



**UNIVERSIDADE DE LISBOA
INSTITUTO SUPERIOR TÉCNICO**

**Isocyanate microcapsules as new cross-linkers for
safer and high performance adhesives**

Mónica de Jesus Veiga Loureiro

Supervisor: Doctor Ana Clara Lopes Marques

Co-Supervisor: Doctor João Carlos Moura Bordado

**Thesis approved in public session to obtain the PhD Degree in
Materials Engineering**

Jury final Classification: Pass with Distinction

2023



**UNIVERSIDADE DE LISBOA
INSTITUTO SUPERIOR TÉCNICO**

**Isocyanate microcapsules as new cross-linkers for
safer and high performance adhesives**

Mónica de Jesus Veiga Loureiro

Supervisor: Doctor Ana Clara Lopes Marques

Co-Supervisor: Doctor João Carlos Moura Bordado

**Thesis approved in public session to obtain the PhD Degree in
Materials Engineering**

Jury final Classification: Pass with Distinction

Jury

Chairperson: Doctor José Paulo Sequeira Farinha, Instituto Superior Técnico, Universidade de Lisboa

Members of the Committee:

Doctor Henrique Aníbal Santos de Matos, Instituto Superior Técnico, Universidade de Lisboa

Doctor Ricardo João Ferreira Simões, Escola Superior de Design, Instituto Politécnico do Cávado e do Ave

Doctor João André Costa Tedim, Universidade de Aveiro

Doctor Maria Amélia Nortadas Lemos, Instituto Superior Técnico, Universidade de Lisboa

Doctor Ana Clara Lopes Marques, Instituto Superior Técnico, Universidade de Lisboa

Funding Institution: FCT: Fundação para a Ciência e a Tecnologia

2023

Abstract

Currently available polyurethane (PU) and polychloroprene (PCP) adhesives use isocyanates as cross-linkers, which are to be added to the adhesive pre-polymer, by the operator, during the adhesive application. New restrictions imposed by the Registration, Evaluation, Authorization and Restriction of Chemicals (REACH) regulations, on the use of diisocyanates, due to their toxicity, make pressure on the companies to develop safer products maintaining the quality of those currently available. The present work focuses on the microencapsulation of isocyanates species for the development of new formulations of PU and PCP adhesives, with main application in the footwear industry. The developed microcapsules (MCs), new solid cross-linkers, release isocyanate where and when needed and eliminate direct contact between the operator and the toxic chemicals.

This work employs two strategies for the encapsulation of monomeric, oligomeric and pre-polymeric isocyanates: development of MCs with a polyurea (PUa) and PU/PUa shell, made by interfacial polymerization, as well as biodegradable MCs, composed of polycaprolactone (PCL) and polyhydroxybutyrate (PHB) shell, made by solvent evaporation, both cases combined with a microemulsion system. MCs with a core-shell morphology, a relatively narrow and monomodal size distribution, with a high encapsulation yield (60 to 80 wt% of their weight in isocyanate), and a satisfactory shelf-life were obtained.

MCs with a biodegradable polyester shell, namely PCL, containing isophorone diisocyanate (IPDI), were considered the most suitable for the application in study. They display a good production process reproducibility and respond to both stimuli of pressure and temperature during the adhesive application. When added to the adhesive pre-polymer, at a weight concentration of 5%, these MCs lead to results identical to those obtained with adhesives formulated with the (non-encapsulated) commercial crosslinkers. This justifies their scale up production in a pilot line implemented at Cipade S.A., paving the way for commercial adhesive formulations without risks for the operators.

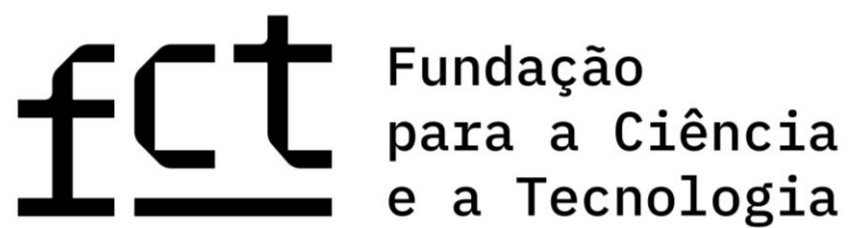
Keywords: Microencapsulation; Adhesives; Isocyanate; Interfacial polymerization; Solvent evaporation.

Resumo

Os adesivos de poliuretano (PU) e policloropreno (PCP) actualmente disponíveis utilizam isocianatos como agentes reticulantes, que necessitam de ser misturados com o pré-polímero adesivo, durante a aplicação, pelo operador. Devido à toxicidade do isocianato, o regulamento de Registro, Avaliação, Autorização e Restrições de Produtos Químicos (REACH) impôs novas restrições relativamente à utilização destes compostos, pressionando as empresas a desenvolver produtos mais seguros, sem prescindir da sua qualidade. O presente trabalho foca-se na microencapsulação de isocianatos para o desenvolvimento de novas formulações de adesivos de PU e PCP, com principal aplicação na indústria do calçado. As novas microcápsulas (MCs), reticulantes sólidos, libertam as espécies de isocianato onde e quando necessário, eliminando o contacto directo entre o operador e os produtos químicos de toxicidade.

Reportam-se duas estratégias para a encapsulação de isocianatos monoméricos, oligoméricos e pré-poliméricos: desenvolvimento de MCs com parede de poliureia (PUa) e PU/PUa, obtidas por polimerização interfacial, assim como MCs com parede biodegradável de policaprolactona (PCL) e polihidroxitirato (PHB), obtidas por evaporação de solvente, ambas associadas a sistemas de microemulsão. Obtiveram-se MCs com morfologia núcleo-parede, distribuição de tamanho relativamente pequena e monomodal, elevado rendimento de encapsulação (entre 60 a 80% do peso em isocianato), e um tempo de vida útil satisfatório. As MCs com parede biodegradável, em particular de PCL, com diisocianato de isoforona (IPDI) encapsulado, foram consideradas as mais adequadas para a aplicação em estudo. Apresentam boa reprodutibilidade do processo de produção e respondem tanto ao estímulo de pressão como de temperatura durante a aplicação do adesivo. Quando adicionadas ao pré-polímero do adesivo, numa concentração mássica de 5%, levam a resultados idênticos aos dos adesivos formulados com reticulantes comerciais (não encapsulados). Isto justifica a sua produção em escala, numa linha piloto implementada na Cipade S.A., abrindo caminho para formulações adesivas comerciais sem riscos para os operadores.

Palavras-chave: Microencapsulação; Adesivos; Isocianato; Polimerização interfacial; Evaporação de solvente;



This work was financially supported by Fundação para a
Ciência e a Tecnologia with PhD grant SFRH/BD/140700/2018

Acknowledgements

I would like to express my sincere gratitude to everyone who, in some way or another, contributed to my PhD.

This work was financially supported by Fundação para a Ciência e a Tecnologia through the PhD grant SFRH/BD/140700/2018, for which I am thankful, as well as projects from ADI – Portugal2020, of reference POCI-01-0247-FEDER-017930 (ECOBOND) and POCI-01-0247-FEDER-046991 (BEYOND ECOBOND).

I want to express my gratitude to Cipade S.A., in particular to Eng. Isabel Pinho, for the technical support, hospitality during my visits to the company and for providing necessary primary materials.

My sincere gratitude to my supervisors, Prof. Ana Clara Lopes Marques and Prof. João Carlos Moura Bordado, for the opportunity, guidance, scientific knowledge and encouragement they have given me over the years. To Dr. Rui Galhano for the all the time and support he always found time to give and to all my colleagues of the Technology Platform on Microencapsulation and Immobilization (TPMI) for the companionship, in particular to António Aguiar and Mahboobeh Attaei who helped me with critical insight into my work and laboratorial support. I want to thank to all co-authors of scientific articles published in the framework of this PhD thesis, for the collaborations and effort.

A special thank you to Mário Vale and António Mariquito not only for their support as research colleagues but also for their friendship, for all the conversations, emotional support, optimism and specially for all the laughs.

I am genuinely grateful to my friends Inês Sebastião and Cláudia Oliveira, for their friendship and for understanding, without judgement, all my absence during the hard times. I will forever be grateful to Rita Antunes for her unconditional friendship, for all the conversations, support and for holding my hand through all the phases of my life.

I would like to thank to my cat and dear companion, Chita, who is no longer here, for being my company during most of the years of this journey, for all the cuddles and emotional support. All the time in confinement would have been very solitary without her.

This work was only possible due to the help of many friends and family members which helped me with their time and support which came in many different ways. I would like to thank to my precious mother, father, and grandmother for all the support with my baby boy, Bruno, which

made it possible for me to write this thesis. A special thank you to my sister for always be present for me and available for a good talk at the distance of a click. My gratitude to Luísa Mendonça for all the support she gave me, in particular this last year, for helping me find the time to conclude this work.

Lastly, I want to thank to my amazing son, Bruno. Your happy personality and tender hugs light me up even in the gloomiest days. Thank you for all the love you brought into my life.

Table of Contents

List of figures	xI
List of tables	xvi
Abbreviations and acronyms.....	xix
Chapter I - Introduction to the thesis.....	3
Research motivation.....	3
Cipade S.A.- Industry and research of adhesive products.....	5
Objectives and main contributions.....	5
Organization of the dissertation.....	6
List of contributions.....	7
Bibliography.....	10
Chapter II - State of understanding.....	14
II.1 Adhesives.....	14
II.1.1 Adhesives in the footwear industry.....	16
II.2 Isocyanates toxicity.....	21
II.3 Microencapsulation.....	21
II.3.1 Interfacial polymerization – Encapsulation of isophorone diisocyanate.....	24
II.3.2 Interfacial polymerization – Encapsulation of other isocyanate species.....	31
II.3.3 Microplastics in isocyanate microencapsulation.....	33
II.3.4 Solvent evaporation.....	33
Bibliography:.....	38
Chapter III - Testing and characterization.....	45
III.1 Emulsions testing and characterization.....	45
III.1.1 Optical microscopy.....	45
III.1.2 Emulsion stability – Sedimentation tests.....	45
III.1.3 Viscosity.....	47
III.2 Microcapsules testing and characterization.....	47
III.2.1 Optical microscopy.....	48
III.2.2 Scanning electron microscopy (SEM).....	48
III.2.3 Fourier transform infrared spectroscopy (FTIR).....	49
III.2.4 Thermogravimetric analysis (TGA).....	49
III.2.5 Gel permeation chromatography (GPC).....	50
III.2.6 Differential scanning calorimetry (DSC).....	50
III.2.7 MCs' behavior to temperature.....	50
Bibliography:.....	52

Chapter IV - Interfacial polymerization technique in combination with a microemulsion system: Reactional parameters and strategies	56
IV.1 Materials.....	56
IV.2 Experimental: MCs synthesis by Interfacial polymerization technique in combination with a microemulsion system.....	59
IV.3 Results and discussion: Reactional parameters and strategies.....	61
IV.3.1 Synthesis duration and temperature.....	62
IV.3.2 Use of two isocyanates and active H sources.....	67
IV.3.3 Effect of the isocyanate source, used for the shell formation, on the microcapsule's final properties.....	79
IV.3.4 Emulsion stabilization	83
IV.4 Scale-up of the syntheses processes	93
IV.5 Final remarks	99
Bibliography	104
Chapter V - Solvent evaporation technique in combination with a double emulsion system: strategies and reactional parameters	122
V.1 Materials.....	122
V.2 Experimental: MCs synthesis by solvent evaporation technique in combination with a microemulsion system.....	124
V.3 Results and discussion: Reactional parameters and strategies	128
V.3.1 The effect of polycaprolactone's molecular weight	130
V.3.2 Design of experiment to control the microcapsules size.....	145
V.3.3 Polymers used for the shell formation	158
V.3.4 Encapsulation of highly reactive isocyanate species	167
V.4 Scale-up of the syntheses processes	171
V.5 Final remarks	176
Bibliography:.....	180
Supplementary Information	186
Chapter VI - Adhesive development	195
VI.1 Adhesives testing and characterization.....	195
VI.1.1 Peeling strength test.....	197
VI.1.2 Creep test.....	197
VI.2 MCs solvent resistance and behavior in the adhesive pre-polymer	198
VI.3 MCs effectiveness as cross-linkers	203
VI.4 Optimization of the final adhesive	209
VI.5 Final remarks	213
Bibliography:.....	215
Supplementary Information	217
Chapter VII – Final remarks and conclusions	221

List of figures

FIGURE I. 1. SCHEMATIC REPRESENTATION OF THE ADHESION PROCESS USING THE 1K ADHESIVE FORMULATION CONTAINING MCS AS CROSS-LINKERS.	4
FIGURE II.1. SCHEMATIC REPRESENTATION OF THE ADHESIVE BONDING MECHANISMS: (A) MECHANICAL INTERLOCKING; (B) BY INTERATOMIC AND INTERMOLECULAR FORCES; (C) CHEMICAL BONDING; (D) INTERDIFFUSION; (E) ELECTROSTATIC ADHESION. IMAGE REPRINTED FROM [9], WITH PERMISSION.	15
FIGURE II.2 ADHESIVE JOINT FOR PEEL TEST (DIMENSIONS IN MILLIMETERS), FOLLOWING THE EN 1392 [26]. IMAGE REPRINTED FROM [13], WITH PERMISSION.	19
FIGURE II.3 TYPES OF FAILURE OF AN ADHESIVE JOINT. ADAPTED FROM [27] AND [28].	20
FIGURE II.4. ADHESIVE JOINT FOR CREEP TEST FOLLOWING THE EN 15307. IMAGE REPRINTED FROM [13], WITH PERMISSION.	21
FIGURE II.5. SCHEMATIC REPRESENTATION OF THE DIFFERENT MCS MORPHOLOGY, A) MATRIX-TYPE MICROCAPSULE OR MICROSPHERE B) MONONUCLEAR MICROCAPSULE OR CORE-SHELL C) POLY-NUCLEAR MICROCAPSULES. THE MCS SHELL IS REPRESENTED AT WHITE. IMAGE REPRINTED FROM [38], WITH PERMISSION.	22
FIGURE II. 6. REPRESENTATION OF THE MCS' RELEASE MECHANISMS: (A) BY THE EFFECT OF TEMPERATURE (MELT) OR SOLVENT DISSOLUTION; (B) PRESSURE (RUPTURE); (C) THROUGH THE MCS' SHELL POROSITY (DIFFUSION).	23
FIGURE II.7. SCHEMATIC REPRESENTATION OF MICROENCAPSULATION BY INTERFACIAL POLYMERIZATION, WHERE THE DISPERSED PHASE OF THE EMULSION IS REPRESENTED AS WHITE (ORGANIC PHASE COMPOSED BY THE ISOCYANATES) AND, AS BLUE, THE CONTINUOUS PHASE (AQUEOUS SOLUTION), WITH THE MONOMERS OF EACH PHASE REPRESENTED AS A AND B, RESPECTIVELY. THE ENCAPSULATED IS REPRESENTED AT PINK AND THE FORMED OLIGOMERS AS BLUE STRIPES. FIGURE ADAPTED FROM [44].	25
FIGURE II.8 THE REACTION OF ISOCYANATES WITH A HYDROXYL GROUP, WITH WATER, AND WITH AN AMINO GROUP.	26
FIGURE II.9. SCHEMATIC REPRESENTATION OF EMULSIONS DESTABILIZATION PHENOMENA, WITH THE DISPERSED PHASE REPRESENTED BY LIGHT GRAY AND THE CONTINUOUS PHASE BY DARK GRAY. FROM [56] UNDER AN OPEN ACCESS CREATIVE COMMON CC BY LICENSE.	30
FIGURE II.10. SCHEMATIC REPRESENTATION OF THE EMULSION'S CLASSIFICATION TYPES, WITH THE WATER PHASE OF THE EMULSION SYSTEM REPRESENTED BY THE LIGHT GRAY COLOR AND THE OIL PHASE BY DARK GRAY COLOR.	34
FIGURE III.1. SCHEMATIC REPRESENTATION OF THE SEDIMENTATION PHENOMENON OBSERVED IN A POLYDISPERSE EMULSION SYSTEM. THE DISPERSED PHASE OF THE EMULSION IS REPRESENTED BY ORANGE SPHERES, WHICH CORRESPONDS TO THE OIL PHASE OF THE EMULSION, COMPOSED BY THE ISOCYANATES. IMAGE REPRINTED FROM [5].	46
FIGURE III.2. VISUAL EXPLANATION OF THE H (TOTAL HEIGHT OF THE INITIAL EMULSION) AND H ₀ (HEIGHT OF THE SEDIMENT) USED FOR EQUATION 2.	47
FIGURE IV.1. SCHEMATIC REPRESENTATION OF THE MCS' SYNTHESIS PROCESS BY THE INTERFACIAL POLYMERIZATION TECHNIQUE COMBINED WITH A MICRO-EMULSION SYSTEM.	60
FIGURE IV.2. SCHEMATIC REPRESENTATION OF THE STRATEGIES ADOPTED TO OPTIMIZE THE MCS OBTAINED BY THE INTERFACIAL POLYMERIZATION TECHNIQUE.	62
FIGURE IV.3. RESULTS OF MCS' AVERAGE SIZE (A) AND S/D RATIO (B), OBTAINED AT DIFFERENT TIMES DURING THE MCS SYNTHESIS AT 30 °C AND AT 70 °C.	64
FIGURE IV.4. SEM PHOTOMICROGRAPHS OF THE MCS' OBTAINED AT 30 °C AND AT 70 °C.	64
FIGURE IV.5. FTIR-ATR OF MCS SAMPLES COLLECTED AT DIFFERENT TIMES DURING THE SYNTHESIS (A). VARIATION OF THE Y VALUE (B) AND FTIR-ATR SPECTRA OF THE MCS_5MIN. 2 AND 7 DAYS AFTER THE MCS' SYNTHESIS.	66
FIGURE IV.6. SEM PHOTOMICROGRAPHS OF THE MCS COLLECTED AFTER 5 AND 15 MINUTES OF SYNTHESIS.	66
FIGURE IV.7. SEM PHOTOMICROGRAPHS OF THE MCS OBTAINED WITH ONE AND WITH TWO ISOCYANATES (A) AND (B) IN THE O PHASE OF THE EMULSION, RESPECTIVELY. RESPECTIVE SIZE DISTRIBUTION (C) AND (D).	68
FIGURE IV.8. FTIR-ATR SPECTRA OF THE MCS OBTAINED WITH ONE AND WITH TWO ISOCYANATES IN THE O PHASE OF THE EMULSION.	69

FIGURE IV.9. SEM PHOTOMICROGRAPHS OF THE MCS OBTAINED USING DIFFERENT ACTIVE H SOURCES AS WELL AS THE REF_MCS, FOR WHICH IT WAS NOT ADDED ANY ACTIVE H SOURCE DURING THE SYNTHESIS.	71
FIGURE IV.10. SEM PHOTOMICROGRAPHS OF A PURPOSEFULLY BROKEN MC (LEFT) AND OF HALF A MCS' SHELL (RIGHT). ..	72
FIGURE IV.11. SIZE DISTRIBUTION HISTOGRAMS OF THE MCS OBTAINED WITH DIFFERENT ACTIVE H SOURCES, AS WELL AS THE REF_MCS, TO WHICH IT WAS NOT ADDED ANY ACTIVE H SOURCE DURING THE SYNTHESIS.	72
FIGURE IV.12. FTIR-ATR SPECTRA OF THE ISOCYANATES AND ACTIVE H SOURCES USED FOR THE MCS' SYNTHESIS (A) AND OF THE OBTAINED MCS (B).	74
FIGURE IV.13. Y VALUE VARIATION OVER TIME, FOR ALL THE MCS IN STUDY, WHILE STORED AT ROOM TEMPERATURE AND 60% OF HUMIDITY.....	75
FIGURE IV.14. SEM PHOTOMICROGRAPHS OF THE O_PEI_N-OTES_MCS (A) AND OF THE O_JEFFAMINE_MCS (B), AS WELL AS THE RESPECTIVE SIZE DISTRIBUTION HISTOGRAMS.	77
FIGURE IV.15. FTIR-ATR SPECTRA OF THE ISOCYANATES AND ACTIVE H SOURCES USED FOR THE MCS' SYNTHESIS (LEFT) AS WELL AS OF THE MCS AFTER THE SYNTHESIS AND AFTER STORED FOR 3 MONTHS AT ROOM TEMPERATURE AND 60% OF RELATIVE HUMIDITY (RIGHT).....	78
FIGURE IV.16. SEM PHOTOMICROGRAPHS OF THE MCS OBTAINED USING DIFFERENT ISOCYANATES FOR THE SHELL FORMATION.....	80
FIGURE IV.17. SIZE DISTRIBUTION HISTOGRAMS OF THE ONGRONAT_MCS (LEFT) AND OF THE DESMODUR_RC_MCS (RIGHT).....	80
FIGURE IV.18. THERMOGRAMS OF THE ISOCYANATES USED FOR THE MCS' SYNTHESIS AND OF THE OBTAINED MCS (LEFT), AND RESPECTIVE DERIVATIVES (RIGHT), NORMALIZED BY THE DIVISION OF EACH POINT BY THE MAXIMUM VALUE.....	82
FIGURE IV.19. SCHEMATIC REPRESENTATION OF THE EMULSION DROPLETS STABILIZATION BY POLYSACCHARIDES, SURFACTANTS, AND RHEOLOGY MODIFIERS. IMAGE REPRINTED FROM [22] UNDER AN OPEN ACCESS CREATIVE COMMON CC BY LICENSE.....	84
FIGURE IV.20. VISUAL OBSERVATION OF THE EMULSIONS USED TO OBTAIN THE GA, DC, GA_DC, PVA, AND GA_PVA MCS, OVER A PERIOD OF 30 MIN. FROM LEFT TO RIGHT: OIL AND WATER PHASE BEFORE EMULSIFICATION, RIGHT AFTER EMULSIFICATION, 14 AND 30 MIN AFTER EMULSIFICATION (STATIC CONDITIONS).....	86
FIGURE IV.21. EVOLUTION OF THE SEDIMENTATION VOLUME FRACTION OVER TIME, OF ALL THE REPORTED EMULSIONS IN STUDY, WHILE AT REST (STATIC CONDITIONS).....	86
FIGURE IV.22. OPTICAL MICROSCOPY PHOTOGRAPHS OF THE EMULSION THAT SUFFERED LESS SEDIMENTATION (GA_PVA_MCS EMULSION) AND THE ONE STABILIZED WITH DC193. OPTICAL PHOTOGRAPHS OF THE EMULSIONS WHILE UNDER EMULSIFICATION (LEFT) AND AFTER 30 MINUTES AT REST (RIGHT), EMULSION AND SEDIMENT PORTIONS.	87
FIGURE IV.23. OPTICAL MICROSCOPY PHOTOGRAPHS OF THE DC_MCS' EMULSION DURING THE FIRST 25 MINUTES OF THE SYNTHESIS. LEFT: AFTER 10 MINUTES OF EMULSIFICATION AT 3200 RPM USING THE ULTRA-TURRAX; RIGHT: AFTER THE FOLLOWING 15 MINUTES UNDER MECHANICAL STIRRING AT 400 RPM (DYNAMIC CONDITIONS).....	87
FIGURE IV.24. SEM IMAGES OF THE OBTAINED MCS AT 80X AMPLIFICATION (LEFT). SEM IMAGES OF ISOLATED MCS' CROSS SECTIONS DELIBERATELY CRUSHED (OBTAINED AT DIFFERENT MAGNIFICATIONS). MCS' SIZE DISTRIBUTION (RIGHT).....	88
FIGURE IV.25. OIL EMULSION DROPLETS AVERAGE DIAMETER AT THE END OF THE EMULSION PREPARATION (10 MIN), AFTER 10 MIN UNDER MECHANICAL AGITATION (20 MIN), AND OF THE FINAL MCS (180 MIN).	90
FIGURE IV.26. FTIR SPECTRA OF THE ISOCYANATES, ACTIVE H SOURCE, AND STABILIZERS (LEFT). FTIR SPECTRA OF THE MCS (RIGHT).....	91
FIGURE IV.27. THERMOGRAM OF THE AS-PREPARED MCS AND THE RESPECTIVE DERIVATIVE CURVES (TOP). THERMOGRAM OF THE ISOCYANATES AND THE RESPECTIVE DERIVATIVE CURVES (BOTTOM), NORMALIZED BY THE DIVISION OF EACH POINT BY THE MAXIMUM VALUE.....	92
FIGURE IV.28. FLOW DIAGRAM OF THE PU/PUA MCS' SYNTHESIS BY THE SOLVENT EVAPORATION METHOD, FOR A VOLUME OF 10L. WITH AN * ARE REPRESENTED TWO ADDITIONAL STEPS ADDED TO THE MCS SYNTHESIS IN THE SCALE-UP PROCESS.	94
FIGURE IV.29. MC'S SYNTHESIS APPARATUS USED FOR THE PRE-SCALE-UP (LEFT) AND FOR THE SCALED-UP VOLUME (RIGHT).	95
FIGURE IV.30. PHOTOGRAPHS OF THE SEVERAL STEPS USED FOR THE MC'S FABRICATION NAMELY THE ADDITION OF THE O PHASE TO THE W PHASE, EMULSIFICATION, POLYMERIZATION PHASE AND MCS' FILTRATION, WITH RESPECTIVE OPTICAL PHOTOGRAPHS OF THE REACTIONAL MEDIUM AND FINAL MCS.	95

FIGURE IV.31. SEM PHOTOMICROGRAPHS OF THE PRE-SCALE-UP_MCS AND OF THE SCALE-UP_MCS (LEFT), AND RESPECTIVE SIZE DISTRIBUTION HISTOGRAMS (RIGHT).....	96
FIGURE IV.32. SCHEMATIC REPRESENTATION OF THE MIXING MECHANISM OF THE ROTOR/STATOR ARRANGEMENT OF ULTRA-TURRAX HOMOGENIZER. IMAGE REPRINTED FROM [34].	97
FIGURE IV.33 - DISPERSION ROTORS USED IN THE PRE-SCALE-UP (A) AND IN THE SCALE-UP (B).....	97
FIGURE IV.34 – STIRRER BLADE USED FOR THE MECHANICAL AGITATION IN THE PRE-SCALE-UP (A) AND IN THE SCALE-UP (B) SYNTHESIS PROCESS.....	98
FIGURE IV.35 - FTIR-ATR OF THE ISOCYANATES AND ACTIVE H SOURCE USED FOR THE MCS' SYNTHESIS (LEFT) AND OF THE MCS OBTAINED FOR THE PRE-SCALE-UP AND FOR THE SCALE-UP REACTIONAL VOLUME (RIGHT).....	98
FIGURE IV. S1. THERMOGRAMS OF THE O_JEFFAMINE_MCS AND OF THE O_PEI_N-OTES_MCS, AS WELL AS OF THE ISOCYANATES USED IN THE SYNTHESIS (TOP) AND RESPECTIVE DERIVATIVES (BOTTOM), NORMALIZED BY THE DIVISION OF EACH POINT BY THE MAXIMUM VALUE.....	109
FIGURE IV. S2. THERMOGRAMS OF THE AGED ONGRONAT_MCS, SUPRASEC_MCS AND DESMODUR RC_MCS, BY 3 MONTHS AT ROOM AND 60WT% HUMIDITY (ABOVE) AND RESPECTIVE DERIVATIVES (BOTTOM), NORMALIZED BY THE DIVISION OF EACH POINT BY THE MAXIMUM VALUE.....	110
FIGURE IV. S3. FTIR SPECTRA OF THE ONGRONAT_MCS, SUPRASEC_MCS AND DESMODUR RC_MCS, AS PREPARED AND AGED (BY 3 MONTHS, AT ROOM TEMPERATURE AND 60WT% OF HUMIDITY).....	111
FIGURE IV. S4. SEM PHOTOMICROGRAPH WITH THE CORRESPONDING AREAS OF THE DC_MCS' EDS ANALYSIS.200μM..	116
FIGURE IV. S5. SEM PHOTOMICROGRAPHS WITH THE CORRESPONDING AREAS OF THE DC_MCS' EDS ANALYSIS.	117
FIGURE IV. S6. THERMOGRAM OF THE SHELL FROM THE MCS OBTAINED WITH DIFFERENT EMULSION STABILIZATION SYSTEMS.	118
FIGURE V.1. OPTICAL MICROSCOPY PHOTOGRAPH OF THE O ₁ /O ₂ EMULSION OBTAINED WITH ONGRONAT® 2500 IN THE O ₁ PHASE OF THE EMULSION.	125
FIGURE V.2. SCHEMATIC REPRESENTATION OF THE SEVERAL STEPS INVOLVED IN THE MCS FORMATION BY THE SOLVENT EVAPORATION TECHNIQUE IN COMBINATION WITH AN EMULSION SYSTEM (A). OPTICAL MICROSCOPY PHOTOGRAPHS OBTAINED IN EACH STEP (B).	126
FIGURE V. 3. OPTICAL MICROSCOPY PHOTOGRAPH THAT SHOWS THE SHELL FORMATION DURING THE MCS FABRICATION, BY THE SOLVENT EVAPORATION METHOD.	127
FIGURE V. 4. SCHEMATIC REPRESENTATION OF THE MCS' FABRICATION PROCESS BY THE SOLVENT EVAPORATION METHOD COMBINED WITH A DOUBLE O ₁ /O ₂ /W EMULSION SYSTEM.	127
FIGURE V.5. OPTICAL MICROSCOPY PHOTOGRAPHS OF THE PCL MCS, OBTAINED BY THE SOLVENT EVAPORATION METHOD, BEFORE THE PRODUCTION PROCESS OPTIMIZATION (FIRST TRIALS).	130
FIGURE V.6. OPTICAL MICROSCOPY PHOTOGRAPHS CAPTURED DURING THE MCS' FABRICATION PROCESS.	131
FIGURE V.7. I_45 AND I_80 EMULSION SIZE DISTRIBUTION.	132
FIGURE V.8. OPTICAL MICROSCOPY IMAGES. TOP: I_45 MCS (A) BEFORE TEARING OF THE SHELL (B) THE SAME MC AFTER THE BREAK OF THE SHELL, EXHIBITING THE RELEASE OF THE CORE CONTENT (ARROW). BOTTOM: I_80 MCS (A) SINGLE CAPSULE PHOTOGRAPH (B) ANOTHER MC AFTER THE BREAK OF THE SHELL, SHOWING ITS CORE-SHELL MORPHOLOGY.	132
FIGURE V.9. SEM IMAGES OF THE I_45 MCS, AT THE TOP, AND OF I_80 MCS, AT THE BOTTOM. THE IMAGES ON THE RIGHT DISPLAY A PURPOSEFULLY BROKEN MC, EVIDENCING A CORE-SHELL MORPHOLOGY, FOR BOTH THE I_45 AND I_80 MCS.	133
FIGURE V.10. SEM IMAGES SHOWING THE TYPICAL MORPHOLOGY OBTAINED FOR MCS WITH A PCL SHELL. (A) IMAGE OF THE I_45 MCS OUTER SHELL. (B) AND (C) IMAGES OF THE I_45 MCS INNER SHELL.	133
FIGURE V.11. I_45 AND I_80 MCS SIZE DISTRIBUTION.	134
FIGURE V.12. FTIR SPECTRA OF THE AS-PREPARED MCS (I_45 AND I_80), THE SHELL-FORMING POLYMER PCL, AND THE ENCAPSULATED ISOCYANATE, IPDI.	136
FIGURE V.13. FTIR SPECTRA OF THE AS-PREPARED I_45 AND I_80 MCS AND OF THE SAME THREE MONTHS AFTER THEIR EXPOSURE IN AN ATMOSPHERE AT ROOM TEMPERATURE AND 60% OF RELATIVE HUMIDITY.	138
FIGURE V.14. REACTION SCHEMES FOR THE FORMATION OF URETHANE AND UREA LINKAGES FROM THE REACTION BETWEEN IPDI AND PCL HYDROLYSIS INTERMEDIATES (REACTIONS 1 AND 1.1.) AND WITH WATER (REACTION 2).	138

FIGURE V.15. (A) THERMOGRAM OF THE AS-PREPARED AND AGED (3 MONTHS) I_45 MCs (TOP), AND THE RESPECTIVE DERIVATIVE CURVES (BOTTOM); (B) THERMOGRAMS OF THE AS-PREPARED AND AGED (3 MONTHS) I_80 MCs (TOP), AND THE RESPECTIVE DERIVATIVE CURVES (BOTTOM).	140
FIGURE V.16. GEL PERMEATION CHROMATOGRAMS OF THE PCL45 AND PCL80 RAW MATERIALS, AS WELL AS THAT OF THE I_45 AND I_80 MCs' SHELLS.	141
FIGURE V.17. DSC THERMOGRAMS OF THE AGED I_45 AND I_80 MCs' SHELL.	142
FIGURE V.18. VISCOSITIES OF THE PRE-POLYMER AND ITS MIXTURES WITH AGED MCs, MEASURED EVERY 10 MINUTES, DURING A 1-HOUR EXPERIMENT.	143
FIGURE V.19. AVERAGE MAXIMUM LOAD OBTAINED IN THE PEELING STRENGTH TESTS FOR THE ADHESIVE JOINTS PREPARED WITH THE FOLLOWING FORMULATIONS: OH PRE-POLYMER WITH IPDI; OH PRE-POLYMER WITH ENCAPSULATED IPDI IN THE FORM OF I_45 MCs AND I_80 MCs.	144
FIGURE V.20. REPRESENTATION OF A GENERAL CENTRAL COMPOSITE FACE DESIGN (CCF), REPRINTED WITH PERMISSION FROM [62] (A) AND THE CCF USED FOR THE OPTIMIZATION OF THE MCs AVERAGE SIZE.	147
FIGURE V. 21. COEFFICIENT PLOT FOR THE DOE SATURATED MODEL, SHOWING THE INFLUENCE OF INDIVIDUAL AND SQUARED TERMS (WHERE * REPRESENTS MULTIPLICATION) ON THE MCs' AVERAGE SIZE.	149
FIGURE V. 22. COEFFICIENT PLOT FOR THE DOE MODEL, CONSIDERING THE SIGNIFICANT TERMS, SHOWING THE INFLUENCE OF INDIVIDUAL AND SQUARED TERMS (WHERE * REPRESENTS MULTIPLICATION) ON THE MCs AVERAGE SIZE.	150
FIGURE V.23. PLOT OF THE CORRELATION BETWEEN THE OBSERVED VS PREDICTED RESULTS.	150
FIGURE V.24. CONTOUR PLOTS OF THE RESPONSE (MCs SIZE, μm) TO THE VARIATION OF GA CONCENTRATION (w/w%) VS VOLUMETRIC RATIO BETWEEN THE O AND W PHASES (v/v %) FOR DIFFERENT PVA CONCENTRATIONS (LEFT) AND THE RESPECTIVE 3-D SURFACE PLOT (RIGHT).	153
FIGURE V.25. SEM IMAGES (LEFT) OF THE MCs OBTAINED IN THE VALIDATION RUNS, N18 AND N19, AND RESPECTIVE SIZE DISTRIBUTION HISTOGRAMS (RIGHT).	154
FIGURE V.26. SEM PHOTOMICROGRAPH OF MCs OBTAINED USING A PVA CONCENTRATION OF 4wt%.	155
FIGURE V.27. SEM PHOTOMICROGRAPHS OF THE N7 AND N15 MCs (LEFT) AND RESPECTIVE SIZE DISTRIBUTION HISTOGRAMS (RIGHT).	156
FIGURE V.28. THERMOGRAM OF THE AS-PREPARED AND AGED (BY 3 MONTHS AT ROOM TEMPERATURE AND 60WT% OF RELATIVE HUMIDITY) N7 MCs AND N15 (LEFT), AND THE RESPECTIVE DERIVATIVE CURVES (RIGHT).	157
FIGURE V. 29. OPTICAL MICROSCOPY PHOTOGRAPHS OF THE PHB MCs OBTAINED USING A MECHANICAL STIRRING OF 750 RPM (A) AND OF 850 RPM (B).	161
FIGURE V.30. OPTICAL MICROSCOPY PHOTOGRAPHS OF PHB MCs OBTAINED WITH 2, 3 AND 4WT% OF PVA IN THE EMULSION W PHASE.	161
FIGURE V.31. OPTICAL MICROSCOPY PHOTOGRAPHS OF PHB MCs OBTAINED USING 5, 8, 10 AND 12 WT% OF PHB IN THE O PHASE OF THE EMULSION.	162
FIGURE V.32. SEM PHOTOMICROGRAPHS OF THE MCs OBTAINED USING 5, 8 AND 10WT% OF PHB IN THE O PHASE OF THE EMULSION.	163
FIGURE V.33. THERMOGRAMS OF THE AS-PREPARED AND AGED MCs OBTAINED USING 5, 8 AND 10 WT% OF PHB IN THE O PHASE OF THE EMULSION, OF THE PHB AND OF THE ENCAPSULATED ISOCYANATE (LEFT), AS WELL AS THE RESPECTIVE DERIVATIVES (RIGHT), NORMALIZED BY THE DIVISION OF EACH POINT BY THE MAXIMUM VALUE.	165
FIGURE V.34. SEM PHOTOMICROGRAPHS OF THE ONGRONAT_MCs AND OF THE SUPRASEC_MCs (RIGHT) AS WELL AS OF THE RESPECTIVE SIZE DISTRIBUTION HISTOGRAMS (LEFT).	168
FIGURE V.35. FTIR-ATR SPECTRA OF THE ONGRONAT_MCs AND SUPRASEC_MCs AS PREPARED AND AGED (BY 3 MONTHS AT ROOM TEMPERATURE AND 60WT% OF RELATIVE HUMIDITY), AND OF THE PCL AND RESPECTIVE ISOCYANATE.	169
FIGURE V.36. THERMOGRAM OF THE ONGRONAT_MCs AS PREPARED AND AGED (BY 3 MONTHS AT ROOM TEMPERATURE AND 60WT% OF RELATIVE HUMIDITY), OF THE SHELL POLYMER AND ENCAPSULATED ISOCYANATE (LEFT) AND RESPECTIVE DERIVATIVES (RIGHT), NORMALIZED BY THE DIVISION OF EACH POINT BY THE MAXIMUM VALUE.	170
FIGURE V.37. FLOW DIAGRAM OF THE SCALE-UP PROCESS FOR THE PCL MCs FABRICATION.	172
FIGURE V.38. PCL MCs' PRODUCTION APPARATUS USED FOR THE PRE-SCALE-UP REACTIONAL VOLUME (A) AND FOR THE SCALE-UP VOLUME (B).	173
FIGURE V.39. STIRRING RODS USED IN THE PRE-SCALE-UP (A), AND IN THE SCALE-UP (B) PROCESS.	173
FIGURE V.40. SEM PHOTOMICROGRAPHS OF THE PRE-SCALE-UP_MCs AND OF THE SCALE-UP_MCs (LEFT) AND RESPECTIVE SIZE DISTRIBUTION HISTOGRAMS (RIGHT).	174

FIGURE V.41. THERMOGRAM OF THE PRE-SCALE-UP_MCs, OF THE SCALE-UP_MCs, SHELL POLYMER AND ENCAPSULATED ISOCYANATE (LEFT) AND RESPECTIVE DERIVATIVE CURVES (RIGHT).	175
FIGURE V. S 1. GEL PERMEATION CHROMATOGRAM OF THE PHB.	186
FIGURE V. S2. THERMOGRAM OF THE PCL MCs CONTAINING ENCAPSULATED SUPRASEC®2234, SUPRASEC_MCs, AFTER THE SYNTHESIS AND AGED (BY 3 MONTHS AT ROOM TEMPERATURE AND 60WT% OF RELATIVE HUMIDITY), AS WELL AS OF THE SUPRASEC®2234 AND PCL.	190
FIGURE V. S3. FTIR-ATR SPECTRA OF THE PCL MCs, CONTAINING ENCAPSULATED IPDI, OBTAINED IN THE PRE-SCALE-UP PROCESS AND IN THE SCALE-UP.	191
FIGURE VI.1. PHOTOGRAPHS OF THE SEVERAL STEPS INVOLVED IN THE ADHESIVE JOINT PREPARATION: (A) ADHESIVE DISPERSION IN THE SUBSTRATE, (B) DRYING, (C) REACTIVATION AND (D) PRESSING.	197
FIGURE VI.2. SPECIMEN UNDER THE CREEP TEST, IN THE CLIMATIC CHAMBER.	198
FIGURE VI.3. ONGRONAT_MCs, SUPRASEC®2234_MCs AND DESMODUR®RC_MCs Y VALUE VARIATION OVER 180H, WHILE SUBMERGED IN ORGANIC SOLVENTS AND WATER.	200
FIGURE VI.4. PCL_MCs, PHB_MCs AND PLC/PHB_MCs Y VALUE VARIATION OVER 180H, WHILE SUBMERGED IN ORGANIC SOLVENTS AND WATER.	201
FIGURE VI.5 VISCOSITY VARIATION, OVER 190 HOURS, OF THE PLASTIK®6275 AND CIPRENE®2000, CONTAINING PU/PUA, PCL OR PHB MCs, TO EVALUATE THE MCs RESISTANCE IN THE ADHESIVE PRE-POLYMERS.	202
FIGURE VI.6. PHOTOGRAPHS EXPOSING AN IMPROPER ADHESIVE DISTRIBUTION ON THE SUBSTRATE.	203
FIGURE VI. 7. PEEL STRENGTH TEST RESULTS OBTAINED WITH PU/PUA MCs CONTAINING SUPRASEC® 2234 AND IPDI, AT 2.5WT% IN THE CIPRENE® 2000 PRE-POLYMER.	205
FIGURE VI.8. OPTICAL MICROSCOPY PHOTOGRAPHS DEPICTING INTACT SUPRASEC 2234_MCs IN THE ADHESIVE JOINT, AFTER ITS OPENING IN THE PEEL STRENGTH TEST.	205
FIGURE VI.9. PHOTOGRAPHS OF SUBSTRATES WITH A HOMOGENEOUSLY DISPERSED ADHESIVE. FORMULATION WITH 5WT% OF PCL MCs (A) AND 5WT% OF PHB MCs (B), BOTH CONTAINING IPDI.	207
FIGURE VI.10. PEEL STRENGTH TEST RESULTS OBTAINED WITH PCL AND PHB MCs IN BOTH THE CIPRENE® 2000 (LEFT) AND THE PLASTIK® 6275 (RIGHT) PRE-POLYMERS, AT 2.5WT%.	208
FIGURE VI.11. PHOTOGRAPHS OF THE OPENED BONDLINES, AFTER THE PEELING STRENGTH TESTS, USING CIPRENE® 2000 AND PCL MCs, CONTAINING IPDI OR ONGRONAT®2500, AS CROSS-LINKERS.	208
FIGURE VI.12. PHOTOGRAPHS OF THE OPENED BONDLINES, AFTER THE PEELING STRENGTH TESTS, USING PLASTIK® 6275 AND PCL MCs, CONTAINING ONGRONAT® 2500, AS CROSS-LINKER.	209
FIGURE VI.13. PEEL STRENGTH TEST RESULTS USING ADHESIVE FORMULATIONS WITH DIFFERENT CONCENTRATIONS OF MCs, BOTH WITH CIPRENE® 2000 (LEFT) AND PLASTIK® 6275 (RIGHT) AS PRE-POLYMERS.	210
FIGURE VI.14. PHOTOGRAPHS DEPICTING A COHESIVE (LEFT) AND MIXTURE OF COHESIVE WITH ADHESIVE TYPE OF FAILURE (RIGHT). SUBSTRATES PREVIOUSLY ADHERED WITH IPDI_MCs AS CROSS-LINKERS IN CIPRENE® 2000.	210
FIGURE VI. 15. PHOTOGRAPHS DEPICTING A SUBSTRATE (LEFT) AND A COHESIVE TYPE OF FAILURE (RIGHT). SUBSTRATES PREVIOUSLY ADHERED WITH IPDI_MCs AS CROSS-LINKERS IN PLASTIK®6275.	211
FIGURE VI. S1. PHOTOGRAPHS OF THE PCL MCs BEFORE (ABOVE) AND AFTER (BOTTOM) BEING SUBMITTED TO THE REACTIVATION PROCESS USED DURING THE ADHESION PROCESS, WHEN USING A PCP ADHESIVE (PLASTIK® 6275).	217

List of tables

TABLE II.1 ADHESIVE CLASSIFICATION. ADAPTED FROM [10].....	16
TABLE II.2 MINIMUM UPPER-SOLE BOND STRENGTH REQUIREMENTS IN THE FOOTWEAR INDUSTRY ACCORDING TO THE STANDARD EN 15307. ADAPTED FROM [13] AND [15].....	17
TABLE II.3 TECHNIQUES USED FOR MICROENCAPSULATION [40, 41].	24
TABLE II. 4. RESUME OF THE ISOCYANATE SPECIES AND ACTIVE H SOURCES USED FOR THE MCs SHELL FORMATION AS WELL AS TYPE AND AMOUNT OF ENCAPSULATED ISOCYANATE OF THE MCs REFERRED IN THIS CHAPTER. (II.3.1.1 ACTIVE H SOURCES AND MICROCAPSULES' SHELL COMPOSITION).	29
TABLE IV. 1. REAGENTS USED IN THE MCs PRODUCTION BY THE INTERFACIAL POLYMERIZATION TECHNIQUE, WITH THE RESPECTIVE COMMERCIAL NAME, PURITY, AND MANUFACTURER.....	57
TABLE IV.2. ISOCYANATES USED FOR THE MCs SYNTHESIS BY THE INTERFACIAL POLYMERIZATION TECHNIQUE AND RESPECTIVE CHEMICAL STRUCTURE, DENSITY, VISCOSITY, NCO CONTENT AND MAIN PROPERTIES.....	58
TABLE IV.3. ACTIVE H SOURCES USED FOR THE MCs SYNTHESIS BY THE INTERFACIAL POLYMERIZATION TECHNIQUE AND RESPECTIVE CHEMICAL STRUCTURE AND TYPE.....	59
TABLE IV. 4. REACTIONAL VARIABLES IN THE SYNTHESIS OF MCs BY INTERFACIAL POLYMERIZATION TECHNIQUE AND RANGES USED.	61
TABLE IV.5. EMULSION COMPOSITION AND ACTIVE H SOURCE FOR THE SYNTHESIS OF THE MCs USED TO STUDY THE EFFECT OF THE SYNTHESIS DURATION ON THE MCs' SHELL THICKNESS AND MORPHOLOGY.	63
TABLE IV.6. EMULSION COMPOSITION AND ACTIVE H SOURCE USED FOR THE SYNTHESIS OF THE MCs USED TO STUDY THE EFFECT OF THE SYNTHESIS DURATION ON THE ENCAPSULATION YIELD.	65
TABLE IV.7. MICROCAPSULES' ACRONYMS AND EMULSION COMPOSITION.	70
TABLE IV.8. MAXIMUM VALUE (MODE) OBTAINED IN THE MC'S SIZE DISTRIBUTION HISTOGRAM.....	73
TABLE IV.9. RELATIVE ENCAPSULATION YIELD (Y VALUE) CALCULATED FOR EACH SAMPLE, BY USING THE FTIR SPECTRA OF THE AS-PREPARED MCs.	74
TABLE IV. 10. MICROCAPSULES' ACRONYMS AND EMULSION COMPOSITION.	76
TABLE IV.11. RELATIVE ENCAPSULATION YIELD (Y VALUE) CALCULATED FOR EACH SAMPLE, BY USING THE FTIR SPECTRA OF THE AS-PREPARED MCs AND 3 MONTHS AGED MCs, WHILE AT ROOM TEMPERATURE AND 60WT% OF RELATIVE HUMIDITY.....	78
TABLE IV.12. MICROCAPSULES' ACRONYMS AND EMULSION COMPOSITION.	79
TABLE IV.13. MASS LOSS (%) OF ENCAPSULATED IPDI (BY TGA), RELATIVE ENCAPSULATION YIELD (Y) CALCULATED USING THE FTIR SPECTRA OBTAINED AFTER THE SYNTHESIS AND 3 MONTHS LATER. THE Y3 IS GIVEN AS A PERCENTAGE OF Y1.....	82
TABLE IV. 14. STABILIZERS USED FOR THE O/W EMULSION STABILIZATION AND RESPECTIVE HLB AND MOLECULAR WEIGHT. 83	
TABLE IV.15. MICROCAPSULES' ACRONYMS AND EMULSION COMPOSITION	85
TABLE IV. 16. MAXIMUM VALUE (MODE) OBTAINED ON THE MCs' SIZE DISTRIBUTION HISTOGRAM.	89
TABLE IV. 17. MASS LOSS (%) OF ENCAPSULATED IPDI (BY TGA), RELATIVE ENCAPSULATION YIELD (Y) CALCULATED USING THE FTIR SPECTRA OBTAINED AFTER THE SYNTHESIS AND 3 MONTHS LATER. THE Y3 IS GIVEN AS A PERCENTAGE OF Y1.....	92
TABLE IV.18. MICROCAPSULES' ACRONYMS AND EMULSION COMPOSITION FOR THE PRE-SCALE-UP AND FOR THE SCALE-UP VOLUME.....	94
TABLE IV.19. RELATIVE ENCAPSULATION YIELD (Y VALUE) OF THE PRE-SCALE-UP_MCs AND OF THE SCALE-UP_MCs AS PREPARED.	98
TABLE IV. 20. STRATEGIES USED TO OPTIMIZE THE MCs' CHARACTERISTICS AND THE MAIN EFFECTS/CONCLUSIONS OF EACH STUDY.....	102
TABLE IV. S1. EMULSION STABILIZERS AND COMBINATIONS TESTED FOR THE MCs' SYNTHESIS BY INTERFACIAL POLYMERIZATION TECHNIQUE.....	112
TABLE IV. S2. OPTICAL MICROSCOPY PHOTOGRAPHS OF ALL THE EMULSIONS TESTED. LEFT: AFTER 10 MINUTES OF EMULSIFICATION AT 3200 RPM USING THE ULTRA-TURRAX; RIGHT: AFTER THE FOLLOWING 15 MINUTES UNDER MECHANICAL STIRRING AT 400 RPM (DYNAMIC CONDITIONS)	113

TABLE IV. S3. EDS ATOMIC CONCENTRATIONS OF THE DC_MCS FOR C, N, O AND SI ATOMS.....	117
TABLE V. 1. REAGENTS USED FOR THE PRODUCTION OF MCS BY THE SOLVENT EVAPORATION METHOD, RESPECTIVE COMMERCIAL NAME, PURITY AND MANUFACTURER.....	123
TABLE V. 2. POLYMERS USED FOR THE MCS' SHELL FORMATION BY THE SOLVENT EVAPORATION METHOD, ITS CHEMICAL STRUCTURE, DENSITY, MELTING POINT AND NUMBER AVERAGE MOLECULAR WEIGHT.	123
TABLE V.3. PROCESS PARAMETERS, FROM THE MCS PRODUCTION BY THE SOLVENT EVAPORATION METHODS, THAT WERE OPTIMIZED AND RESPECTIVE RANGE VALUES.	129
TABLE V. 4. MICROCAPSULES' ACRONYMS AND EMULSION COMPOSITION	131
TABLE V.5. MCS' AVERAGE SHELL THICKNESS (S) AS WELL AS THE MCS' DIAMETER (D) AND S/D RATIO	135
TABLE V.6. RELATIVE ENCAPSULATION YIELD (Y) AND MASS LOSS (%) OF ENCAPSULATED IPDI FOR EACH EXPERIMENT	140
TABLE V.7. SELECTED INDEPENDENT VARIABLES AND RESPECTIVE RANGES	147
TABLE V. 8. PROPOSED EXPERIMENTS, BY THE DOE SOFTWARE, AND RESPECTIVE EXPERIMENTAL AND PREDICTED RESPONSES.	148
TABLE V. 9. RESULTS OF THE MULTIPLE REGRESSION ANALYSIS.	151
TABLE V.10. COEFFICIENTS OF MODEL #2 AND ITS STATISTICAL SIGNIFICANCE.	152
TABLE V. 11. EXPERIMENTAL RUNS FOR VALIDATION OF THE MODEL AND RESPECTIVE PREDICTED AND EXPERIMENTAL RESULTS.	154
TABLE V.12. N7, N15 AND I_45MCS AVERAGE DIAMETER (D), SIZE DISTRIBUTION MODE AND S/D RATIO.	156
TABLE V.13. RELATIVE ENCAPSULATION YIELD (Y VALUE) AND MASS LOSS (%) OF ENCAPSULATED IPDI FOR THE N7_MCS AND N15_MCS, AS PREPARED AND AGED BY 3 MONTHS (AT ROOM TEMPERATURE AND 60WT% OF RELATIVE HUMIDITY).	158
TABLE V.14. OPTIMIZED PARAMETERS FOR THE PHB MCS PRODUCTION, AND STUDIED RANGE OF VALUES.....	160
TABLE V. 15. MASS LOSS (%) OF ENCAPSULATED IPDI FOR THE AS-PREPARED PHB MCS OBTAINED WITH 5, 8 AND 10 WT% OF DISSOLVED POLYMER IN THE O PHASE OF THE EMULSION, AS WELL AS FOR THE AGED MCS (BY 3 MONTHS AT ROOM TEMPERATURE AND 60WT% OF RELATIVE HUMIDITY).....	166
TABLE V.16. OPTIMIZED VALUES FOR THE REACTIONAL PARAMETERS TO PRODUCE PHB MCS.....	166
TABLE V.17. MICROCAPSULES' ACRONYMS AND EMULSION COMPOSITION.	167
TABLE V.18 MASS LOSS (%) OF ENCAPSULATED IPDI, BY TGA AND RELATIVE ENCAPSULATION YIELD (Y VALUE) OF THE AS- PREPARED MCS AND AGED BY 3 MONTHS (AT ROOM TEMPERATURE AND 60WT% OF RELATIVE HUMIDITY).	170
TABLE V.19. MICROCAPSULES' ACRONYMS AND EMULSION COMPOSITION.	171
TABLE V.20. MASS LOSS (%) OF ENCAPSULATED IPDI, BY TGA, RELATIVE ENCAPSULATION YIELD (Y VALUE) AND S/D RATIO FOR THE AS-PREPARED PRE-SCALE-UP_MCS AND SCALE-UP_MCS.....	175
TABLE V. S1. GPC RESULTS FOR THE PCL POLYMERS WITH 45000 DA AND 80000 DA AND FOR THE I_45 AND I_80 MCS' SHELL.	187
TABLE V. S2. PRELIMINARY PEELING STRENGTH TEST RESULTS OF ADHESIVE BONDS ADHERED USING THE I_45 AND I_80 MCS AS CROSS-LINKERS.....	188
TABLE V. S3. COEFFICIENTS OF MODEL #1 AND ITS STATISTICAL SIGNIFICANCE.....	189
TABLE VI.1. PU AND PCP PRE-POLYMERS, AS WELL AS ISOCYANATE CROSS-LINKERS (TO BE ENCAPSULATED AND BENCHMARK) USED IN THE DEVELOPMENT OF THE NEW ADHESIVE FORMULATION.	196
TABLE VI.2. SOLVENTS USED TO TEST THE CHEMICAL RESISTANCE OF THE DEVELOPED MCS, THEIR PURITY AND MANUFACTURER.	199
TABLE VI.3. PEEL STRENGTH TEST RESULTS OBTAINED FOR THE IPDI, ONGRONAT®2500 AND RESPECTIVE BENCHMARKS, AT 2.5 WT%, IN BOTH THE PU AND PCP PRE-POLYMERS.	204
TABLE VI. 4. RESULTS OBTAINED IN THE CREEP TESTS FOR SUBSTRATES ADHERED WITH THE PRE-POLYMER AND ADHESIVE FORMULATIONS CONTAINING SUPRASEC®2234 AND IPDI AS CROSSLINKERS, AS WELL AS MCS WITH THE ENCAPSULATED ISOCYANATES, USING CIPRENE® 2000 AS PRE-POLYMER.....	206

TABLE VI.5. RESULTS OBTAINED IN THE CREEP TESTS FOR SUBSTRATES ADHERED WITH A PRE-POLYMER AND ADHESIVE FORMULATIONS CONTAINING DESMODUR®RC AND IPDI AS CROSSLINKERS, AS WELL AS PCL AND PHB MCS CONTAINING THE LAST, USING PLASTIK®6275 AS PRE-POLYMER.	212
TABLE VI.6. RESULTS OBTAINED IN THE CREEP TESTS FOR SUBSTRATES ADHERED WITH A PRE-POLYMER AND ADHESIVE FORMULATIONS CONTAINING SUPRASEC®2234 AND IPDI AS CROSSLINKERS, AS WELL AS PCL AND PHB MCS CONTAINING THE LAST, USING CIPRENE®2000 AS PRE-POLYMER.....	212
TABLE VII. 1. RANGE OF VALUES FOR THE STUDIED REACTIONAL PARAMETERS THAT ALLOW TO OBTAIN SATISFACTORY MCS BY INTERFACIAL POLYMERIZATION TECHNIQUE.	224
TABLE VII. 2. RANGE OF VALUES FOR THE STUDIED REACTIONAL PARAMETERS THAT ALLOW TO OBTAIN SATISFACTORY MCS BY THE SOLVENT EVAPORATION TECHNIQUE, USING PCL AS SHELL FORMING POLYMER.....	226
TABLE VII. 3. RANGE OF VALUES FOR THE STUDIED REACTIONAL PARAMETERS THAT ALLOW TO OBTAIN SATISFACTORY MCS BY THE SOLVENT EVAPORATION TECHNIQUE, USING PCL AS SHELL FORMING POLYMER.....	227
TABLE VII. 4. PEEL STRENGTH AND CREEP TEST RESULTS OBTAINED WITH ADHESIVE FORMULATIONS COMPOSED BY THE CIPRENE®2000 PRE-POLYMER AND THE OPTIMIZED MCS' CONCENTRATION, FOR EACH TYPE OF MCS.....	228
TABLE VII. 5. PEEL STRENGTH AND CREEP TEST RESULTS OBTAINED WITH ADHESIVE FORMULATIONS COMPOSED BY THE PLASTIK®6275 PRE-POLYMER AND THE OPTIMIZED MCS' CONCENTRATION, FOR EACH TYPE OF MCS.	228
TABLE VII.6. ADVANTAGES AND DISADVANTAGES OF EACH MCS' PRODUCTION METHOD AND OF THE RESPECTIVE MCS CHARACTERISTICS.....	230

Abbreviations and acronyms

BGE - 1-butyl glycidyl ether
BSA - Bovine serum albumin

CCD - Central composite design
CCF - Central composite face design
CI - Creaming index
CTAB- Cetrimonium bromide

DBTL - Dibutyltin dilaurate
DETA - Diethylenetriamine
DGEBPA - Diglycidyl ether of bisphenol A
DOE - Design of experiment
DSC - Differential scanning calorimetry
DTG - Derivative thermogravimetry
EDS - Energy Dispersive X-ray Spectroscopy

FTIR - Fourier transform infrared spectroscopy
F-value - Fischer test value

GA - Gum arabic
GPC - Gel permeation chromatography

H - Hydrogen
HDI - Hexamethylene diisocyanate
HLB - Hydrophilic–lipophilic balance
HMDS - Hexamethyldisilazane

IPDI - Isophorone diisocyanate

MCs - Microcapsules
MDI - Methylene diphenyl diisocyanate
MPAN - Multi-polyaniline
MF - Melamine formaldehyde
MW - Molecular weight

n-OTES - n-octyl triethoxysilane

O/W - Oil-in-water
O - Oil

PAPI - Polymethylene polyphenyl isocyanate
PEA - Polyether amine
PEI - Polyethylenimine
PCL - Polycaprolactone
PCP - Polychloroprene
PHA - Polyhydroxyalkanoate (PHA)
PHB - Polyhydroxybutyrate

PLA - Polylactic acid
PLGA – Poly (lactic-co-glycolic acid)
PMMA – Poly (methyl methacrylate)
PU - Polyurethane
PUa - Polyurea
PUF – Poly (urea formaldehyde)
PVA - Polyvinyl alcohol
PVP - Polyvinylpyrrolidone

REACH - Registration, Evaluation, Authorization and Restriction of Chemicals
rpm - Rotations per minute
RSM - Response surface methodology

SBS - Styrene–butadiene–styrene
SBR - Styrene–butadiene rubber
SDBS – Sodium Dodecyl benzene sulfonate
SDS - Sodium dodecyl sulfate
SEM - Scanning Electron Microscopy
SIS – Styrene-isoprene-styrene

TDI - Toluene 2,4-diisocyanate
TETA – Triethylenetetramine
TGA - Thermogravimetric Analysis
THF - Tetrahydrofuran

S/D - Shell thickness to MC's diameter

UF - Urea formaldehyde
UV-Vis - Ultraviolet-visible

VOCs - Volatile organic compounds

W - Water
W/O - Water-in-oil
W/O/W - Water-in-oil-in-water

Y value – Relative encapsulation Yield

1K – One-component
2K - Two-component

Chapter I

Introduction to the thesis

Chapter I - Introduction to the thesis

Research motivation

The market size for adhesives and sealants is projected to grow from 67.64 thousand million euros in 2021 to 81.28 thousand millions euros in 2026 [1]. The increase demand for adhesives is mainly related with its use in the medical industry, building and construction, and growth in the appliances industry [1]. However, adhesives are used in a wide variety of industries and applications as in the automobile, footwear, aeronautics, furniture, among others. Particularly, in the footwear industry there is a high requirement for adhesives as the industry depends on the assembly of the various components used for the shoes manufacture, for which different adhesives are used [2, 3]. The adhesive joint performance depends on several factors, including the joint design, the surface treatments, the type of adhesive and the type of substrate material to joint [2, 3]. The joining of the upper-to-sole joints is the most requiring process in footwear manufacturing as it demands a high bond strength. PCP and PU adhesives are the main adhesives used for this type of joints due to their high versatility and capability to join a wide range of materials, associated with their high strength resistance. PCP adhesives show good results with leather, textiles, vulcanized rubbers, among others. However, the increased use of plasticizers in plastic materials made it necessary to introduce the use of PU adhesives, which have a higher versatility and performance than PCP [2-5]. Both PCP and PU adhesives are currently supplied as two-component (2K) formulations, one a pre-polymer and the other a cross-linking agent, usually isocyanate-based. Although both adhesives can be used as one component (1k) adhesive (pre-polymer) the addition of a cross-linker can improve the final characteristics of the adhesive joint. PCP adhesives are limited by their poor heat resistance and bond strength, but by adding an isocyanate-based cross-linker it is possible to improve its thermal stability and cohesive strength, and, in many cases, it significantly increases the adhesion to certain substrates [2, 5]. Regarding PU adhesives, the addition of an isocyanate cross-linker highly increases the adhesive joint durability [2].

However, isocyanates have a high toxicity which is a primary concern when applied to adhesives. Isocyanates are powerful irritants, mainly affecting the mucous membranes of eyes, respiratory and gastrointestinal tracts as well as skin inflammation, when in direct contact, and its prolonged exposure can lead to severe asthma attacks and even death [6]. To prevent health hazards, on February 2020, the REACH committee approved the European Commission's proposal for a restriction on diisocyanates. The Restriction, which applies from 24 August 2023, prohibits the

commercialization of diisocyanates as substances on their own and as a constituent in other substances or in mixtures for industrial and professional use when in concentrations above 0.1% wt [7].

The incorporation of isocyanate cross-linkers is essential in the footwear industry to provide a strong and long-lasting adhesive formulation fitter to the upper-to-sole joint, at concentrations well above 0.1wt% in the adhesive formulation. The footwear industry is one of the most important sectors of the Portuguese economy, globally recognized for its high-quality products. Accordingly, it is important to maintain the quality of its products and, at the same time, respecting the new regulations.

With this thesis, in collaboration with Cipade, S.A., an adhesive producer/supplier, it is intended to develop a new PU and PCP adhesive formulation for the footwear industry in which the cross-linkers are polymeric MCs containing the isocyanate species, crucial for the required high-quality adhesive joints. By protecting the isocyanate inside a polymeric MC, its direct contact with the operator is avoided. The isocyanate is only to be released during the joint preparation, by melting, due to the effect of temperature (up to 70°C), by breaking, due to the effect of pressure (4kg/cm²), or a combination of both. The new adhesive could be supplied as 1K, in which the MCs and the pre-polymer are mixed or as a 2K adhesive with both components being supplied separately. The schematical representation of the adhesion process with the 1K formulation, containing the MCs as cross-linkers, is depicted in Figure I. 1.

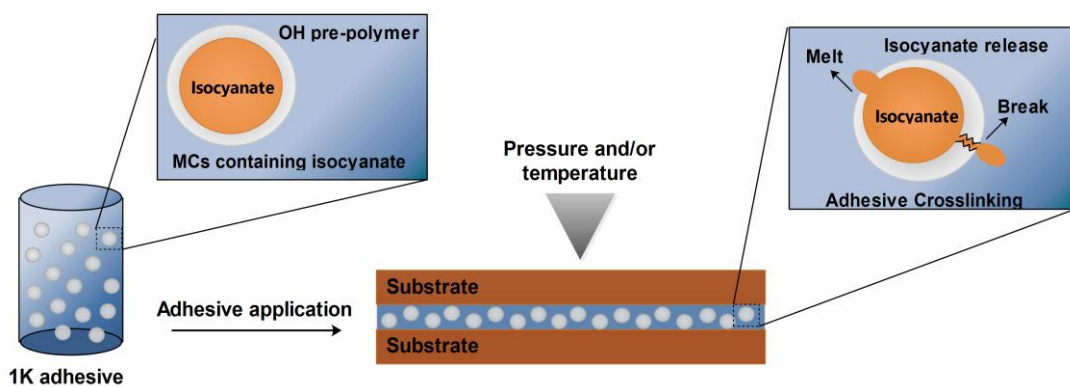


Figure I. 1. Schematic representation of the adhesion process using the 1K adhesive formulation containing MCs as cross-linkers.

Encapsulation is an evolving area with a significant importance in many industrial sectors as for example pharmaceutical, agrochemical, cosmetics, among others, with the MCs serving as storage, carrier and protector, of the encapsulated content, from the environment [8]. For this

application the MCs serve as storage as well as a protector avoiding the reaction of the isocyanates with the exterior environment, until the stimuli of pressure and/or temperature is applied during the adhesive joint preparation. It is mandatory that the encapsulated isocyanate does not contact the pre-polymer before the adhesive application (for 1K adhesive formulations) or does not react with the air moisture than could eventually penetrate the MCs' shell (for 2K adhesive formulations). The major challenge of this thesis regards the development of suitable MCs, capable to encapsulate a satisfactory amount of isocyanate content, of at least 40% of the MCs total weight, at the same time offering an adequate protection from the environment, during a period of at least 3 months, and efficiently responding to the stimuli applied during the adhesive joint preparation, leading to the isocyanate release and its reaction, establishing cross-linking points within the adhesive joint, at the desired moment.

Cipade S.A.- Industry and research of adhesive products

Cipade is a company that produces a complete range of products in all types of industrial glues for different industry sectors, such as footwear, wood, leather goods, building industry, automotive, paper, among others. The company started in 1968 and has been a certified company since 1995 under the ISO 9001, ISO 14001 and ISO 45001 standards. Cipade production is structured in three main production areas which are dry compounds (raw material) formulated for the production of solvent based glues, solvent based glues and water based glues. In parallel with the production activity, CIPADE devotes to research and development of adhesives. The company R&D activities are aimed at improving the performance of production processes, quality of manufactured products and product compatibility, to increase the company's competitive advantages in the market.

Objectives and main contributions

The aim of this thesis is to develop a solution to the 2K adhesives formulations used in the footwear industry, by avoiding the direct contact between the operator and the toxic isocyanate species, at the same time ensuring an identical performance to the adhesive formulations that are currently commercially available.

Therefore, the objectives of this thesis are:

- 1) Synthesis and development of polymeric MCs, containing encapsulated isocyanate species, with the necessary characteristics to be used as efficient cross-linkers for PU and PCP adhesives.

2) Experimental development and optimization of new adhesives formulations containing the polymeric MCs as cross-linkers. 3) Feasibility studies of the new adhesives at the CIPADE, S.A. using internal validation tests.

Organization of the dissertation

Chapter II contains the state of understanding regarding adhesive properties, its classification, and applications. The close relation between the adhesive and footwear industry is there clarified, as well as the details regarding the type of materials to adhere, difficulties encountered in the industry and the characterization tests and respective norms that usually apply.

Microencapsulation is presented as the solution to avoid the direct contact between the operators and the toxic isocyanate species during the adhesive application process. First, it is given a brief explanation on microencapsulation following with an in-depth discussion of the state of the art regarding isocyanate microencapsulation. The strategy used to obtain MCs with the desired final characteristics is disclosed, and more details are given regarding the use of interfacial polymerization and solvent evaporation microencapsulation techniques: method, state of the art, and finally advantages and limitation of each.

Chapter III regards the MCs characterization techniques and respective test conditions.

The synthesis of MCs by interfacial polymerization in combination with a microemulsion system is addressed in Chapter IV. This chapter includes the optimization of the microemulsion stabilization, for which different emulsion stabilizers and combinations between them were tested, the effect of some parameters, as duration of the synthesis and isocyanates combinations used, as well as which active H sources lead to the most satisfying MCs.

Chapter V regards the production of MCs by the solvent evaporation technique in combination with a microemulsion system. It includes a discussion on the polymers used for the shell formation, the effect of their molecular weight on the MCs characteristics, and the results of a design of experiment study with the aim of controlling the MCs size and size distribution.

Finally, in chapter VI, the development and characterization of the new adhesive, containing the MCs are addressed. The cross-linking effect of each isocyanate in both the PU and PCP pre-polymer is studied, followed by the optimization of the MCs' percentage in the formulation. A conclusion on the most suitable MCs for this application is given, regarding the isocyanate type and polymeric shell composition. Lastly, Chapter VII presents a summary of the thesis together with main conclusions of this work.

List of contributions

Papers (related to the thesis)

- **Loureiro, M.V.**; Aguiar, A.; Santos, R. G.; Bordado, J.C.; Pinto, I.; Marques, A.C. “Design of Experiment for Optimizing Microencapsulation by the Solvent Evaporation Technique”, *Polymers* 16 (2024) 111. DOI: doi.org/10.3390/polym16010111
- **Loureiro, M. V.**; Mariquito, A.; Vale, M.; Bordado, J. C.; Pinho, I.; Marques, A. C. “Emulsion Stabilization Strategies for Tailored Isocyanate Microcapsules”, *Polymers* 15 (2023) 403. Doi: 10.3390/polym15020403
- **Loureiro, M. V.**, Vale, M., Galhano, R.; Matos, S.; Bordado, J. C.; Pinho, I., Marques, A. C. “Microencapsulation of Isocyanate in Biodegradable Poly(ϵ -caprolactone) Capsules and Application in Monocomponent Green Adhesives”, *ACS Applied Polymer Materials* 2 (2020) 4425–4438. Doi: 10.1021/acsapm.0c00535
- **Loureiro, M. V.**; Attaei, M.; Rocha, S.; Vale, M.; Bordado, J. C.; Simões, R.; Pinho, I.; Marques, A. C. “The role played by different active hydrogen sources in the microencapsulation of a commercial oligomeric diisocyanate”, *Journal of Materials Science* 55 (2020) 4607–4623. DOI: doi.org/10.1007/s10853-019-04301-1
- **Loureiro, M.V.**; Bordado, J.C.; Galhano, R.; Gonçalves, D.; Pinto, I.; Marques, A.C. “Bioderived and biodegradable polyhydroxybutyrate for the isocyanate microencapsulation to develop of a new adhesive cross-linker”. *In preparation*.

Papers (Collaborations)

- António, A.; **Loureiro, M. V.**; Pinho, I.; Marques, A. C. “Efficient encapsulation of isocyanates in PCL/PLA biodegradable microcapsules for adhesives”, *Journal of Materials Science* 58 (2023) 2249–2267. Doi: 10.1007/s10853-023-08160-9
- Costa, M.; Pinho, I.; **Loureiro, M. V.**; Marques, A. C.; Simões, C. L.; Simões, R.; “Optimization of a microfluidic process to encapsulate isocyanate for autoreactive and ecological adhesives”, *Polymer Bulletin* 79 (2022) 3951–3970. Doi: 10.1007/s00289-021-03690-1
- Costa, M.; Pinho, I.; **Loureiro, M. V.**; Marques, A. C.; Simões, C. L.; Simões, R.; “Optimization of a microfluidic process to encapsulate isocyanate for autoreactive and ecological adhesives”, *Polymer Bulletin* 79 (2022) 3951–3970. Doi: 10.1007/s00289-021-03690-1
- Costa, M.; Dias, J. P.; Pinho I.; **Loureiro, M. V.**; Marques, A. C.; Simões, R. “Development of a Microfluidic Device to Encapsulate Isocyanate for Autoreactive and Ecological Adhesives”, *IOP Conference Series: Materials Science and Engineering* 520 (2019) DOI: 10.1088/1757-899X/520/1/012007
- Attaei, M.; **Loureiro M. V.**; Vale, M.; Condeço, J.; Pinho, I.; Bordado J. C.; Marques, A. C., " Isophorone Diisocyanate (IPDI) Microencapsulation for Mono-Component Adhesives: Effect of the Active H and NCO Sources", *Polymers* 10 (2018) 825. DOI: 10.1016/j.micromeso.2016.10.039

Oral presentations

- **Mónica V. Loureiro**, António Aguiar, Isabel Pinho, João C. Bordado, Ana C. Marques, “Advances in isocyanate microencapsulation for new ecological and mono-component adhesives”, 2nd CERTBOND Training School - Sustainable Composite Bonded Joints, from the COST Action CA18120 “Reliable roadmap for certification of bonded primary structures”, 17-19 of October 2022, Guimarães, Portugal.
- **Mónica V. Loureiro**, António Aguiar, Isabel Pinho, João C. Bordado, Ana C. Marques, “Advances in isocyanate microencapsulation for new ecological and mono-component adhesives”, Junior Euromat 2022, 19-22 of July 2022, Coimbra, Portugal
- **Mónica V. Loureiro**, Sofia F. Rocha, Mahboobeh Attaei M, Mário Vale, Ricardo Simões, Mariana Costa, Isabel Pinho, João C. Bordado, Ana C. Marques, “Isocyanate Microcapsules For Composite One-Component Adhesives”, Twenty-Seventh Annual International Conference on Composites/Nano Engineering (ICCE-27), 14–20 of July 2019, Granada, Spain.
- **Mónica V. Loureiro**, Sofia F. Rocha, Mahboobeh Attaei, Mário Vale, Ricardo Simões, Mariana Costa, Isabel Pinho, João C. Bordado, Ana C. Marques, “Microencapsulation of highly reactive isocyanates for new ecological and mono-component adhesives”, XIX Congresso da Sociedade Portuguesa de Materiais and X International Symposium on Materials (MATERIAIS 2019), 14-17 of April 2019, Lisbon, Portugal.
- Mariana Costa, José P. Dias, Isabel Pinho, **Mónica V. Loureiro**, Ana C. Marques, Ricardo Simões, “Development of a microfluidic device to encapsulate isocyanate for autoreactive and ecological adhesives”, 4th International Conference on Mechanical, Manufacturing, Modeling and Mechatronics (IC4M 2019), 22-24 of February 2019, Nice, France.
- Mariana Costa, M. Osorio, Carla L. Simões, Isabel Pinho, **Mónica V. Loureiro**, A. Marques, Ricardo Simões, “Synthesis of novel autoreactive and ecological monocomponent adhesives for the shoe industry”, 9th International Conference on Biopolymers and Polymer Sciences, 19-21 of November 2018, Bucharest, Romania.
- Mariana Costa, M. Borges, Carla L. Simões, Isabel Pinho, **Mónica V. Loureiro**, Ana C. Marques, Ricardo Simões, “Development of a continuous method to produce autoreactive and ecological monocomponent adhesives”, Fifth International Symposium on Green Chemistry, Sustainable Development and Circular Economy, 30 of September to 3 of October, 2018, Skiathos, Greece.
- Ricardo Simoes, M. Borges, Mariana Costa, Carla L. Simões, Isabel Pinho, João C. Bordado, **Mónica V. Loureiro**, Ana C. Marques, “Development of novel autoreactive and ecological monocomponent adhesives”, 24th IUPAC Conference on Physical Organic Chemistry (ICPOC24), 1- 6 July 2018, Faro, Portugal.

Invited lectures and colloquia:

- “Polyurethane/Polyurea microcapsules as new crosslinkers for safer and high-performance adhesives (Ecobond)”, Workshop TPMI2023 - Technology Platform on Microencapsulation and Immobilization 2023, 8-12 May, Instituto Superior Técnico, Universidade de Lisboa, Portugal.
- “Fundamentals on microencapsulation by interfacial polymerization”, Workshop TPMI2023 - Technology Platform on Microencapsulation and Immobilization 2023, 8-12 May, Instituto Superior Técnico, Universidade de Lisboa, Portugal. “Isocyanate Microcapsules For Composite One-Component Adhesives”, COST Action CA18120-CERTBOND - Reliable roadmap for certification of bonded primary structures, Virtual Meeting, 12 of January 2021.
- “Encapsulation of isocyanate by a biodegradable polymer for eco-innovative adhesives”, CERENA Seminar - Sustainable Innovation, 17 of February 2020.

Posters in Conferences

- Mónica V. Loureiro, António Aguiar, Isabel Pinho, João C. Bordado, Ana C. Marques. “Isocyanate microencapsulation for one-component, self-reactive and eco-innovative adhesives”, Encontro Ciência 2022, 16-18 of May, Lisbon, Portugal.
- Ana C. Marques, Mário Vale, Mónica V. Loureiro, Elisabete Silva, João C. Bordado, Elena Tervoort, Murielle Schreck, Markus Niederberger, “Porous Microspheres for Chemical Immobilization”, 20th International Sol-Gel Conference, 25-30 of August 2019, St. Petersburg, Russia.
- Mahboobeh Attaei, Mónica V. Loureiro, Mário Vale, João C. Bordado, Isabel Pinho, Ana C. Marques, “Isocyanate Microencapsulation: New Crosslinking Strategy for One Component, Self-Reactive and Eco-Innovative Adhesives”, Polymers: Design, Function and Application, 21-23 of March 2018, Barcelona, Spain.

Patents

- Ana C. Marques, Mónica V. Loureiro, Sofia F. Rocha, Mahboobeh Attaei, João C. Bordado, Isabel Pinho, CIPADE S.A., “Microencapsulation of highly reactive isocyanate species” “Microencapsulação de espécies de isocianato altamente reativas”, Publication reference PT 115312 A. (Filing date: 14/02/2019; Publication date 09/09/2020); **PATENT GRANTED**: 2021.07.16; Publication: 2021.07.21 - PT 115312 B

Bibliography

- 1 *Adhesives & Sealants Market by Adhesive Formulating Technology (Water-based, Solvent-based, Hot-melt, Reactive), Sealant Resin Type (Silicone, Polyurethane, Plastisol, Emulsion, Polysulfide, Butyl), Application, Region - Global Forecast to 2026. 2022*; Available from: <https://www.marketsandmarkets.com/Market-Reports/adhesive-sealants-market-421.html>.
- 2 Orgilés-Calpena, E.;Arán-Ais, F.;Torró-Palau, A. M.;Sánchez, M., *Adhesives in the Footwear Industry: A Critical Review*. *Reviews of Adhesion and Adhesives*, **2019**, 7, 69-91.
- 3 Paiva, R. M. M.;Marques, E. A. S.;da Silva, L. F. M.;António, C. A. C.;Arán-Ais, F., *Adhesives in the footwear industry*. *Proceedings of the Institution of Mechanical Engineers, Part L: Journal of Materials: Design and Applications*, **2015**, 230, 357-374.
- 4 Associação Portuguesa dos Industriais de Calçado, Componentes, Artigos de Pele e seus Sucedâneos. *Facts and Numbers Portuguese Shoes 2023*. Available from: <https://www.apiccaps.pt/publications/facts--numbers/126.html>.
- 5 Adhesives & Sealants Industry. *Polychloroprene Contact Adhesives. Water-Based Systems Make Inroads Into Traditional Solvent-Borne Technology*. Available from: <https://www.adhesivesmag.com/articles/85273-polychloroprene-contact-adhesives>.
- 6 Centers for Disease Control and Prevention. The National Institute for Occupational Safety and Health. *Isocyanates. Overview. 2008*; Available from: <https://www.cdc.gov/niosh/topics/isocyanates/default.html>.
- 7 ECHA - European Chemicals Agency. *ECHA - Annex XVII to REACH - Conditions of Restriction. Restrictions on the Manufacture, Placing on the Market and Use of Certain Dangerous Substances, Mixtures and Articles*. Available from: <https://echa.europa.eu/documents/10162/503ac424-3bcb-137b-9247-09e41eb6dd5a>.
- 8 Mishra, M., *Handbook of Encapsulation and Controlled Release. 2015*, Boca Raton: CRC Press.

Chapter II

State of Understanding

Chapter II - State of understanding

II.1 Adhesives

Adhesives, when applied between the surfaces of same or dissimilar materials, are used to hold, fasten, or bond them together [1, 2]. Adhesives have been increasingly used as they are cost-efficient, of simple and fast application, allow a homogeneous stress distribution between the bonded surfaces, can produce suitable joints for a wide range of mechanical loads, and can efficiently bond a variety of substrates, such as metals, alloys, composites, and natural materials [1-3]. Adhesives are an increasingly used alternative to mechanical joining methods, such as rivets, providing several advantages over conventional mechanical fasteners as for example its superior fatigue strength, homogeneous stress distribution, flexibility, resistance to corrosion, to damage and its low structural weight [1-3]. However, due to their organic nature, they have the disadvantage of its mechanical properties to be influenced by environmental factors such as moisture absorption, temperature, joining process and curing cycle parameters. Also, the bonded joint is considered permanent as it is very difficult to disassemble without suffering irreparable damages [2, 3]. Adhesives have been used in a large variety of applications, but it is estimated that over 20% are used for building and construction [1, 4]. Another emergent area of interest for adhesives refers to its application in lightweight composite structures, although both mechanical fasteners and adhesives can be used. Composites used in aircraft are usually joined by a combination of both methods while the composites used in automobiles are often joined only with adhesives [2, 5]. There are five main primary mechanisms that contribute to the development of an efficient adhesive bond, which are classified as mechanical adhesion, adsorption and wetting, chemical bonding, diffusion, and electrostatic adhesion. By mechanical adhesion, the bonding can be expected to be purely from the mechanical interlocking of the adhesive in both substrates, occurring only on a microscopic level. For this case, the adhesion properties are related with the adhesive viscosity, the geometry of the substrate pores, the counterpressure of the gas enclosed in the pore, the surface tension of the substrate, its wetting properties, and the degree of roughness of the substrates, with the shear strength increasing significantly with the increase of roughness [5]. The adhesive fills the pores, cracks, and indentations in the substrate surface, resulting in a mechanical anchoring once the adhesive has hardened [5]. In which regards the adsorption and wetting interaction, they occur due to the action of interatomic and intermolecular forces, as van der Waal forces, between adhesive and substrate. Although these are the weakest of all intermolecular forces, their contribution to the strength of the adhesive joints is significant [5-7]. Chemical bonding occurs by the reaction

between a functional group of the substrate and the adhesive. The substrates to adhere are usually subject to surface treatments to create compatible groups to promote the formation of strong covalent or hydrogen bonds [5, 7]. By diffusion the adhesion occurs through the interdiffusion of molecules between the adhesive and the substrate. This type of adhesion is particularly important when both the adhesive and substrate are polymers with relatively long-chain molecules capable of movement. Finally, electrostatic adhesion takes place through attraction between moieties from charged or ionized surfaces, with different electrical potentials [8]. The schematical representation of each mechanism of adhesive bonding are represented in Figure II.1

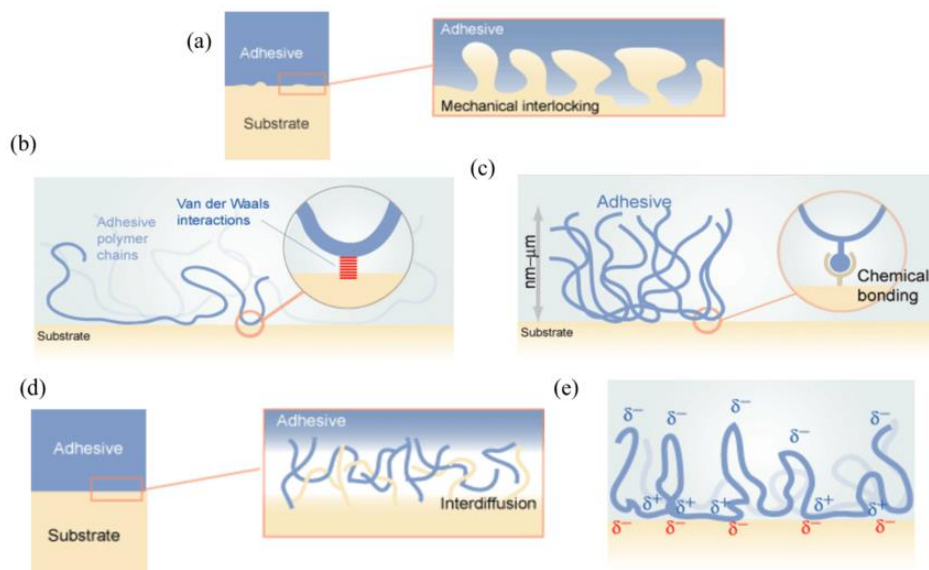


Figure II.1. Schematic representation of the adhesive bonding mechanisms: (a) mechanical interlocking; (b) by interatomic and intermolecular forces; (c) chemical bonding; (d) interdiffusion; (e) electrostatic adhesion. Image reprinted from [9], with permission.

There is a large variety of adhesives, which can be classified according to Table II.1.

Table II.1 Adhesive classification. Adapted from [10].

Group	Type
Animal	Gelatina; Casein; Albumen
Vegetable	Starch; Cellulose acetate; Cellulose nitrate
Mineral	Asphalt/Bitumen
Elastomeric	Natural rubber; SBR; Nitrile rubber; Polyurethane rubber; Silicone rubber
Thermoplastic	PVA; Polystyrene; Cyanoacrylates; liquid acrylic
Thermosetting	Phenol-formaldehyde; Urea-formaldehyde; Unsaturated polyesters; Epoxy resins; Polyurethane

There has been an increased use of adhesive bonding in all industries, with the diversity of substrates and the continuous development and introduction of new processes and materials contributing to its increasing market [1]. The use of the light weight composite structures in a variety of applications as in aeronautical, aerospace, and automotive industries, has also contributed to its increase [2, 4]. It is projected for the adhesives and sealants market to grow from 67.64 thousand million euros in 2021 to 81.28 thousand million euros in 2026 [2, 4].

II.1.1 Adhesives in the footwear industry

The footwear and adhesive industry are in close association as adhesives are essential to join the several materials employed in the shoe manufacture [11-13]. A wide range of materials is used in this industry as for example synthetic leather, plastics materials, rubber and synthetic fibers [11, 13]. Different types of adhesives are applied for the shoe manufacture, depending on the materials to be joint, which will influence the application method, surface treatment, drying time, and adhesive hazard classification [14]. The upper-to-sole joint, which refers to the joint between the upper shoe and its sole, is the one with higher technical requirements in this industry, as it demands a high bond strength [13]. There are several methods that can be used to assemble the upper shoe with the sole, including by welding, molding, when pre-formed as units, or adhered [13]. When using adhesives, it is recommended, independently of the materials to be used, that the adhesive joint follows the standard EN 15307 regarding the

minimum strength values, in the peel strength test, for the bonding of the upper-to-sole joint (Table II.2).

Table II.2 Minimum upper-sole bond strength requirements in the footwear industry according to the standard EN 15307. Adapted from [13] and [15].

Shoes	Peel Strength per unit width (upper/sole)*
Class A: Low stress when in use: Infants footwear, indoor footwear, fashion footwear	≥ 2.5 N/mm
Class B: Medium stress when in use: Town footwear, cold weather footwear, casual footwear	≥ 3.0 N/mm, or ≥ 5.5 N/mm with material failure
Class C: High stress when in use: Children footwear, general sports footwear	≥ 4.0 N/mm, or ≥ 3.0 N/mm with material failure
Class D: Very high stress when in use: Mountain footwear	≥ 5.0 N/mm, or ≥ 3.5 N/mm with material failure

* Peel strength per unit width after a 4-day storage in standard atmosphere of 23°C and 50% of relative humidity.

II.1.1.1 Adhesives for the upper-to-sole joints

Nitrocellulose adhesives were among the first to be introduced in the footwear industry, at 1906, which were posteriorly replaced by PCP in 1949. PCP adhesives showed an increased versatility, being good to use with leather, textiles, and vulcanized rubbers [12, 13]. However, the introduction of plastic materials, containing plasticizers, made it necessary to introduce adhesives based on thermoplastic PU in 1970. Regarding the upper-to-sole joints, the solvent-based PCP and PU contact adhesives are the most currently used adhesives, as they are the ones that can guarantee high demanding strength resistance joints. The bonding strengths obtained with the PCP and PU adhesives are similar, the main differences lying in the adequate substrates for each adhesive and the open time, which is longer for the PCP. As for the other parts of the shoe, styrene–isoprene–styrene (SIS), styrene–butadiene–styrene (SBS), styrene–butadiene rubber (SBR) latex and hotmelt (polyamide, EVA based), are the most used [13, 16, 17]. PU adhesives are characterized by their flexibility and performance at low temperatures, excellent adhesion and cohesion strength, and a rapid curing, forming covalent bonds when the substrates have active hydrogen atoms in the surface [13, 16, 18]. PCP adhesives have a chlorine atom in each monomer of the polymer which provides a strong polarity and enables the

development of physical interactions with the substrate. This type of adhesives has a high initial bond strength and the ability to form bonds with minimum pressure during the substrate's assembly [13, 19, 20]. While PCP adhesives show good results with leather, textiles, vulcanized rubbers, among others, PU adhesives are essential to adhere plastic materials containing large quantities of plasticizers [15].

PU and PCP adhesives are both commercially available as 1K and 2K adhesives. 1K adhesives are supplied as one component which is responsible to form the adhesive joint usually by the effect of pressure [21, 22]. 2K adhesive formulations are supplied as two components, one is an adhesive pre-polymer and the second a cross-linking compound, usually isocyanate-based, the two to be mixed during the adhesive application. The 2K adhesives have the advantage of having an accelerated cure, as well as an increased resistance to temperature and durability, due to the cross-linking effect by isocyanates [13, 14, 17].

II.1.1.2 Joint preparation in the footwear industry

The type of materials to be joint and the model of the shoe are the two main factors to have in consideration for the selection of the most suitable method to use. The model of the shoe dictates the joining method, which can be by adhesion, stitching or a combination of both. The type of substrate dictates the type of adhesive to use and the necessity or not to apply a surface treatment before the application [12, 14, 15]. There are four main types of surface treatments that can be applied to improve the final adhesion characteristics, which are the following: physical, chemical, primer, and solvent wiping [13]. Physical treatment regards the carding of the substrate by using sandpaper or abrasives, which increases the surface area, and the chemical treatment is used to change the polarity of the surface. An adhesive primer is usually a dilute solution of an adhesive in an organic solvent. Its application helps to optimize the adhesion, to improve the adhesive compatibility to the substrate or to modify certain characteristics of the joint, such as its peel. Finally, the solvent wiping is used to eliminate some agents present in the substrate surface that could lead to adhesion problems [13, 23-25]. As an example, leather has a porous nature that facilitates the adhesion, but it has a weak grain layer that must be firstly removed by roughening. In addition, for this case, it can be necessary to apply a primer, due to the presence of grease [15]. For the application of PU adhesives, after its application in both substrates, the solvents are let to dry for about 5 to 10 minutes, step after which the adhesive loses its tackiness. The adhesive must be subjected to an extra reactivation step, during which infrared radiation is applied during 2 to 6 seconds, leading to a surface

temperature between 55 to 80 °C, which allows the adhesive to soften and to have the necessary tackiness [17, 18]. Posteriorly, the two substrates are brought together and a pressure of 4 bar is applied for 5 seconds, the adhesive joint cools and the adhesive film dries in seconds [13]. Regarding the solvent-based PCP adhesive, it has a much longer open time which can range from a few minutes to hours, depending on the formulation. The dry adhesive film has tackiness at room temperature which avoids the need for the reactivation step [13, 14, 19]. PCP must be applied in both substrates to be bonded and allowed to dry for 15 to 20 minutes. After the solvent evaporation, a pressure of 4 bar must be applied during 5 seconds for the two substrates to be bonded [13].

II.1.1.3 Testing of the adhesive joints in the footwear industry

There are two main mechanical properties of relevance when evaluating adhesive joints in the footwear industry: peel strength, and creep strength [13]. In particular, the minimum strength test requirements for the upper-to-sole joint creep test must follow the EN 15307 requirements (Table II.2)[13, 15]. The peel strength test, in the footwear industry, must follow the standard EN 1392. For this, the test must be done 72 hours after the substrates bonding at a speed of 100 mm/min and using an angle of 180 °C, as depicted in Figure II.2 [26].

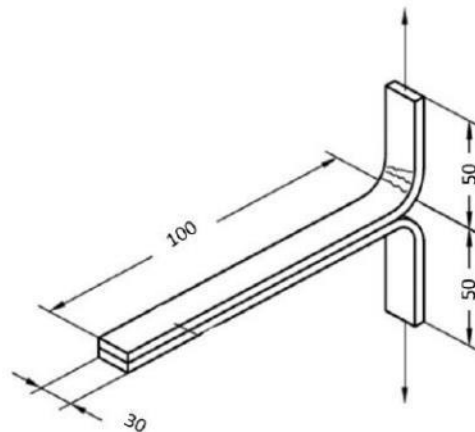


Figure II.2 Adhesive joint for peel test (dimensions in millimeters), following the EN 1392 [26]. Image reprinted from [13], with permission.

The peel strength is calculated by the ratio between the average force (Newton, N) and the average width (millimeter, mm) of the bonded joints. In addition, it is important to consider not only peel strength but also the type of failure, depicted in Figure II.3, which can provide useful information about the performance of the adhesive joint [27].

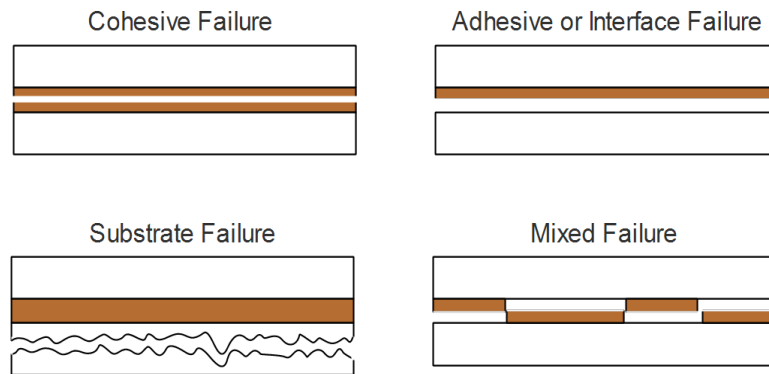


Figure II.3 Types of failure of an adhesive joint. Adapted from [27] and [28].

Adhesive failure occurs by delamination of the bonded layer, and it occurs due to an improper surface preparation, wrong adhesive selection or high peel stress. An improper surface preparation reduces the mechanical interlocking between adhesive and the substrate, while the selection of an inappropriate adhesive reduces its adhesion with the substrate [28]. Cohesive failure occurs at the adhesive, and it is due to a higher bonding strength between the adhesive and the substrate than its individual strength. Substrate failure occurs when the substrate fails before the adhesive. Cohesive failure or substrate failure is the preferred type of failure as the maximum strength of the joint has been reached [28, 29]. The creep strength allows to conclude regarding the resistance of the joint to the effect of temperature [13]. After the bonding of the substrates is complete, the specimen is subjected to 60 °C for 1h, after which it must be loaded with a constant weight of 1.5kg, as depicted in Figure II.4, for 10 minutes and the deformation of the specimen is measured in millimeters, while still loaded. After this analysis, the time necessary to obtain a complete separation is also determined [26].



Figure II.4. Adhesive joint for creep test following the EN 15307. Image reprinted from [13], with permission.

II.2 Isocyanates toxicity

Isocyanates are currently used in both PU and PCP 2K adhesives formulations, as cross-linkers. However, isocyanates are considered to have a high toxicity, which is a primary concern in the adhesive application. Isocyanates can be powerful irritants, leading to skin inflammation and affecting mucous membranes, as eyes, respiratory and gastrointestinal tracts [30]. It is also suspected that a prolonged exposure to isocyanates can cause cancer and severe damage to organs [31]. For these reasons, the REACH regulation approved, in February 2020, the European Commission's proposal for restricting the use/commercialization of diisocyanates. According to Annex XVII of REACH (Council Directive 76/769/EEC of the European Union), from August 2023 diisocyanates cannot be placed on the market as substances on their own, as a constituent in other substances or in mixtures for industrial and professional use(s), i.e. to be used by any worker or self-employed worker, in concentrations above 0.1% by weight [31]. From August 2023, it should not be used unless it is in a concentration lower than 0.1% or if guaranteed that the industrial or professional user(s) have successfully completed training on the safe use of diisocyanates [31]. In the footwear industry, the adhesives used contain free diisocyanate in amounts well above 0.1% (m/m), as these are the amounts that enable to meet the demands of the adhesive joints in this sector. Thus, an adaptation, not only from the adhesive industry but other sectors, will be necessary to offer new products which are in accordance with the new regulations and those to come, at the same time guarantying the same quality of the products.

II.3 Microencapsulation

Microencapsulation is the process of enclosing solids or droplets of liquids or gases inside a second polymeric or inorganic material [32-34]. The process of encapsulation dates from 1930s, when Barrett Green, an employee of the National Cash Register Company, started to work on

encapsulation of a dye-precursor in gelatin spheres, by the coacervation technique, to develop a new typing paper. The process of a liquid microencapsulation was later patented, in 1955 [35]. The process of encapsulation developed by Barrett Green was the foundation for the development and application of MCs in various industries as pharmaceuticals, foods, cosmetics, nutritional supplements, agricultural, detergents, among others [35].

MCs are composed by two parts, the surrounding material which is usually referred as “shell” and the encapsulated material, referred as “core”. Microencapsulation is gaining importance in several industrial sectors as they serve various purposes, including i) protection of the encapsulated materials from detrimental conditions (increased stability); ii) separation of incompatible components iii) promotion of an easier handling iv) control of the moment at which the encapsulated compound is released v) control of the release profile of the core material vi) control of the release of different encapsulated materials [32, 34, 36]. According to their morphology, MCs can be classified as matrix-type or microspheres, mononuclear or core-shell, and polynuclear MCs [37]. Representations of the referred morphologies are depicted in Figure II.5.

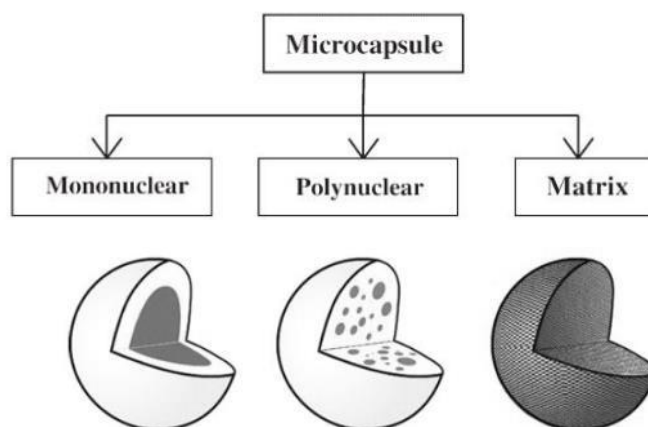


Figure II.5. Schematic representation of the different MCs morphology, a) matrix-type microcapsule or microsphere b) mononuclear microcapsule or core-shell c) poly-nuclear microcapsules. The MCs shell is represented at white. Image reprinted from [38], with permission.

Matrix-type MCs or microspheres are characterized for having the core homogeneously integrated within the matrix of the shell material, as for the mononuclear or core-shell MCs they are characterized by having a single core, surrounded by the shell or multiple layers of shell, lastly the polynuclear MCs have several different sized cores enclosed within the shell [36, 39]. There are different mechanisms by which the MCs can release its encapsulated content, which

can provide controlled, sustained, or targeted release of core material. The most common mechanisms are by diffusion of the core through the shell, by mechanical rupture, dissolution, and melting/fusion of the shell, as depicted in Figure II. 6 [36, 38, 40]. Although less common, biodegradation can also lead to the release of the core material [36].

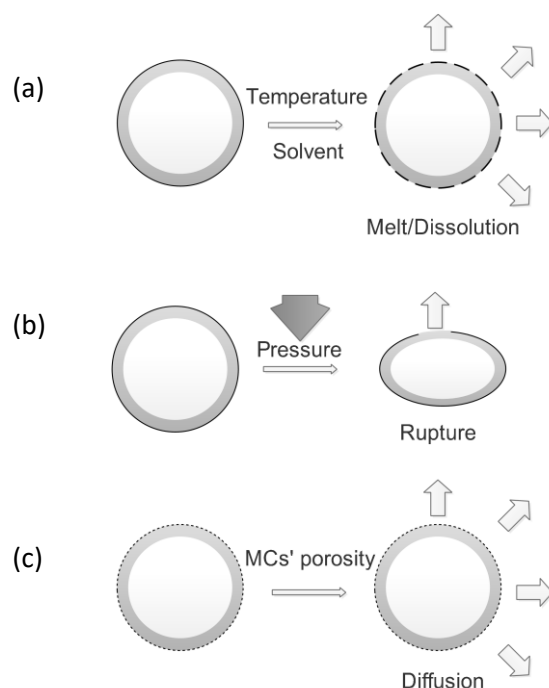


Figure II. 6. Representation of the MCs' release mechanisms: (a) By the effect of temperature (melt) or solvent dissolution; (b) pressure (rupture); (c) through the MCs' shell porosity (diffusion).

The release profile can be controlled by the MCs' characteristics as its pore size, shell chemical composition, shell thickness and permeability, among others. The today large abundance of polymers, both natural or man-made, provide a wide choice of shell materials, each offering different characteristics regarding permeability, elasticity, biodegradability, stiffness, and others. Although not so common, inorganic materials as silica and titania can also be used to obtain the MCs' shell [36, 40]. There are several encapsulation techniques which can be broadly divided into two main categories, namely chemical and physical techniques, with the last being subdivided into physico-chemical and physico-mechanical techniques, according to Table II.3 [36, 40]. The choice of the adequate microencapsulation method depends on the nature of the material used for the shell, as well as of the compound to be encapsulated. Different appropriate combinations of materials and synthesis methods can be used to produce MCs with a wide variety of compositional and morphological characteristics [36].

Table II.3 Techniques used for microencapsulation [40, 41].

Chemical	Physical	
	Physico-chemical	Physico-mechanical
<ul style="list-style-type: none"> • Suspension polymerization • Emulsion polymerization • Interfacial polymerization • <i>In-situ</i> polymerization 	<ul style="list-style-type: none"> • Coacervation • Layer-by-layer assembly • Supercritical CO₂-assisted • Phase separation • Ionic gelation 	<ul style="list-style-type: none"> • Spray-drying • Vibration nozzle • Fluidized bed coating • Centrifugal techniques • Vacuum encapsulation • Solvent evaporation

Chemical microencapsulation techniques include those involving polymerization processes, using monomers, oligomers, or pre-polymers as starting materials for the shell formation [39, 42]. By physical processes the starting materials for the shell are polymers, and no chemical reactions are involved. By a physico-chemical microencapsulation process the shell-forming material is previously dissolved, and the encapsulation occurs by precipitation of the polymer due to variations of pH value or electrolyte concentrations [36]. By the physico-mechanical methods, the process is based on physical and mechanical principles, with the formation of the shell depending only on solid–liquid phase transitions under the effect of temperature or by solubility reduction due to solvent evaporation [36, 43].

II.3.1 Interfacial polymerization – Encapsulation of isophorone diisocyanate

Microencapsulation by interfacial polymerization involves chemical reactions on the surface of emulsion droplets, leading to the formation of the shell. The choice of the emulsion system depends on the hydrophilic/lipophilic nature of the compound to be encapsulated. The reaction takes place at the interface between the continuous and dispersed phases of the emulsion system, each containing a monomer or reactant. If the formed oligomers are soluble in the dispersed phase of the emulsion, then its diffusion inwards to the droplet occurs and a matrix-type MC is formed. On the other hand, if the formed oligomers are soluble in the continuous phase, then the polymeric shell is formed at the emulsion droplet interface, leading to the formation of mononuclear, or core-shell, microcapsules [44]. This process is depicted in Figure II.7.

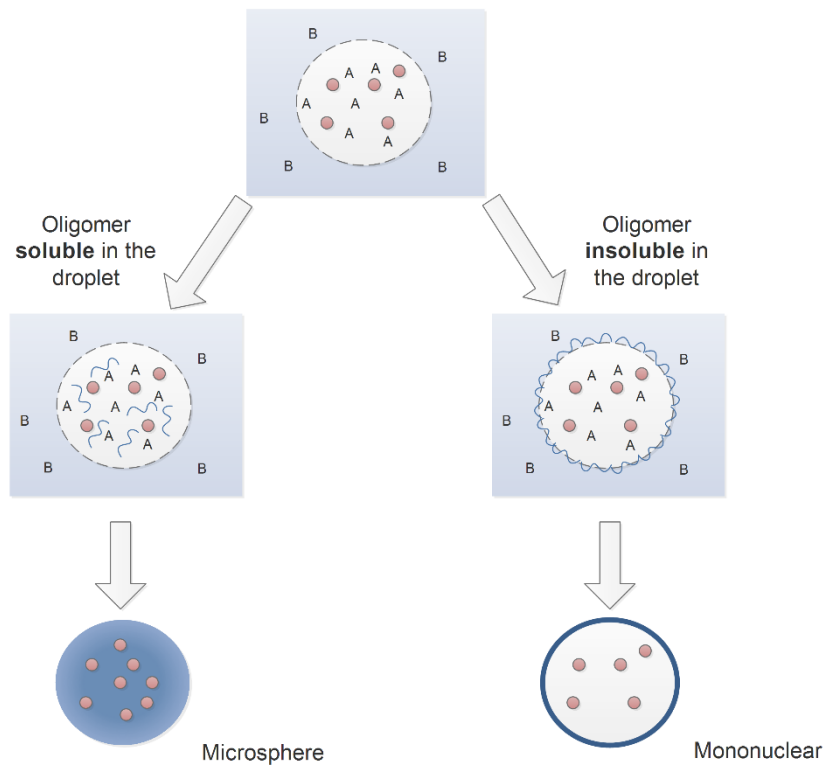


Figure II.7. Schematic representation of microencapsulation by interfacial polymerization, where the dispersed phase of the emulsion is represented as white (organic phase composed by the isocyanates) and, as blue, the continuous phase (aqueous solution), with the monomers of each phase represented as A and B, respectively. The encapsulated is represented at pink and the formed oligomers as blue stripes. Figure adapted from [44].

The encapsulation of a liquid isocyanate was reported for the first time by *Yang et al.*, who described the microencapsulation IPDI as a healing agent via the interfacial polymerization technique [43]. Interfacial polymerization technique, in combination with an oil-in-water (O/W) microemulsion system, is the most common method reported for the isocyanate encapsulation. By this technique, there are at least two reactants in a pair of immiscible liquids. The water (W) phase of the emulsion system is usually composed by water, an emulsion stabilizer, and compounds with active hydrogen (H) groups, while the oil (O) phase is composed by the isocyanate. The two phases are dispersed into each other under a high shear rate. This is followed by the diffusion of the reactants which become in contact at the interface of the O droplets of the emulsion system. When in contact, polymerization reactions, represented in Figure II.8, lead to the formation of an initially thin PUa or PU polymeric shell. It should be noted that the initial reaction of water and isocyanate forms an unstable carbamic acid intermediate that immediately decomposes to amine and CO₂ [42].

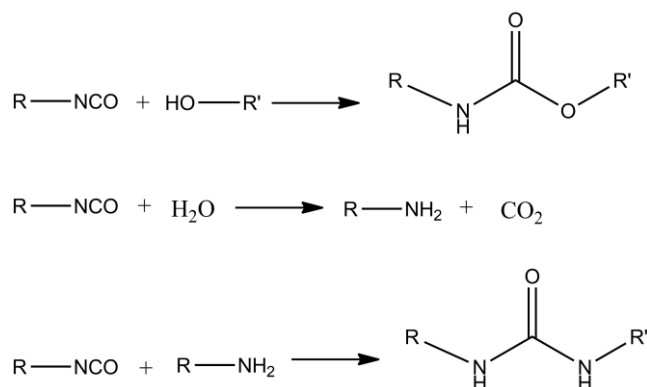


Figure II.8 The reaction of isocyanates with a hydroxyl group, with water, and with an amino group.

Further reactions will lead to the thickening of the shell until no more reactant species are in contact. Since the polymerization reactions are mainly controlled by diffusion, the growth's rate of the MCs shell decreases as the shell thickness increases [45]. The high reactivity of the isocyanate with water or other active H sources makes it difficult to obtain MCs with a high core content. In addition, the possible diffusion of water from the air moisture to the inside of the MCs, while stored, leads, by reaction with the encapsulated isocyanates, to a low shelf-life of the MCs [46].

In 2008, *Yang et al.* used a toluene 2,4-diisocyanate (TDI) pre-polymer dissolved in chlorobenzene as precursor for the shell formation. The highly reactive TDI was posteriorly mixed with IPDI, and the solution was added to an aqueous phase, at 70 °C, composed by water and gum arabic (GA), an emulsion stabilizer, to form an O/W emulsion system. 1,4-Butanediol was posteriorly added, at 50 °C, to act as a chain extender. The temperature was switched off, and the emulsion was maintained under agitation until a solid shell was formed [43]. The TDI higher reactivity when compared with IPDI ensured the encapsulation of the last, while the TDI reacted with the aqueous phase reactants to form the polymeric shell. The obtained MCs are reported to contain up to 68 wt% of core content, composed both by IPDI and chlorobenzene. The IPDI content varied from 63 to 45 wt% depending on the mechanical agitation rate employed in the synthesis and consequently the final MCs' size [43]. Most of the efforts, reported in the state of the art, regarding isocyanate microencapsulation refer to the encapsulation of monomeric IPDI for self-healing applications, following similar synthesis methodologies than the one reported by *Yang et al* [43].

II.3.1.1 Active H sources and microcapsules' shell composition

Several parameters which influence the isocyanate encapsulation have been studied and optimized over the years. The presence of chemicals with active hydrogen (H) groups, available to react with the isocyanate species (active H sources), or cross-linkers, as well as the MCs' shell composition were evaluated by several authors. Some examples of active H source reported in the state of the art are the glycerol, 1,4-butanediol and 1,6-hexanediol for a PU shell formation and DETA, triethylenetetramine (TETA), PEA D230 and PEA D400 (which are both commercial polyether amines) for a PUa' shell. Regarding the precursors for the shell formation, TDI pre-polymers are commonly used although there are also some studies referring methylene diphenyl diisocyanates (MDI) pre-polymers for this purpose. Double layered MCs of PU/ Poly(urea formaldehyde) (PUF) and PUa/melamine formaldehyde (MF) have also been reported. *Sondari et al.* reported, in 2010, on the encapsulation of IPDI intended for self-healing applications using a TDI pre-polymer as the shell forming material, which was synthesized using a TDI monomer and glycerol. After the O/W emulsion was obtained, glycerol was also added as polyol [47]. In 2013, *Credico et al.* reported MCs containing IPDI prepared using two different shell compositions: PU and a bi-layer PU/PUF shell. The PU MCs were obtained by interfacial polymerization of a TDI pre-polymer using 1,4-butanediol as active H source. As for the PU/PUF MCs, interfacial polymerization was initially used to form the PU shell, followed by in situ PUF microencapsulation [48]. The IPDI content of the PU and PU/PUF MCs was of 50 and 72 wt% respectively, with a drop to 47 wt% after 6 months for the PU MCs. In 2015 *Kardar et al.* studied the effect of different polyols including 1,4-butanediol, 1,6-hexanediol and glycerol on the encapsulation of IPDI, by interfacial polymerization, for self-healing purposes. A TDI pre-polymer was used for the shell formation, which was synthesized using a TDI monomer and each one of the polyols previously mentioned [49]. During the interfacial polymerization reaction each polyol was also added to the synthesis to promote the PU shell formation. The author refers on a lower IPDI encapsulation content using glycerol, with a difference of 25 wt% when comparing with the MCs obtained with 1,6-hexanediol [49]. In 2016, *Ming et al.* reported on the encapsulation of IPDI in PUa/ MF double-layered MCs, using a TDI pre-polymer for the PUa shell formation. Three different active H sources were used, namely TETA, PEA D230 and PEA D400. Not only the active H sources have led to different encapsulation contents but also contributed with different morphological features to the final MCs. Active H sources with longer soft segment led to lower encapsulation contents. In accordance, TETA has led to the MCs with a higher encapsulation, 78.09 wt% of IPDI, which decreased only 2.97% after a heat-moisture treatment for 2h. However, since TETA has no soft segments, the PUa shell was relatively brittle

[50]. In 2020, *Sun et al.* studied the effects of different shell materials for the IPDI encapsulation, using DETA as active H source. An MDI pre-polymer and of polymethylene polyphenyl isocyanate (PAPI) were used as shell materials, in addition to a composite shell of polyvinyl alcohol (PVA)/PUa. Regarding the composite shell, PVA formed intramolecular hydrogen bonds and the PUa moieties were obtained by the reaction of PAPI with DETA [51]. The MCs with a composite shell were the ones with the higher IPDI encapsulation content. It was concluded that not only the shell material played an important role for the encapsulation, but also the MCs' size, as previously reported by *Yang et al.* The bigger the MCs, the higher the encapsulation [51]. No values were commented regarding the MC's shelf-life.

Two main strategies have been reported intended to lead to a higher encapsulation content: i) the use of an isocyanate with a higher reactivity intended for the shell formation, ideally a pre-polymer as a PU or PUa shell can be quickly achieved; ii) the use of active H sources, or cross-linkers, which contribute not only to decrease the reaction time but also to bring some hydrophobicity and an increased cross-linking to the MC' shell. By decreasing the reaction time, the exposure of the isocyanate to the W phase is decreased and, with it, the extent of the polymerization reactions, leading to a higher encapsulation content. The hydrophobicity of the shell, as well as the storage conditions, with no moisture, seem the most significant parameters for an extended MCs' shelf-life.

Table II. 4. resumes the isocyanates species used for the MCs shell formation, the used active H sources and type and amount of encapsulated content of the MCs referred in this chapter.

Table II. 4. Resume of the isocyanate species and active H sources used for the MCs shell formation as well as type and amount of encapsulated isocyanate of the MCs referred in this chapter. (II.3.1.1 Active H sources and microcapsules' shell composition).

Reference	Isocyanate precursors for the shell formation	Encapsulated isocyanate	Active H sources	Core content (isocyanate or its mixture with solvents)
[43]	TDI pre-polymer	IPDI	1,4 - butanediol	68 wt%
[47]	TDI pre-polymer	IPDI	Glycerol	-
[48]	Desmodur L-75 (aromatic polyisocyanate based on TDI) for the synthesis of PU (PU/PUF shell)	IPDI	1,4- butanediol	50 wt%
[49]	TDI pre-polymer	IPDI	1,4- butanediol	57 wt%
			1,6- hexanediol	64 wt%
			Glycerol	39 wt%
[50]	TDI pre-polymer for the synthesis of PUa (PUa/MF shell)	IPDI	TETA	80.68 wt%
			PEA D230	78.09 wt%
			PEA D400	77.50 wt%
[51]	MDI pre-polymer and PAPI	IPDI	DETA	67.4 wt% to 79.2wt%

II.3.1.2 Microcapsules' size and size distribution – Emulsion stability

Besides the MCs' core content and shelf-life, it is also important to be able to control the MCs size and size distribution. As the interfacial polymerization reactions occur in the O/W emulsions interface, the size of the O droplets dictates the size of the final MCs.

Emulsion systems, even when the two phases are immiscible liquids, are thermodynamically unstable and tend to breakdown over time. There are several emulsion destabilization phenomena, which are gravitational separation, flocculation, Ostwald ripening and coalescence, schematically depicted in Figure II.9. Gravitational separation phenomena occur by sedimentation or creaming of the emulsion droplets, due to the viscosity differences of the W and O emulsion phases. Flocculation occurs when two or more droplets associate with each other while maintaining their individual integrities and Ostwald ripening, due to mass diffusion from smaller to larger droplets [52-55]. Coalescence or Ostwald ripening are irreversible

emulsion destabilization phenomena, as a change in droplet size occurs, which makes it impossible to restore the emulsion initial state [56].

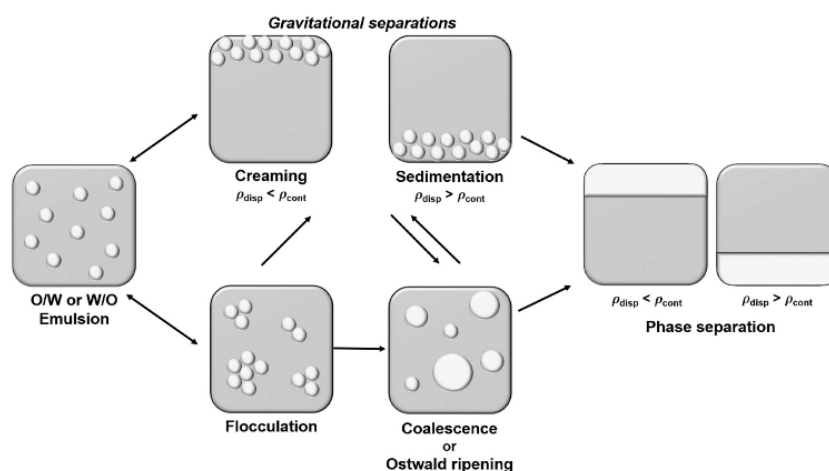


Figure II.9. Schematic representation of emulsions destabilization phenomena, with the dispersed phase represented by light gray and the continuous phase by dark gray. From [56] under an open access Creative Common CC BY license.

To avoid this destabilization phenomena, stabilizers are usually used in the dispersant medium of the emulsion system, which can be surfactants, amphiphilic polymers, or solid particles [53]. Surfactants stabilize the emulsion by forming an electrostatic or steric barrier around the emulsion droplets, which decreases attractive interactions [54]. Polymers act by the entropic effect caused by the entanglement of polymeric chain' segments in the emulsion droplets interface, limiting conformational rearrangements. Regarding solid particles, its adsorption creates a mechanical barrier against coalescence. An alternative to common stabilizers is the use of rheology or texture modifiers, which, by increasing the viscosity of the continuous phase, help to restrict the droplets movement and to increase its kinetic stability [53].

Particularly, for O/W emulsion systems, the instability is a result of gravitational separation and flocculation, which might lead to coalescence of the O droplets [53, 57]. The polysaccharide GA is one of the stabilizers most commonly used in the synthesis of isocyanate containing MCs obtained by the interfacial polymerization method. GA has a good water solubility, low solution viscosity, good surface activity, and ability to form a protective film around emulsion droplets[58, 59]. There are several studies reporting on the optimization of the GA concentrations in the W phase, intended to increase the stability of the O/W emulsion and consequently lead to smaller and more homogeneous MCs [51, 59, 60]. *Huang et al.* report on the study of different GA concentrations and its effect on the MCs' final morphology. The authors tested GA concentrations ranging from 2 to 10 wt% in the W phase, observing a significant decrease in the MCs size when the GA concentration increased from 1.5 to 3 wt%,

followed by a plateau with the MCs maintaining similar diameters for GA concentrations above 3 wt% [59]. *Xiang et al.* have also tested different GA concentrations of 5, 7.5 and 12.5% in the W phase and concluded that as the GA concentration increased the sphericity and uniformity of the MCs improved [60]. GA in a concentration above 12.5% has been shown to significantly increase the aqueous solution viscosity, which strongly leads to a reduction in the MCs size as two stabilization effects are combined, the effect of GA as a polysaccharide and its rheological effect as viscosity modifier [60]. In addition to GA, and although not so common, it has been reported the use of other stabilizers for this purpose. Some examples are the Tween80, Tween20, Sodium dodecyl sulfate (SDS), SPAN20, PVA, dodecyl benzene sulfonate (SDBS) and combinations of GA with cetrimonium bromide (CTAB), PVA with SDS and SDBS with polyvinylpyrrolidone (PVP) [51, 61, 62]. *Sun et al.* studied the effect of several stabilizers and its concentration on the final MCs' characteristics. A decrease on the MCs size with the increase of the stabilizer concentration, up to a certain amount, was observed. GA was the stabilizer leading to bigger MCs, and which needed to be present at higher concentrations [51]. It is composed by arabinogalactan (868.4%), arabinogalactan protein (10.4%), and glycoprotein (1.24%), with its emulsifying property attributed only to arabinogalactan protein, which explains its use in a greater amount for achieving stable emulsions [58]. A combination of SDBS/PVP and PVA were concluded to be the best emulsifying systems [51].

II.3.2 Interfacial polymerization – Encapsulation of other isocyanate species

Besides IPDI it has already been reported the encapsulation of other isocyanates species by interfacial polymerization, although in a significantly less extent. An example is the hexamethylene diisocyanate (HDI), either in the form of monomer, dimer, and trimer. *Huang et al.* and *Wu et al.* report on the encapsulation of its monomeric form, by using an MDI pre-polymer and an urea formaldehyde (UF) pre-polymer, respectively [59, 63]. *Wu et al.* have also encapsulated an HDI dimer using the same shell material [63]. *Nguyen et al.* encapsulated an HDI trimer using a more reactive commercial MDI, Suprasec 2020 [46].

For the encapsulation of the monomeric HDI in PU MCs, *Huang et al.* used an MDI pre-polymer as shell material and 1,4-butanediol as active H source [59]. The obtained MCs had a maximum core content of 63 wt%, which dropped to 45 wt% while stored in an open-air environment for a month, and to below 20 wt% upon its immersion in water for 24 hours [59]. For the encapsulation of both the monomeric HDI and the HDI dimer, in PUF MCs, *Wu et al.*, used a UF pre-polymer as shell precursor and the MCs were obtained by in situ polymerization. The author reports on an encapsulation content ranging from 82–90 wt%, with a reduction to 78% in 45

days. For the production of the MCs containing liquid HDI-trimer, *Nguyen et al.* reported on the use of an MDI-trimer and a 2,4,6-triaminopyrimidine for the shell formation [46, 63]. Several functionalizing agents were tested for the shell, namely the 2-ethylhexylamine, 3,4-difluorobenzylamine, 1H,1H,2H,2H-Perfluorodecylamine, and combinations between them. This were to bring some hydrophobicity to the shell and to increase the MCs' core content. The use of hexamethyldisilazane (HMDS) was also tested, aimed to induce reactions between isocyanate groups to reinforce the PUa shell structure. The use of HDMS enabled to obtain a core-content of 76 wt% of HDI, and the hydrophobic functionalization improved the encapsulation content by 18 to 27 wt% when compared to non-functionalized MCs [46].

The referred works all report on the encapsulation of HDI, which although slightly more reactive than IPDI, was able to be encapsulated as a monomer, a dimer and a trimer. The encapsulation of higher molecular weight (MW) isocyanates has also been reported, although in a significantly small extent. In 2019 *Ma et al.* was able to encapsulate liquid PAPI dissolved in n-hexadecane, using the same isocyanate for the shell formation and without the addition of any active H source. The encapsulation content, composed by both PAPI and n-hexadecane, was of 77 wt%, decreasing to 59.7 wt% within a 6-month period [64]. In 2020, *Lubis et al.* reported on the encapsulation of polymeric 4-4 diphenyl methane diisocyanate, with 31% of –NCO content, using the same for the shell formation and 1,4 butanediol as active H source. The obtained MCs had an encapsulated content that varied from 60.8 to 63.5 wt% of the total MCs weight. However, the MCs were poorly spherical, with some aggregation and big sizes and size distribution varying from ca. 50 to 300 μm [61]. Lastly, *Xiang et al.*, in 2022, refer the encapsulation of an aliphatic isocyanate pre-polymer using a commercial polyurethane (Bayer L-75), which is an aromatic polyisocyanate based on TDI, along with 1,4 butanediol, for the shell formation. The encapsulated content varied from 31.56% to 40.88% [60].

The state of the art regarding isocyanates microencapsulation mainly refers to MCs with a PU/PUa shell enclosing monomeric or low MW isocyanate species. Although the encapsulation of monomeric isocyanates, by interfacial polymerization, is widely documented in the state of the art, improvements regarding these MCs shelf-life, size to core content and size distribution are still a necessity. Also, the state of the art regarding the encapsulation of oligomeric or pre-polymeric isocyanate species is very scarce, mainly due to the high viscosity and reactivity of these species which leads to MCs with a poorly spherical shape, large size distributions and low encapsulation yield.

II.3.3 Microplastics in isocyanate microencapsulation

Interfacial polymerization in combination with an O/W emulsion is a well-established method for isocyanate microencapsulation. However, the MCs obtained by this method are not considered to be biodegradable making them microplastics. In 2021, the ECHA completed a restrictions proposal regarding the use of intentionally added microplastics in products available at the European Union/European Economic Area market [65]. Following the European Commission request, ECHA proposed that the concentration of microplastic in a mixture should not exceed 0.01%, which is equivalent to its ban. The proposal is still to be approved but it is expected to come into force [65, 66].

Some PUs have been reported to present some biodegradability, to a certain extent, depending on the properties of the polymer as for example its molecular orientation, crystallinity, cross-linking and the presence of certain chemical groups which can promote degradability by certain enzymes [67].

In 2019, *Xiao et al.* reported on the production of PU MCs containing encapsulated IPDI presenting some biodegradability when subjected to simulated physiological conditions. For the MCs' production, a polycaprolactone (PCL) diol and poly(ethylene glycol) were made to react with an MDI to form a PU pre-polymer to be further used for the shell formation [68]. The PU MCs, obtained by interfacial polymerization, exhibited some degradation into smaller fragments after exposed to phosphate buffer saline solution for 30 days. However, there is no reference to further degradation after this time.

The strategy followed in this thesis to address the microplastics issue took into account the employment of biodegradable plastics for the MCs' shell. The next sub-chapter explains the theory behind the MCs' preparation process in this case.

II.3.4 Solvent evaporation

As an alternative to the absent or limited biodegradability of the MCs obtained by interfacial polymerization, it is possible to obtain biodegradable MCs using other techniques.

The solvent evaporation technique has been used to obtain MCs by precipitation. By this method no chemical reactions occur, and the MCs are obtained only by physical phenomena. Instead of monomers or pre-polymers as starting materials for the shell formation, in this case, polymers (including bio-derived and biodegradable polymers) can be used, offering a wider range of options.

By this technique, a first aqueous phase is dispersed into an organic phase composed by a dissolved polymer, forming the primary emulsion system, W_1/O . This emulsion is then dispersed into an aqueous phase containing an emulsifier, leading to the double $W_1/O/W_2$ emulsion system formation. The double emulsion is then left under agitation until all the solvent present in the O phase has evaporated, leading to the polymer precipitation at the W_1/O emulsion interface and to the MCs formation [69].

This technique enables to use biodegradable polymers as shell material for the MCs formation, with PCL being the most referred in the literature for this use. PCL is an aliphatic polyester with low glass transition temperature and a melting point of 60 °C with its biodegradability occurring by means of bulk ester hydrolysis into carboxylic acids and alcohols [70-73]. PCL has been widely studied as MCs' shell material mainly for controlled drug release applications due to its biocompatibility and FDA approval for use in humans [70, 71]. However, most works reporting its use refer to the encapsulation of hydrophilic compounds, usually temperature sensitive, by means of a $W/O/W$ emulsion system [74-78].

For the encapsulation of isocyanates using this technique, it is necessary to use an $O/O/W$ emulsion system, since the core content would not be hydrophilic but lipophilic.

II.3.4.1 Double emulsion system

Emulsions can be divided into simple emulsion systems, consisting of two immiscible liquids dispersed in one another or double/multiple emulsion systems consisting of three or more different fluids, as depicted in Figure II.10.

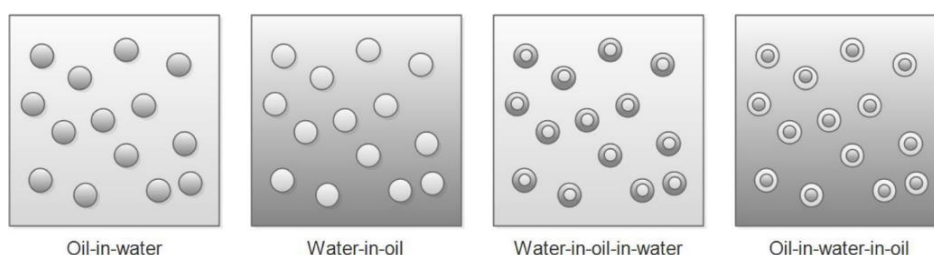


Figure II.10. Schematic representation of the emulsion's classification types, with the water phase of the emulsion system represented by the light gray color and the oil phase by dark gray color.

Seifriz W. reported, in 1924, on double emulsions system formation, for the first time, classifying them as complex polydisperse systems, which can be placed into two categories: $W/O/W$ or $O/W/O$ [79]. Although $W/O/W$ is the most commonly double emulsion system used in combination with the solvent evaporation technique, there is also reference, in the state of the

art, for the use of O/O templates and, more commonly, W/O/O double-emulsion systems. Microencapsulation using an O/O emulsions have been reported later on by *Sturesson et al.*, 1993, regarding the encapsulation of timolol maleate using poly(lactic-co-glycolic acid) through the solvent evaporation method, leading to a drug load of about 2% (w/w) [80]. The use of O/O templates or the adaptation of the latter one in a double emulsion system brought the possibility to obtain a higher encapsulation yield for water soluble compounds since these species tend to diffuse to the aqueous outer phase on the conventional emulsion systems [81, 82]. Despite its importance, references regarding the use of O/O emulsion systems are still reduced, mainly due to the difficulty to achieve a stable system. For that it is essential to identify appropriate solvent pairs that drive phase separation into an emulsion. The most referred combinations regard the use of nonpolar solvents for the polymer dissolution, such as hydrocarbons, and highly polar solvents (e.g., dichloromethane, polyols, formamide, and methanol), and mineral or vegetable oil for an external O phase [82]. *Jelvehgari M.* and *Montazam S. H.* reported on encapsulation of theophylline using W/O/O and O/O emulsion systems through solvent evaporation/extraction technique using various shell forming materials, obtaining a high encapsulation yield of 90% with Eudragit RS and an O/O template [81]. *Ramesh D. V.* studied the encapsulation of Vitamin B12 in PCL microspheres by the solvent evaporation technique using the following emulsion systems: O/O, W/O/W, and O/O obtained by melt, in which the Vitamin B12 was added directly in melted PCL without the need of a solvent. The most favorable result was obtained with the O/O template [82]. *Iwata* and *McGinity* have developed a multiple emulsion system of the W/O/O/O type through which multiphase MCs of poly(lactic-co-glycolic acid) (PLGA) containing W/O emulsions were prepared by solvent evaporation technique, using acetonitrile for the polymer dissolution and mineral oil for the continuous phase, obtaining loading efficiencies of 80-100%. [83]. In addition, W/O/O templates have also been described by *Zheng et al.* as a method to produce double-shell MCs containing a hydrophilic content, with a PU/PMF shell through combinations of both interfacial polymerization and polymer precipitation techniques [84].

II.3.4.2. Microencapsulation for adhesive formulations

Microencapsulation can be of use in adhesive industry to increase the compatibility of certain ingredients, to minimize component poisoning and product degradation [38]. Other advantage offered by microencapsulation is the possibility to activate the adhesive at a specified time [85]. However, despite the offered advantages very little development has been carried out in this field. In the adhesive industry, encapsulation can be used to enclose a reactive component, a

catalyst or a cross-linker, enabling the production of latent adhesives. This type of adhesive is not active until the breakage of the MCs at the desired moment. It is also possible to encapsulate other incompatible, sensitive, or volatile compounds of adhesive formulations, as antioxidants, flame retardants, solvents, biocides, dyes, among others [38, 86].

Most of the work reported in the state of the art combining microencapsulation and adhesives refers to self-healing applications. As a title of example *Yuan et al.* described on the encapsulation of a liquid epoxy resin adhesive, composed by a mixture of diglycidyl ether of bisphenol A and 1-butyl glycidyl ether in MCs with a PUF shell, to be used as a healing adhesive to self-healing composites [87]. *Celestine et al.* encapsulated anisole with dissolved poly(methyl methacrylate) (PMMA) in PU/PUF MCs to be part of a self-healing PMMA formulation. The MCs were only to release the core content when subjected to a fracture. When subjected to a Mode I fracture, while in the PMMA matrix, the MCs were able to release its content and lead to a healing efficiency of 89% after 3 days, for a formulation containing 5 wt% of MCs [88]. Although in a fewer amount there are also some publications regarding the encapsulation of curing agents for adhesives formulations. *Zhang et al.* reported, in 2019, on the encapsulation of 2-phenylimidazole to act as an accelerator to a 1K epoxy thermoset resin. Imidazole is one of the most used accelerators for epoxy resins, however its intrinsic high reactivity, even when at room temperature, makes it unfeasible to be added directly to the resin formulation. Here the MCs act as latent accelerators, only releasing the encapsulated component by the effect of temperature, allowing the addition of the imidazole to the formulation [89]. *You et al.*, refer, in 2020, the production of MCs via microfluidic-assisted fabrication, containing oxalic acid, and by using ethoxylated trimethylolpropane triacrylate pre-polymer for the shell formation. The MCs are intended to be used on UF pressure-sensitive adhesives for plywood boards [90]. Also, in 2020 *Ni et al.* reported on polyetherimide (PEI) shell' MCs containing a multi-polyaniline (MPAN) on its core, to be released due to an external stimulus of pressure, heat or light. The MCs were able to release the core content at the temperature of 120 °C leading to the epoxy resin cure [91]. In 2021 *Messersmith et al.* reported on the encapsulation of a polyol cross-linker, glycerol, and a tertiary amine catalyst, DABCO, to be added to a polyurethane adhesive intended to a rapid cure under water. The MCs were composed by a PUa shell and demonstrated to be able to release its content in response to a mechanical stimulus [92].

Regarding the production of MCs containing encapsulated isocyanate species for adhesive formulations, in 2020 *Lubis et al.* reported on the encapsulation of polymeric 4,4 methylene diphenyl isocyanate in PU MCs to be used for the modification of urea UF adhesives. The authors showed an increased performance of the adhesive with the addition of the MCs when comparing

with the UF adhesive on its own. However, it is referred the importance of reducing the MCs size, which reached 300 μm , to improve its performance [93].

The application of MCs in adhesive formulations is still very scars, in particular the use of isocyanate containing MCs. For the MCs to be used as cross-linkers, in adhesive formulations, it is necessary for them to respond to the stimuli applied during the adhesive application, have a good dispersion in the adhesive, have small sizes and size distributions (to guarantee a good homogeneity) and, in case of 1K adhesives, need to resist the solvent present in the formulation. In this work, the development of adequate MCs, with the required characteristics, is here addressed, as well as the formulation of a final PU and PCP adhesive containing the new solid cross-linkers.

Bibliography:

- 1 Jeevi, G.;Nayak, S. K.;Kader, M. A., *Review on adhesive joints and their application in hybrid composite structures*. Journal of Adhesion Science and Technology, **2019**, 33, 1497-1520.
- 2 Marques, A. C.;Mocanu, A.;Tomić, N. Z.;Balos, S.;Stammen, E.;Lundevall, A.;Abrahami, S. T.;Günther, R.;de Kok, J. M. M.;Freitas, S. T., *Review on Adhesives and Surface Treatments for Structural Applications: Recent Developments on Sustainability and Implementation for Metal and Composite Substrates*. Materials, **2020**, 13.
- 3 Banea, M. D.;Silva, L. F. M., *Adhesively bonded joints in composite materials: An overview*. Proceedings of the Institution of Mechanical Engineers, Part L: Journal of Materials: Design and Applications, **2009**, 223, 1-18.
- 4 *Adhesives & Sealants Market by Adhesive Formulating Technology (Water-based, Solvent-based, Hot-melt, Reactive), Sealant Resin Type (Silicone, Polyurethane, Plastisol, Emulsion, Polysulfide, Butyl), Application, Region - Global Forecast to 2026*. **2022**; Available from: <https://www.marketsandmarkets.com/Market-Reports/adhesive-sealants-market-421.html>.
- 5 Duncan, B.;Abbott, S. G.;Court, R. W.;Roberts, R.;Leatherdale, D., *A review of adhesive bonding assembly processes and measurement methods*, **2003**, National Physical Laboratory, Teddington, Middlesex, UK.
- 6 George, W., *Handbook of Adhesion Promoters*. 2nd ed. **2023**: Elsevier.
- 7 Adams, R. D., *Adhesive Bonding: Science, Technology and Applications*. 2nd ed. **2021**: Woodhead Publishing.
- 8 Maia, B. S., *Study on the Effect of Surface Energy of Polypropylene/Polyamide12 polymer Hybrid Matrix Reinforced with Virgin and Recycled Carbon Fiber*, **2017**, Master Degree, Faculty of Forestry, University of Toronto.
- 9 *Adhesion Theory - Mechanical Interlocking*. **2008**; Available from: <http://www.specialchem4adhesives.com/resources/adhesionguide/index.aspx?id=theory4>.
- 10 Mays, G. C.;Hutchinson, A. R., *Adhesives in Civil Engineering*. 1st ed. **1992**: Cambridge University Press.
- 11 Mayan, O.;Pires, A.;Neves, P.;Capela, F., *Shoe Manufacturing and Solvent Exposure in Northern Portugal*. Applied Occupational and Environmental Hygiene, **1999**, 14, 785-790.
- 12 *The role of adhesives in the shoe industry*. **2007**; Available from: www.specialchem.com
- 13 Paiva, R. M. M.;Marques, E. A. S.;da Silva, L. F. M.;António, C. A. C.;Arán-Ais, F., *Adhesives in the footwear industry*. Proceedings of the Institution of Mechanical Engineers, Part L: Journal of Materials: Design and Applications, **2015**, 230, 357-374.
- 14 Falco, A. P. S. D., *Avaliação de Adesivos Utilizados em Solados de Calçados de Uso da Marinha do Brasil*, **2007**, Master Degree, Universidade Federal do Rio de Janeiro, COPPE.
- 15 Orgilés-Calpena, E.;Arán-Ais, F.;Torró-Palau, A. M.;Sánchez, M., *Adhesives in the Footwear Industry: A Critical Review*. Reviews of Adhesion and Adhesives, **2019**, 7, 69-91.
- 16 Minford, J. D., *Handbook of Adhesives*. 2nd ed. **1977**: Van Nostrand Reinhold Company.
- 17 Pizzi, A.;Mittal, K. L., *Handbook of adhesive technology*. 2nd ed. **1994**, New York: Marcel Dekker.
- 18 Silva, L. F. M.;Öchsner, A.;Adams, R. D., *Handbook of Adhesion Technology*. 2nd ed. **2018**: Springer
- 19 Paiva, R. M. G. M., *Composição e propriedades de produtos adesivos de base solvente*, **2009**, Master degree, Universidade de Aveiro, Portugal.

- 20 CIPADE – Indústria e Investigação de Produtos Adesivos. Available from:
www.cipade.com,.
- 21 Silva, L. F. M.;Magalhães, A. G.;Moura, M. F. S. F., *Juntas Adesivas Estruturais*. **2007**:
Publindústria.
- 22 Sánchez-Adsuar, M. S.;Martín-Martínez, J. M., *Structure, composition, and adhesion
properties of thermoplastic polyurethane adhesives*. Journal of Adhesion Science and
Technology, **2000**, 14, 1035 - 1055.
- 23 Saikumar, C., *Adhesives in the leather industry - perspectives for changing needs*. Journal
of Adhesion Science and Technology, **2002**, 16, 543-563.
- 24 Romero-Sánchez, M. D.;Pastor-Blas, M. M.;Martín-Martínez, J. M., *Improved peel
strength in vulcanized sbr rubber roughened before chlorination with
trichloroisocyanuric acid*. The Journal of Adhesion, **2002**, 78, 15 - 38.
- 25 Paiva, R. M. M.;Marques, E. A. S.;Silva, L. F. M.;António, C. A. C., *Effect of the surface
treatment in polyurethane and natural leather for the footwear industry*.
Materialwissenschaft und Werkstofftechnik, **2015**, 46, 47-58.
- 26 EN 1392:2006 - *Adhesives for leather and footwear materials-Solvent-based and
dispersion adhesives-Testing of bond strength under specified conditions*, **2006**.
- 27 Kweon, J.-H.;Jung, J.-W.;Kim, T.-H.;Choi, J.-H.;Kim, D.-H., *Failure of carbon composite-to-
aluminum joints with combined mechanical fastening and adhesive bonding*. Composite
Structures, **2006**, 75, 192-198.
- 28 Singh, Y.;Kumar, J.;Singh, I.;Rakesh, P. K., *Joining behavior of natural fiber reinforced
polymer composites*. Joining Processes for Dissimilar and Advanced Materials. **2022**:
Woodhead Publishing.
- 29 Ebnesajjad, S., *Surface Treatment of Materials for Adhesive Bonding*. 2nd ed. **2014**:
Elsevier.
- 30 Centers for Disease Control and Prevention. The National Institute for Occupational
Safety and Health. *Isocyanates. Overview*. **2008**; Available from:
<https://www.cdc.gov/niosh/topics/isocyanates/default.html>.
- 31 ECHA - European Chemicals Agency. *ECHA - Annex XVII to REACH - Conditions of
Restriction. Restrictions on the Manufacture, Placing on the Market and Use of Certain
Dangerous Substances, Mixtures and Articles*. Available from:
<https://echa.europa.eu/documents/10162/503ac424-3bcb-137b-9247-09e41eb6dd5a>.
- 32 Choudhury, N.;Meghwal, M.;Das, K., *Microencapsulation: An overview on concepts,
methods, properties and applications in foods*. Food Frontiers, **2021**, 2, 426-442.
- 33 Jyothi, N. V. N.;Prasanna, P. M.;Sakarkar, S. N.;Prabha, K. S.;Ramaiah, P. S.;Srawan, G. Y.,
Microencapsulation techniques, factors influencing encapsulation efficiency. Journal of
Microencapsulation, **2010**, 27, 187-197.
- 34 Singh, M. N.;Hemant, K. S.;Ram, M.;Shivakumar, H. G., *Microencapsulation: A promising
technique for controlled drug delivery*. Research in Pharmaceutical Sciences, **2010**, 5, 65-
77.
- 35 Sonawane, S. H.;Bhanvase, B. A.;Sivakumar, M.;Potdar, S. B., *Encapsulation of Active
Molecules and Their Delivery System*. **2020**: Elsevier.
- 36 Dubey, R., *Microencapsulation Technology and Applications*. Defence Science Journal,
2009, 59, 82-95.
- 37 Ciriminna, R.;Sciortino, M.;Alonzo, G.;Schrijver, A. d.;Pagliaro, M., *From Molecules to
Systems: Sol-Gel Microencapsulation in Silica-Based Materials*. Chemical Reviews, **2011**,
111, 765-789.
- 38 Arán-Ais, F.;Pérez-Limiñana, M. Á.;Sánchez-Navarro, M. M.;Orgilés-Barceló, C.,
Developments in Microencapsulation Technology to Improve Adhesive Formulations.
The Journal of Adhesion, **2012**, 88, 391-405.
- 39 Fanger, G. O., *Microencapsulation: Processes and Applications*. 1st ed, ed. J.E.
Vandegaer. **1974**, Boston, MA: Springer US.

- 40 Ghosh, S. K., *Functional Coatings: By Polymer Microencapsulation*. 1st ed. **2006**: Wiley-VCH Verlag GmbH & Co. KGaA.
- 41 Al-Shannaq, R.;Farid, M. M.;Ikutegbe, C. A., *Methods for the Synthesis of Phase Change Material Microcapsules with Enhanced Thermophysical Properties—A State-of-the-Art Review*. *Micro and Nanosystems*, **2022**, 2, 426-474.
- 42 Saunders, K. J., *Organic polymer chemistry : an introduction to the organic chemistry of adhesives, fibres, paints, plastics, and rubbers*. 2nd ed. **1988**: Springer Dordrecht.
- 43 Yang, J.;Keller, M. W.;Moore, J. S.;White, S. R.;Sottos, N. R., *Microencapsulation of Isocyanates for Self-Healing Polymers*. *Macromolecules*, **2008**, 41, 9650-9655.
- 44 Munin, A.;Edwards-Lévy, F., *Encapsulation of natural polyphenolic compounds; a review*. *Pharmaceutics*, **2011**, 3, 793-829.
- 45 Mishra, M., *Handbook of Encapsulation and Controlled Release*. **2015**, Boca Raton: CRC Press.
- 46 Nguyen, L.-T. T.;Hillewaere, X. K. D.;Teixeira, R. F. A.;van den Berg, O.;Du Prez, F. E., *Efficient microencapsulation of a liquid isocyanate with in situ shell functionalization*. *Polymer Chemistry*, **2015**, 6, 1159-1170.
- 47 Sondari, D.;Septevani, A. A.;Randy, A.;Triwulandari, E., *Polyurethane microcapsule with glycerol as the polyol component for encapsulated self healing agent*. *International Journal of Engineering and Technology*, **2010**, 2, 466-471.
- 48 Di Credico, B.;Levi, M.;Turri, S., *An efficient method for the output of new self-repairing materials through a reactive isocyanate encapsulation*. *European Polymer Journal*, **2013**, 49, 2467-2476.
- 49 Kardar, P., *Preparation of polyurethane microcapsules with different polyols component for encapsulation of isophorone diisocyanate healing agent*. *Progress in Organic Coatings*, **2015**, 89, 271-276.
- 50 Ming, Y.;Hu, J.;Xing, J.;Wu, M.;Qu, J., *Preparation of polyurea/melamine formaldehyde double-layered self-healing microcapsules and investigation on core fraction*. *Journal of Microencapsulation*, **2016**, 33, 307-14.
- 51 Sun, Y.;Wang, S.;Dong, X.;Liang, Y.;Lu, W.;He, Z.;Qi, G., *Optimized synthesis of isocyanate microcapsules for self-healing application in epoxy composites*. *High Performance Polymers*, **2020**, 32, 669-680.
- 52 Tadros, T., *Encyclopedia of Colloid and Interface Science*. 1st ed. **2013**: Springer Berlin, Heidelberg.
- 53 Lian, X.;Liao, S.;Xu, X.-Q.;Zhang, S.;Wang, Y., *Self-Stabilizing Encapsulation through Fast Interfacial Polymerization of Ethyl α -Cyanoacrylate: From Emulsions to Microcapsule Dispersions*. *Macromolecules*, **2021**, 54, 10279-10288.
- 54 Costa, C.;Medronho, B.;Filipe, A.;Mira, I.;Lindman, B.;Edlund, H.;Norgren, M., *Emulsion Formation and Stabilization by Biomolecules: The Leading Role of Cellulose*. *Polymers*, **2019**, 11, 1570.
- 55 Walstra, P., *Physical Chemistry of Foods*. 1st ed. **2001**: CRC Press, Boca Raton.
- 56 Perrin, L.;Desobry-Banon, S.;Gillet, G.;Desobry, S., *Review of High-Frequency Ultrasounds Emulsification Methods and Oil/Water Interfacial Organization in Absence of any Kind of Stabilizer*. *Foods*, **2022**, 11, 2194.
- 57 Wang, B.;Tian, H.;Xiang, D., *Stabilizing the Oil-in-Water Emulsions Using the Mixtures of *Dendrobium Officinale* Polysaccharides and Gum Arabic or Propylene Glycol Alginate*. *Molecules*, **2020**, 25, 759.
- 58 Niu, F.;Niu, D.;Zhang, H.;Chang, C.;Gu, L.;Su, Y.;Yang, Y., *Ovalbumin/gum arabic-stabilized emulsion: Rheology, emulsion characteristics, and Raman spectroscopic study*. *Food Hydrocolloids*, **2016**, 52, 607-614.
- 59 Huang, M.;Yang, J., *Facile microencapsulation of HDI for self-healing anticorrosion coatings*. *Journal of Materials Chemistry*, **2011**, 21, 11123-11130.

- 60 Xiang, G.;Tu, J.;Xu, H.;Ji, J.;Liang, L.;Li, H.;Chen, H.;Tian, J.;Guo, X., *Preparation and Self-Healing Application of Isocyanate Prepolymer Microcapsules*. *Coatings*, **2022**, 12, 166.
- 61 Lubis, M. A. R.;Suryanegara, L.;Pramesti, M. A., *Synthesis of polymeric isocyanate microcapsules via interfacial polymerization and their characterisation using spectroscopy and microscopy techniques*. *IOP Conference Series: Materials Science and Engineering*, **2020**, 935, 012053.
- 62 Ma, Y.;Jiang, Y.;Tan, H.;Zhang, Y.;Gu, J., *A Rapid and Efficient Route to Preparation of Isocyanate Microcapsules*. *Polymers*, **2017**, 9, 274.
- 63 Wu, G.;An, J.;Tang, X.-Z.;Xiang, Y.;Yang, J., *A Versatile Approach towards Multifunctional Robust Microcapsules with Tunable, Restorable, and Solvent-Proof Superhydrophobicity for Self-Healing and Self-Cleaning Coatings*. *Advanced Functional Materials*, **2014**, 24, 6751-6761.
- 64 Ma, Y.;Lu, P.;Chen, W.;Zhang, Y.;Gu, J., *Preparation of isocyanate microcapsules as functional crosslinking agent by minimalist interfacial polymerization*. *Advanced Powder Technology*, **2019**, 30, 1995-2002.
- 65 ECHA - European Chemicals Agency. *Microplastics*. Available from: <https://echa.europa.eu/hot-topics/microplastics>.
- 66 European Parliament. *Reduction of the release of microplastics in the environment and restriction of microplastics intentionally added to products*. **2023**; Available from: <https://www.europarl.europa.eu/legislative-train/theme-a-european-green-deal/file-microplastics>.
- 67 Howard, G. T., *Biodegradation of polyurethane: a review*. *International Biodeterioration & Biodegradation*, **2002**, 49, 245-252.
- 68 Xiao, Y.;Wu, B.;Fu, X.;Wang, R.;Lei, J., *Preparation of biodegradable microcapsules through an organic solvent-free interfacial polymerization method*. *Polymers for Advanced Technologies*, **2019**, 30, 483-488.
- 69 Ibraheem, D.;Iqbal, M.;Agusti, G.;Fessi, H.;Elaissari, A., *Effects of process parameters on the colloidal properties of polycaprolactone microparticles prepared by double emulsion like process*. *Colloids and Surfaces A: Physicochemical and Engineering Aspects*, **2014**, 445, 79-91.
- 70 Azimi, B.;Nourpanah, P.;Rabiee, M.;Arbab, S., *Poly (ϵ -caprolactone) Fiber: An Overview*. *Journal of Engineered Fibers and Fabrics*, **2014**, 9.
- 71 Ansari, T. H.;Hasnain, M.;Hoda, M. N.;Nayak, A. K., *Microencapsulation of pharmaceuticals by solvent evaporation technique: A review*. *Elixir Pharmacy*, **2012**, 47, 8821-8827.
- 72 Cai, Q.;Shi, G.;Bei, J.;Wang, S., *Enzymatic degradation behavior and mechanism of Poly(lactide-co-glycolide) foams by trypsin*. *Biomaterials*, **2003**, 24, 629-638.
- 73 Mark, H. F., *Encyclopedia of Polymer Science and Technology*. 4th ed. **2014**: John Wiley & Sons, Inc.: New York.
- 74 Iqbal, M.;Valour, J.-P.;Fessi, H.;Elaissari, A., *Preparation of biodegradable PCL particles via double emulsion evaporation method using ultrasound technique*. *Colloid and Polymer Science*, **2015**, 293, 861-873.
- 75 Lamprecht, A.;Ubrich, N.;Pérez, M. H.;Lehr, C.;Hoffman, M.;Maincent, P., *Influences of process parameters on nanoparticle preparation performed by a double emulsion pressure homogenization technique*. *International Journal of Pharmaceutics*, **2000**, 196, 177-82.
- 76 Hwang, Y. M.;Pan, C. T.;Lin, Y.-M.;Zeng, S.-W.;Yen, C. K.;Wang, S.-Y.;Kuo, S. W.;Ju, S.-P.;Liang, S.-S.;Zong-Hsin, L., *Preparation of Biodegradable Polycaprolactone Microcarriers with Doxorubicin Hydrochloride by Ultrasonic-assisted Emulsification Technology*. *Sensors and Materials*, **2019**, 31, 301-310.

- 77 Iqbal, M.;Zafar, N.;Fessi, H.;Elaissari, A., *Double emulsion solvent evaporation techniques used for drug encapsulation*. International Journal of Pharmaceutics, **2015**, 496, 173-190.
- 78 Imbrogno, A.;Dragosavac, M. M.;Piacentini, E.;Vladislavljević, G. T.;Holdich, R. G.;Giorno, L., *Polycaprolactone multicore-matrix particle for the simultaneous encapsulation of hydrophilic and hydrophobic compounds produced by membrane emulsification and solvent diffusion processes*. Colloids and Surfaces B: Biointerfaces, **2015**, 135, 116-125.
- 79 Seifriz, W., *Studies in Emulsions. III-V*. The Journal of Physical Chemistry, **1925**, 29, 738-749.
- 80 Stureson, C.;Carlfors, J.;Edsman, K.;Andersson, M., *Preparation of biodegradable poly(lactic-co-glycolic) acid microspheres and their in vitro release of timolol maleate*. International Journal of Pharmaceutics, **1993**, 89, 235-244.
- 81 Jelvehgari, M.;Montazam, S. H., *Comparison of microencapsulation by emulsion-solvent extraction/evaporation technique using derivatives cellulose and acrylate-methacrylate copolymer as carriers*. Jundishapur Journal of Natural Pharmaceutical Products **2012**, 7, 144-52.
- 82 Ramesh, D. V., *Comparison of Oil-in-Oil, Water-in-Oil-in-Water and Melt Encapsulation Techniques for the Preparation of Controlled Release B12 Poly (ϵ -caprolactone) Microparticles*. Trends in biomaterials & artificial organs, **2009**, 23.
- 83 Iwata, M.;McGinity, J. W., *Preparation of multi-phase microspheres of poly(D,L-lactic acid) and poly(D,L-lactic-co-glycolic acid) containing a W/O emulsion by a multiple emulsion solvent evaporation technique*. Journal of Microencapsulation, **1992**, 9, 201-14.
- 84 Zheng, T.;Pilla, S., *Encapsulating Hydrophilic Solution by PU-PMF Double-Component Capsule Based on Water-In-Oil-In-Oil Emulsion Template*. Macromolecular Chemistry and Physics, **2018**, 219, 1700418.
- 85 Attaei, M.;Loureiro, M. V.;Vale, M.;Condeço, J.;Pinho, I.;Bordado, J. C.;Marques, A. C., *Isophorone Diisocyanate (IPDI) Microencapsulation for Mono-Component Adhesives: Effect of the Active H and NCO Sources*. Polymers, **2018**, 10, 825.
- 86 Bagheri Kashani, M.;Salimi, A.;Zohuriaan-Mehr, M. J.;Hanifpour, A., *Preparation of poly (urea-formaldehyde) microcapsules for use in capsular adhesive*. Journal of Polymer Research, **2019**, 26, 270.
- 87 Yuan, L.;Liang, G.-Z.;Xie, J.-Q.;Guo, J.;Li, L., *Thermal stability of microencapsulated epoxy resins with poly(urea-formaldehyde)*. Polymer Degradation and Stability, **2006**, 91, 2300-2306.
- 88 Celestine, A.-D. N.;Sottos, N. R.;White, S. R., *Autonomic healing of PMMA via microencapsulated solvent*. Polymer, **2015**, 69, 241-248.
- 89 Zhang, B.;Zhao, Y.;Sun, X.;Fei, X.;Wei, W.;Li, X.;Liu, X., *Microcapsules derived from Pickering emulsions as thermal latent curing accelerator for epoxy resins*. Journal of Industrial and Engineering Chemistry, **2020**, 83, 224-234.
- 90 You, X.;Wang, B.;Xie, S.;Li, L.;Lu, H.;Jin, M.;Wang, X.;Zhou, G.;Shui, L., *Microfluidic-Assisted Fabrication of Monodisperse Core-Shell Microcapsules for Pressure-Sensitive Adhesive with Enhanced Performance*. Nanomaterials, **2020**, 10.
- 91 Ni, D.;Luo, Y.;Cong, Y., *Polyamine microcapsules featured with high storage stability used for one-component epoxy adhesive*. Journal of Applied Polymer Science, **2021**, 138.
- 92 Messersmith, R. E.;Bartlett, M. E.;Rose, D. J.;Smith, D. A.;Patchan, M. W.;Benkoski, J. J.;Trexler, M. M.;Hoffman, C. M., *Rapid Underwater Adhesive Utilizing Crosslinker and Amine Catalyst-Filled Microcapsules*. **2021**, 3, 996-1002.
- 93 Lubis, M. A. R.;Park, B.-D.;Lee, S.-M., *Microencapsulation of polymeric isocyanate for the modification of urea-formaldehyde resins*. International Journal of Adhesion and Adhesives, **2020**, 100, 102599.

Chapter III

Testing and characterization

Chapter III - Testing and characterization

III.1 Emulsions testing and characterization

The stability of the O/W emulsion systems is directly correlated with the size and size distribution of the MCs. For that purpose, emulsions were evaluated both under static and dynamic conditions, by optical microscopy and sedimentation tests. The following tests were used to evaluate the O/W emulsions that were combined with the interfacial polymerization process for the achievement of the MCs.

III.1.1 Optical microscopy

An optical microscope, Kruss MSZ 5600 (Hamburg, Germany) was used to evaluate the emulsion stability and droplets' size variation over time. The emulsions were studied both while at rest (static conditions) and during the MCs' synthesis (dynamic conditions), subject to a stirring at 400 rpm, for a maximum of 30 minutes. Interfacial polymerization reactions take place at the emulsion droplets surface, and it is not possible to guarantee that no solid film has been formed after that time. For the emulsion evaluation under static conditions, photographs were taken after 10 minutes of emulsification and after 20 minutes at rest, which corresponds to 30 minutes of synthesis. For the evaluation at dynamic conditions, the photos were taken after 10 minutes of emulsification and after 15 minutes under mechanical agitation, which is equivalent to 20 minutes of synthesis. The photographs were used to determine the average diameter and size distribution of the emulsion droplets, using the Fiji software in a sample of 100 droplets per image [1].

III.1.2 Emulsion stability – Sedimentation tests

Gravitational separation is one of the most common emulsion instability mechanisms when the two phases have a significant density disparity, and, in particular for O/W emulsions, creaming is the most predominant phenomenon [1]. Due to this, the creaming index (CI) is usually used to study O/W emulsions stability, by using the following Equation 1:

$$CI = 100 \frac{H_S}{H_E} \quad \text{Equation 1}$$

where H_s is the height of the serum layer and H_e the total height of the emulsion [2].

However, the emulsion gravitation separation was evaluated by calculating the sedimentation volume fraction instead of the CI, for two main reasons: i) isocyanates lead to such an increase of the O phase density that it surpasses that of the W phase, with a consequent tendency for the droplets to move downwards (sedimentation) [1, 3]; ii) the emulsions are polydisperse in terms of droplet size distribution, having different sedimentation velocities, as schematically represented in Figure III.1. The smaller droplets remain dispersed in the upper part of the emulsion during a prolonged time not allowing to form a clean serum layer during the time of the study, which is required for the CI calculation [4].

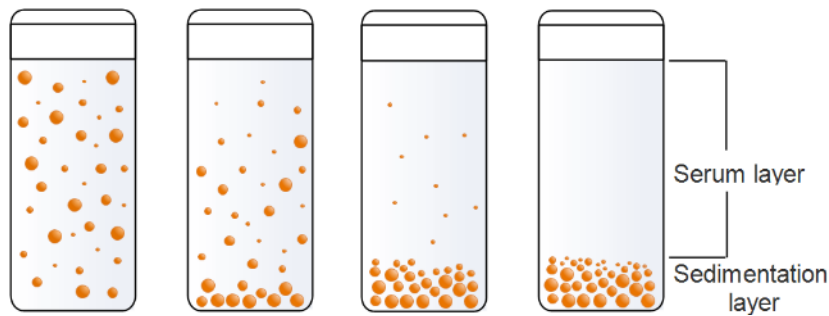


Figure III.1. Schematic representation of the sedimentation phenomenon observed in a polydisperse emulsion system. The dispersed phase of the emulsion is represented by orange spheres, which corresponds to the oil phase of the emulsion, composed by the isocyanates. Image reprinted from [5].

For these reasons, instead of the CI it was determined the sedimentation volume fraction of the emulsion, by using the following Equation 2:

$$\text{Sedimentation} = \frac{\pi \times r^2 \times h_0}{\pi \times r^2 \times h} \quad \text{Equation 2}$$

where h is the total height of the initial emulsion in the vessel, h_0 is the height of the sediment formed at the bottom, as depicted in Figure III.2, and r is the radius of the vessel used to calculate the volume.

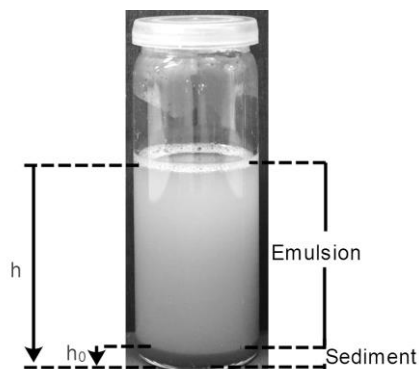


Figure III.2. Visual explanation of the h (total height of the initial emulsion) and h_0 (height of the sediment) used for Equation 2.

For the sedimentation tests, the emulsions were prepared using an organic dye, Oil Red O dye (Sigma Aldrich, USA) in the O phase, to better distinguish both phases. After the emulsification, a 30 ml sample was collected to a vessel of 2.6 cm of diameter by 7.7 cm of height. The collected sample was let at rest and followed for 30 minutes. During that time photographs were taken at periodic intervals of 1 minute, during the first 5 minutes, and then every 2 minutes. The photographs were used to calculate the sedimentation volume fraction of the emulsion.

III.1.3 Viscosity

The viscosity of the W phase of the emulsions systems were measured to understand its effect on the emulsion stabilization. For that purpose, it was used a BROOKFIELD DV-II+Pro digital viscosimeter, with a CFE - 52 spindle, at a speed of 60 rpm and a temperature of 20 °C. All the measurements were made in triplicate.

III.2 Microcapsules testing and characterization

In the course of this work, the MCs were characterized according to their morphological characteristics, their core content, shelf-life, chemical resistance, behavior in the adhesive pre-polymer and capacity to release its content during the adhesive application.

The morphological characterization of the MCs, namely its morphology type, physical shape, size and size distribution, were accessed by microscopy techniques. The MCs chemical composition, quantification of its core content and shelf-life were confirmed by Fourier transform infrared

spectroscopy, thermogravimetric analysis, and its derivative. Differential scanning calorimetry were used to confirm the melting temperature of the MCs' shell as well as the MW of the polymers used for its MCs' production.

III.2.1 Optical microscopy

Optical microscopy was used during the MCs production process, to evaluate the emulsion' droplets size and stability, as well as to assess the MCs' shell maturity during the process, i.e. its rigidity, which enabled to qualitatively evaluate its capacity to endure the vacuum filtration process. For bigger sized MCs, its final morphology was, in some cases, accessed by optical microscopy, however scanning electron microscopy was the preferred technique for that purpose.

The optical microscope used was a Kruss MSZ 5600 optical microscope (Hamburg, Germany).

III.2.2 Scanning electron microscopy (SEM)

SEM was used to characterize the MCs regarding its morphological type, shell' roughness, porosity, shell thickness, average diameter and size distribution. For that purpose, the samples were immobilized in a sample holder by using a conductive double-sided adhesive tape and coated with a conductive 15 nm layer of gold-palladium (Au/Pd) thin film, through sputtering, by using a turbomolecular pumped coater, Quorum Technologies sputter coater, model Q150T ES (Lewes Road, Laughton, UK). The average diameter, size distribution, and shell thickness of the MCs were evaluated using photomicrographs obtained through SEM and employing the Fiji software in a sample of 100 MCs [6].

Three different SEM equipment's were used, namely:

A field emission gun scanning electron microscope FEG-SEM operating at 15 kV, JEOL JSM7001F (JEOL, Tokyo, Japan). The elemental analysis over the MCs' sample was carried out using an Oxford Energy Dispersive Spectrometer (EDS) light elements detector, model INCA 250.

An analytical scanning electron microscope, model Hitachi S2400 (Chiyoda, Tokyo, Japan), with Bruker light elements EDS detector.

A Phenom ProX G6 benchtop SEM (ThermoScientific, Waltham, MA, USA) equipped with an EDS with integrated element identification (EID) software.

III.2.3 Fourier transform infrared spectroscopy (FTIR)

FTIR spectroscopy was used to confirm the chemical structure of the MCs' shell and to assess the relative encapsulation yield (Y value), which represents an indirect measure of the isocyanate encapsulation efficiency, used to evaluate the shelf-life of the MCs. For that purpose, the FTIR spectra were obtained at 4 cm⁻¹ resolution and 8 scans of data accumulation, between 500 and 4000 cm⁻¹.

The following Equation 3 was used to determine the Y value:

$$Y = \frac{Area_{NCO (2260\text{ cm}^{-1})}}{Area_{shell (x)}} \quad \text{Equation 3}$$

where Y is considered a relative, indirect measure value of the isocyanate encapsulation efficiency, $Area_{NCO (2600\text{ cm}^{-1})}$ the area of the isocyanate' NCO peak and $Area_{shell (x)}$, the area of a peak regarding the MCs' shell that does not significantly change over time. For PU and PUa MCs, it was used the area of the peak at 1300 cm⁻¹ related to the C-O stretching vibration and, for the PCL and PHB MCs' the area of the peak at 1720 cm⁻¹ related to the polymer's carbonyl group. The FTIR peaks areas were obtained by using the Origin Pro 2016 software [7]. The Y value and the corresponding methodology herein described to calculate it, have been previously reported in published papers under my co-authorship [5, 8-10].

By comparing the Y value obtained after the MCs synthesis with that of the 3 months old MCs, it is possible to conclude about its shelf-life, directly related to the shell permeability to moisture. If the MCs' shell does not offer enough protection, moisture can diffuse to the MCs interior and react with the free NCO groups, leading to a loss of encapsulated compound, together with an increase of the shell's thickness and a decrease of the Y value.

The FTIR equipment used was a Spectrum Two from PerkinElmer (Waltham, MA) equipped with a UATR Two accessory.

III.2.4 Thermogravimetric analysis (TGA)

TGA resulting thermograms and its derivative curves (DTG) were used to quantify the amount of the MCs' core content and to conclude about its aging, as well as to corroborate the FTIR findings regarding the MCs' composition. The analyses were performed under a controlled nitrogen atmosphere with a flow of 200 mL/min, at a temperature increase rate of 10 °C/min, in the range 30–600 °C. The equipment used was a Hitachi STA 7200 Thermal Analysis System (Ibaraki, Japan).

III.2.5 Gel permeation chromatography (GPC)

GPC enabled to study the MW of the polymers used to obtain the MCs' shell, namely of the PCL and PHB, and to evaluate the effect of the microencapsulation process on the MW of the polymeric MCs' shell. For that purpose, all the samples were prepared at a concentration of 5 g/L in tetrahydrofuran (THF). The calibration curve was established by using polystyrene standards from PSS – Polymer Standards Service GmbH. For the analysis it was followed an isocratic method using THF as the mobile phase at a flow rate of 1 mL/min at 40 °C.

The equipment used was a Jasco system (Tokyo, Japan) equipped with a refractive index detector, model RI4030 and an ultraviolet-visible (UV-Vis) detector, model UV-4070 (set at 254 nm). The equipment is equipped with a SDV (styrene-divinylbenzene) precolumn and a set of two SDV linear columns.

III.2.6 Differential scanning calorimetry (DSC)

The DSC analysis enabled to confirm the melting temperature of the PCL polymer, used for the MCs' shell fabrication. The DSC analyses were performed using a DSC Q200 V24.4 differential scanning calorimeter, from TA Instruments (New Castle, Delaware, USA) under a controlled nitrogen atmosphere with a flow of 50 mL/min and a temperature increase rate of 10 °C/min, in the range of 20 to 300 °C.

III.2.7 MCs' behavior to temperature

To evaluate the thermos-responsive MCs behavior to temperature, two different tests were performed:

In a first test the MCs were placed in an oven at 30 °C and exposed to increasingly higher temperatures, until melted. This enabled to confirm the maximum temperature at which the MCs can be exposed without melting. The oven's temperature was increased by 10 °C each hour and the MCs were optically evaluated.

In a second test, the MCs were added to an adhesive pre-polymer formulation, which contains OH groups available to react (OH pre-polymer), supplied by CIPADE S.A (São João da Madeira, Portugal), and exposed to 50 °C in an oven. This test enabled to study the responsiveness of the MCs' shell to temperature. The melting of the MCs' shell leads to the isocyanate release and contact with the OH pre-polymer with consequent formation of urethane crosslinks, which

contributes to an increase of the pre-polymer viscosity. The viscosity of the pre-polymer was monitored along the time, including that of reference samples which consisted of only the pre-polymer, without MCs, exposed to both 50 °C and at RT. The viscosities were measured every 10 minutes, during a period of 1 hour, at 27 °C, using a multi speed digital cone and plate viscometer with variable control, from REL (London, United Kingdom).

Bibliography:

- 1 McClements, D. J., *Critical review of techniques and methodologies for characterization of emulsion stability*. Critical Reviews in Food Science and Nutrition, **2007**, 47, 611-49.
- 2 Grumezescu, A.;Oprea, A., *Nanotechnology Applications in Food - Flavor, Stability, Nutrition and Safety*. 1st Edition ed. **2017**: Elsevier Inc.
- 3 Schindelin, J.;Arganda-Carreras, I.;Frise, E.;Kaynig, V.;Longair, M.;Pietzsch, T.;Preibisch, S.;Rueden, C.;Saalfeld, S.;Schmid, B.;Tinevez, J. Y.;White, D. J.;Hartenstein, V.;Eliceiri, K.;Tomancak, P.;Cardona, A., *Fiji: an open-source platform for biological-image analysis*. Nat Methods, **2012**, 9, 676-82.
- 4 *Origin(Pro), Version 2016*. OriginLab Corporation, Northampton, MA, USA.
- 5 Loureiro, M. V.;Mariquito, A.;Vale, M.;Bordado, J. C.;Pinho, I.;Marques, A. C., *Emulsion Stabilization Strategies for Tailored Isocyanate Microcapsules*. Polymers (Basel), **2023**, 15.
- 6 Kopinke, F. D.;Remmler, M.;Mackenzie, K., *Thermal decomposition of biodegradable polyesters—I: Poly(β -hydroxybutyric acid)*. Polymer Degradation and Stability, **1996**, 52, 25-38.
- 7 *Scaling Up a Rotor-Stator Homogenization Process*. **2019**; Available from: <https://homogenizers.net/blogs/blog/rotor-stator-homogenization-scaleup>.
- 8 Attaei, M.;Loureiro, M. V.;Vale, M.;Condeço, J.;Pinho, I.;Bordado, J. C.;Marques, A. C., *Isophorone Diisocyanate (IPDI) Microencapsulation for Mono-Component Adhesives: Effect of the Active H and NCO Sources*. Polymers, **2018**, 10, 825.
- 9 Loureiro, M. V.;Attaei, M.;Rocha, S.;Vale, M.;Bordado, J. C.;Simões, R.;Pinho, I.;Marques, A. C., *The role played by different active hydrogen sources in the microencapsulation of a commercial oligomeric diisocyanate*. Journal of Materials Science, **2020**, 55, 4607-4623.
- 10 Loureiro, M. V.;Vale, M.;Galhano, R.;Matos, S.;Bordado, J. C.;Pinho, I.;Marques, A. C., *Microencapsulation of Isocyanate in Biodegradable Poly(ϵ -caprolactone) Capsules and Application in Monocomponent Green Adhesives*. ACS Applied Polymer Materials, **2020**, 2, 4425–4438.

Chapter IV

Interfacial polymerization technique in combination with a microemulsion system

Chapter IV - Interfacial polymerization technique in combination with a microemulsion system: Reactional parameters and strategies

This chapter exposes the production of MCs by the interfacial polymerization technique in combination with an O/W microemulsion system. By this technique, the MCs synthesis occur due to polymerization reactions on the emulsion droplets interface, which leads to the formation of the polymeric shell. Several strategies and reactional parameters optimizations are reported in this chapter, intended to improve the MCs final characteristics in particular to increase its encapsulation yield and shelf-life as well as to reduce the MCs size distribution. A laboratorial scale-up of the MCs production process is also described, which refers to an increase of the reactional volume from 1.5L to 10L.

Published papers with results exposed in this chapter:

- Loureiro, M. V.; Mariquito, A.; Vale, M.; Bordado, J. C.; Pinho, I.; Marques, A. C. "Emulsion Stabilization Strategies for Tailored Isocyanate Microcapsules", *Polymers* 15 (2023) 403. Doi: 10.3390/polym15020403

IV.1 Materials

The materials used for the MCs production, by the interfacial polymerization technique in combination with a microemulsion system, can be classified as isocyanates, active H sources, and emulsion stabilizers. All reagents used are listed in Table IV. 1 and the essential information regarding the isocyanates and the active H sources are described on Table IV.2 and Table IV.3 , respectively.

Table IV. 1. Reagents used in the MCs production by the interfacial polymerization technique, with the respective commercial name, purity, and manufacturer.

Classification	Chemical	Commercial name	Purity	Manufacturer
Isocyanate	Isophorone diisocyanate (IPDI)	Desmodur® I	98%	Covestro AG
	Methylene diphenyl diisocyanate (MDI)	Ongronat® 2500	-	BorsodChem
		Suprasec® 2234	-	CIPADE S.A.
	Toluene diisocyanate (TDI)	Desmodur® RFE	-	Covestro AG
		Desmodur® RC	-	CIPADE S.A.
Active H source	Polyetheramine	Jeffamine® D2000	-	Huntsman
	Poly(ethyleneimine (PEI)	-	≤99%	Sigma-Aldrich
	Triethoxy(octyl)silane (n-OTES)	-	97%	Sigma-Aldrich
	1,6-Hexanediol	-	97%	Acros Organics
Emulsion stabilizers	Gum arabic (GA)	-	>95	Fisher Chemical
	Poly(vinyl alcohol) (PVA)	-	-	Alfa Aesar
	Polyoxyethylenesorbitan Trioleate	Tween® 85	≥50% (GC)	Sigma-Aldrich
	Sorbitan laurate	Span® 20	≥44% (GC)	Fluka
	Poly(ethylene glycol)-block-poly(propylene glycol)-block-poly(ethylene glycol)	Pluronic®	-	Sigma-Aldrich
		P 123	-	Sigma-Aldrich
-	Dabco® DC193	-	Air Products	

Table IV.2. Isocyanates used for the MCs synthesis by the interfacial polymerization technique and respective chemical structure, density, viscosity, NCO content and main properties.

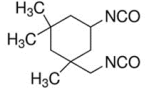
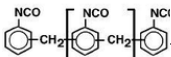
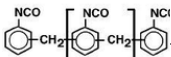
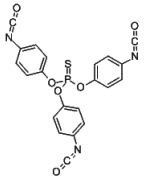
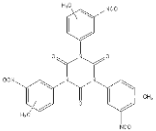
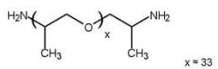
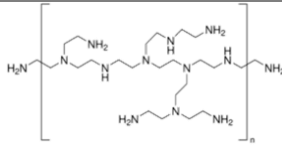
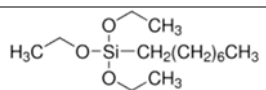
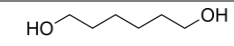
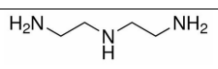
Commercial name	Chemical Structure	$\rho, 20^{\circ}\text{C}$ (g.cm-3)	$\eta, 20^{\circ}\text{C}$ (mPa.s)	NCO content (%)	Properties
Desmodur® I		1.049	15	≥ 37.5	Aliphatic diisocyanate with two isomers, cis and trans, with the same reactivity. Secondary -NCO group has a higher reactivity (for most cases) than the primary -NCO group.
Ongronat® 2500		1.24	520-680	30-32	Oligomeric MDI.
Suprasec® 2234		1.13	2500	15.9	Pre-polymeric MDI.
Desmodur® RFE		1.000	3	7.2 ± 0.2	Aromatic poly-isocyanate pre-polymer supplied as a solution of tris(p-isocyanatophenyl) thiophosphate (27%) in ethyl acetate.
Desmodur® RC		1.01	3	7.0 ± 0.2	Supplied as a solution of a poly-isocyanurate of TDI (35%) in ethyl acetate.

Table IV.3. Active H sources used for the MCs synthesis by the interfacial polymerization technique and respective chemical structure and type.

Name	Chemical Structure	Type of active H source
Polyetheramine (PEA) (Jeffamine® D2000)		Amine
Poly(ethyleneimine) (PEI)		Amine
Triethoxy(octyl)silane (n-OTES)		Silane (Latent active H source)
1,6-Hexanediol		Polyol
Diethylenetriamine (DETA)		Amine

IV.2 Experimental: MCs synthesis by Interfacial polymerization technique in combination with a microemulsion system

PUa and PU/PUa MCs were synthesized via an O/W microemulsion system combined with *in-situ* polymerization at the O/W droplets surface.

The synthesis of MCs by interfacial polymerization involves, at least, two reactants in a pair of immiscible liquids, which is typically achieved by an O/W micro-emulsion system. The continuous aqueous solution is composed by one or more reactants with NH or OH groups and at least one emulsion stabilizer, as for the dispersed phase it is composed by the isocyanates. To obtain the microemulsion, the two phases are mixed together and subjected to a high shear rate. This is followed by the diffusion of the reactants, which become in contact at the interface of the O droplets of the emulsion system and begin to react to form an initially thin PUa and/ or PU/PUa polymeric shell, composed mainly by oligomers or pre-polymeric species. The isocyanate reacts readily and quicker with water, resulting in the formation of an unstable carbamic acid intermediate that immediately decomposes to amine and CO₂ [1]. Amines react with isocyanates and are autocatalytic, further leading to PUa formation [1]. In case of polyols in the W phase, PU is also formed. With further polymerization reactions the thickness of the initially thin polymeric shell surrounding the O phase droplets increases in thickness until no more reactant species are allowed to be in contact. In this synthesis technique, the polymerization reactions are mostly controlled by the diffusion of the W phase reactants to the O phase of the emulsion, which leads to a decrease of the MCs' shell growth's rate as the shell

thickness increases. The main reactions that take place during the synthesis of MCs by interfacial polymerization are summarized in Figure II.8 and Figure IV.1.

In more detail, for the O/W microemulsion preparation, both phases were mixed under vigorous stirring, at 3400 rpm with the use of an Ultra-Turrax, IKA T25 digital (Germany), during 10 min at a predefined temperature. The microemulsion was then submitted to mechanical stirring, using an Heidolph RZR 2051 (Germany) mechanical stirrer, under a controlled temperature. After 10 minutes under mechanical agitation, the OH and or NH reactants, from now on designated as active H sources, were added to the emulsion. When the MCs' shell had attained enough maturity, they were filtrated using a vacuum filtration system, while washed with water. The final MCs were dried at atmospheric pressure and room temperature for 48 h before stored. The maturity of the MCs shell was constantly evaluated, during the time of the synthesis, by means of optical microscopy, using a Kruss MSZ 5600 optical microscope (Hamburg, Germany).

The general synthesis procedure is depicted in Figure IV.1.

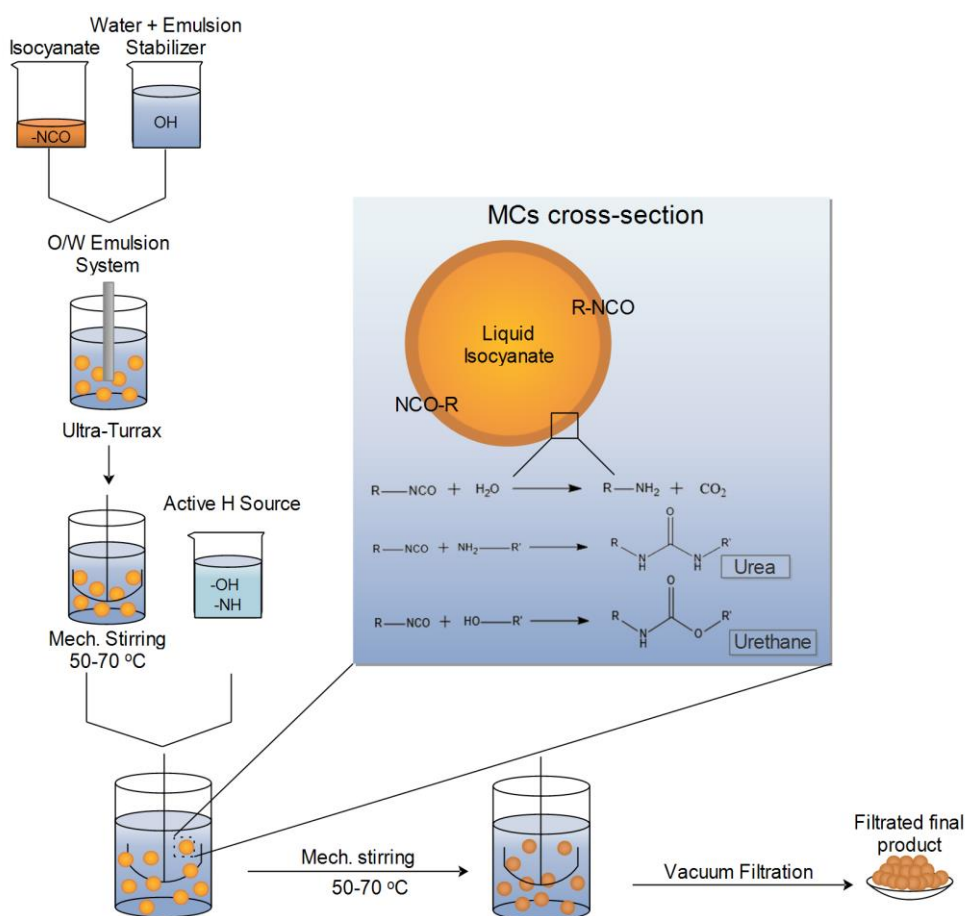


Figure IV.1. Schematic representation of the MCs' synthesis process by the interfacial polymerization technique combined with a micro-emulsion system.

There are several parameters which are considered as reactional variables. Table IV. 4 lists the ranges of temperature used, synthesis duration, emulsification time and mechanical agitation used. The choice of the synthesis temperature, duration and emulsification time was made having into consideration the reactivity of the isocyanates employed in the synthesis. The choice of the mechanical agitation to use was based on the viscosity and density of the O phase.

Table IV. 4. Reactional variables in the synthesis of MCs by interfacial polymerization technique and ranges used.

Reactional parameters	Ranges
Synthesis temperature	40 - 70 °C
Synthesis duration	1h – 5h
Emulsification time	5 – 10 minutes
Emulsification stirring	3200 rpm – 3600 rpm
Mechanical stirring	380 – 600 rpm

The isocyanates, active H sources and emulsion stabilizer used are described in Table IV.2 and Table IV.3.

A scale-up of the synthesis process is described in the sub-chapter “VI.4 Scale-up of the syntheses processes”. For that, a 10L water heated jacketed glass reactor was used and, for the heating system, a Huber (Offenburg, Germany) heating bath circulation thermostat, model CC-304B coupled with a thermal bath, at 30 °C. For the emulsification, an ULTRA-TURRAX (model T50, from IKA (Staufen, Germany)) was used. An ULTRA-TURRAX (model T50, from IKA (Staufen, Germany)) was used for emulsification.

IV.3 Results and discussion: Reactional parameters and strategies

The most reported technique for the isocyanates microencapsulation is by an O/W microemulsion system combined with interfacial polymerization. However, there are still some challenges regarding this process, particularly the usually wide size distributions of the obtained MCs, a low encapsulation yield, and short shelf-life. To decrease and control the MCs size distribution, several emulsion stabilizers, and different combinations between them, were tested. As for the encapsulation yield, the effect of the synthesis duration and temperature were tested, as well as the combined effect of using active H sources on the W phase and two different

isocyanates on the O phase of the emulsion. For the MCs' shelf-life, the effect of different isocyanates for the shell formation and different active H sources, to improve the MCs' shell hydrophobicity, were studied.

Figure IV.2 depicts the schematic representation of the strategies adopted to optimize the PUa and PU/PUa MCs obtained by interfacial polymerization technique.

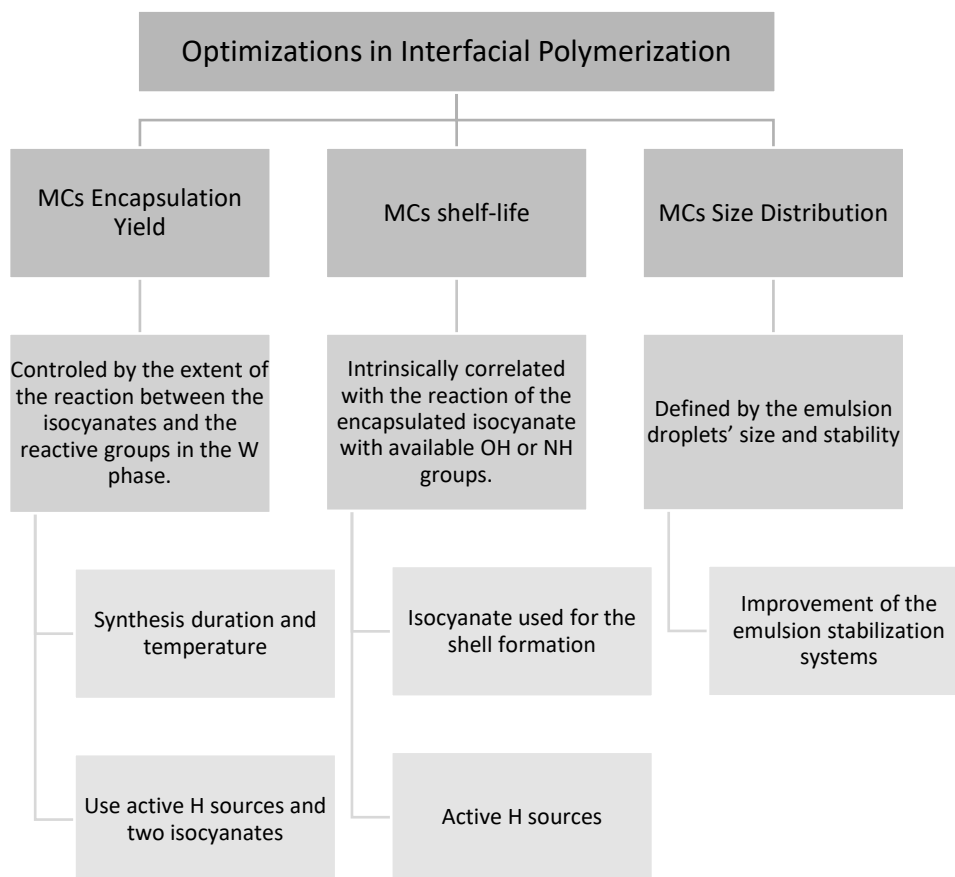


Figure IV.2. Schematic representation of the strategies adopted to optimize the MCs obtained by the interfacial polymerization technique.

IV.3.1 Synthesis duration and temperature

The MCs' shell formation occurs in two main steps. Primarily, an initial thin PUa and/or PU/PUa shell, composed by oligomers or pre-polymeric species, is formed, followed by an increase of the shell thickness, due to the continuing of the polymerization reactions. The extent of the reaction is controlled by diffusion, and the shell growth rate tends to decrease as the shell thickness increases [2, 3].

The influence of the synthesis duration on the MCs' shell thickness and morphology was assessed. For that, samples of MCs were filtrated at different times during syntheses done at 70 °C and at 30 °C, and evaluated by SEM. The syntheses were followed for 5h, and the samples collected after 30, 120 and 300 minutes. The reactants used for both syntheses were identical and are described in Table IV.5, as well as the reactional parameters, with exception of the temperature.

Table IV.5. Emulsion composition and active H source for the synthesis of the MCs used to study the effect of the synthesis duration on the MCs' shell thickness and morphology.

Water phase (wt%)	Oil phase (wt%)	Active H source (wt% of the W phase)
Water Gum arabic (93 wt% of the emulsion)	Ongronat® 2500 (Shell) IPDI (Core content) (7 wt% of the emulsion)	Diethylenetriamine (DETA) (4 wt%)

Figure IV.3 shows the evolution of the MC's size and the ratio of shell thickness to MC's diameter (S/D ratio) over the duration of the syntheses. The MCs' size was not significantly affected by the duration of the synthesis as its average size only varied ca. 11 µm during the process, for the synthesis at 30 °C, and 1.5 µm for the synthesis at 70 °C, which represents a variation of 17 and 1.9% of the overall MCs' size, respectively. On the contrary, the S/D ratio increased, mainly for the syntheses conducted at 30 °C. This can be explained by the necessary time for the shell to be formed, the quicker its formation the sooner the reactants diffusion tends to decrease as well as the shell growth rate. Indeed, higher temperatures promote the transfer of the aqueous reactants to the O phase by increasing its diffusion and partition coefficient which results into an increase in the reaction rate [3-5]. It is most likely that the initial barrier around the O emulsion droplets was formed earlier in the synthesis at 70 °C, slowing the condensation reactions and protecting the isocyanate to be encapsulated. These results confirm that the shell growth occurs inwards, consuming the isocyanate to be encapsulated.

After 5h of synthesis, the MCs obtained at 30 °C have several debris and show some aggregation, which is not observed for the MCs obtained at 70 °C, as depicted in Figure IV.4. This indicates that these MCs were still maturing and were not ready to undergo vacuum assisted filtration.

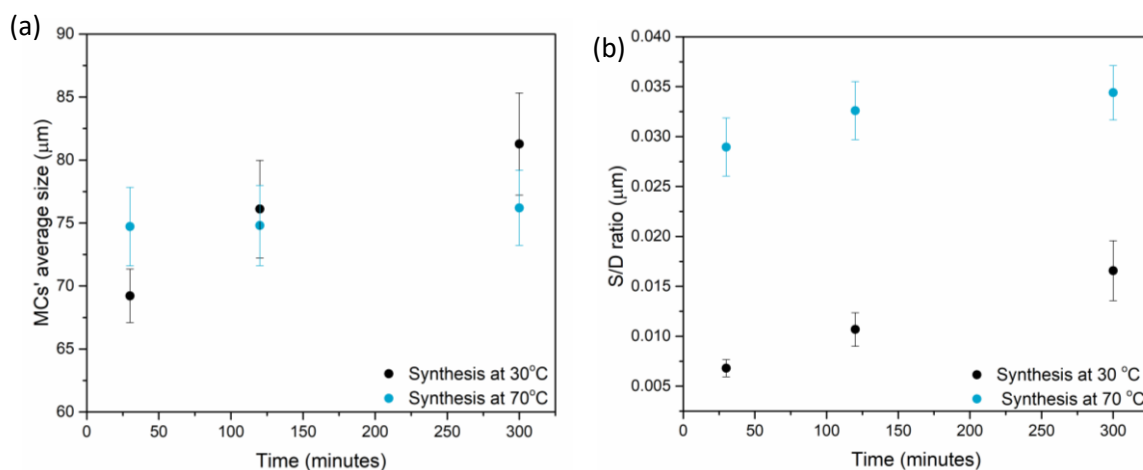


Figure IV.3. Results of MCs' average size (a) and S/D ratio (b), obtained at different times during the MCs synthesis at 30 °C and at 70 °C.

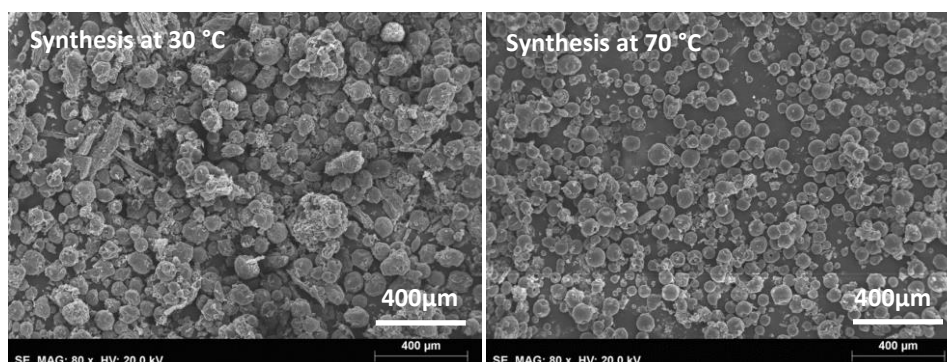


Figure IV.4. SEM photomicrographs of the MCs' obtained at 30 °C and at 70 °C.

In agreement with the obtained results, it was chosen to further use higher, rather than lower, temperatures for the MCs' synthesis.

In a second study, the effect of the synthesis duration on the MCs' encapsulation yield was evaluated. For that purpose, MCs' samples were collected during the synthesis and evaluated by FTIR, which was used to calculate the Y value. For this study, the reactants used for the synthesis are described in Table IV.6.

Table IV.6. Emulsion composition and active H source used for the synthesis of the MCs used to study the effect of the synthesis duration on the encapsulation yield.

Water phase (wt%)	Oil phase (wt%)	Active H source (wt% of the W phase)
Water Gum arabic (93% of the emulsion)	Desmodur® RC (Core content) (7% of the emulsion)	-

A very reactive polyisocyanurate of TDI, Desmodur® RC, was used both to be encapsulated and for the shell formation. The synthesis of these MCs is considerably quick, occurring in less than 15 minutes, due to this isocyanate high reactivity. To conclude about the synthesis duration effect, a sample was collected after 5, 8, 10 and 15 minutes from the beginning of the synthesis and evaluated by FTIR (Figure IV.5 (a)). The encapsulated isocyanate can be detected by the band peaked at ca. 2260 cm^{-1} , which corresponds to the N=C=O bond stretching vibration. The MCs' polymeric shell exhibits characteristic peaks at $1730\text{--}1715\text{ cm}^{-1}$ and at $1700\text{--}1680\text{ cm}^{-1}$, related to the presence of the PU and PUa carbonyl groups vibration peaks, respectively, at 1214 cm^{-1} , related to the presence of the C–O–C group, and at 1300 cm^{-1} , due to C–O stretching. The NCO peak, at 2260 cm^{-1} , its found to decrease in intensity with the progression of the synthesis and is no longer visible for the sample collected after 15 minutes, indicating that there is no more free, unreacted, isocyanate species. Figure IV.5 (b) shows the evolution of the Y value over the course of the synthesis, for which the value calculated for the MCs_5min. was considered to be 100%. It is clear the correlation between a longer duration of the synthesis and the decrease in the encapsulated content. Nevertheless, the maturity of the shell is also to consider. The first collected sample, MCs_5min., was evaluated over time, by FTIR-ATR (Figure IV.5(c)), while stored at room temperature and 60% of relative humidity. After the MCs filtration, the 2260 cm^{-1} peak has a significant intensity which rapidly decreases to be no longer detectable in the spectra of the MCs stored for a week, indicating that the MCs no longer had unreacted, encapsulated isocyanate after that period. This occurs due to the isocyanate reaction with OH or NH groups that might get in contact, usually OH groups from the air moisture that can enter the MCs interior through the shell.

By comparing the photomicrographs of the MCs obtained after 5 and 15 minutes of synthesis, Figure IV.6, the difference in the shell is notorious, with the 5min._MCs having holes in its surface, not visible in the 15min._MCs. This might have occurred due to the lack of time for a homogeneous shell to be formed and/or to the inability of the 5min._MCs to endure the vacuum filtration process.

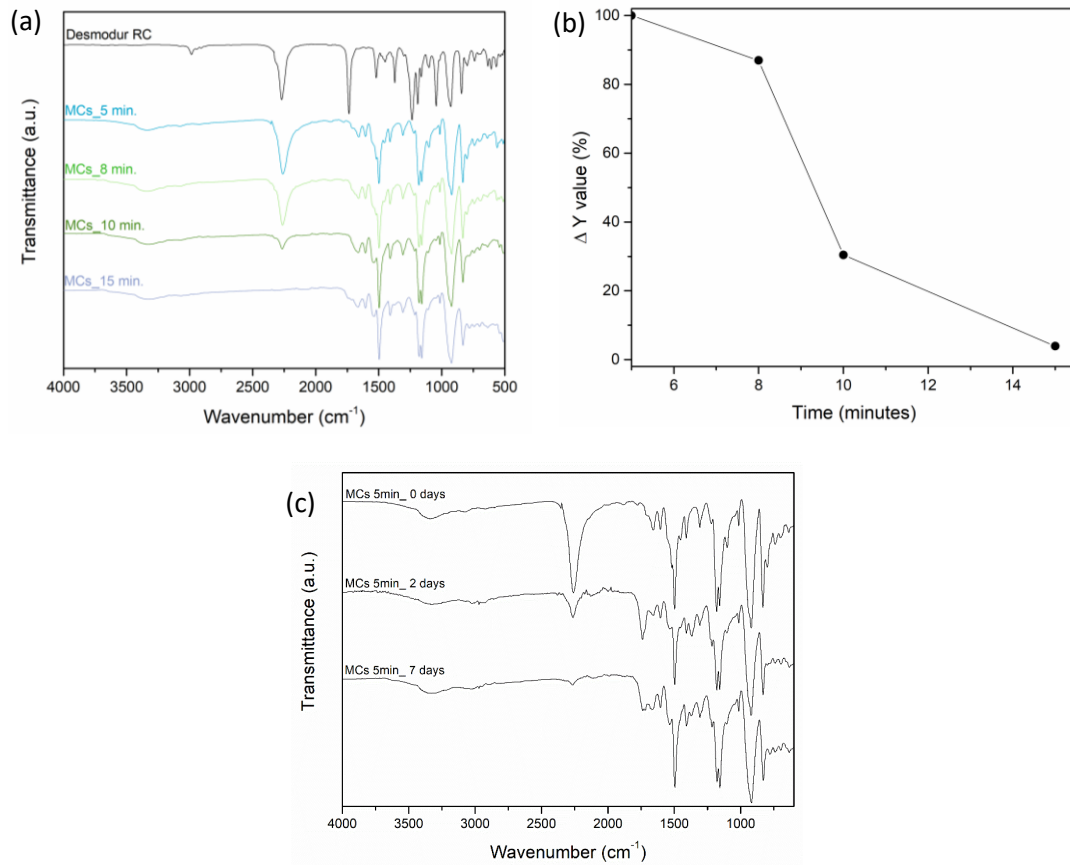


Figure IV.5. FTIR-ATR of MCs samples collected at different times during the synthesis (a). Variation of the Y value (b) and FTIR-ATR spectra of the MCs_5min. 2 and 7 days after the MCs' synthesis.

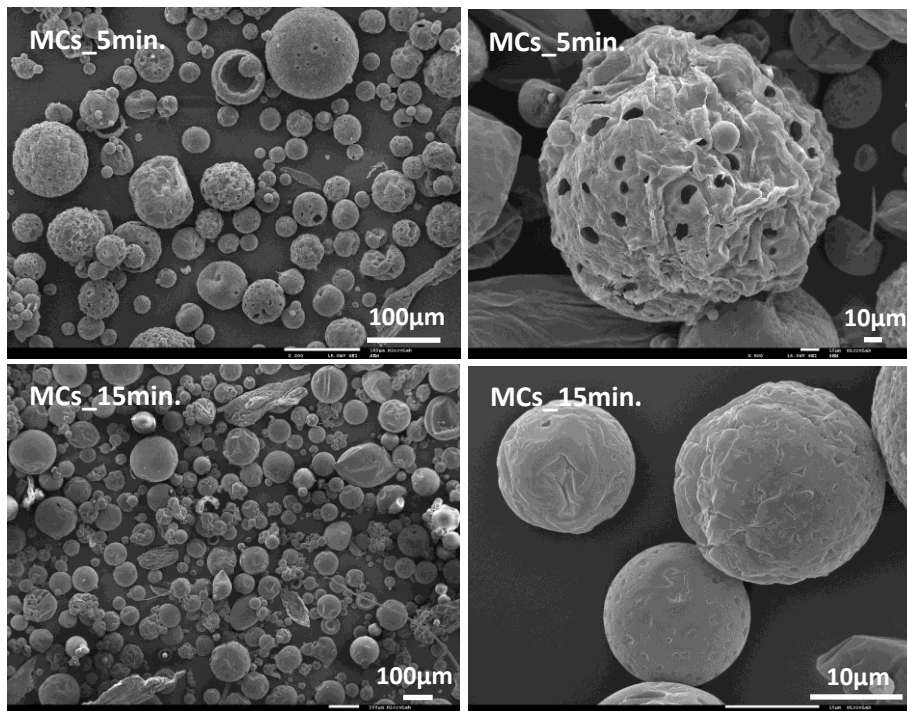


Figure IV.6. SEM photomicrographs of the MCs collected after 5 and 15 minutes of synthesis.

The duration of the MCs' synthesis has a notorious impact on the both the encapsulation yield and maturity of the MCs' shell, with longer reaction times leading to a lower isocyanate content and a more mature shell. It is essential to achieve a compromise between the optimum reaction time to achieve a sufficiently mature shell while enabling the encapsulation of a significant amount of unreacted isocyanate. It was implemented to filtrate several aliquots over the synthesis duration to better understand the moment at which the MCs can stand the vacuum assisted filtration process, and, as this, optimize the synthesis duration.

IV.3.2 Use of two isocyanates and active H sources

The synthesis of MCs by the interfacial polymerization technique involves the reaction of OH or NH groups, present in the emulsion W phase, with the isocyanates of the O phase. The higher the extent of the reaction the lower the available encapsulated isocyanate. Aimed at increasing the encapsulation yield, the use of two isocyanates in the O phase of the emulsion, one to be encapsulated and the other, the most reactive, to form the shell, was tested. To complement this strategy, active H sources were added to the aqueous phase of the emulsion, as an attempt to lead to a quicker initial shell formation. This initial and immature shell reduces the diffusion of water species into the O phase of the emulsion and decreases the extent of the shell formation, ideally contributing to a higher encapsulation content. The use of active H sources can also impact the morphology and final properties of the MCs. Molecules with different structures can influence the morphology, porosity, permeability, and thermal and mechanical resistance of the shell, which have an impact on the release performance and/or the shelf-life of the MCs [2]. Active H sources with a higher functionality have more readily available sites for reaction, leading to a higher degree of cross-linking and, therefore, an increased hardness of the shell. Linear structures decrease the mechanical resistance of shell. On the other hand, branched active H sources lead to a thicker shell formation due to the presence of bulkier groups. It is therefore important to have the chemical structure of the active H source into consideration during its selection, to meet the required specifications for the MCs.

This combined strategy was studied on the encapsulation of Suprasec®2234 and later used for the encapsulation of Ongronat® 2500. Suprasec®2234 is a pre-polymeric MDI, which makes its encapsulation particularly difficult, due to its higher reactivity and a high viscosity, of 2500cP. Usually, for these cases, organic solvents are added to the O phase of the emulsion, to decrease its viscosity [6, 7]. The isocyanate used for the shell formation was Desmodur® RC which is a poly-isocyanurate of TDI with a low free NCO value, supplied in 75% of ethyl acetate, and a

viscosity of 3cP. Its low viscosity contributes to decrease the one of the O phase, avoiding the need for extra organic solvent.

The SEM images and respective size distribution of the MCs obtained with one and two isocyanates in the O phase are shown in Figure IV.7. The decrease of the O phase viscosity (Suprasec® 2234 and Desmodur® RC) has a positive impact on the MCs' morphology. They exhibit a narrower and monomodal size distribution. It has been reported that emulsions with less viscous dispersed phase lead to MCs with narrower size distributions, as opposed to those with a higher viscosity [8]. As the dispersed phase viscosity increases, the size of the largest and smallest drops tends to increase and decrease, respectively. For higher viscosities there is some resistance for the droplets to deform under shear rate and an increased difficulty for the emulsion stabilizers to adsorb around the emulsion droplets, resulting in larger droplets [9-11]. The formation of smaller sized droplets seems to be correlated with the droplets rupture, by pressure, by drop-vortex collisions or by its elongation into threads prior to the break-up, due to viscous stresses [10, 12].

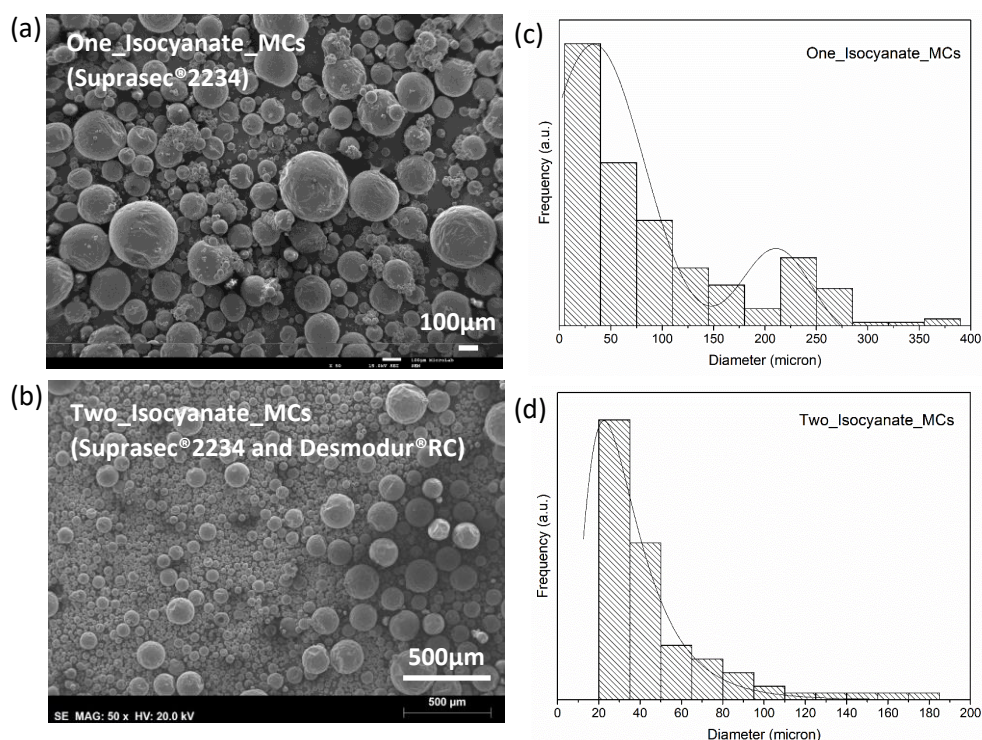


Figure IV.7. SEM photomicrographs of the MCs obtained with one and with two isocyanates (a) and (b) in the O phase of the emulsion, respectively. Respective size distribution (c) and (d).

When encapsulating pre-polymeric isocyanates, it is difficult to accurately quantify the encapsulation content by thermogravimetric techniques, as there are overlaps of thermal events from the MCs' core content and the shell. Due to this, the encapsulation of

Suprasec®2234 and the MCs' shelf-life was evaluated by FTIR, using the relative encapsulation yield (Y). The FTIR spectra of the MCs obtained with one and two isocyanates in the O phase of the emulsion are exposed in Figure IV.8. Unfortunately, for this case, it is not possible to compare the Y value between the two samples in study as the backbone of the isocyanates used for the shell formation is different, which will influence the wavenumber and intensity of the respective peaks. However, it is possible to state that the MCs to which were added two isocyanates had a significantly higher encapsulation content, confirmed by the differences in the N=C=O bond stretching peak vibration, at 2260 cm^{-1} .

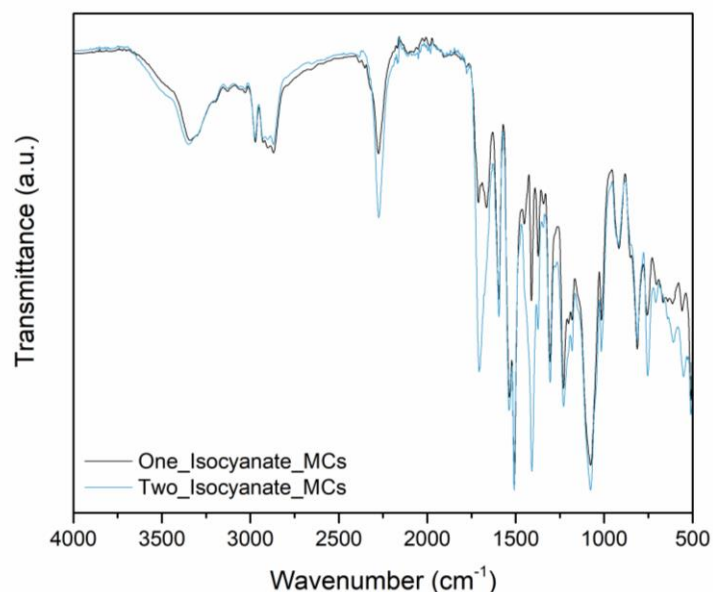


Figure IV.8. FTIR-ATR spectra of the MCs obtained with one and with two isocyanates in the O phase of the emulsion.

In addition to the use of two isocyanates in the O phase of the emulsion, it was tested the addition of several active H sources, and combinations, in the W phase. Table IV.7 lists the synthesis compositions for the MCs to which active H sources were added, as well as for a reference. All syntheses were carried out under the same emulsification and mechanical stirring velocities, temperature range, organic and aqueous mixture, and so it is reasonable to assume that the morphological and encapsulation yield differences among samples are due to the different active H sources. It is to notice that the maturity of the MCs was continuously evaluated during the synthesis and so the reactions times were optimized for each case.

Table IV.7. Microcapsules' acronyms and emulsion composition.

MCs acronym	Water phase (wt%)	Oil phase (wt%)	Active H source (wt% of the W phase)	Time of synthesis
Ref_MCs			-	2h20
n-OTES_MCs			n-OTES (0.72 wt%)	1h45
Hexanediol_MCs			1,6-Hexanediol aqueous solution at 5 0wt% (5.8 wt%)	2h10
	Water	Suprasec® 2234 (Core content)		
PEI_MCs	Gum arabic (89% of the emulsion)	Desmodur® RC (Shell)	Aqueous solution of PEI at 17 wt% (2.2 wt%)	1h40
Jeffamine_MCs		(11% of the emulsion)	Aqueous solution of Jeffamine D 2000 at 17wt% (2.2 wt%)	1h20
PEI_n-OTES_MCs			Aqueous solution of PEI at 17 wt% (2.2 wt%) n-OTES (0.72 wt%)	1h50

Three different types of active H sources were tested, namely a silane, a polyol and polyamines. The isocyanate NCO groups react with the OH or NH groups from the active H sources to form urethane or urea moieties, respectively. The main factor influencing the activity and reaction of these chemicals in emulsions are their solubility and diffusion rate towards the emulsion droplets interface [13]. Reactions in emulsions interfaces can be controlled by diffusion or by activation. Reactions with a low activation energy are controlled by diffusion, as its reaction time is negligible in comparison with that required for the diffusion of the molecules to occur. For cases with reaction times much higher than those required for the diffusion of the reactants, the reactions are controlled by activation [13].

The reaction of the isocyanates NCO group with NH groups has a higher reaction rate than that with OH groups. Silanes can be considered “latent” active H sources, since, when added to the synthesis, they are not readily able to react. It is expected that the n-OTES addition to the W phase would lead to its alkoxy groups hydrolysis, with the formation of silanol groups. These may react among each other by polycondensation reactions, leading to the formation of siloxane

moieties, but also with the isocyanate' NCO groups leading to the formation of urethane moieties, forming a PU/PUa/Silica hybrid shell.

The photomicrographs of the obtained MCs are displayed in Figure IV.9, where a general view of each sample is displayed. All the syntheses led to loose, disaggregated MCs, with a fairly spherical shape, however with distinct size distributions. Both MCs to which the n-OTES was added show some roughness. Its 8-carbon aliphatic chain of hydrophobic nature, have low affinity with the W phase and might contribute to local inhomogeneous compositions and reaction kinetics, together with the different diffusion rates of the active H sources, water and isocyanates present in the O phase [14, 15]. This different reaction kinetics and diffusion rates might have contributed to the roughness of the shell.

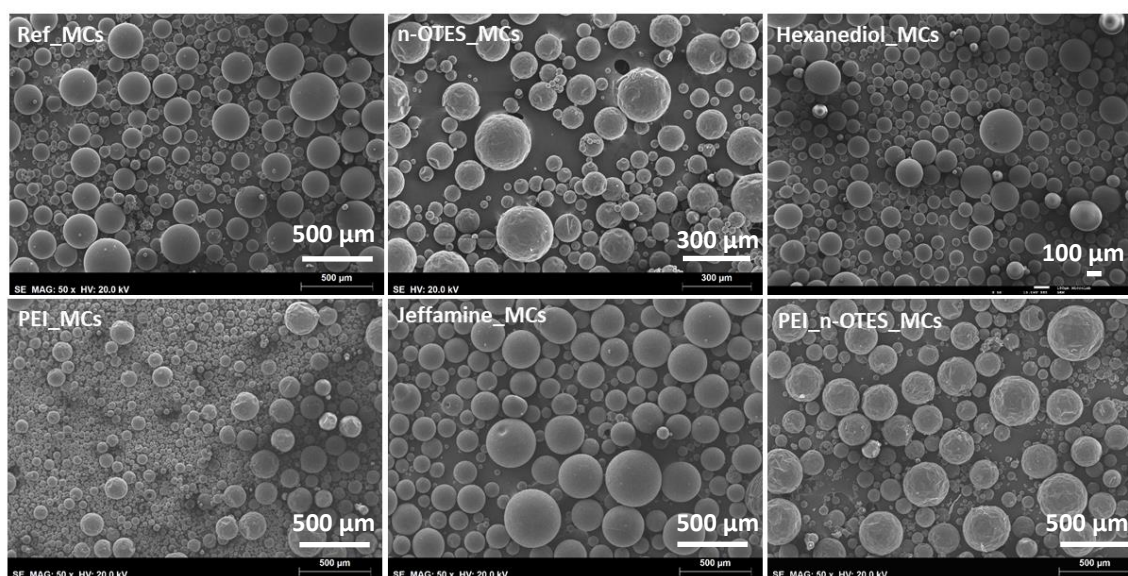


Figure IV.9. SEM photomicrographs of the MCs obtained using different active H sources as well as the Ref_MCs, for which it was not added any active H source during the synthesis.

On Figure IV.10 are a photomicrograph of a broken MCs, on the left, and of a broken shell, on the right, confirming its core-shell morphology, which is the desired morphology that enables a higher encapsulation content.

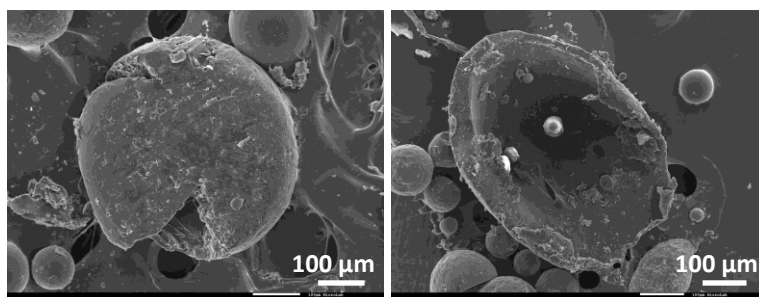


Figure IV.10. SEM photomicrographs of a purposefully broken MC (left) and of half a MCs' shell (right).

Figure IV.11 depicts the size distribution histograms for all the MCs in study, and in Table IV.8 the maximum value for each case, which corresponds to the mode of the MCs sizes. The presence of n-OTES as “latent” active H source was found to lead to a multimodal and more heterogeneous MC’s size distributions, while the Ref_MCs and the PEI_MCs are the ones showing a lower heterogeneity. N-OTES might lead to a less stable emulsion, due to its hydrophobicity and its tendency to lead to local inhomogeneous compositions and reaction kinetics. The same phenomena might have occurred with the addition of Jeffamine® D2000, due to its repeating oxypropylene hydrophobic backbone, as this MCs also have a broad size distribution comparing not only to the Ref_MCs but also to the ones to which PEI and Hexanediol were added.

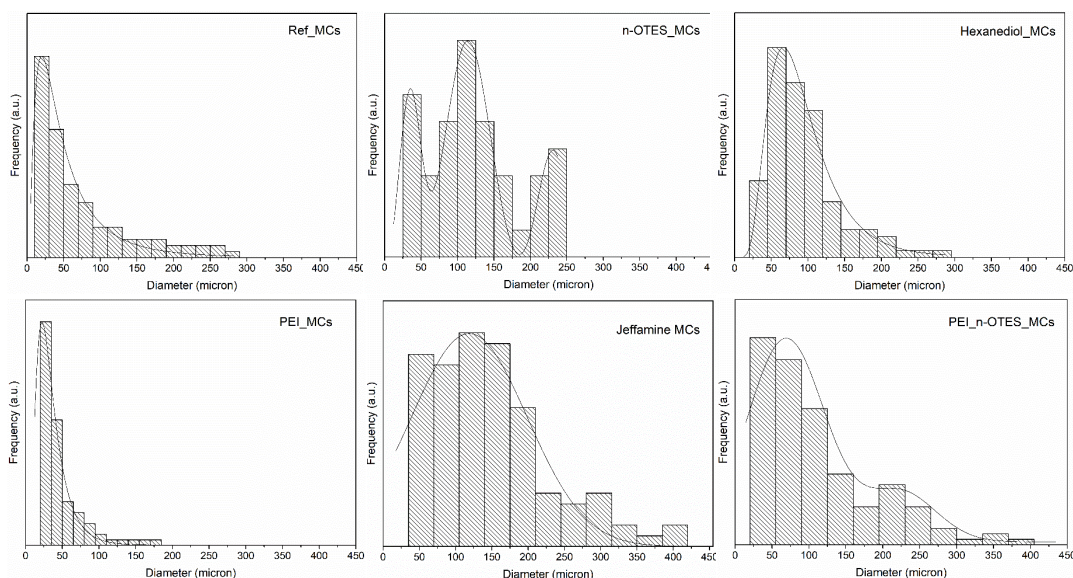


Figure IV.11. Size distribution histograms of the MCs obtained with different active H sources, as well as the Ref_MCs, to which it was not added any active H source during the synthesis.

Table IV.8. Maximum value (mode) obtained in the MC's size distribution histogram.

MCs' acronym	Ref_ MCs	n-OTES_MCs	Hexanediol_MCs	PEI_MCs	Jeffamine_MCs	PEI_n-OTES_MCs
MC's diameter (mode) (μm)	21.5	38.8 112.9 237.1	60.1	28.6	119.4	40.4 212.5

The FTIR spectra of the MCs as well as those of the active H sources and unreacted isocyanates are exposed in Figure IV.12. The presence of an intense band peaked at ca. 2260 cm^{-1} , in all the MCs' spectra, related to the presence of a N=C=O bond stretching vibration, confirms the presence of encapsulated, unreacted, isocyanate species. The PU and PUa MCs' shell composition is confirmed by the presence of its carbonyl groups vibration peaks, detected at $1730\text{--}1715\text{ cm}^{-1}$ and at $1700\text{--}1680\text{ cm}^{-1}$, respectively, and from the presence of C–O–C group at 1214 cm^{-1} and C–O stretching at 1300 cm^{-1} . Both PU and PUa were expected as the Desmodur[®] RC reaction with the water forms PUa while its eventual reaction with GA forms PU. Although the GA is added to the synthesis as an emulsion stabilizer, it has several OH groups possible to react with the isocyanates present in the O phase, and thus act as a polyol. For all the samples, the carbonyl peak ascribed for the PU has a higher intensity than the one of PUa, indicating a more significant contribution of the first in the MCs' shell composition. The MCs with the most intense PUa carbonyl peak are the ones with PEI. The n-OTES has characteristic peaks at 1103 cm^{-1} and at 1076 cm^{-1} , from the Si-O-CH₂-CH₃ group. Unfortunately, these peaks cannot be detected in the MCs to which n-OTES was added during the synthesis. It has been reported that the peak related with the Si–O–Si asymmetric stretching vibrations (TO component) is located at ca. 1070 cm^{-1} , whereas the presence of a shoulder at ca. 1200 cm^{-1} corresponds to the LO component of the asymmetric stretch [16]. Its absence in the MCs' spectra indicates the lack of a hybrid PU/PUa/Silica shell. The Desmodur[®] RC is very reactive, quickly forming an initial thin polymeric shell around the O droplets, which makes this synthesis probably quite fast for the n-OTES silane to have time to hydrolyse and posteriorly react with the isocyanate. Although it was not possible to show evidence of the hydrolysis, condensation, or polymerization of the silane, i.e. of the hybrid character of the n-OTES and PEI_n-OTES_MCs, it is still possible for some n-OTES molecules to be entrapped in the MCs' shell structure.

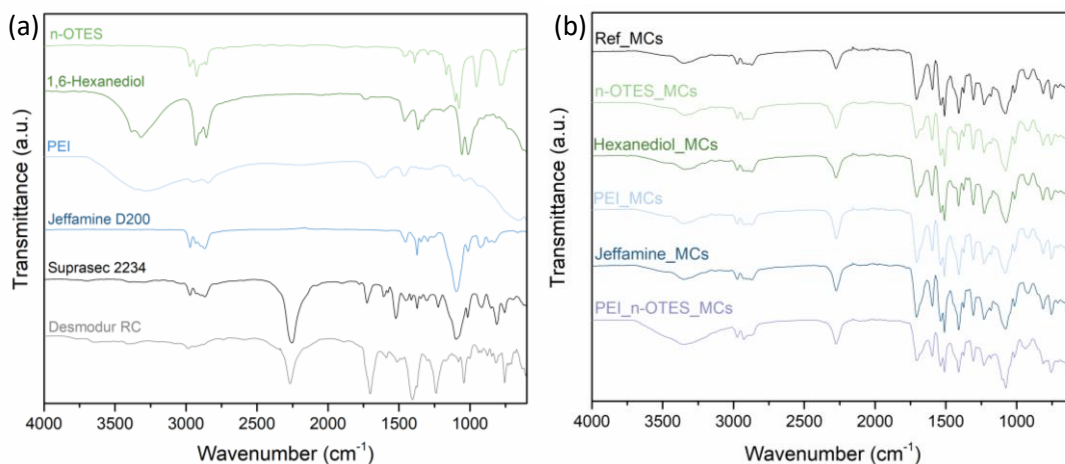


Figure IV.12. FTIR-ATR spectra of the isocyanates and active H sources used for the MCs' synthesis (a) and of the obtained MCs (b).

The relative encapsulation yield (Y) was used to conclude regarding the MCs' encapsulation efficiency, exposed in Table IV.9. All the MCs to which active H sources were added during the synthesis present a higher encapsulation yield than the Ref_MCs. The faster formation of the MCs' shell, due to the reaction between the NCO groups from Desmodur[®] RC and the extra active H sources, created an early barrier between the NCO groups and the aqueous medium, which led to a higher amount of encapsulated isocyanate. For the Ref_MCs, the formation of the shell is only due to the reaction between the isocyanate and the less reactive OH groups from the water and, possibly, with GA, leading to a slower shell formation, which increases the exposure of the isocyanate to the W phase.

Right after the synthesis, the PEI_n-OTES_MCs and the n-OTES_MCs are the ones which exhibit a higher encapsulation content. In contrast with PEI, the Hexanediol and the Jeffamine[®] D2000 only have two reactive groups per molecule, offering far less reactive H groups. Hexanediol was chosen due to its small linear molecule which could be associated with a fast diffusion through the immature shell towards the O phase. The higher Y value of the Jeffamine_MCs, comparing with that of the Hexanediol_MCs, is explained by the faster reaction of primary amines with the NCO groups, which have a relative uncatalyzed reaction rate, at 25 °C, 1000 times higher than that of primary hydroxyls and water [17].

Table IV.9. Relative encapsulation yield (Y value) calculated for each sample, by using the FTIR spectra of the as-prepared MCs.

MCs' acronym	Ref_MCs	n-OTES_MCs	Hexanediol_MCs	PEI_MCs	Jeffamine_MCs	PEI_n-OTES_MCs
Y value	2.94	3.41	3.33	4.15	3.65	4.38

On Figure IV.13 is the evolution of the ΔY value of each sample, while stored at room temperature and 60% of humidity, over time. Although all the active H sources contributed to a more protective shell, the most promising shelf-life was obtained for the Jeffamine_MCs and for the PEI_n-OTES_MCs, corresponding to a loss of 49% and 43%, respectively, of the Y_i after 3 months. Hexanediol_MCs were the ones showing the most significant decrease of the Y_i , of 67%. Jeffamine® D2000 has repeating oxypropylene units in its backbone, which brings some hydrophobicity to the MCs, contributing to prevent moisture from penetrating across the shell. PEI brings an enhanced cross-linking to the shell, that comes from the branched structure rich in NH groups and the n-OTES, due to its long aliphatic carbohydrate chain, is anticipated to contribute to increase the shell hydrophobicity.

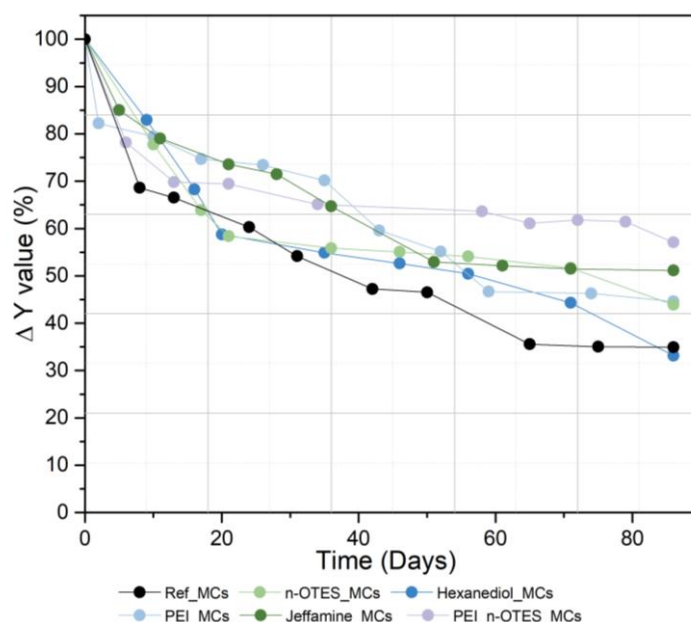


Figure IV.13. ΔY value variation over time, for all the MCs in study, while stored at room temperature and 60% of humidity.

The addition of active H sources to the MCs synthesis is expected to also influence its mechanical properties. It is desired for the MCs to be sufficiently robust to survive transportation and the blending within the pre-polymer formulation, but at the same time be able to burst during the adhesive joint preparation, by the effect of the applied pressure. The siloxane moieties of the n-OTES can be responsible to promote an improved mechanical strength and thermal resistance to the MCs. As for the addition of PEI, the resulting increased cross-linking of shell typically results in more stable MCs with higher thermal and mechanical resistance. Jeffamine® D2000, due to its long repeating oxypropylene units is expected to bring some flexibility to the shell.

One of the main problems associated with the PU/PUa MCs are the high toughness of its shell, which makes it difficult for some of the MCs to break during the adhesive application, especially when encapsulating such reactive isocyanate species. Although the PEI_n-OTES_MCs were the ones with the higher encapsulation content and the most promising shelf-life over the period of three months, its increased cross-linking, from PEI, and enhanced mechanical properties, from n-OTES, might difficult its breakage during the adhesive application. Jeffamine® D2000 provides an increased flexibility to the MCs' shell, an improvement to the relative encapsulation yield and an increased shelf-life, when comparing with the Ref_MCs, which makes this an interesting active H source for the current application.

This strategy was applied for the encapsulation of other highly reactive isocyanate, Ongronat®2500, an oligomeric MDI with increased functionality. Desmodur® RC was used for the shell formation with to two different active H source combinations, namely Jeffamine D®2000 and the combination of PEI and n-OTES, according to the Table IV. 10.

Table IV. 10. Microcapsules' acronyms and emulsion composition.

MCs acronym	Water phase (wt%)	Oil phase (wt%)	Active H source (wt% of the W phase)	Time of synthesis
O_Jeffamine_MCs	Water Gum arabic	Ongronat® 2500 (Core content)	Aqueous solution of Jeffamine D 2000 at 17 wt% (2.2 wt%)	75min.
O_PEI_n-OTES_MCs	(91% of the emulsion)	Desmodur® RC (Shell) (9% of the emulsion)	Aqueous solution of PEI at 17 wt% (2.2 wt%) n-OTES (0.72 wt%)	45min.

The photomicrographs of both MCs samples are displayed in Figure IV.14, along with the respective size distribution histograms. Both syntheses led to loose, disaggregated MCs, with a fairly spherical shape. As in the MCs obtained with Suprasec®2234, the ones with the combination of PEI and n-OTES have a rougher surface, while the O_Jeffamine_MCs have a smoother surface.

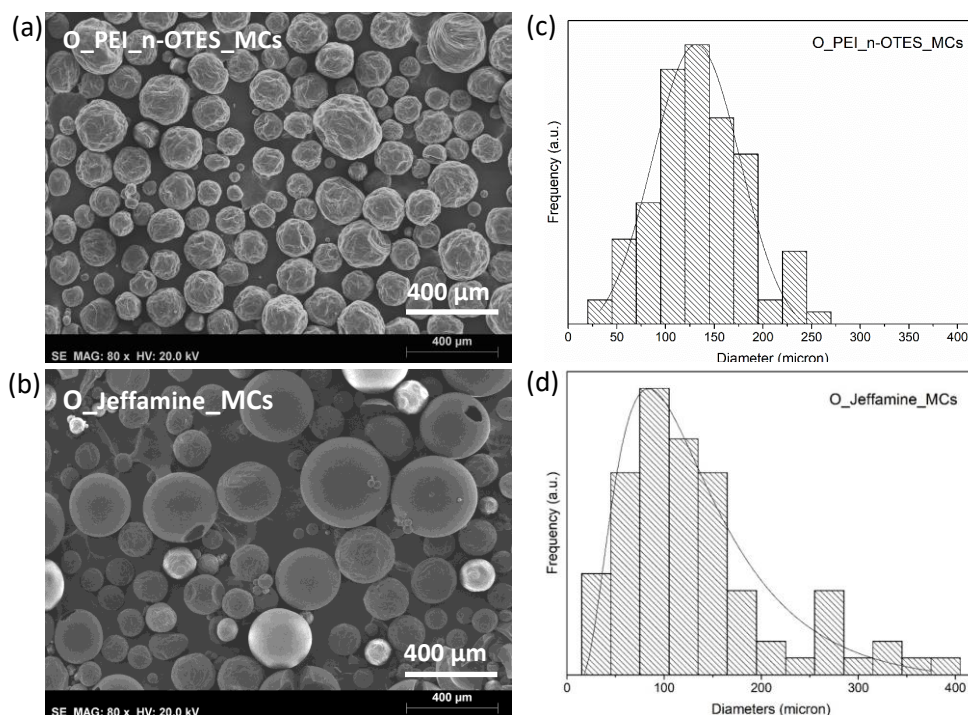


Figure IV.14. SEM photomicrographs of the O_PEI_n-OTES_MCs (a) and of the O_Jeffamine_MCs (b), as well as the respective size distribution histograms.

Figure IV.15 exposes the FTIR spectra of the active H sources, unreacted isocyanates and of the MCs, after the synthesis and aged by 3 months. The presence of the N=C=O bond stretching vibration peak, at ca. 2260 cm^{-1} , confirms the presence of the encapsulated isocyanate. By the Pu and PUa carbonyl peaks, at $1730\text{--}1715\text{ cm}^{-1}$ and at $1700\text{--}1680\text{ cm}^{-1}$, respectively, it is possible to confirm the MCs' shell composition which is mainly composed by PU, for both cases. Although only a NH terminated active H source was used for the O_Jeffamine_MCs synthesis, promoting the PUa formation along with the water, the PU peak is still more intense. This is probably due to the significantly higher concentration of GA, ca. 10 times higher, in the W phase compared to Jeffamine® D2000. When looking at the 3 months old MCs, it is possible to notice an increase in the PUa formation, indicating that water, from the air moisture, must have entered the MCs and reacted with the encapsulated Ongronat®2500. The n-OTES has strong peaks at 1103 cm^{-1} and at 1078 cm^{-1} , which can be seen in the O_PEI_n-OTES_MCs, confirming the presence of the silane in the MCs' shell. The Si–O–Si asymmetric stretching vibration, located at 1070 cm^{-1} is not visible in the MCs' spectra, indicating that the lack of a hybrid PU/PUa/Silica [16].

Due to the overlap of thermal events in these samples thermograms, Figure IV. S1, from Supplementary Information, the quantity of encapsulated content was not possible to be quantified from TGA. Instead, the Y value was used to conclude regarding the encapsulation yield and shelf-life. The Y values of the as prepared and 3 months aged MCs, are displayed at the

Table IV.11. Similarly, to the results obtained for the encapsulation of Suprasec® 2234, the combination of PEI with n-OTES led to the higher encapsulation content and shelf-life.

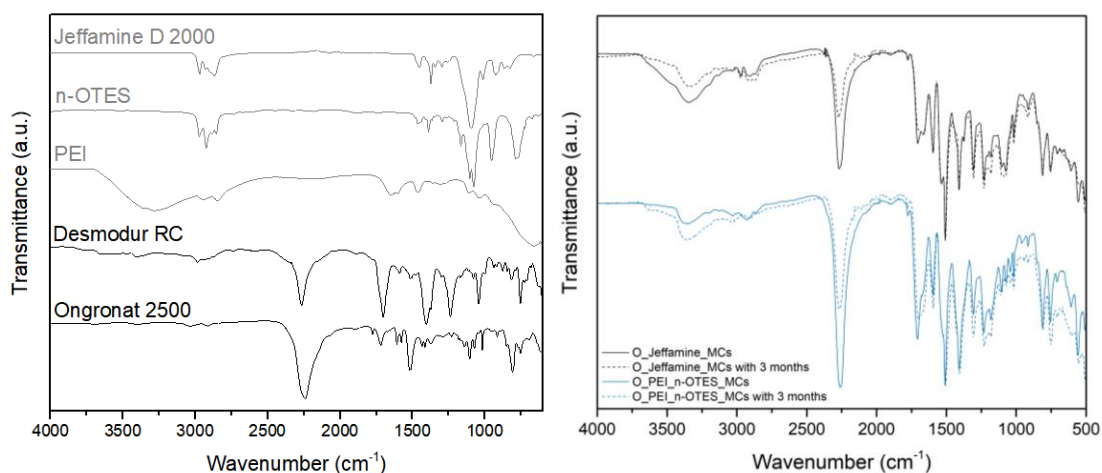


Figure IV.15. FTIR-ATR spectra of the isocyanates and active H sources used for the MCs' synthesis (left) as well as of the MCs after the synthesis and after stored for 3 months at room temperature and 60% of relative humidity (right).

Table IV.11. Relative encapsulation yield (Y value) calculated for each sample, by using the FTIR spectra of the as-prepared MCs and 3 months aged MCs, while at room temperature and 60wt% of relative humidity.

MCs' acronyms	Y value	Y (%) 3 months after the synthesis
O_Jeffamine_MCs	8.67	38.06
O_PEI_n-OTES_MCs	14.54	52.75

The strategy of using two isocyanates in the O phase of the emulsion, one to be encapsulated and the other to form the shell, in combination with active H sources in the W phase, has enabled to obtain PU/PUa MCs containing oligomeric and pre-polymeric isocyanate species. The active H sources have also a role in the MCs characteristics influencing its morphology, porosity, permeability and thermal and mechanical resistance, which directly impact the MCs performance as cross-linkers in the adhesive.

The majority of isocyanate containing PU/PUa MCs reported in the state of the art refer the encapsulation of monomeric species. The encapsulation of higher MW isocyanates mainly refers to the encapsulation of PAPI, more precisely PAPI 44V20 [6, 7]. This isocyanate has an NCO content of approximately 30, which is equivalent to the one of Ongronat® 2500. It is to refer that the NCO content of Suprasec® 2234 is of 15.9. To the best of my knowledge, the encapsulation of an isocyanate with such low NCO content and such high reactivity, was not yet reported.

IV.3.3 Effect of the isocyanate source, used for the shell formation, on the microcapsule's final properties

The diffusion of air humidity to the MCs interior is the major obstacle to PU and PUa MCs' shelf-life, leading to its decrease. As different isocyanates can affect the thermal, mechanical, and morphological properties of the MCs' shell, due to distinct intermolecular interactions, it is here proposed that different isocyanates can also lead different permeabilities of the shell to the air moisture diffusion [18, 19].

Three different isocyanates were tested for the shell formation, namely Ongronat®2500, Desmodur® RC and Suprasec® 2234. Its general properties and chemical structure are exposed in Table IV.2. Ongronat®2500 and Suprasec® 2234 are MDIs with different polymerization degrees and functionality. Desmodur® RC is a poly-isocyanurate of TDI. The MCs' synthesis parameters are summarized on Table IV.12. The Desmodur® RC was added to the respective synthesis having into consideration that 65% of its composition is ethyl acetate. The amount of IPDI was maintained for the three syntheses.

Table IV.12. Microcapsules' acronyms and emulsion composition.

MCs acronym	W phase	W phase (wt% in the emulsion)	O phase	O phase (wt% in the emulsion)	Isocyanate for the shell formation (% in the O phase)
Ongronat_MCs	Water	90 wt%	Isocyanate for the shell formation	10 wt%	Ongronat® 2500 (30%)
Suprasec_MCs	Gum arabic	90 wt%		10 wt%	Suprasec® 2234 (30%)
Desmodur RC_MCs	Jeffamine® D2000	88 wt%		IPDI (core content)	12 wt%

Figure IV.16 exposes The SEM photomicrographs of the obtained MCs. Ongronat and Desmodur RC_MCs are loose and disaggregated and have a spherical morphology. On the contrary, the use of Suprasec®2234 led to irregular aggregates. Several attempts were made to optimize this MCs synthesis though without success. Suprasec®2234 is an isocyanate with a significantly higher viscosity which might have contributed to the emulsion destabilization, due to the resistance of the O droplets to deform under the applied shear rate, and the difficulty to achieve a good

dispersive mixture of droplets. Regardless the aggregated particles, the Suprasec_MCs were used to draw conclusions regarding the use of this isocyanate on the MCs' properties.

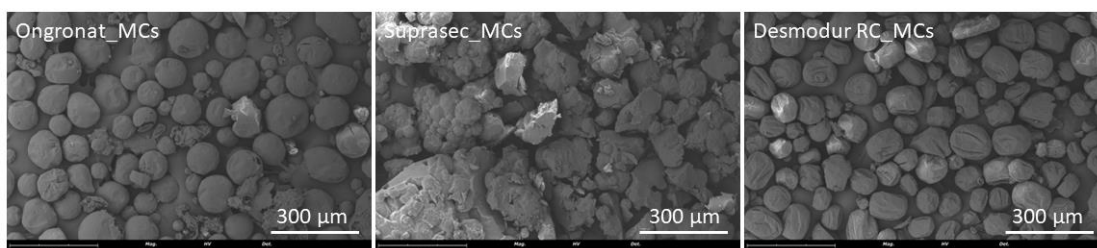


Figure IV.16. SEM photomicrographs of the MCs obtained using different isocyanates for the shell formation.

The Ongronat_MCs have a broader size distribution than the Desmodur_RC_MCs, shown in Figure IV.17, which might be related to its higher viscosity (520-680 mPa.s), compared to the one of Desmodur[®] RC (3 mPa.s). It was not possible to conclude about the Suprasec_MCs size distribution, as the Fiji software uses the area of a circle to calculate the MCs' diameter.

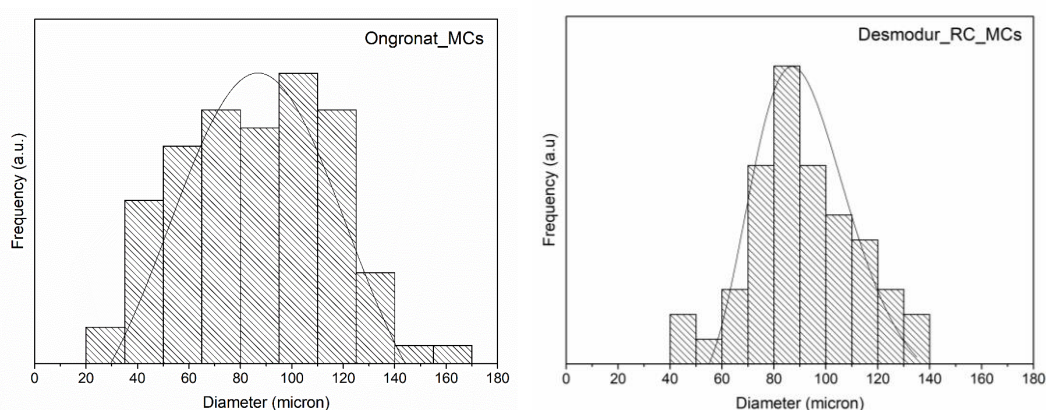


Figure IV.17. Size distribution histograms of the Ongronat_MCs (left) and of the Desmodur_RC_MCs (right).

Figure IV.18 shows the thermograms and respective derivative curves of the MCs and those of IPDI and the isocyanates used for the shell formation. The ones corresponding to the aged MCs, by 3 months, are available in Figure IV. S2., at the Supplementary Information. Due to the polymerization degree of the IPDI on the aged MCs, the Y value was used to conclude about the MCs shelf-life. IPDI has its first thermal event starting above 100 °C, with the major mass loss occurring at 225 °C, while the MDIs have its most significant loss occurring between 200 and 350 °C, approximately. Desmodur[®] RC has 65 wt% of ethyl acetate, with its thermal event occurring at lower temperatures than that of the isocyanate, which occurs between 430 and 500 °C, approximately. The decomposition of the PUa and PU shell, in particular the soft segments, start

to occur typically around 300 °C [20]. Having this into account, the first slope of the as-prepared MCs thermograms was used to quantify the encapsulated isocyanate, IPDI, with its values listed in Table IV.13 along with the ones of the relative encapsulation yield, determined by FTIR. The FTIR spectra are available in Figure IV. S3, from Supplementary Information. It is to notice that, for this study, the Y values are not comparable between different synthesis, as the MCs' shell composition varies, and it should only be used to draw conclusions about the MCs' shelf-life.

The MCs encapsulation content, calculated by TGA, did not significantly varied between the different synthesis. By interfacial polymerization technique, the main factor affecting the encapsulated content is the quick formation of a physical barrier between the W phase and the O phase (isocyanates) of the emulsion. Suprasec® 2234 and Ongronat® 2500 are both MDIs with a high degree of polymerization resulting in MCs with similar encapsulation contents. Desmodur® RC was expected to lead to the highest degree of encapsulation, what was not observed. This isocyanate is a polyisocyanurate of TDI which has a significantly lower free NCO content than the MDIs in study, meaning lesser free groups to react, promoting a quicker shell formation. The Desmodur_RC_MCs' DTG shows some higher MW isocyanates, at ca. 230 °C, not visible for the other MCs. Adding, this isocyanate led the to MCs with the poorer shelf-life, with a decrease of almost 67% in the Y value in a period of 3 months, while stored at room temperature and 60% of relative humidity. This might be due to the Desmodur® RC bulky aromatic trifunctional monomer, a structure with potentially more free volume, which might lead to a lesser protective shell, enabling some further reactions between the W phase and the IPDI. In contrast, the shell resulting from the MDI is expected to be more packed and more crystalline [21]. It is reported that the permeation in polymers occurs preferentially in non-crystalline regions and, the higher the crystalline content, the lower the permeability [19, 21]. The MDIs led not only to a higher encapsulation yield but also to a better shelf-life, particularly the Ongronat® 2500. MCs obtained with this isocyanate, have the better resistance to the air moisture permeability, from the Y value. Ongronat® 2500 is, from the isocyanates in study, the most promising to be used for the envisaged MCs' shell formation.

The resistance of each MCs' shell to organic solvents and water diffusion, while immersed, was also evaluated, and the results are exposed on Chapter VI.

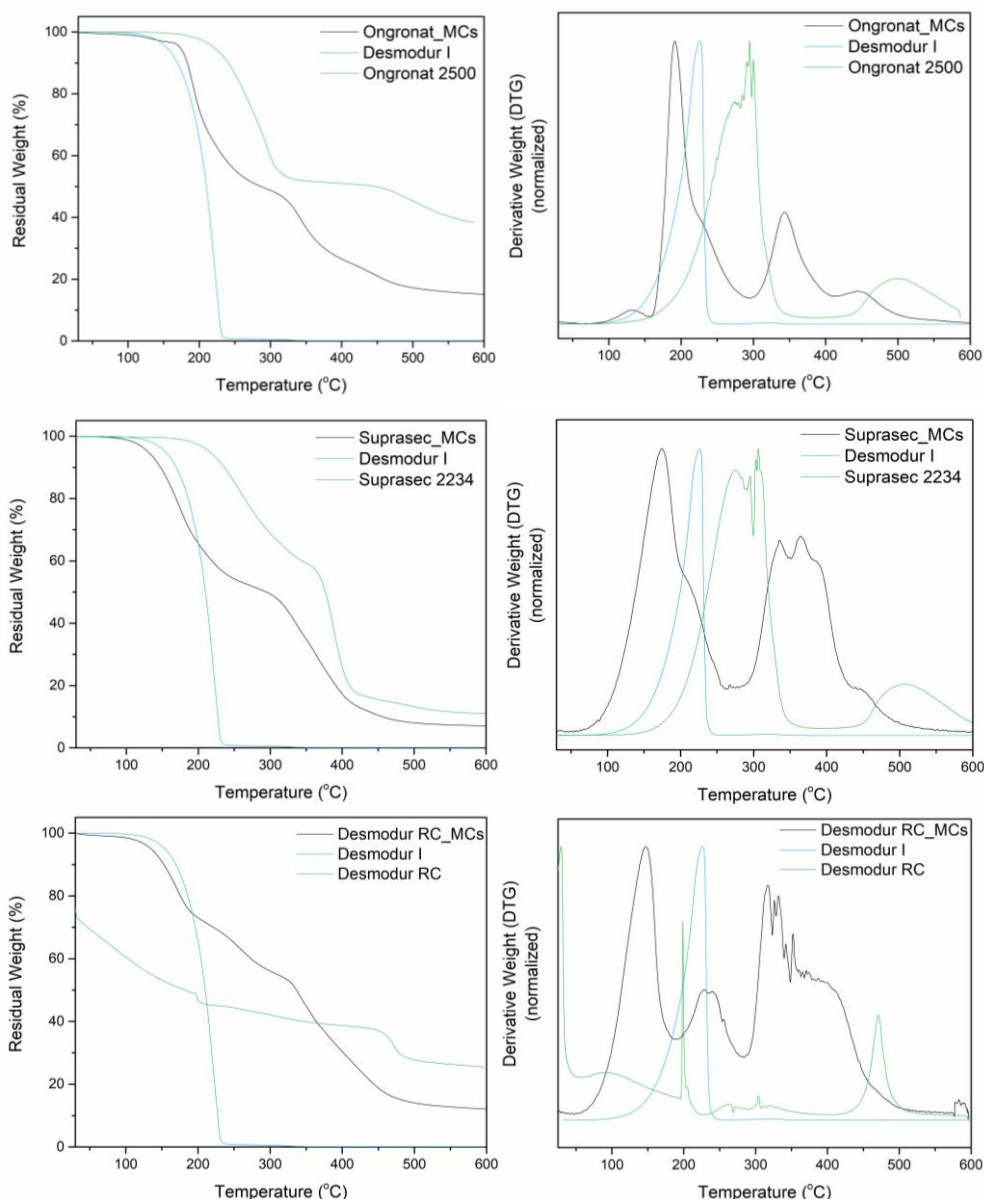


Figure IV.18. Thermograms of the isocyanates used for the MCs' synthesis and of the obtained MCs (left), and respective derivatives (right), normalized by the division of each point by the maximum value.

Table IV.13. Mass loss (%) of encapsulated IPDI (by TGA), relative encapsulation Yield (Y) calculated using the FTIR spectra obtained after the synthesis and 3 months later. The Y₃ is given as a percentage of Y_i.

MCs' acronym	Mass loss (%) from TGA (encapsulated isocyanate) (115 – 320 °C *)	Initial relative encapsulation yield (Y _i)	Y ₃ (%) 3 months after the synthesis
Ongronat_MCs	42.34	15.9	41.0
Suprasec_MCs	43.47	15.8	38.7
Desmodur RC_MCs	37.68	30.8	33.1

*Range of temperatures used for the encapsulated isocyanate quantification. The temperature range varied slightly depending on the MCs thermograms.

IV.3.4 Emulsion stabilization

The results exposed in this sub-chapter “IV.3.4 Emulsion stabilization” are published in our paper “Emulsion Stabilization Strategies for Tailored Isocyanate Microcapsules” [22].

In MCs synthesis by interfacial polymerization, the size of the emulsion droplets typically defines the size of the final MCs, as the polymerization reactions occur at the droplets interface leading to the formation of the shell. As so, the stabilization and control of the emulsion droplets sizes throughout the synthesis is of great importance to be able to tailor the final MCs sizes and size distribution. For O/W emulsion systems, the most common instability phenomenon is a result of gravitational separation and flocculation, which might lead to coalescence [23, 24].

With the intend to obtain small sized MCs, with a narrow size distribution, and with no to little variation between the initial O droplets size to that of the final MCs, several emulsion stabilizers, and different combinations between them, were tested. The used stabilizers are described in Table IV. 14.

Table IV. 14. Stabilizers used for the O/W emulsion stabilization and respective HLB and molecular weight.

Type of stabilizer	Stabilizer	HLB	Molecular Weight (Da.)
Polysaccharide	Gum arabic (GA)	n.a.	250 000
	DC [®] 193	12	3 200
Surfactant	Span [®] 20	8.6	346
	Tween [®] 85	11	16.04
	Pluronic [®] P123	8	5 800
Polymer	PVA	n.a.	57 000 -66 000

Each of these stabilizers was tested in different concentrations and combinations. A general overview for all cases can be found at the Table IV. S1, from Supplementary Information.

The polysaccharide GA was here used as the benchmark as it is the most commonly used emulsion stabilizers, reported in the literature, for the synthesis of PU/PUa MCs by interfacial polymerization combined with an O/W emulsion system. It has a good water solubility, low solution viscosity, good surface activity, and ability to form a protective film around emulsion droplets. However, GA needs to be used in high amounts to lead to a stable emulsion.

All the tested surfactants were chosen having into consideration its hydrophilic–lipophilic balance (HLB) value, which ranged from 8 to 12 as, for an O/W emulsions system, it must be higher than 8. However, from all the four different surfactants tested, only DC193 led to a stable emulsion. DC193 is a non-ionic silicone surfactant and was chosen not only based on its HLB value but also on its low surface tension and its use in the PU and footwear industry.

SPAN20 and Tween85, which are both hydrocarbon chain surfactants, led to a complete emulsion destabilization while under mechanical agitation and no MCs were obtained. This is possibly due to their lower HLB values of 11 and 8.6, respectively, when comparing with the ones of DC193, which gives them a lower affinity for the W phase. Pluronic® P-123 is a non-ionic, difunctional block copolymer with terminating primary hydroxyl groups, and, depending on the tested concentration, it led to a completely or partial destabilization of the emulsion. For the cases of partial destabilization, the resultant particles had big dimensions and an irregular morphology and were not considered viable for this application.

Partially hydrolysed PVA, is a non-toxic and biodegradable water-soluble polymer and was used as a rheology modifier, intended to increase the continuous phase viscosity and, as this, reduce the tendency for the emulsion droplets to suffer from sedimentation and coalescence.

The emulsion stabilization mechanisms of polysaccharides, surfactants and rheology modifiers are schematized in Figure IV.19.

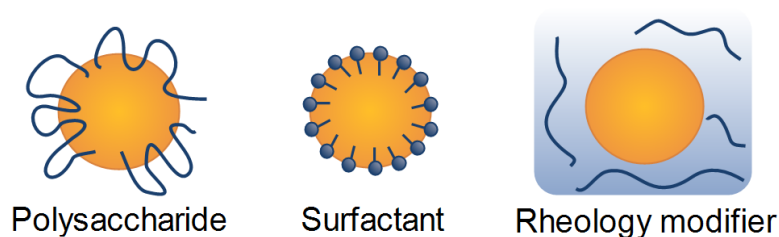


Figure IV.19. Schematic representation of the emulsion droplets stabilization by polysaccharides, surfactants, and rheology modifiers. Image reprinted from [22] under an open access Creative Common CC BY license.

The best 5 emulsion stabilization systems, which represented different strategies, are listed in Table IV.15 along with its concentrations and the O and W phases emulsion compositions. A general overview of all cases tested can be found in Table IV. S1, from the Supplementary Information. Optical microscopy photographs, of all the emulsions tested, were taken after 10 minutes of emulsification (at the end of the emulsification) and after 15 minutes under mechanical stirring, as it is not possible to guarantee that no solid film has been formed after

that time. The optical microscopy photographs are reported on Table IV. S2, from the Supplementary Information.

Table IV.15. Microcapsules' acronyms and emulsion composition

MCs' Acronym	Water phase	Oil phase	Emulsion stabilizer (wt% added to the W phase)
GA_MCs	Water Emulsion stabilizer Jeffamine® D2000 (93 wt% of the emulsion)	Ongronat®2500 IPDI (7 wt% of the emulsion)	GA (5%)
DC_MCs			DC193 (4%)
GA_DC_MCs			GA (4%) DC193 (1%)
PVA_MCs			PVA (2%)
GA_PVA_MCs			GA (1.30%) PVA (2%)

For O/W emulsion systems, the most common instability phenomenon is a result of gravitational separation, in particular the occurrence of creaming [23, 24]. However, in this case, the droplets tend to sediment, as Ongronat®2500 greatly contributes to increase the O phase density, to a final value of 1.114 g/cm³. Gravitational separation phenomena in emulsions can be reduced by decreasing the density difference between the W and O phases, by increasing the viscosity of the continuous phase, or by decreasing the size of the emulsion droplets [25].

Figure IV.20 show the photographs of the selected emulsion at 0, 15 and 30 minutes after the emulsification, while at rest and, Figure IV.21 shows the volume percentage of sediment along the time, determined from the first.

DC193 was the stabilizer that led to the higher degree of sedimentation as well the only leading to the occurrence of coalescence. This last phenomenon may also contribute to a quicker sedimentation, as it increases size of the emulsion droplets. The poorer stabilization might be correlated with the small size of DC193 molecule, compared to the other stabilizers in study, which makes it more difficult to avoid the attractive interactions between the isocyanate droplets [26]. The combining effect of GA and DC193 led to improvements in the emulsion stability when comparing with the two stabilizers acting alone. As for the use of PVA as a rheology modifier, it led to significant improvements in decreasing the sedimentation. With the use of 2 wt% of PVA it was possible to increase the viscosity of the continuous phase to 5.78 cP, and to 7.64 cP, when in combination with GA, which demonstrated to significantly decrease the gravitational separation phenomena in emulsions [7, 8].

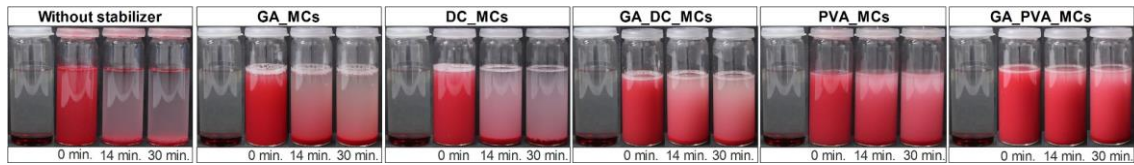


Figure IV.20. Visual observation of the emulsions used to obtain the GA, DC, GA_DC, PVA, and GA_PVA MCs, over a period of 30 min. From left to right: oil and water phase before emulsification, right after emulsification, 14 and 30 min after emulsification (static conditions).

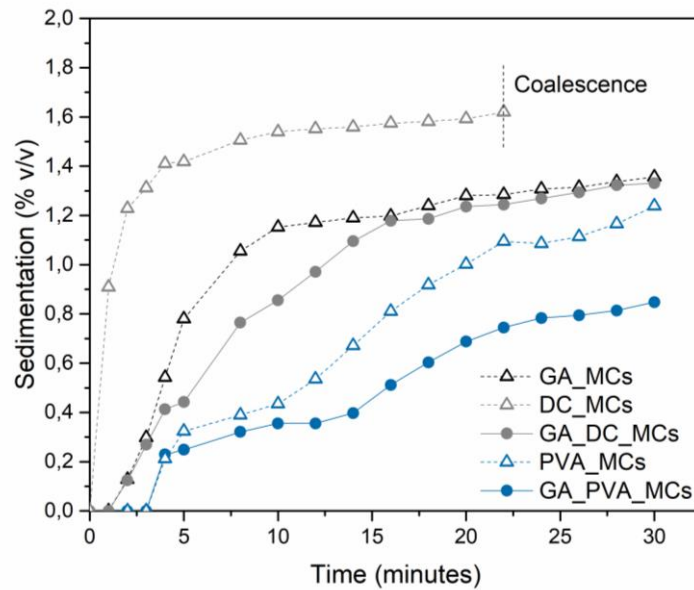


Figure IV.21. Evolution of the sedimentation volume fraction over time, of all the reported emulsions in study, while at rest (static conditions).

Figure IV.22 compares the best performing emulsion, obtained with GA and PVA, i.e. the one that suffered less sedimentation, with the one obtained with DC193. After 30 minutes at rest, the density of droplets in the emulsion phase stabilized by DC193 is significantly less than that of the emulsion phase stabilized by GA_PVA, and the occurrence of coalescence in the sediment phase is notorious, revealing some inadequacy of the DC193 for this application.

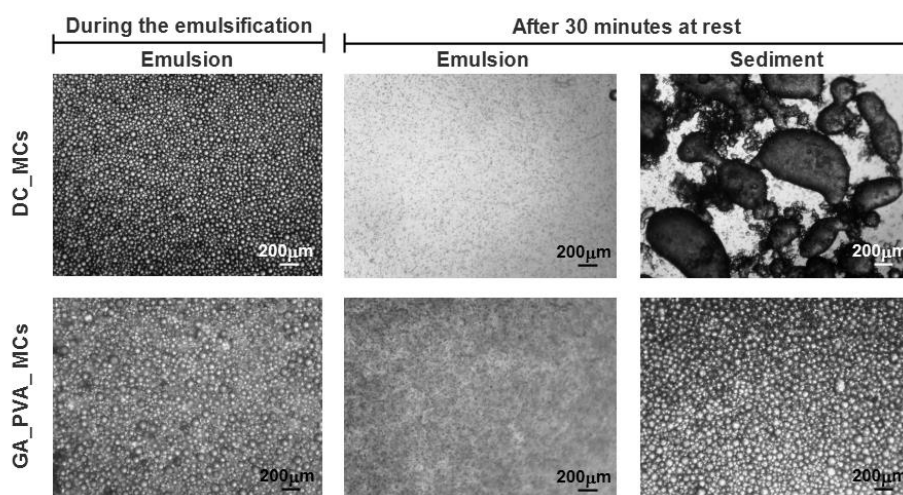


Figure IV.22. Optical microscopy photographs of the emulsion that suffered less sedimentation (GA_PVA_MCs emulsion) and the one stabilized with DC193. Optical photographs of the emulsions while under emulsification (left) and after 30 minutes at rest (right), emulsion and sediment portions.

In addition to the static tests, the emulsion systems were also evaluated when under dynamic conditions. For that purpose, the emulsions were followed by optical microscopy during the first 25 minutes of the synthesis. As was observed for static conditions, the emulsion stabilized by DC193 was the only suffering from coalescence (Figure IV.23), with no major changes reported in the other stabilizing systems.

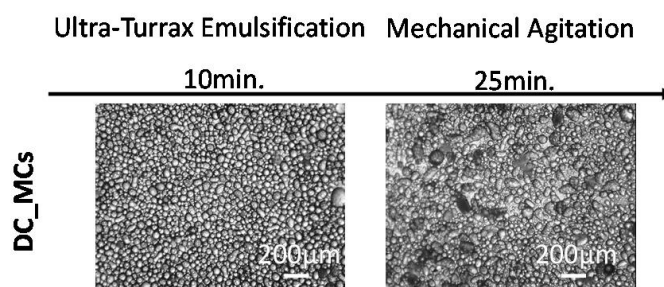


Figure IV.23. Optical microscopy photographs of the DC_MCs' emulsion during the first 25 minutes of the synthesis. Left: after 10 minutes of emulsification at 3200 rpm using the Ultra-Turrax; Right: after the following 15 minutes under mechanical stirring at 400 rpm (dynamic conditions).

Figure IV.24 exposes the SEM photomicrographs of the obtained MCs. All the syntheses led to loose MCs, with a core-shell morphology and a spherical shape, excepting the one with DC193 as stabilizer, which led to some irregular shaped MCs and debris. The MCs show some roughness or buckling due to fluid-induced shear forces related with the mechanical stirring and due to inhomogeneous reaction kinetics between the isocyanate, the added active H sources and water. Another explanation is a slow shell formation that leads to an initially thin and flexible

shell preceding the reduction of the MCs size, due to the progress of the interfacial polymerization reactions [14, 15, 27].

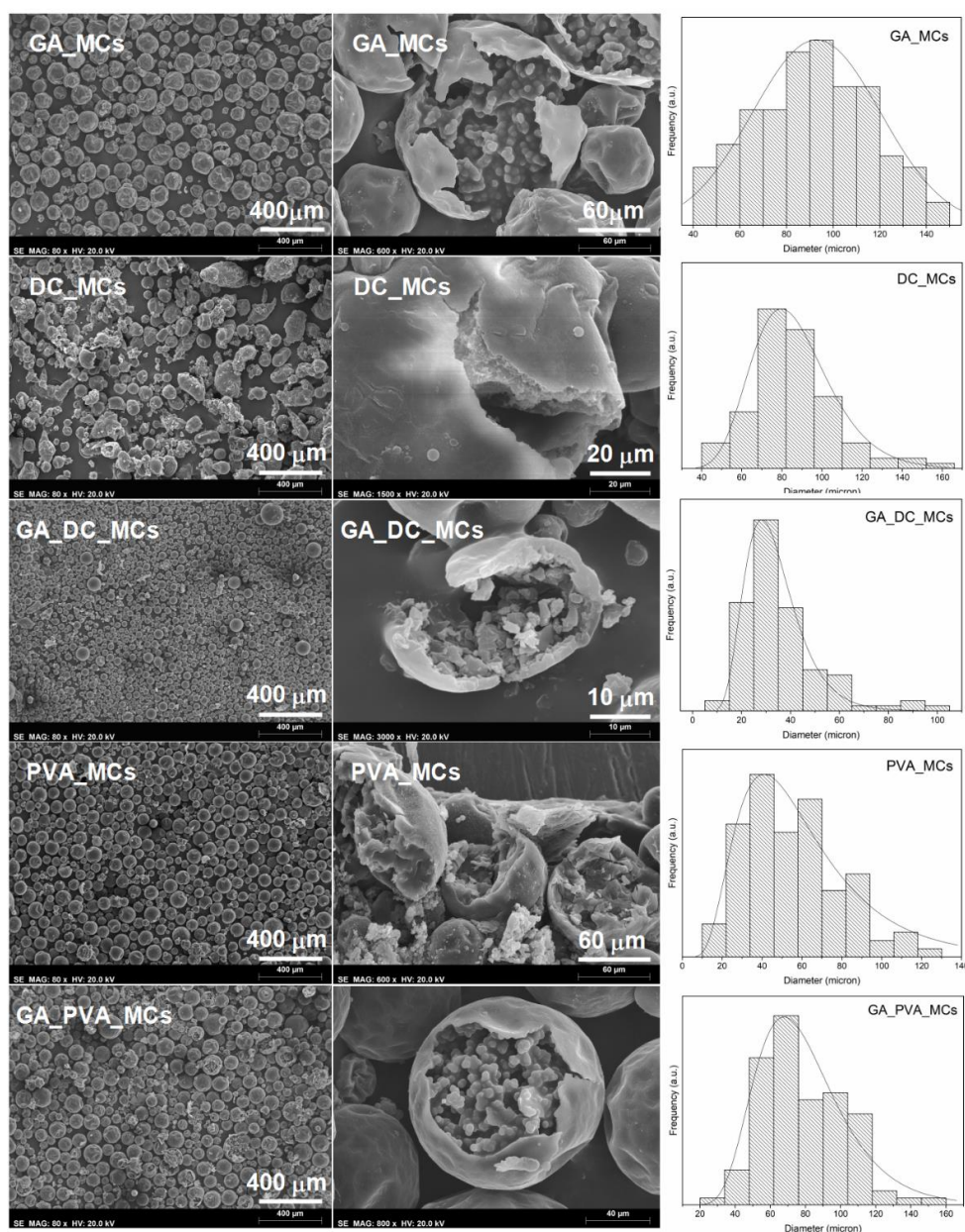


Figure IV.24. SEM images of the obtained MCs at 80x amplification (left). SEM images of isolated MCs' cross sections deliberately crushed (obtained at different magnifications). MCs' size distribution (right).

The combining effect of DC193 and GA, at a ratio of 1:4, led to the smallest MCs. It is possible that both the strong steric effect of the GA and the low surface tension provided by the DC193 surfactant contributed to the emulsion stability in the GA_DC_MCs synthesis. It has been referred that when the two stabilizers coexist and reach an equilibrium state, the silicone surfactant preferentially migrates to the emulsion droplets interface, and when this is at low concentrations the GA can also partially adsorb [12]. Indeed, the DC193/GA ratio of ca. 1:1 led

to bigger MCs with a broader size distribution, as can be seen in Table IV. S2, from Supplementary Information.

Figure IV.24 depicts the MCs' size distribution histograms and, Table IV. 16 the maximum value for each case, which corresponds to the mode of the MCs sizes. It is important to refer that no debris or non-spherical MCs were considered for the size distribution determination, which is particularly relevant for the DC_MCs.

Table IV. 16. Maximum value (mode) obtained on the MCs' size distribution histogram.

MCs' acronym	GA_MCs	DC_MCs	GA_DC_MCs	PVA_MCs	GA_PVA_MCs
MC's diameter (mode) (μm)	92.74	80.15	28.24	40.85	65.32

All the samples follow a monomodal distribution with GA_MCs having the broadest profile. On the other hand, the combination of GA with DC193 led to the narrowest, with most of the MCs having between 14.8 and 45 μm in diameter. PVA, present at only 2 wt%, greatly increased the viscosity of the aqueous solution to 5.8 cP. By comparing with GA that, when present at 5 wt% lead to a viscosity of 1.3 cP, it is possible to state that PVA is a more efficient rheology modifier, which plays an important role in emulsion stabilization. However, a further increase of the PVA concentration was found to lead to bigger sized MCs and a larger size distribution, which might be associated with an excessive viscosity of the continuous phase. The same has occurred to the GA_PVA emulsion, with a viscosity of 7.6 cP, resulting in larger MCs compared to the PVA_MCs. For the GA_PVA emulsion two different effects can be acting on the emulsion. The higher viscosity of the aqueous phase requires more energy to break the O phase into smaller droplets and hinders the diffusion of GA and adsorption onto the O droplets, contributing to a less stable emulsion [28, 29]. Also, it has been reported that excessive free, non-adsorbed, polysaccharide emulsifiers on the continuous phase of O/W emulsions can lead to depletion-induced flocculation [28, 29]. O/W emulsion system with excess free polymer in the W phase can suffer from depletion-induced flocculation through an osmotic effect, as there is a region surrounding each droplet where the polymer concentration is depleted. This results in an osmotic pressure between the depletion zone and the bulk polymer solution, with a thermodynamic tendency for the decreasing of the water volume in this zone. When the two O droplets approach each other, the system tends towards droplet association and drives flocculation [30, 31]

There is an optimum viscosity value for the continuous phase to lead to a stable emulsion, namely between 5-6 cP for the present system.

Figure IV.25 represents the average diameter of the O emulsion droplets at the end of the emulsification process, after 10 minutes under mechanical agitation and of the final MCs. DC193 led to the largest variation between the initial emulsion and the final MCs' size, even when excluding the debris and non-spherical particles, followed by GA. GA_PVA_MCs suffered a final variation identical to the one obtained with GA, however with a more noticeable destabilization in the first 10 minutes. PVA_MCs suffered the lowest variation, which proves the PVA capability as stabilizer, offering the possibility of a better tuning of the MCs. By using PVA as emulsion stabilizer it is possible to define the MCs size by controlling the size of the initial emulsion droplets.

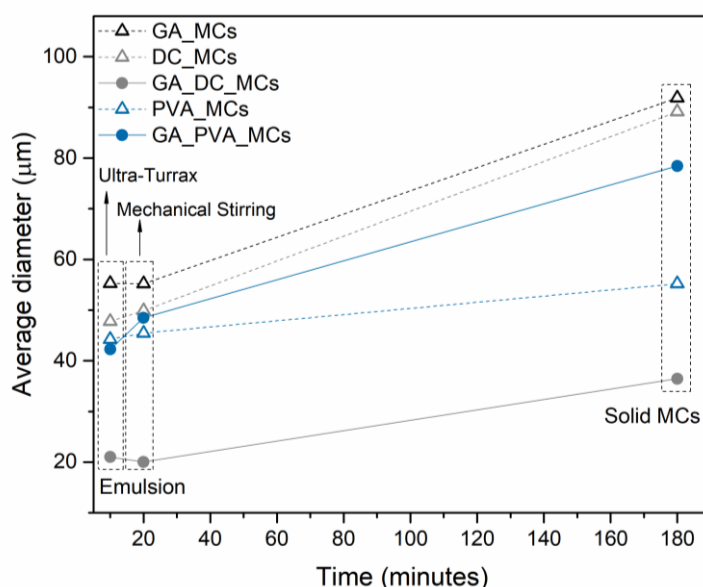


Figure IV.25. Oil emulsion droplets average diameter at the end of the emulsion preparation (10 min), after 10 min under mechanical agitation (20 min), and of the final MCs (180 min).

Figure IV.26 shows the ATR-FTIR spectra of the MCs and those of the isocyanates, active H source, and stabilizers. The presence of encapsulated unreacted isocyanate is confirmed by the presence of the NCO peak at 2260 cm^{-1} in the MCs spectra. By the similarity of the MCs' NCO peak with that of the IPDI it is possible to confirm that this is the encapsulated isocyanate, and not Ongronat®2500.

The presence of PU and PUa can be confirmed by the presence of its respective carbonyl peaks, at $1780\text{-}1760\text{ cm}^{-1}$ and $1760\text{-}1700\text{ cm}^{-1}$, respectively, and by the peak at 1214 cm^{-1} from the C–O–C group and at 1300 cm^{-1} from the stretching of C–O linkages. PUa carbonyl groups are clearly detected in all the MCs spectra while the ones from PU are only slightly visible. DC_MCs are the

ones which exhibit a stronger PU carbonyl peak, which suggests that DC193 OH end groups reacted with the Ongronat® 2500 in a higher extent than the other stabilizers. Indeed, a broad band between 1115 cm^{-1} and 1060 cm^{-1} in the DC_MCs and GA_DC_MCs spectra indicate the presence of siloxane (Si-O-Si) groups brought by DC193 [16, 32]. An additional EDS analysis, Table IV. S3 and Figure IV. S5, from the Supplementary Information, confirmed the presence of Si atoms in the DC_MCs. The presence of GA and PVA cannot be confirmed by ATR-FTIR as none of its characteristic peaks can be identified, or are hidden, in the respective MCs spectra.

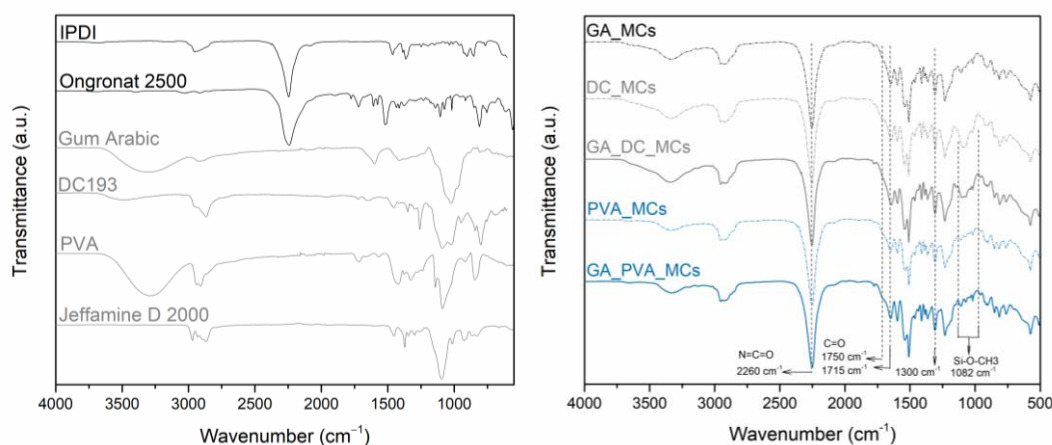


Figure IV.26. FTIR spectra of the isocyanates, active H source, and stabilizers (left). FTIR spectra of the MCs (right).

The Y value of the as-prepared MCs (Y_i), and those aged by 3 months, with the latter given as a percentage of Y_i , were used to conclude about the MCs shelf-life. The obtained values are reported in Table IV. 17. For the period of 3 months, most of the MCs had a decrease in the Y value between 37.7 and 54.2%. The GA_DC_MCs had the most significant decrease, of almost 66%, possibly because these MCs smaller, therefore, with a larger surface area which contributes to a greater diffusion of air moisture to its core and the consequent isocyanate polymerization.

The thermograms and respective derivative curves of the MCs, as well as those of the isocyanates used in the synthesis, are represented in Figure IV.27. The major mass loss of IPDI occurs at 225 $^{\circ}\text{C}$, while the Ongronat®2500 has its most significant loss occurring at 294 $^{\circ}\text{C}$. The PUa and PU MCs' shell decomposition, especially the soft segments, start to occur typically around 300 $^{\circ}\text{C}$, as can be seen in Figure IV. S6, from Supplementary Information [19]. Having this into account, the first mass loss in the MCs thermograms was considered to calculate the amount of encapsulated isocyanate which is listed in Table IV. 17. All the MCs have around 30 wt% of unreacted encapsulated isocyanate, with exception for PVA_MCs and GA_PVA_MCs,

both having ca. 46 wt%. PVA is the emulsion stabilizer that is expected to have the lowest contribution to the MCs' shell as it does not act at the emulsion droplet interface, stabilizing only by increasing the viscosity of the W phase, which might explain the larger encapsulation observed.

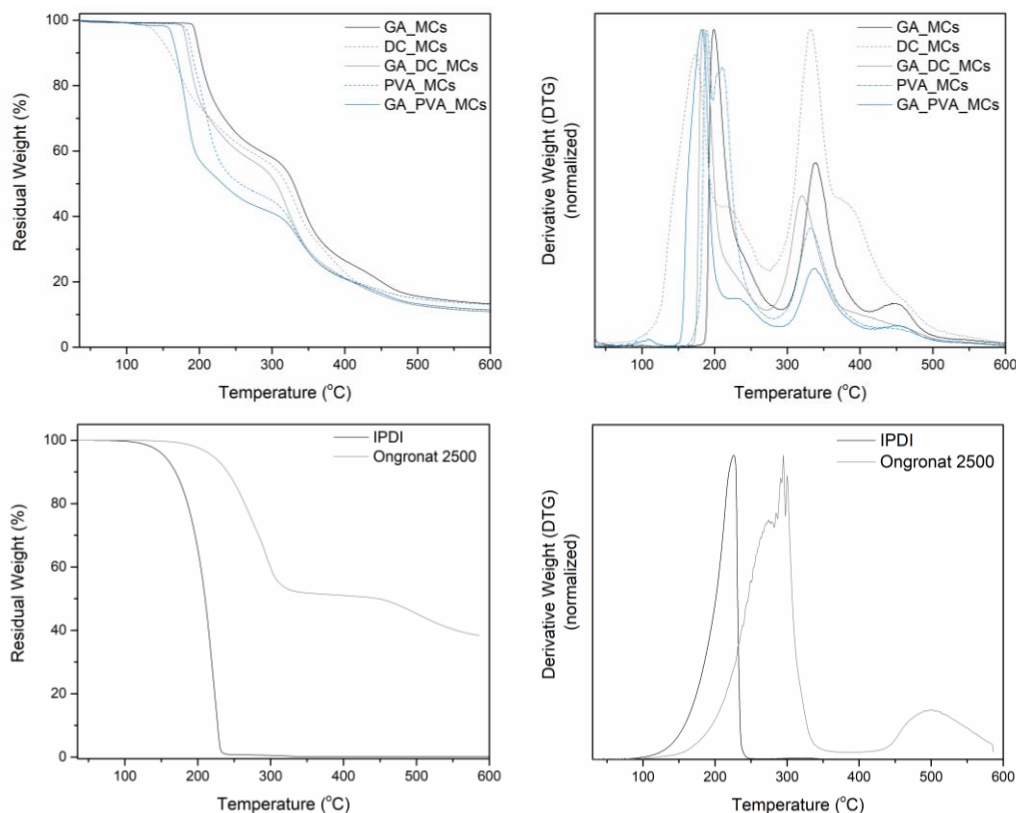


Figure IV.27. Thermogram of the as-prepared MCs and the respective derivative curves (top). Thermogram of the isocyanates and the respective derivative curves (bottom), normalized by the division of each point by the maximum value.

Table IV. 17. Mass loss (%) of encapsulated IPDI (by TGA), relative encapsulation Yield (Y) calculated using the FTIR spectra obtained after the synthesis and 3 months later. The Y₃ is given as a percentage of Y_i.

MCs' acronym	Mass loss (%) from TGA (encapsulated isocyanate) (from 116-188 to 320 °C *)	Initial relative encapsulation yield (Y _i)	Y ₃ (%) 3 months after the synthesis
GA_MCs	31.2 wt%	14	50.3
DC_MCs	30.6 wt%	13.7	62.3
GA_DC_MCs	32.9 wt%	14.3	34.2
PVA_MCs	46 wt%	15.3	45.8
GA_PVA_MCs	46.3 wt%	16.1	53.3

*Range of temperatures used for the encapsulated isocyanate quantification. The temperature range varied depending on the MCs thermograms.

To conclude, all the studied stabilization systems enabled loose, spherical, and core-shelled MCs, with the exception of DC193.

PVA and its combination with GA led to a significant reduction of the gravitational separation phenomenon, with the continuous phase viscosity having the most significant impact in the emulsion stabilization. The MCs obtained with the combination of both these stabilizers were also the ones with the highest encapsulation content (46.4 wt%). However, PVA alone, besides leading to a similar encapsulation amount, showed a better performance during the MCs' synthesis leading to the smallest variation in size of the droplet to particle process, and allowing a finer tuning and control of the MCs' size. Rheology modification is found to be the most effective strategy to stabilize O/W emulsion systems for the PUa MCs' synthesis by interfacial polymerization. The increased viscosity of the continuous phase, achieved with PVA at 2 wt% in the W phase of the emulsion, is shown to be an effective strategy for this purpose.

IV.4 Scale-up of the syntheses processes

A laboratorial scale-up of the synthesis process was made at IST facilities, with the intent to produce a higher number of MCs to be tested in the pre-polymer by CIPADE and, posteriorly, by its customers. The laboratorial scale-up refers to a reaction volume increase from 1.5L to 10L, which corresponds to an increase of almost 7 times its initial volume. The initial volume was already scaled-up from an initial protocol which involved a reactional volume of 77ml. The 77ml reactional volume was used to make the initial studies regarding the choice and impact of the active H sources and isocyanates used on the synthesis. All the other reactional optimizations were made using the 1.5L volume. The transition to 10L required adaptations to the process, more specifically to the filtration process, represented by an asterisk in the flow diagram, Figure IV.28, as it became a time-consuming operation.

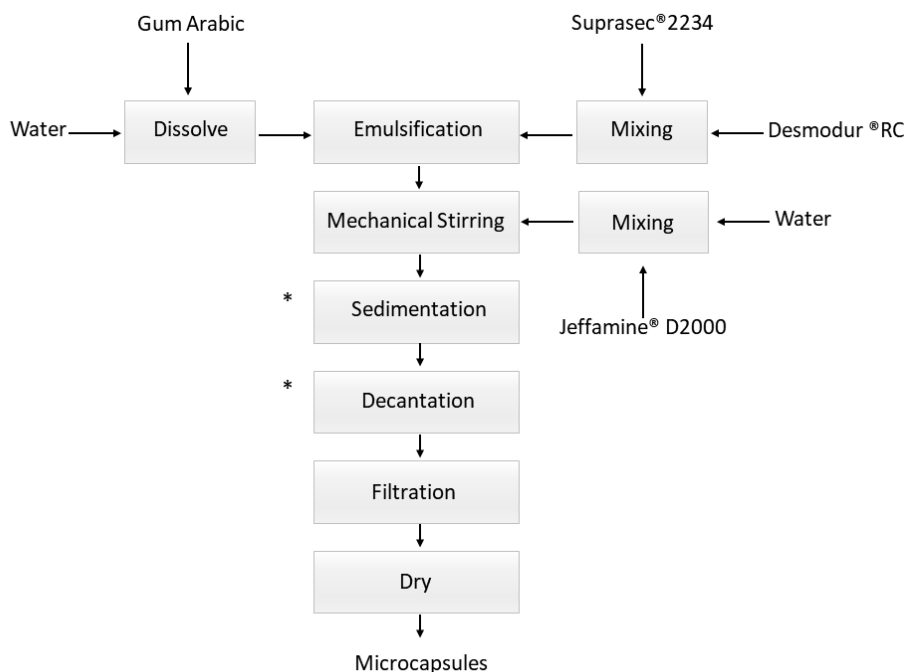


Figure IV.28. Flow diagram of the PU/PUa MCs' synthesis by the solvent evaporation method, for a volume of 10L. With an * are represented two additional steps added to the MCs synthesis in the scale-up process.

As per request of the company CIPADE, Suprasec®2234 containing MCs were the selected ones for the scale up tests. Table IV.18 lists the emulsion composition and time of synthesis for both cases.

Table IV.18. Microcapsules' acronyms and emulsion composition for the pre-scale-up and for the scale-up volume.

MCs acronym	Synthesis volume	Water phase (wt%)	Oil phase (wt%)	Active H source (wt% in the W phase)	Time of synthesis
Pre-scale-up_MCs	1.5L	Water Gum arabic	Suprasec® 2234 (Core content)	Aqueous solution of Jeffamine D	1h20
Scale_Up_MCs	10L	(89% of the emulsion)	Desmodur® RC (Shell) (11% of the emulsion)	2000 at 17 wt% (2.2 wt%)	1h

The reaction apparatus of the small-scaled synthesis as well as for the scaled-up volume are depicted in Figure IV.29. In Figure IV.30, are exposed the major steps of the MCs' synthesis process, with the microscopy photographs obtained in each phase as well as of the final MCs.

Initially the O phase, composed by the Suprasec®2234 and the Desmodur®RC, is added to the W phase by a glass funnel connected with a metallic tube, which allows the O phase to enter directly in the water. This is followed by the emulsification. The ULTRA-TURRAX is then manually exchanged for the mechanical stirrer, and the active H source, Jeffamine® D2000 is added. Once the MCs attain enough maturity, the stirring is stopped, and the MCs are let to sediment. This step is followed by the decantation of the upper water phase, and the filtration and washing of the MCs.

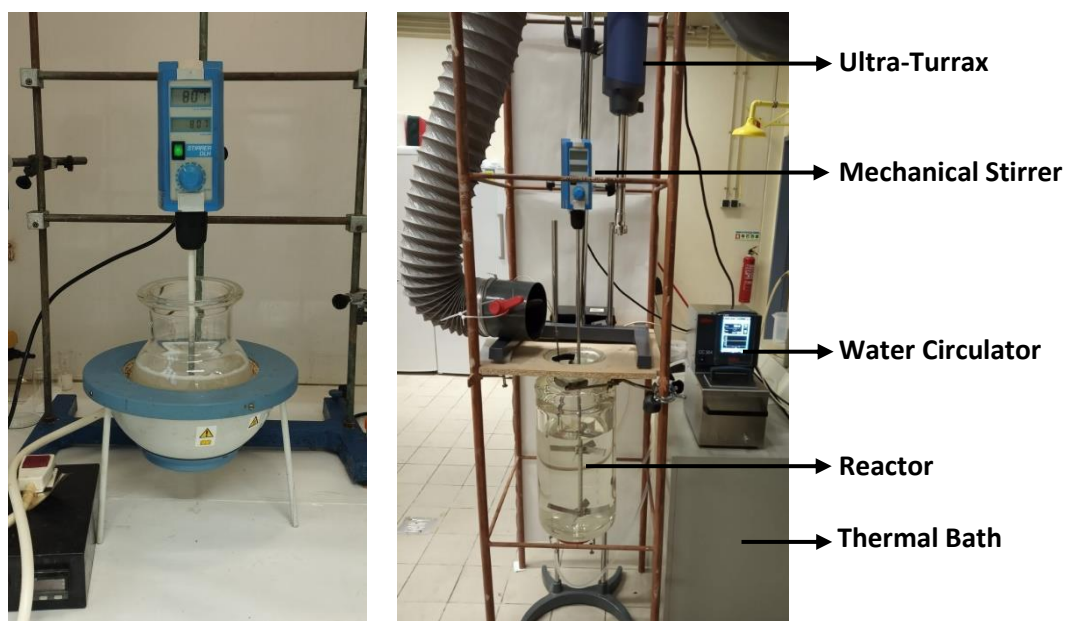


Figure IV.29. MC's synthesis apparatus used for the pre-scale-up (left) and for the scaled-up volume (right).

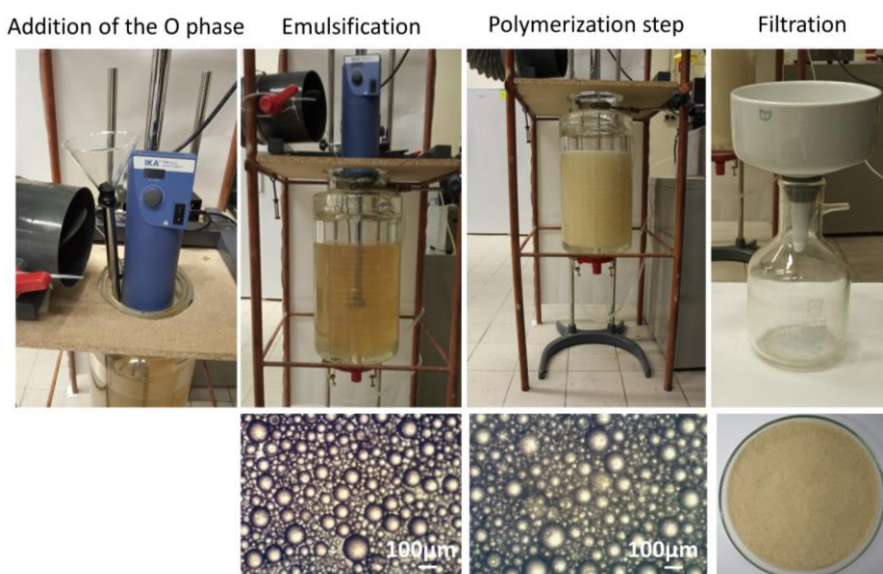


Figure IV.30. Photographs of the several steps used for the MC's fabrication namely the addition of the O phase to the W phase, emulsification, polymerization phase and MCs' filtration, with respective optical photographs of the reactional medium and final MCs.

The SEM photomicrographs of both samples are exposed in Figure IV.31, along with the MCs size distribution histogram. Both syntheses resulted in loose MCs, with the V0_MCs having a bimodal size distribution and the 5V0_MCs a monomodal distribution.

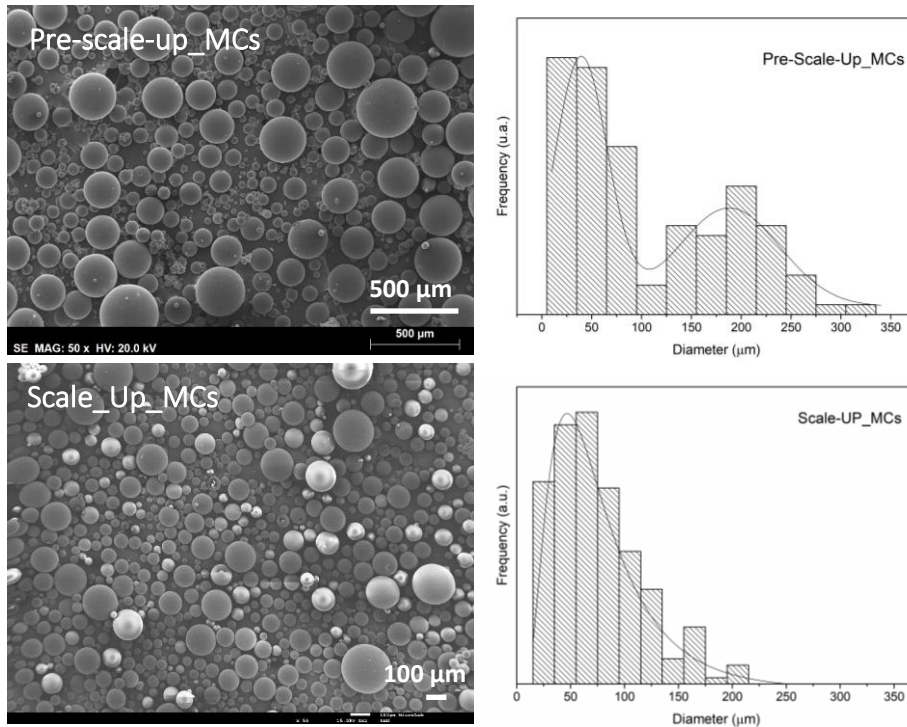


Figure IV.31. SEM photomicrographs of the Pre-Scale-Up_MCs and of the Scale-Up_MCs (left), and respective size distribution histograms (right).

The scale-up process resulted in a decrease of the medium MCs' size along with an uniformization of the size distribution. This can be related with the different ULTRA-TURRAX dispersion rotor used in the scale-up. Figure IV.32 shows the schematization of an ULTRA-TURRAX, which enabled a better emulsification and homogenization of the emulsion droplets. As depicted, a metal shaft (rotor) rotates inside a stationary casing (stator). During the emulsification process, the sample is drawn into the narrow space between the rotor and stator, which creates shear forces. The level of shear is affected by the speed as well as the size of the gap between the rotor and the stator. Those changes, between dispersion rotors, need to be compensated by an adaptation to the applied rotations per minute (rpm). The speed of the rotor relates with the rpm by the Equation 4 [33]. When increasing the rotor diameter, the rpm value should be decreased to maintain the same tip velocity.

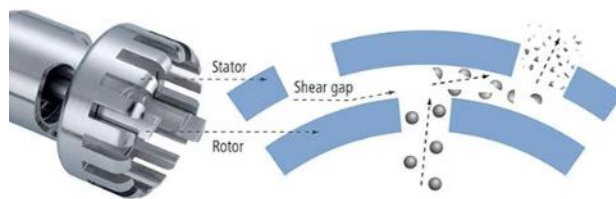


Figure IV.32. Schematic representation of the mixing mechanism of the rotor/stator arrangement of Ultra-Turrax homogenizer. Image reprinted from [34].

$$V = \frac{R\pi d}{60} \quad \text{Equation 4}$$

where, V is the rotor speed (m/s), R the rpm (rev/min) and d the rotor diameter (m). As this, the emulsification was decreased from 3600rpm to 1600rpm. Figure IV.33 depicts the dispersion rotor used in the pre-scale up synthesis, (a), and in the scale-up one, (b).

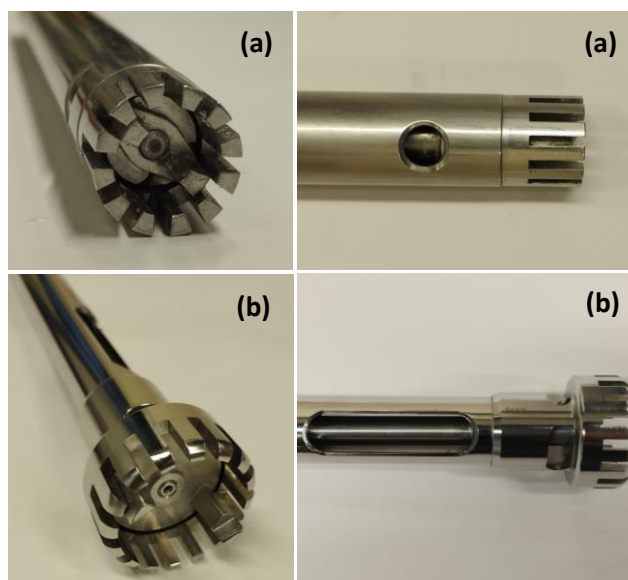


Figure IV.33 - Dispersion rotors used in the pre-scale-up (a) and in the scale-up (b).

Regarding the mechanical stirring, in the pre-scale-up synthesis a mechanical agitation of 200 rpm was applied, using a rod with 7 cm blades. For the scaled-up synthesis a rod with 13.5 cm blades was used and an agitation of 100 rpm was applied, calculated using the Equation 4. Due to the cylindrical nature of the reactor, the used rod had two sets of blades distanced vertically by 23 cm. The stirrer blade used in the pre-scale up synthesis as well as that of the scale-up are shown in Figure IV.34, (a) and (b) respectively.

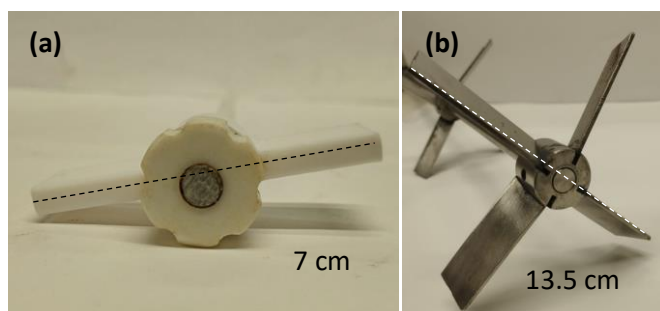


Figure IV.34 – Stirrer blade used for the mechanical agitation in the pre-scale-up (a) and in the scale-up (b) synthesis process.

Figure IV.35 depicts the FTIR-ATR spectra of the Pre-scale-up_MCs and Scale-Up_MCs, as well as those of the isocyanates and active H source used for the MC's synthesis. By comparing the MCs' spectra it is possible to state that both syntheses led to MCs with an identical chemical composition, as their spectra have the same fingerprint. When looking at the intensity of the N=C=O bond stretching peak, it can be stated that the scale-up led to MCs with an identical, only slightly lower, encapsulation content. The Y values calculated for both syntheses are listed in Table IV.19. These facts reveal the success of the implemented scale up process.

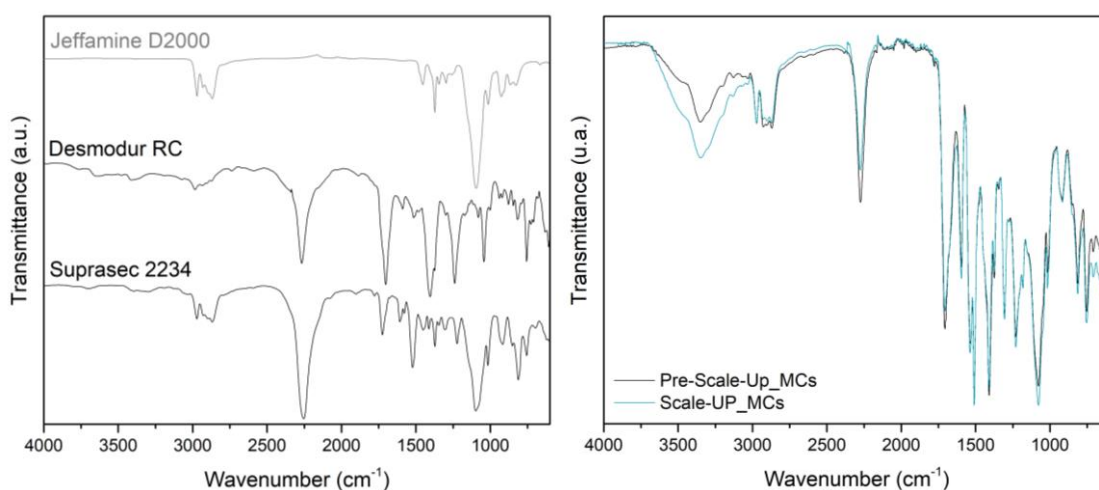


Figure IV.35 - FTIR-ATR of the isocyanates and active H source used for the MCs' synthesis (left) and of the MCs obtained for the pre-scale-up and for the scale-up reactional volume (right).

Table IV.19. Relative encapsulation yield (Y value) of the Pre-scale-up_MCs and of the Scale-up_MCs as prepared.

MCs' acronym	Initial relative encapsulation yield (Yi)
Pre-scale-up_MCs	4.20
Scale-Up_MCs	3.52

By this laboratorial scale-up the number of obtained MCs was increased from 75g, in the 1.5L volume batch, to 400g of MCs per synthesis, at the same time maintaining the characteristics of the product. This confirms the viability of implementing this synthesis process in a larger scale.

IV.5 Final remarks

Interfacial polymerization technique combined with an O/W microemulsion system is the most reported method to produce PUa and/or PU/PUa MCs. Although this is a well-established technique, there are still some challenges regarding this process, in particular the wide size distributions of the obtained MCs, its low encapsulation yield, and its short shelf-life. In this work several approaches to tackle these issues and to optimize the isocyanate containing PU/PUa MCs, obtained by the interfacial polymerization technique, were tested.

Encapsulation Yield

The main factor affecting the encapsulation yield is the extent of the reaction between the isocyanates to be encapsulated and the reactive groups of the W phase of the emulsion. Having this into consideration, it was tried to decrease the contact between the isocyanate and the W phase of the emulsion by promoting a quicker formation of the initial, immature, shell at the O droplets surface. For that purpose, the effect of the synthesis duration and temperature, as well as the use of two different isocyanates on the O phase in combination with the addition of active H sources, were studied.

Both the **duration and temperature at which the synthesis is performed** have proven to strongly impact the encapsulation yield. It was found that the duration of the synthesis influences the MCs' shell thickness, mainly when using a temperature of 30 °C. This result is explained by the longer time necessary for the formation of the shell as higher temperatures increase the diffusion and partition coefficient of the reactants, consequently increasing the reaction rate. **It was found that by using higher temperatures and by optimizing the duration of the reaction, by recurrently observing an aliquot of the reaction medium at the microscope, it is possible to obtain MCs with a smaller S/D ratio and with an adequate balance between an enough mature shell and a good encapsulation content.**

Another strategy is to use **two isocyanates in the O phase of the emulsion, the most reactive for the shell formation and the other to be encapsulated, along with the addition of active H sources.** All the synthesis to which active H sources were added led to a higher encapsulation

content, particularly those with PEI. Indeed, primary amines have a faster reaction with NCO than primary hydroxyls and water. However, PEI has a branched structure rich in NH groups resulting in a very cross-linked shell. Although this active H source would be ideal to be used to encapsulate isocyanate species for other applications, for this case it might condition the MCs' performance as cross-linkers. One of the main difficulties on the use of PU/PUa MCs for this application is to guarantee its breakage during the adhesive application, by the effect of pressure. As this, it is proposed the use of Jeffamine® D2000, which has a long linear structure, composed by repeating oxypropylene units and only two NH end groups per molecule. It is expected for this amine to provide some flexibility and hydrophobicity to the MCs' shell. In addition, **Jeffamine® D2000 led to significant improvements in the encapsulation yield and shelf-life of the MCs**, comparing with the ones obtained without active H sources.

Although it was possible to increase the encapsulation yield by using the proposed strategies, the maximum value obtained in the developed work was of ca. 46.3 wt% of IPDI, which does not represent a significant improvement to the state of the art. Values ranging from 30 to ca. 60 wt% of encapsulated content have been reported, using this technique, by other authors. However, in most of the cases there is evidence that the MCs core is composed not only by the isocyanate but also by an organic solvent.

For other cases, higher encapsulation values are only obtained for large sized MCs, as reported by *Yang et al.* In this case, 68% of encapsulation is achieved for MCs with diameters between 200 and 400 µm, decreasing to 32 wt% of IPDI for lower diameters MCs [14]. In our case, the developed PU/PUa MCs have average diameters between 30 to 100 µm with the majority having ca. of 60 µm. An exception is the MCs containing encapsulated Ongronat® 2500 and Suprasec® 2234 which have larger size diameters, probably related to this isocyanate's high viscosity.

Shelf-life

The MCs' shelf-life is intrinsically correlated with the reaction of the encapsulated isocyanate with available OH or NH groups. Although some reactive groups, from the active H sources, might still be available to react in the moments after the MCs' synthesis, it is the diffusion of the air moisture, to the MCs interior, that mostly affects its shelf-life. As an attempt to decrease the rate of this diffusion, the effect of different isocyanates used for the shell formation and different active H sources were studied.

Three different isocyanates, namely Ongronat® 2500, Suprasec® 2234, which are both MDIs with different polymerization degrees, and Desmodur® RC, a poly-isocyanurate of TDI, were tested

to be used for the shell formation. It is expected for the shell obtained with the MDIs to be denser and more crystalline than that obtained with the Desmodur® RC, as it has a bulky aromatic trifunctional monomer. Indeed, MCs synthesized with MDI compounds showed an improved shelf-life, with the **Ongronat_MCs exhibiting the lowest isocyanate loss in a period of 3 months while stored at room temperature and 60% of relative humidity.**

The addition of active H sources was used to tailor the MCs, in the sense that chemical backbone of the active H sources might influence the MCs' chemical and mechanical properties. Several active H sources, namely two amines, PEI and Jeffamine® D2000, a polyol, 1, 6 – Hexanediol and a silane, n-OTES were tested. All the MCs to which active H sources were added during the synthesis presented an increased resistance to the air moisture diffusion, with Jeffamine® D2000 and the combination of PEI and n-OTES leading to the most protective shells. The repeating oxypropylene units of Jeffamine® D2000, as well as the long aliphatic carbohydrate chain of n-OTES might have brought some hydrophobicity to the shell. PEI contributed with an increase in the cross-linking of the shell, due to its branched structure rich in NH groups. By using active H sources, the MCs' shell resistance to the water diffusion was increased. **After a period of 3 months, the PEI_n-OTES and Jeffamine_MCs showed a reduction of only 43 and 48.5 wt% of the initial Y value, which contrasts with the 66.2 wt% of loss obtained without active H source.**

Size Distribution

By interfacial polymerization technique, the MCs size distribution is defined by the emulsion droplets' size and stabilization, as the polymerization reactions occur at the droplets surface leading to the formation of the shell. As so, several stabilization systems comprising emulsifiers, a polysaccharide and a rheology modifier, as well as combinations between them, were tested with the intent to decrease the emulsion destabilization that occurs during the first moments of the synthesis. Although GA is the most used emulsion stabilizer to obtain this type of MCs, it was by rheology modification that the most stable system was achieved. In this sense, PVA was the rheology modifier employed, either alone or in combination with GA. When used alone it led to the most stable system, but in combination with GA it led to the highest encapsulation content. An increase of the W phase viscosity to 5-6 cP, enabled by 2wt% PVA, resulted in a minimum variation between the size of the initial emulsion droplets and that of the final MCs, enabling a finer control over the MCs size. **Rheology modification is herein shown to be the most effective strategy to stabilize O/W emulsion systems for the PUa MCs' synthesis by interfacial polymerization, namely by adding PVA to the W phase of the emulsion.**

Table IV. 20 summarizes each strategy used to optimize the MCs' characteristics as well as the main conclusions draw from each study.

Table IV. 20. Strategies used to optimize the MCs' characteristics and the main effects/conclusions of each study.

Characteristics to optimize	Strategy used for the optimization	Effect on the MCs
Encapsulation Yield	Synthesis temperature	- Shell formation (higher temperatures result in a quicker shell formation); - MCs' S/D ratio (higher temperature result in a lower S/D ratio); -Maturity of the shell (higher temperature result in a more mature shell).
	Synthesis duration	-Maturity of the shell (longer duration result in a more mature shell); -Encapsulation yield (longer durations result in lower encapsulation yield).
	Use of two isocyanates	- Higher encapsulation content.
	Active H sources	- Use of active H sources lead to a higher encapsulation yield; - Amines led to higher encapsulation yield than polyols.
Shelf-life	Type of isocyanate for the shell formation	- The use of MDI for the shell formation, over TDI, led to an extended shelf-life.
	Active H sources	- Adding hydrophobic active H sources led to an extended shelf-life.
Size Distribution	Emulsion stabilization	- Rheology modification enables a better emulsion stabilization and control over the MCs sizes.

Contributions:

- Effect of the synthesis temperature and duration on the MCs size and shell thickness.
- The effect of several active H sources, and their combination, on the encapsulation yield and MCs' shelf-life. The use of the active H source Jeffamine® D2000 had not been yet reported on the state of the art for this application.

- The effect of different isocyanates on the chemistry and mechanical properties of the MC's shell. Suprasec® 2234 and Desmodur® RC had not been yet reported in the literature to be used for the MCs' shell synthesis. As for Ongronat®2500, its use was only reported by our group [32, 35].
- Comparative study on the effect of a polysaccharide, a surfactant, a polymer, and their combinations, for the O/W emulsion stabilization.
- Fine-tuning of the PU/PUa final MCs' size and size distribution by means of the emulsion W phase rheology modification. Determination of the optimum viscosity for the system in study.
- Encapsulation of high MW isocyanates, with a NCO value lower than 30, by the interfacial polymerization technique in combination with an microemulsion system.

Bibliography

- 1 Szycher, M., *Szycher's Handbook of Polyurethanes*. 2nd ed. **2012**, Boca Raton: CRC Press.
- 2 Mishra, M., *Handbook of Encapsulation and Controlled Release*. **2015**, Boca Raton: CRC Press.
- 3 Gaudin, F.;Sintes-Zydowicz, N., *Correlation between the polymerization kinetics and the chemical structure of poly(urethane–urea) nanocapsule membrane obtained by interfacial step polymerization in miniemulsion*. *Colloids and Surfaces A: Physicochemical and Engineering Aspects*, **2012**, 415, 328-342.
- 4 Parsottamdas, C. U., *Studies on Synthesis, Characterization and Applications of Microencapsulation Process via Interfacial Polymerization*, **2021**, Doctor of Philosophy dissertation, Gujarat Technological University.
- 5 Perignon, C.;Ongmayeb, G.;Neufeld, R.;Frere, Y.;Poncelet, D., *Microencapsulation by interfacial polymerisation: membrane formation and structure*. *Journal of Microencapsulation*, **2015**, 32, 1-15.
- 6 Haghayegh, M.;Mirabedini, S. M.;Yeganeh, H., *Microcapsules containing multi-functional reactive isocyanate-terminated polyurethane prepolymer as a healing agent. Part 1: synthesis and optimization of reaction conditions*. *Journal of Materials Science*, **2016**, 51, 3056-3068.
- 7 Ma, Y.;Jiang, Y.;Tan, H.;Zhang, Y.;Gu, J., *A Rapid and Efficient Route to Preparation of Isocyanate Microcapsules*. *Polymers*, **2017**, 9, 274.
- 8 Salisu, J., *Effect of Dispersed Phase Viscosity on Stability of Emulsions Produced by a Rotor Stator Homogenizer*. *International Journal of Sciences: Basic and Applied Research*, **2022**, 25, 256-267.
- 9 Fournier, C. O.;Fradette, L.;Tanguy, P. A., *Effect of dispersed phase viscosity on solid-stabilized emulsions*. *Chemical Engineering Research and Design*, **2009**, 87, 499-506.
- 10 Liu, C. W.;Li, M. Z., *Effect of Dispersed Phase Viscosity on Emulsification in Turbulence Flow*. *Applied Mechanics and Materials*, **2014**, 446-447, 571-575.
- 11 Abbott, S., *Surfactant Science: Principles and Practice*. **2015**: DEStech Publications, Inc.
- 12 Briceño, M.;Salager, J. L.;Bertrand, J., *Influence of Dispersed Phase Content and Viscosity on the Mixing of Concentrated Oil-in-Water Emulsions in the Transition Flow Regime*. *Chemical Engineering Research and Design*, **2001**, 79, 943-948.
- 13 Costa, M.;Paiva-Martins, F.;Losada-Barreiro, S.;Bravo-Díaz, C., *Modeling Chemical Reactivity at the Interfaces of Emulsions: Effects of Partitioning and Temperature*. *Molecules*, **2021**, 26, 4703.
- 14 Yang, J.;Keller, M. W.;Moore, J. S.;White, S. R.;Sottos, N. R., *Microencapsulation of Isocyanates for Self-Healing Polymers*. *Macromolecules*, **2008**, 41, 9650-9655.
- 15 Kardar, P., *Preparation of polyurethane microcapsules with different polyols component for encapsulation of isophorone diisocyanate healing agent*. *Progress in Organic Coatings*, **2015**, 89, 271-276.
- 16 Almeida, R. M.;Marques, A. C., *Handbook of Sol-Gel Science and Technology: Processing, Characterization and Applications*. 2nd ed. **2018**: Springer.
- 17 Arnold, R. G.;Nelson, J. A.;Verbanc, J. J., *Recent Advances In Isocyanate Chemistry*. *Chemical Reviews*, **1957**, 57, 47-76.
- 18 Matyjaszewski, K.;Möller, M., *Polymer Science: A Comprehensive Reference*. 2nd ed. **2012**: Elsevier B.V. .
- 19 Krohn, J.;Tate, R.;Jordy, D., *Factors Affecting the Permeability of PE Blown Films*. *Journal of Plastic Film & Sheeting*, **1997**, 13, 327-335.
- 20 Stuart L. Cooper, J. G., *Advances in Polyurethane Biomaterials*. **2016**: Woodhead Publishing, Elsevier.

- 21 Van Goethem, C.;Mulunda, M. M.;Verbeke, R.;Koschine, T.;Wübbenhorst, M.;Zhang, Z.;Nies, E.;Dickmann, M.;Egger, W.;Vankelecom, I. F. J.;Koeckelberghs, G., *Increasing Membrane Permeability by Increasing the Polymer Crystallinity: The Unique Case of Polythiophenes*. *Macromolecules*, **2018**, 51, 9943-9950.
- 22 Loureiro, M. V.;Mariquito, A.;Vale, M.;Bordado, J. C.;Pinho, I.;Marques, A. C., *Emulsion Stabilization Strategies for Tailored Isocyanate Microcapsules*. *Polymers (Basel)*, **2023**, 15.
- 23 Lian, X.;Liao, S.;Xu, X.-Q.;Zhang, S.;Wang, Y., *Self-Stabilizing Encapsulation through Fast Interfacial Polymerization of Ethyl α -Cyanoacrylate: From Emulsions to Microcapsule Dispersions*. *Macromolecules*, **2021**, 54, 10279-10288.
- 24 Walstra, P., *Physical Chemistry of Foods*. 1st ed. **2001**: CRC Press, Boca Raton.
- 25 McClements, D. J., *Critical review of techniques and methodologies for characterization of emulsion stability*. *Critical Reviews in Food Science and Nutrition*, **2007**, 47, 611-49.
- 26 McClements, D. J.;Jafari, S. M., *Improving emulsion formation, stability and performance using mixed emulsifiers: A review*. *Advances in Colloid and Interface Science*, **2018**, 251, 55-79.
- 27 Loxley, A.;Vincent, B., *Preparation of Poly(methylmethacrylate) Microcapsules with Liquid Cores*. *Journal of Colloid and Interface Science*, **1998**, 208, 49-62.
- 28 Yao, X.;Xu, Q.;Tian, D.;Wang, N.;Fang, Y.;Deng, Z.;Phillips, G.;Lu, J., *Physical and Chemical Stability of Gum Arabic-Stabilized Conjugated Linoleic Acid Oil-in-Water Emulsions*. *Journal of agricultural and food chemistry*, **2013**, 61, 4639-4645.
- 29 Moschakis, T.;Murray, B. S.;Dickinson, E., *Microstructural evolution of viscoelastic emulsions stabilised by sodium caseinate and xanthan gum*. *Journal of Colloid and Interface Science*, **2005**, 284, 714-28.
- 30 Grundy, M. M. L.;McClements, D. J.;Ballance, S.;Wilde, P. J., *Influence of oat components on lipid digestion using an in vitro model: Impact of viscosity and depletion flocculation mechanism*. *Food Hydrocolloids*, **2018**, 83, 253-264.
- 31 McClements, D. J., *Comments on viscosity enhancement and depletion flocculation by polysaccharides*. *Food Hydrocolloids*, **2000**, 14, 173-177.
- 32 Attaei, M.;Loureiro, M. V.;Vale, M.;Condeço, J.;Pinho, I.;Bordado, J. C.;Marques, A. C., *Isophorone Diisocyanate (IPDI) Microencapsulation for Mono-Component Adhesives: Effect of the Active H and NCO Sources*. *Polymers*, **2018**, 10, 825.
- 33 Coker, A. K., *Modeling of Chemical Kinetics and Reactor Design*. 1st ed. **2001**: Gulf Professional Publishing.
- 34 *Scaling Up a Rotor-Stator Homogenization Process*. **2019**; Available from: <https://homogenizers.net/blogs/blog/rotor-stator-homogenization-scaleup>.
- 35 Loureiro, M. V.;Attaei, M.;Rocha, S.;Vale, M.;Bordado, J. C.;Simões, R.;Pinho, I.;Marques, A. C., *The role played by different active hydrogen sources in the microencapsulation of a commercial oligomeric diisocyanate*. *Journal of Materials Science*, **2020**, 55, 4607-4623.

Supplementary Information

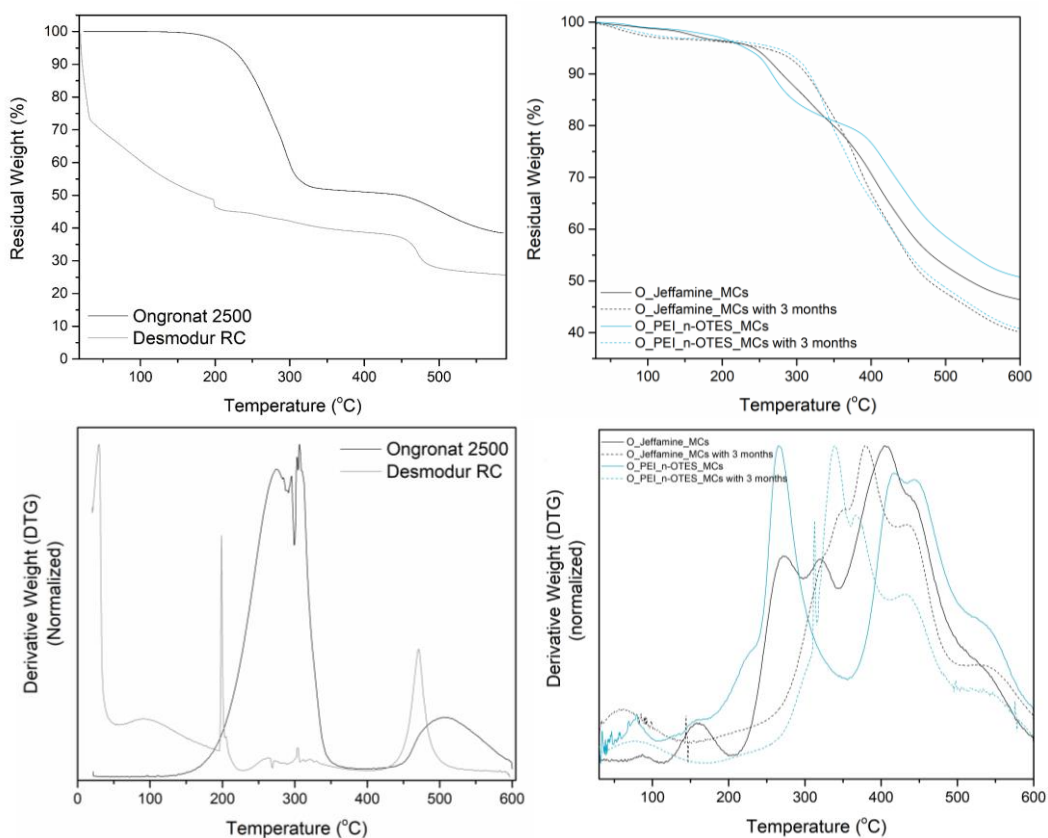


Figure IV. S1. Thermograms of the *O_Jeffamine_MCs* and of the *O_PEI_n-OTES_MCs*, as well as of the isocyanates used in the synthesis (top) and respective derivatives (bottom), normalized by the division of each point by the maximum value.

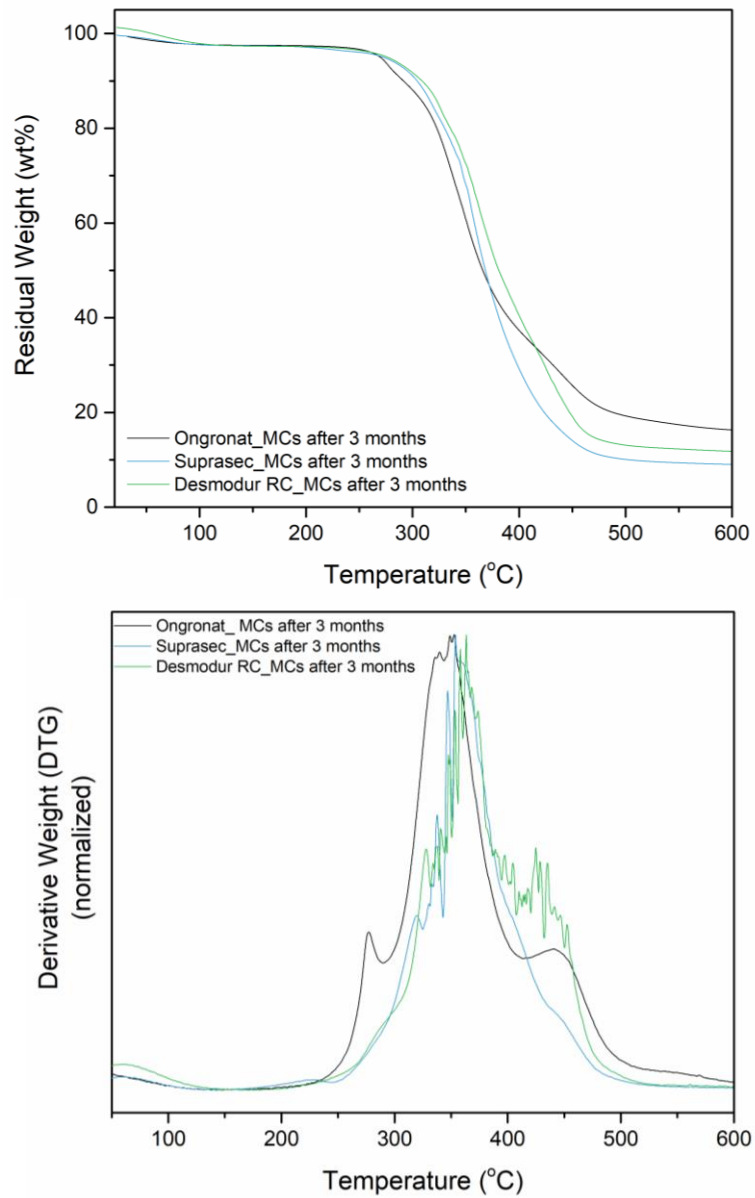


Figure IV. S2. Thermograms of the aged Ongronat_MCs, Suprasec_MCs and Desmodur RC_MCs, by 3 months at room and 60wt% humidity (above) and respective derivatives (bottom), normalized by the division of each point by the maximum value.

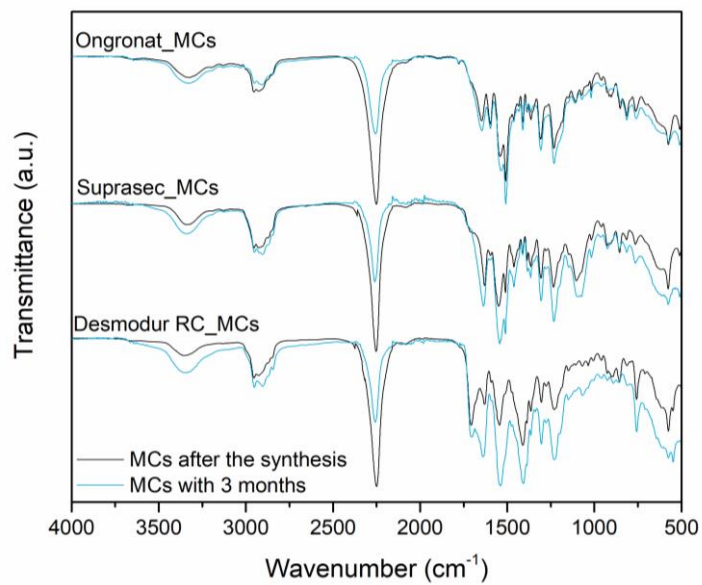
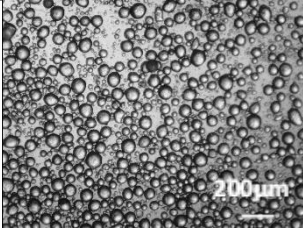
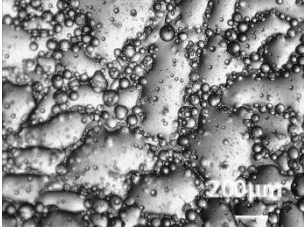
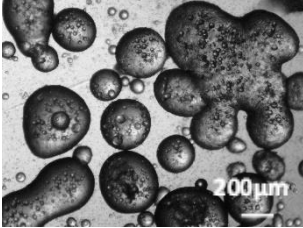
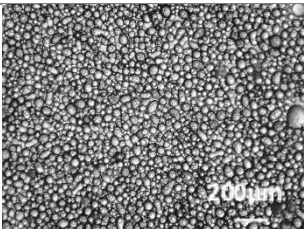
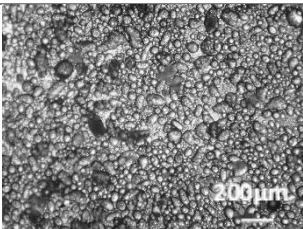
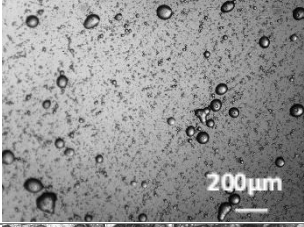
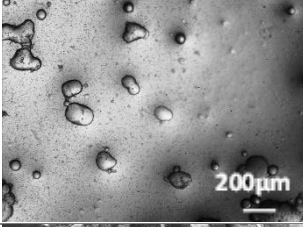
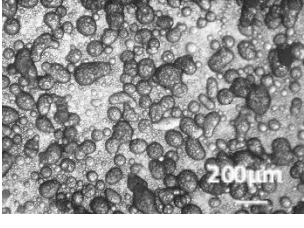
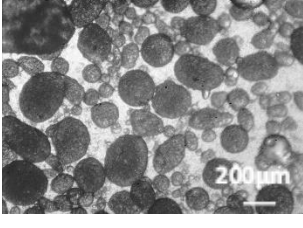
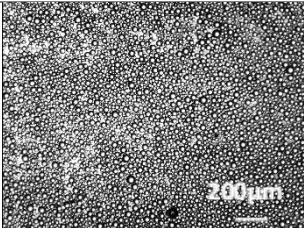
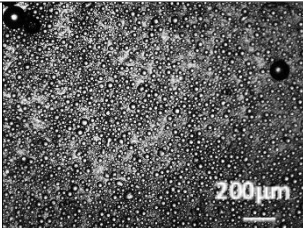


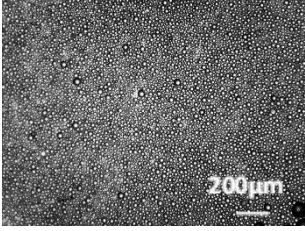
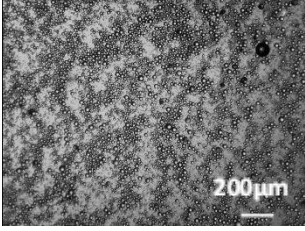
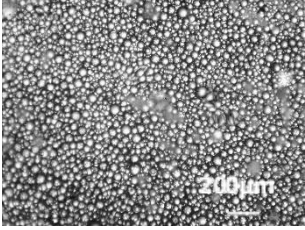
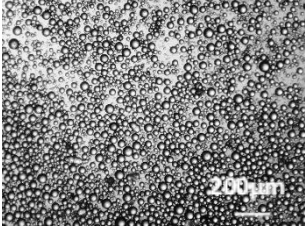
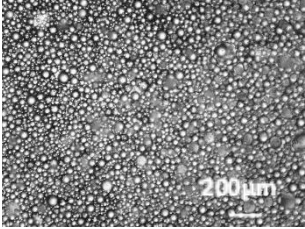
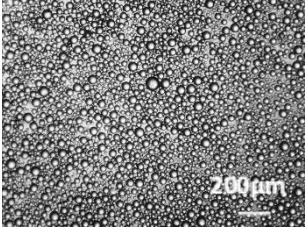
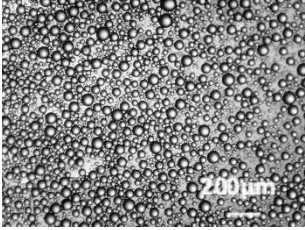
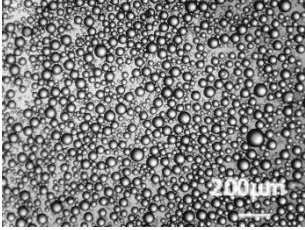
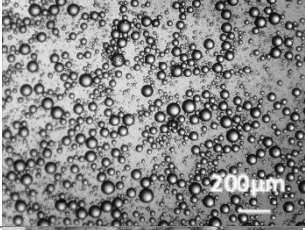
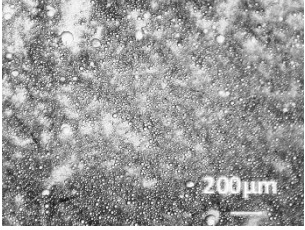
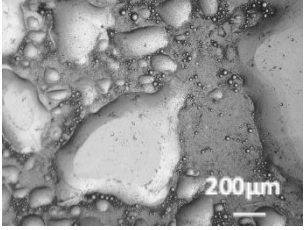
Figure IV. S3. FTIR spectra of the Ongronat_MCs, Suprasec_MCs and Desmodur RC_MCs, as prepared and aged (by 3 months, at room temperature and 60wt% of humidity).

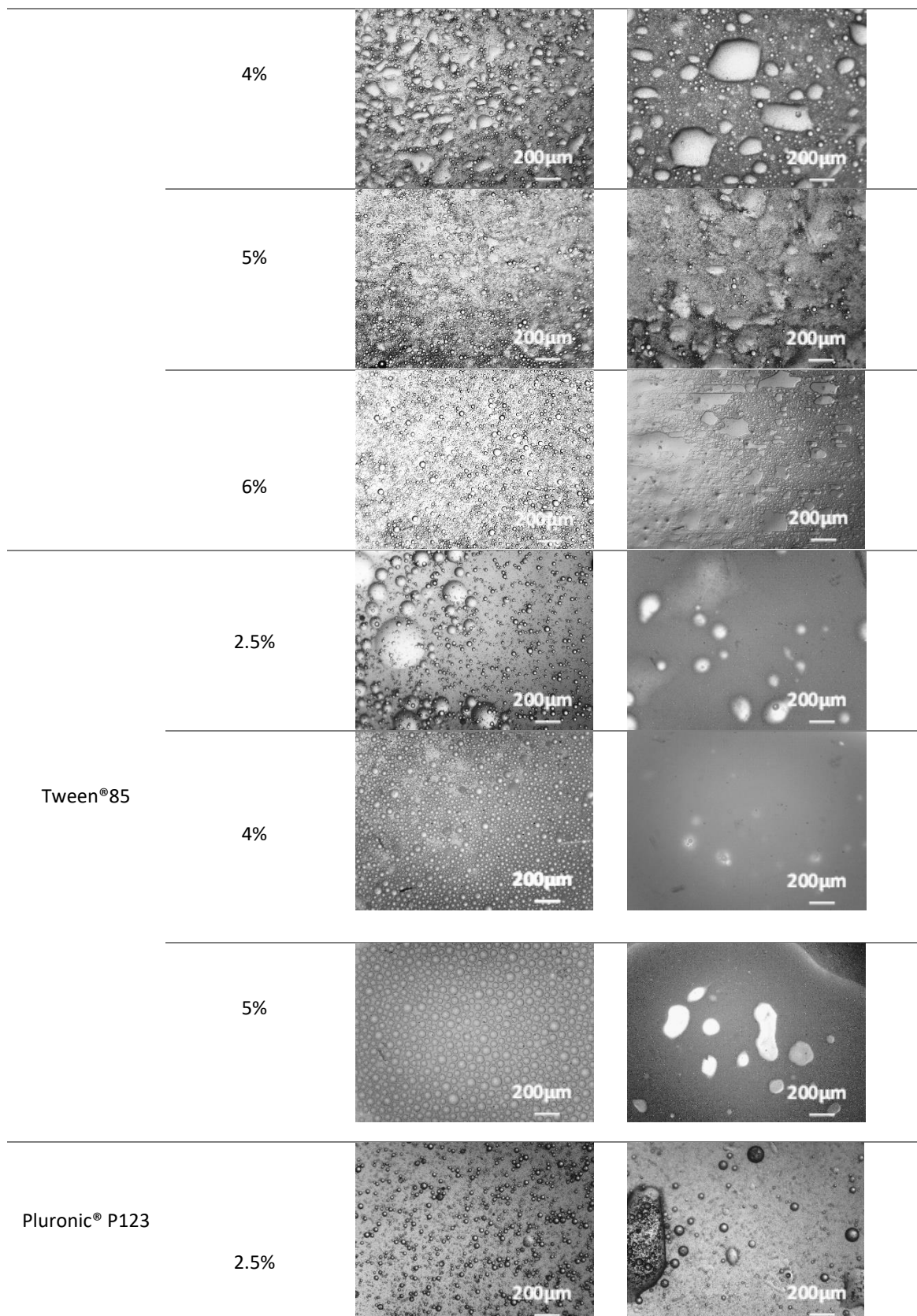
Table IV. S1. Emulsion stabilizers and combinations tested for the MCs' synthesis by interfacial polymerization technique.

Emulsion stabilizer	Gum arabic (GA)	DC193	DC193 and GA	Polyvinyl alcohol (PVA)	PVA and GA	SPAN®20	Tween®85	Pluronic® P123	Pluronic® P123 and GA
Stabilizer (wt% added to the W phase)	5%	2.5%	2% (DC193) and 2.5% (GA)	2%	2% (PVA) and 1.30% (GA)	2.5%	2.5%	2.5%	2% (Pluronic P123) and 2.5% (GA)
		4%		3%		4%	4%	4%	
		5%				5%	5%	5%	
		6%				6%		6%	
			4% (DC193) and 1% (GA)		2 wt% (PVA) and 2.5% (GA)				1% (Pluronic P123) and 4% (GA)

Table IV. S2. Optical microscopy photographs of all the emulsions tested. Left: after 10 minutes of emulsification at 3200 rpm using the Ultra-Turrax; Right: after the following 15 minutes under mechanical stirring at 400 rpm (dynamic conditions)

Emulsion stabilizer	Stabilizer (wt% added to the W phase)	Ultra-Turrax emulsification	Mechanical Agitation
Gum arabic (GA)	5%		
	2.5%		
DC193	4%		
	5%		
	6%		
DC193 and GA	2% (DC193) and 2.5% (GA)		

	4% (DC193) and 1% (GA)		
Polyvinyl alcohol (PVA)	2%		
	3%		
PVA and GA	2% (PVA) and 1.30% (GA)		
	2 wt% (PVA) and 2.5% (GA)		
SPAN®20	2.5%		



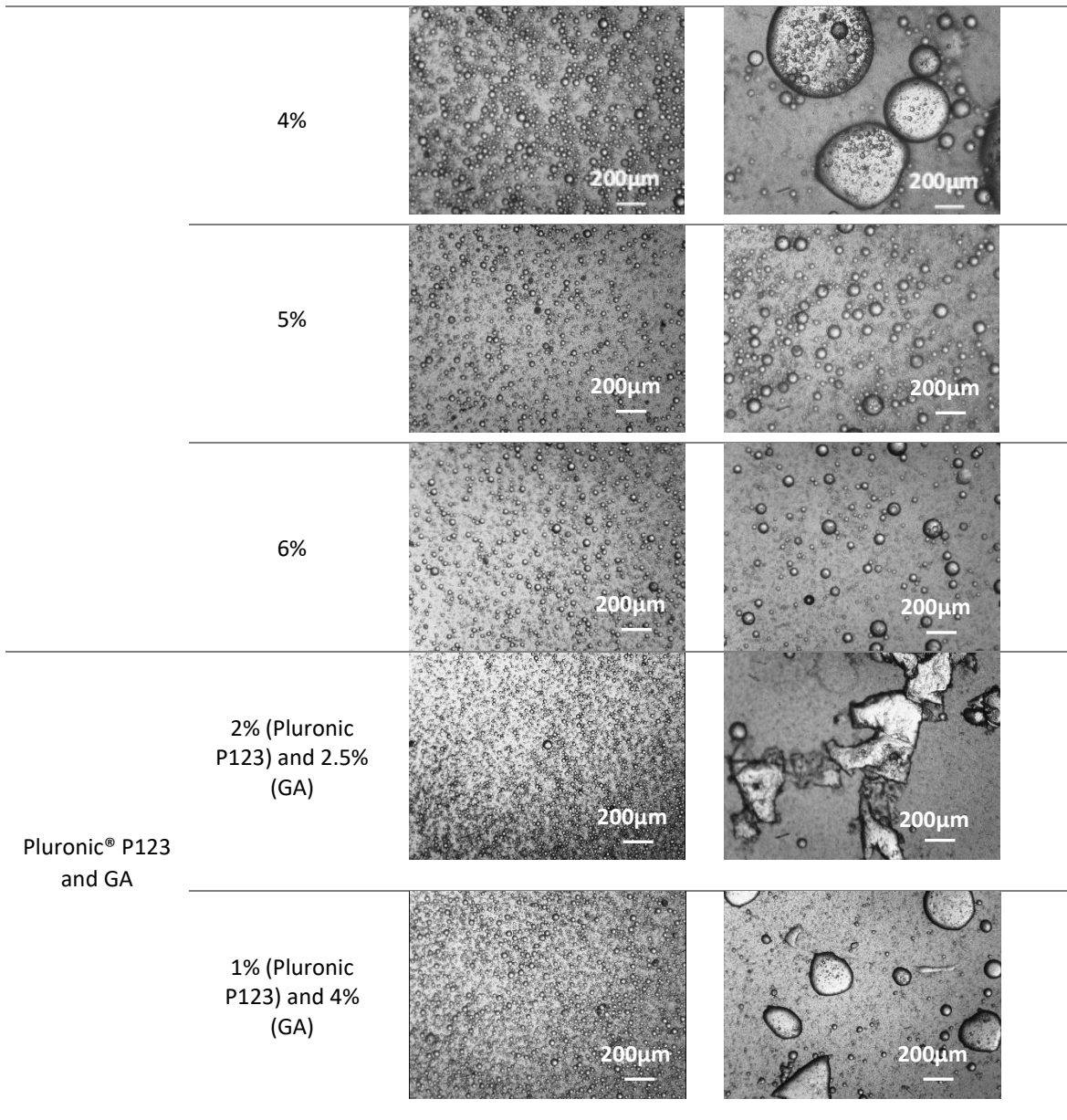


Table IV. S3. EDS atomic concentrations of the DC_MCs for C, N, O and Si atoms

Analysis	Atomic concentration			
	C	N	O	Si
Area 1	61.782	26.95	10.24	1.03
Area 2	61.084	27.49	10.73	0.70
Area 3	70.502	19.58	6.68	3.24

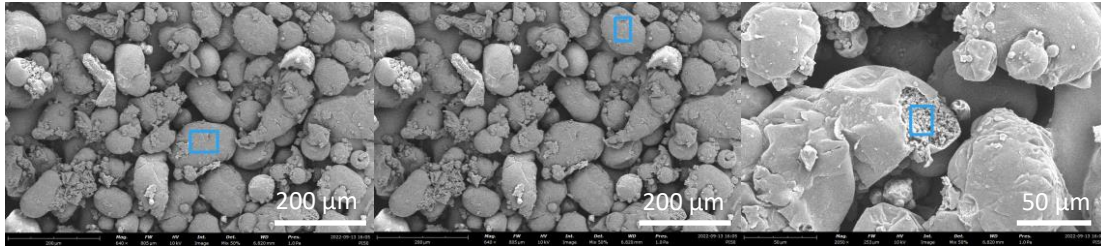


Figure IV. S5. SEM photomicrographs with the corresponding areas of the DC_MCs' EDS analysis.

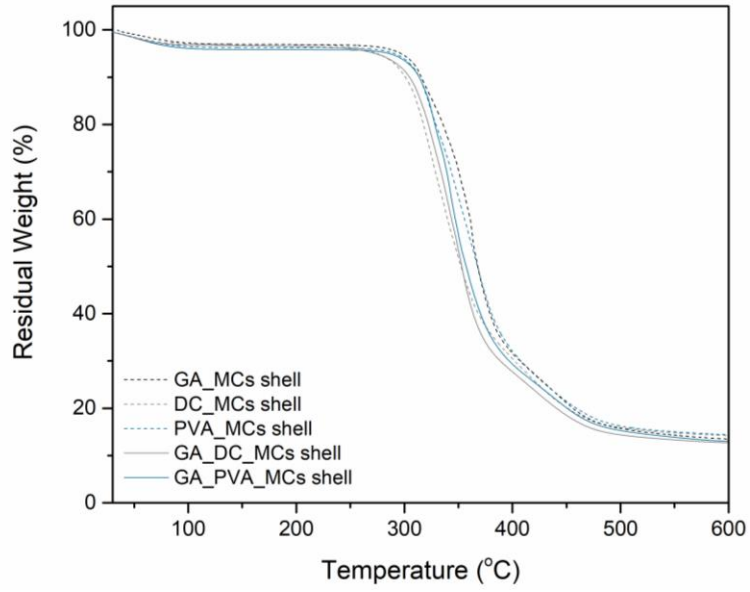


Figure IV. S6. Thermogram of the shell from the MCs obtained with different emulsion stabilization systems.

Chapter V

**Solvent evaporation technique in
combination with a microemulsion system**

Chapter V - Solvent evaporation technique in combination with a double emulsion system: strategies and reactional parameters

This chapter exposes the production of MCs by the solvent evaporation technique in combination with a microemulsion system. By this method, the MCs production occurs due to the precipitation of a dissolved polymer on the emulsion droplets interface, leading to the formation of a solid polymeric shell, without the occurrence of chemical reactions. This method was not yet reported for the encapsulation of isocyanate species which required process adaptations and several parameters' optimizations, reported in this chapter. Two distinct biodegradable polymers were used for the MCs' shell formation, intended to encapsulate not only monomeric but also oligomeric isocyanate species. A laboratorial scale-up of the MCs production process is also described, referring to an increase of the reactional volume from 85 ml to 425 ml.

Published papers with results exposed in this chapter:

- Loureiro, M. V., Vale, M., Galhano, R.; Matos, S.; Bordado, J. C.; Pinho, I., Marques, A. C. "Microencapsulation of Isocyanate in Biodegradable Poly(ϵ -caprolactone) Capsules and Application in Monocomponent Green Adhesives", *ACS Applied Polymer Materials* 2 (2020) 4425–4438. Doi: 10.1021/acsapm.0c00535
- Loureiro, M.V.; Aguiar, A.; Santos, R. G.; Bordado, J.C.; Pinto, I.; Marques, A.C. "Design of Experiment for Optimizing Microencapsulation by the Solvent Evaporation Technique", *Polymers* 16 (2024) 111. DOI: doi.org/10.3390/polym16010111

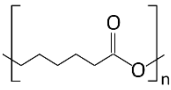
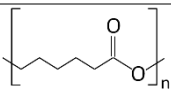
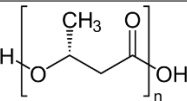
V.1 Materials

The reagents used for the MCs production, by the solvent evaporation technique in combination with a microemulsion system, can be classified as isocyanates, polymers for the shell formation, emulsion stabilizers and solvents. Table V. 1 lists all the reagents used for these MCs fabrication. The essential information regarding the isocyanates and polymers, can be found in Table IV.2 and Table V. 2, respectively. Reagents used for the production of MCs by the solvent evaporation method, respective commercial name, purity and manufacturer.

Table V. 1. Reagents used for the production of MCs by the solvent evaporation method, respective commercial name, purity and manufacturer.

Classification	Chemical	Commercial name	Purity (%)	Manufacturer
Isocyanate	Isophorone diisocyanate (IPDI)	Desmodur® I	98%	Covestro AG
	Methylene diphenyl diisocyanate (MDI)	Ongronat® 2500	-	BorsodChem
Polymers	Polycaprolactone (PCL)	-		Sigma Aldrich
	Polycaprolactone (PCL)	-	<0.5% water	Sigma Aldrich
	Polyhydroxybutyrate (PHB)			-
Emulsion stabilizers	Gum arabic (GA)	-		Fisher Chemical
	Poly(vinyl alcohol) (PVA)	-		Alfa Aesar
Solvents	Dichloromethane	-		Alfa Aesar
	Chloroform	-		Alfa Aesar

Table V. 2. Polymers used for the MCs' shell formation by the solvent evaporation method, its chemical structure, density, melting point and number average molecular weight.

Commercial name	Chemical Structure	ρ , 25°C (g/mL)	Melting point (°C)	Average Mn
Polycaprolactone (PCL)		-	60 °C	45000
Polycaprolactone (PCL)		1.145	60 °C	80000
Polyhydroxybutyrate (PHB)		-	175 °C - 180 °C	-

The information regarding the number average molecular weight of the PHB used was not provided. Therefore, GPC analysis was carried out to conclude about its molecular weight distribution, with the respective gel permeation chromatogram being reported in Figure V. S 1.

V.2 Experimental: MCs synthesis by solvent evaporation technique in combination with a microemulsion system

The solvent evaporation technique in combination with a microemulsion system enabled to obtain MCs with a shell composed by the biodegradable PCL and PHB.

To the best of our knowledge, the encapsulation of hydrophobic compounds by the solvent evaporation technique has only been reported for the encapsulation of drugs, mineral and essential oils and, in a particular case, the catalyst dibutyltin dilaurate (DBTL), with low encapsulation loads. Polymers, namely PLGA, polylactic acid (PLA), PLGA/PCL and less common PMMA, poly(phthalaldehyde) and polyethylene oxide-block-polycaprolactone were the ones applied for the shell [1-5]. The encapsulation of isocyanates, using this technique was not previously reported, nor its encapsulation in a biodegradable shell, by this or any other methodology. According with the literature, microencapsulation using PCL through solvent evaporation technique is conventionally used for the encapsulation of hydrophilic and lipophilic compounds, particularly those which are sensitive to high temperatures [6-10]. As for PHB, its reference in microencapsulation is very scarce and it is referred to be used on its own or in combination with clays, for the encapsulation of drugs, urea, bovine serum albumin (BSA) and the trifluralin herbicide [11-15]. Its use for the encapsulation of isocyanates is not yet reported in the state of the art.

The most commonly reported process for producing MCs by the solvent evaporation technique involves the use of a water-in-oil-in-water (W/O/W) emulsion system. For that, it is first dispersed an aqueous phase, containing the compound to be encapsulated, in a non-miscible organic solvent, containing a dissolved polymer for the shell, which forms the primary emulsion system W_1/O . Following, the dispersion of the first emulsion into an aqueous phase containing an emulsifier leads to the double $W_1/O/W_2$ emulsion system. The subsequent evaporation of the solvent, present in the organic phase, leads to the polymer precipitation at the W_1/O emulsion interface and to the MCs formation [16].

An adaptation of this process was made for the encapsulation of isocyanate. Instead of an initial W_1/O , it was tried to obtain a non-aqueous O_1/O_2 emulsion system in which O_1 corresponded to the isocyanate to be encapsulated and O_2 the dissolved polymer. These emulsions can be achieved by adding viscosity modifiers in the continuous phase or by using two immiscible oils, with different polarities [17, 18]. The addition of surfactants to stabilize O/O emulsions is less common, instead it is reported the use of co-polymers or solid particles for Pickering emulsions, both contributing to a steric stabilization [18, 19]. For our case, the addition of co-polymers or

solid particles would mean its later presence in the MCs shell, for that reason its use was avoided. As our O_1 phase is only composed by the isocyanate to be encapsulated the use of solvents with different polarities was not possible. Instead, PCL was used to act as both a shell-forming material and a viscosity modifier, which can promote the formation of an O_1/O_2 emulsion. By increasing the O_2 phase viscosity it is possible to control the diffusion kinetics of the isocyanate and improve the emulsion stability [17]. However, both the polymers used for the shell and the isocyanates are soluble in dichloromethane and chloroform, and that might affect the O_1/O_2 emulsion stability. The existence of this emulsion, when prepared with IPDI, was not possible to confirm, as this isocyanate is not visually distinguishable in the O_2 phase by optical microscopy observation. Due to the lack of evidence, the emulsions obtained with IPDI were considered O/W, with the O phase composed by the dissolved polymer and the IPDI. When using Ongronat® 2500 the existence of an O_1/O_2 emulsion was verified, exposed in Figure V.1. Nevertheless, the O_1 droplets have a much smaller size than that of the final MCs, which leads to believe that in the $O_1/O_2/W$ emulsion system several isocyanate droplets must be enclosed in a droplet of dissolved polymer, posteriorly merging. The stability of this emulsion was not studied.

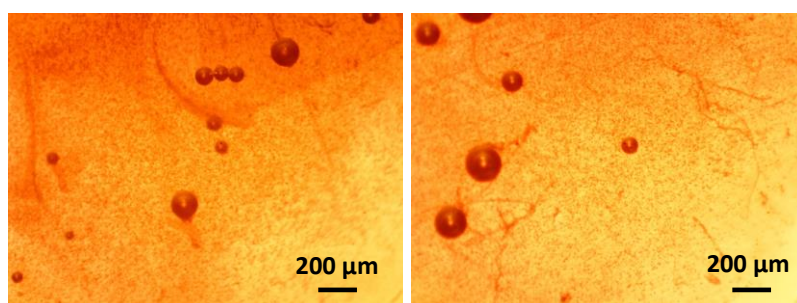


Figure V.1. Optical microscopy photograph of the O_1/O_2 emulsion obtained with Ongronat® 2500 in the O_1 phase of the emulsion.

Due to the uncertainties associated with the O_1/O_2 emulsion with IPDI, the organic phase was considered to be composed by a single O phase containing the polymer dissolved in the respective solvent, i.e. dichloromethane for the PCL and chloroform for the PHB, and the isocyanate to be encapsulated. The dissolved polymer and the isocyanate were mixed together by applying a vigorous agitation of 10000 rpm, for a volume of 65 mL in a cylindrical flask of 150 mL, using an Ultra-Turrax (IKA T25 digital ULTRA TURRAX (Staufen, Germany)), during 5 min at room temperature. The O phase was then dispersed in the W phase, containing dissolved PVA and GA, while under mechanical stirring, at 750 rpm, at room temperature. The emulsion was let under agitation, for several hours, depending on the experiment, during which the solvent gradually diffused to the continuous phase and evaporates. The process reported in the state of

the art for the formation of MCs by this method, when using a simple emulsion system, involves the formation of small polymeric domains that change the O droplets nature from one phase to a two-phase particle. This leads to interfacial tension interactions between the liquid core, the polymer and the aqueous phase, resulting in the migration of the polymer-rich domains to the O/W droplets interface. These domains tend to merge, forming a shell around the O droplets. The evaporation of the remaining solvent leads to the polymer precipitation, resulting in a solid shell [20, 21]. This process leads to the formation of core-shell MCs, as depicted in Figure V.2 (a). It is reported that, for this MCs' production method, the morphology of the MCs is determined by the thermodynamics to assure the minimum total interfacial free energy [21].

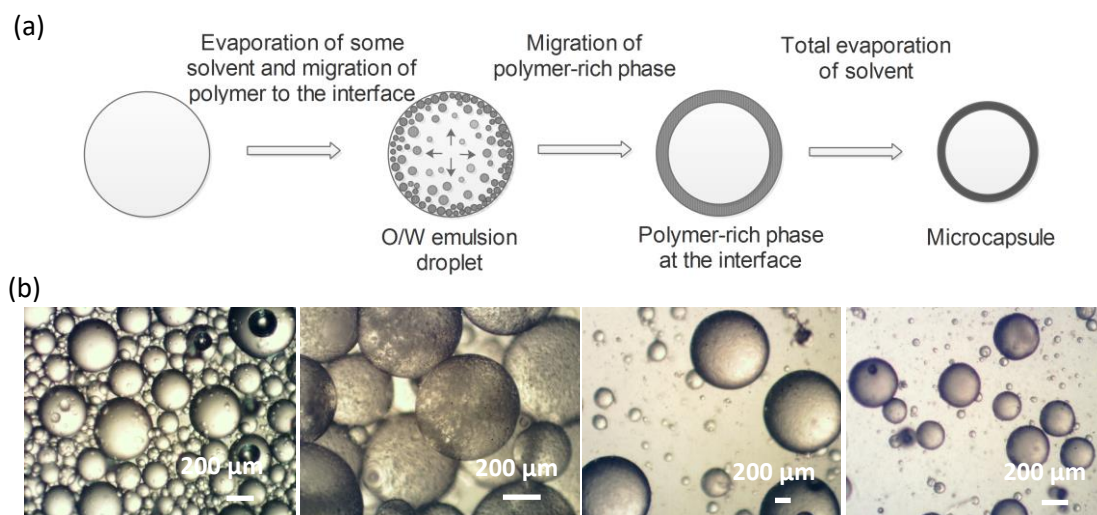


Figure V.2. Schematic representation of the several steps involved in the MCs formation by the solvent evaporation technique in combination with an emulsion system (a). Optical microscopy photographs obtained in each step (b).

Optical microscopy photographs obtained during the MCs' synthesis, exposed in Figure V.2 (b), seem to represent the process of the shell formation described in the literature. It is to notice that the photographs are not of the same synthesis nor are at the same scale but are the ones that are more representative of each step of the process. All the photographs were taken during the fabrication of PCL MCs containing encapsulated IPDI.

In Figure V. 3 is an optical microscopy photograph which shows the shell formation during the MCs' fabrication process. It is clearly possible to visualize areas in the O droplets in which there is still no solid polymer precipitation. This is in accordance with the process described in the literature [21].

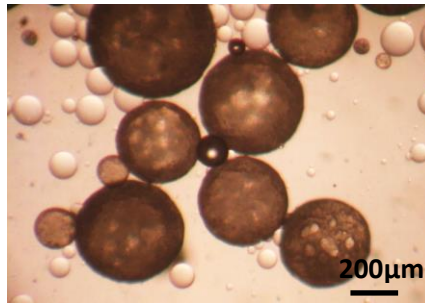


Figure V. 3. Optical microscopy photograph that shows the shell formation during the MCs fabrication, by the solvent evaporation method.

The MCs fabrication process was followed by optical microscopy enabling to monitor the maturity of the MCs' shell and conclude regarding the shortest production time for each experiment. The MCs were filtrated by using a vacuum filtration system, while being washed with water. The obtained MCs were left to dry at atmospheric pressure and at room temperature for 48 h. The schematic representation of the MCs fabrication, using a double $O_1/O_2/W$ emulsion system, is represented in Figure V. 4.

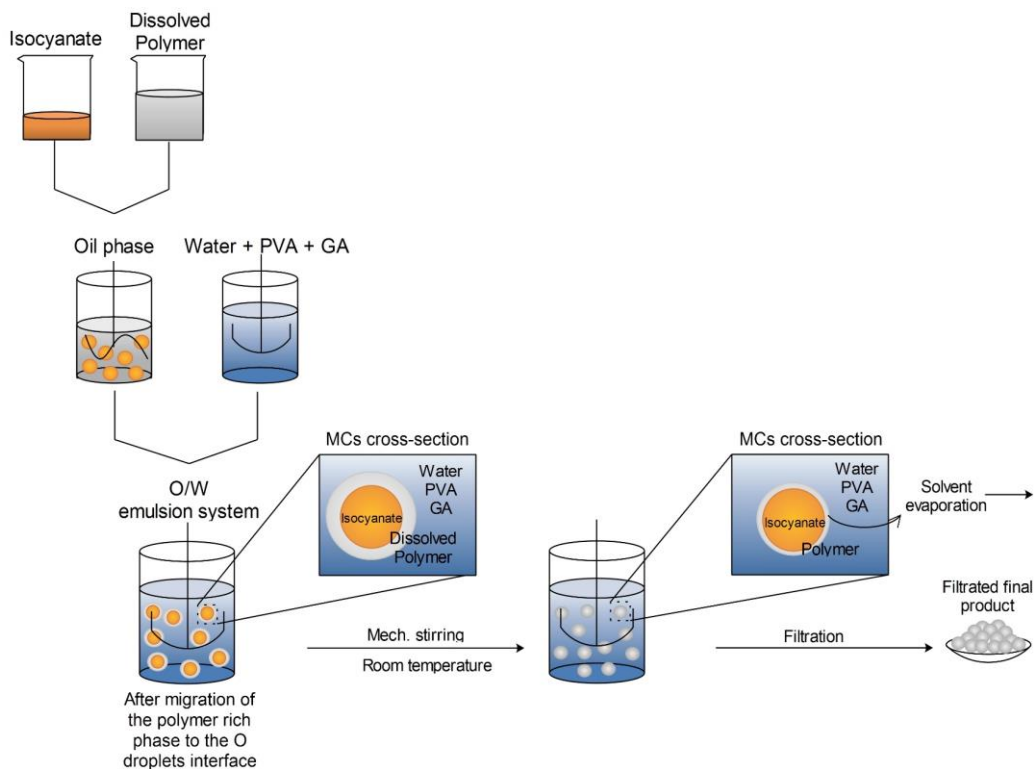


Figure V. 4. Schematic representation of the MCs' fabrication process by the solvent evaporation method combined with a double $O_1/O_2/W$ emulsion system.

To obtain MCs of PCL shell dichloromethane was used as organic solvent due to its ability to dissolve the chosen polymer and its low boiling point. Its high saturated vapor pressure contributes to a high solvent evaporation rate, which decreases the MCs' production time. Despite the advantaged of chloroform, as its lower vapor pressure, higher boiling point and higher toxicity, it was necessary to use dichloromethane to dissolve the PHB [1].

A scale-up of the process is described in the sub-chapter "VI.4 Scale-up of the syntheses processes". For that the ULTRA-TURRAX equipment used for the pre-scale-up was maintained, as it is suitable for volumes up to 2L. The agitation was adjusted according to Equation 4, Chapter IV. For the synthesis it was used a glass reactor of 500ml and the mechanical stirring rod was replaced by one with a larger blade, due to the reactor diameter that was doubled.

V.3 Results and discussion: Reactional parameters and strategies

The encapsulation of isocyanates using solvent evaporation method had not yet been described in the state of the art. So, it was necessary to optimize several synthesis parameters to obtain MCs with the desired characteristics for the current application. Some of the results and discussion below presented have been published in our paper our paper "Microencapsulation of Isocyanate in Biodegradable Poly(ϵ -caprolactone) Capsules and Application in Monocomponent Green Adhesives", which consists of the first report on isocyanate microcapsules with biodegradable shell, prepared by solvent evaporation technique [22]. The process parameters that were optimized are described in Table V.3, along with the tested ranges.

Table V.3. Process parameters, from the MCs production by the solvent evaporation methods, that were optimized and respective range values.

Reactional parameters	Ranges
PVA concentration	2 - 4 wt% in the W phase
GA concentration	0 - 3.5 wt% in the W phase
Emulsification time	5 - 10 minutes
Emulsification stirring	5000 -10000 rpm
Mechanical stirring	500 -850 rpm
Polymer concentration	8-16 wt% in the organic solvent
Isocyanate concentration	16-20 wt% of the O phase
O/W ratio	28 - 39 wt%

The studies regarding the production of MCs by the solvent evaporation method were mainly focused on the PLC MCs containing IPDI in its core. PCL is a synthetic biodegradable aliphatic polyester, which has a low glass transition temperature, of about -60°C , and a melting point of 60° , it has been widely used in encapsulation, mainly for drug controlled-release, due to its biocompatibility and FDA approval for use in humans [23, 24]. For the present work, its low melting temperature, in the range of temperatures used during the adhesive application in the footwear industry, would enable the MCs to release its content not only by break but also by the melting of the shell.

The MCs initially obtained by this method were loose particles, with a spherical shape, however with very large dimensions, as depicted in Figure V.5. Despite this, the non-optimized MCs had an encapsulation yield of ca. 50 wt% which was a promising indicator of the adequacy of this technique for the isocyanate encapsulation. Indeed, by this process there are no chemical reactions involved and the MCs production occurs only due to the organic solvent evaporation, leading to the polymer precipitation around the isocyanate droplets. It is a physical method for the MCs production. This should lead to MCs with a higher encapsulation yield than the ones obtained by interfacial polymerization method, by which some of the isocyanate must react for the shell formation.

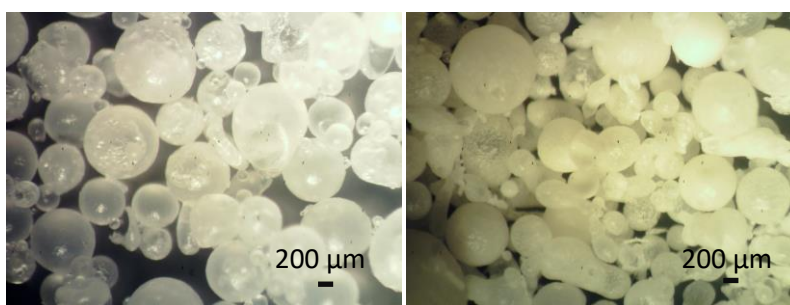


Figure V.5. Optical microscopy photographs of the PCL MCs, obtained by the solvent evaporation method, before the production process optimization (first trials).

Two PCL grades with different MW, of 45000 and 80000 Da were tested as polymers for the encapsulation of IPDI. The effect of the polymer MW on the MCs' typology, size and size distribution, encapsulation yield, shelf-life and temperature response and performance in the final application was studied.

A Design of Experiment (DOE) study, intended to decrease the MCs' average size and to achieve a finer control over these MCs' morphology, was made, by which the effects of the GA and PVA concentrations as well as the O emulsion phase volume on the MCs sizes was evaluated. It was intended to develop a model, which enabled to predict the optimum values for each variable in study, that led to the production of tailored MCs within a predefined size range.

After the optimization of the PCL MCs production process, the PHB was tested as polymer for the MCs' shell. The performance of the PCL and PHB MCs on the adhesive formulation, i.e. resistance to the solvents used in the adhesive (pre-polymer) formulation, as well as their effectiveness as cross-linkers, was studied and it is described in Chapter VI.

V.3.1 The effect of polycaprolactone's molecular weight

The results exposed in this sub-chapter "V.3.1 The effect of polycaprolactone's molecular weight" are published in our paper "Microencapsulation of Isocyanate in Biodegradable Poly(ϵ -caprolactone) Capsules and Application in Monocomponent Green Adhesives" [22].

Two PCL grades with different MW, of 45000 (PCL45) and 80000 Da (PCL80), were used as shell material to conclude about the effect of the polymer MW on the MCs' final characteristics, in what regards encapsulation yield and resistance to moisture inwards diffusion. The composition of the W and O phase of the emulsions used for the MCs production is listed in Table V. 4.

Table V. 4. Microcapsules' acronyms and emulsion composition

MCs acronym	Water phase (wt%)	Oil ₁ phase (wt%)	Oil ₂ phase (wt%)
I_45MCs	PVA aqueous solution	IPDI (7.1% of the emulsion)	PCL with 45000 Da at 16 wt% in DCM (26% of the emulsion)
I_80MCs	GA (66.9 % of the emulsion)		PCL with 80000 Da at 16 wt% in DCM (26% of the emulsion)

Optical microscopy and SEM were used to assess the MCs' morphology, size distribution, and average shell thickness. Figure V.6 shows optical microscopy photographs of the emulsions and respective I_45 MCs and I_80 MCs at different stages of their fabrication process. For both cases, it is possible to distinctly observe the formation of a solid shell, by the increased opacity of the MCs after 45 and 60 min from the beginning of fabrication progress. Looking at the initial emulsions it can be observed a smaller average size of the droplets when using PCL80 as the shell-forming polymer. Indeed, PCL80 leads to an O phase with significantly higher viscosity, of 6150 cP, than that obtained with the PCL45, of 570 cP and, for the same emulsification speed a higher viscosity might result on smaller droplets of the dispersed phase [25-28]. On the other hand, it should be stressed that if the viscosity of the O phase is too high and the solution, or dispersion, is not homogeneous, issues may arise in the stability of the emulsion, which might result, for instance, in a broader size distribution of the MCs. The respective emulsions size distribution histogram is depicted in Figure V.7, based on the optical microscope photographs shown in Figure V.6, at 0 minutes.

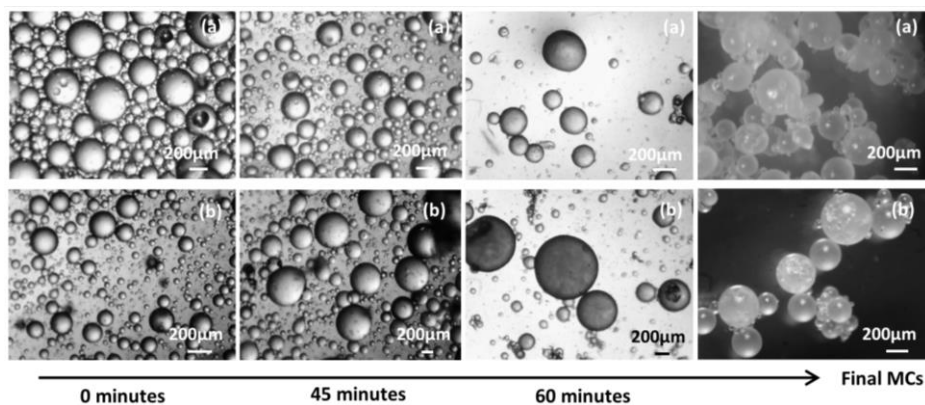


Figure V.6. Optical microscopy photographs captured during the MCs' fabrication process.

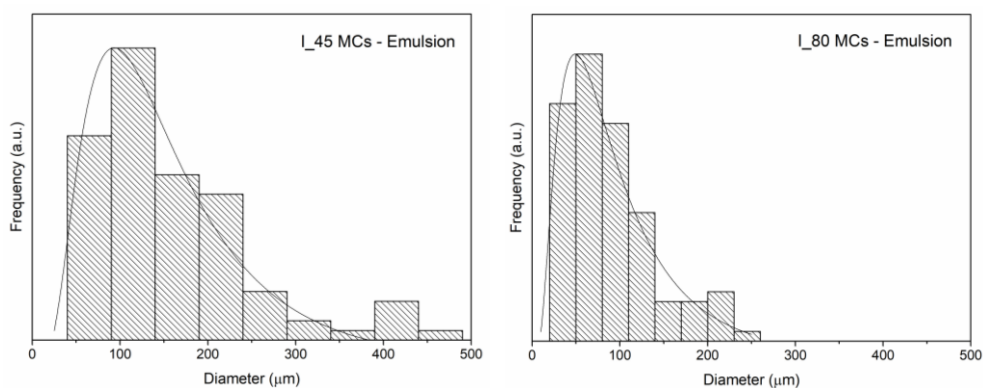


Figure V.7. I_45 and I_80 emulsion size distribution.

It is possible to observe a single I_45 MCs' shell breakage due to mechanical tearing, with a needle (I_45MCs (b)), leading to the release of a significant amount of liquid from its core in Figure V.8. This is expected to be IPDI, as the MCs are assumed to be only composed by the encapsulated isocyanate and the solidified PCL shell, to be further corroborated by FTIR and TGA analyses. A single I_80 MCs, prepared with PCL of higher Mw (PCL80), is also displayed in Figure V.8, as well as a ruptured MCs' shell revealing a core-shell morphology.

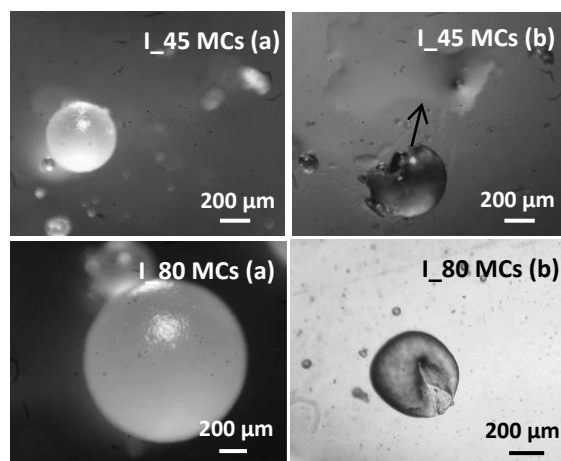


Figure V.8. Optical microscopy images. Top: I_45 MCs (a) before tearing of the shell (b) the same MC after the break of the shell, exhibiting the release of the core content (arrow). Bottom: I_80 MCs (a) single capsule photograph (b) another MC after the break of the shell, showing its core-shell morphology.

Figure V.9 shows the SEM photomicrographs of the I_45 and I_80 MCs. Some MCs were purposely crushed to assess their morphology and shell thickness. The MCs' fabrication using both PCL45 and PCL80 led to loose, disaggregated MCs with a core-shell morphology and a

spherical shape, with the I_80 MCs showing a smoother outer shell, probably due to the longer polymeric chains of PCL80, which are less prone to crystallization than shorter chains. Figure V.10 shows more magnified images of the outer (a) and inner (b, c) part of the I_45 MCs' shell, showing some lamellar bundles. The interior of the shell has more defined structures with an irregular orientation, which might be attributed to the semicrystalline state of the polymer [29]. This difference between the exterior and interior of the MCs' shell might be correlated to a slower DCM evaporation rate in the inner face, in comparison with the rate experienced at the outer face, and/or due to the smoothing effect of the shear forces that occur at the surface of the droplets/MCs upon their movement within the continuous phase (water-rich medium). In addition, the water may also cause a constraining effect on the polymer, restricting the PCL' chains movement [29, 30]. Some small superficial heterogeneous pores can also be observed in the shell, resulting from the large arrangement of the lamellae. The possible semicrystalline nature of PCL is mainly identified in the PCL45 MCs possibly due to its smaller chain sizes, which enables more movement freedom and consequently a better rearrangement of the polymer chains.

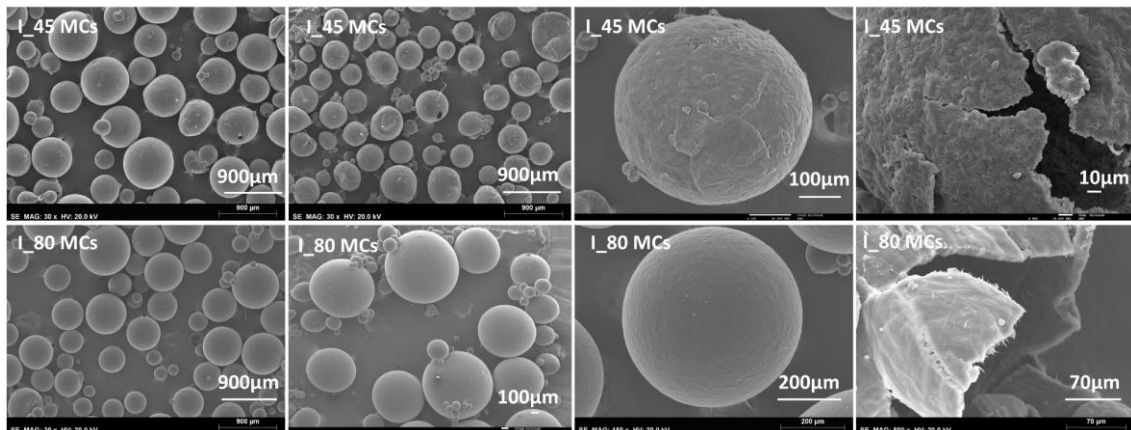


Figure V.9. SEM images of the I_45 MCs, at the top, and of I_80 MCs, at the bottom. The images on the right display a purposefully broken MC, evidencing a core-shell morphology, for both the I_45 and I_80 MCs.

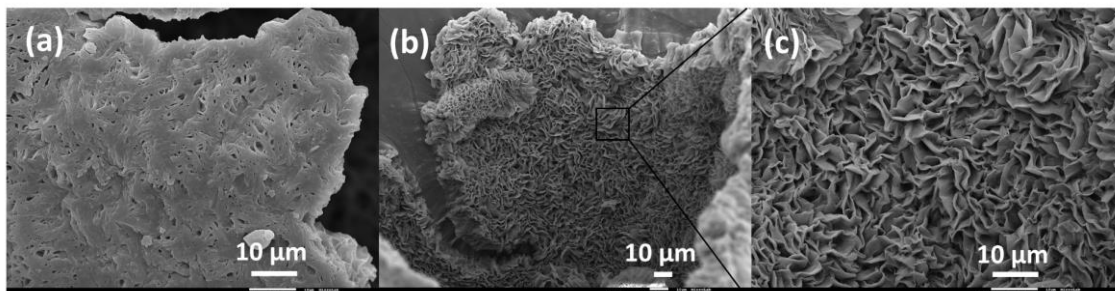


Figure V.10. SEM images showing the typical morphology obtained for MCs with a PCL shell. (a) Image of the I_45 MCs outer shell. (b) and (c) images of the I_45 MCs inner shell.

Figure V.11 displays the MCs' size distribution, which follows a multimodal distribution for both cases, showing the polydisperse nature of the MCs. By comparing the size distribution of the I_45 MCs and I_80 MCs, it is possible to conclude about the emulsion stability, namely, in what regards the effect of the O phase viscosity on the overall system and obtained MCs. Although both samples have a significantly broad size distribution, the majority of the I_45 MCs have between 225 and 525 μm with the I_80 MCs having a broader distribution, from 150 to 750 μm . The I_80 MCs larger size distribution might be due to the higher viscosity or/and to a less homogeneous O emulsion phase, which tends to destabilize the emulsion, consequently leading to some droplet coalescence. Due to the PCL80 higher MW, its ideal concentration in the DCM should probably be higher than the one needed for the PCL45 dissolution. However, the aim of this work was to keep constant all the fabrication parameters, except for the MW of the PCL, to conclude about its effect.

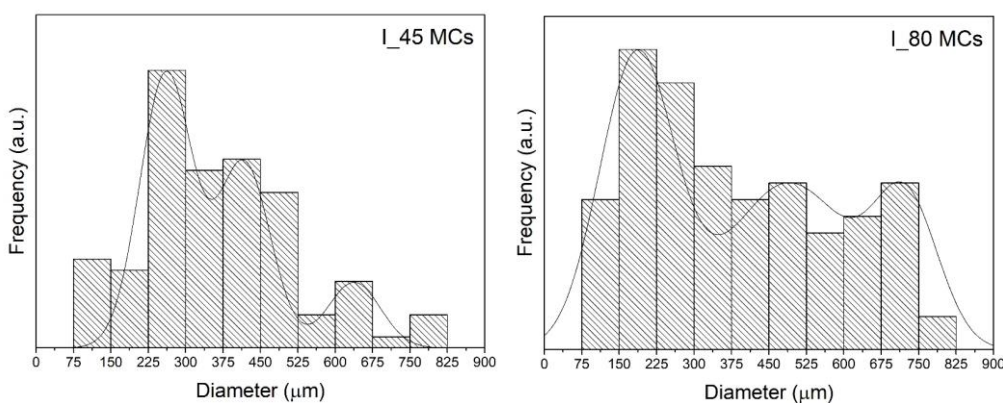


Figure V.11. I_45 and I_80 MCs size distribution.

The value of each size distribution peak, which corresponds to the modes of the MCs' sizes, as well as the average shell thickness are displayed in Table V.5. To calculate the shell thickness and respective mean deviation, 15 measurements, at the cross sections of several MCs, were made using the Fiji software [31]. It is also reported the S/D ratio, which is an indicator of the contribution of the shell to the MCs overall morphology, with higher values indicating a higher shell contribution.

Table V.5. MCs' average shell thickness (S) as well as the MCs' diameter (D) and S/D ratio

MCs acronym	S, av shell thickness (μm)	D, MC's diameter (peak max, mode) (μm)	S/D (ratio)
I_45MCs	29.65 ± 7	264, 416, and 637	0.11, 0.071, and 0.046
I_80MCs	28.24 ± 6	191, 491, and 710	0.14, 0.057, and 0.039

I_80 MCs have a slightly thinner average shell and an overall lower S/D ratio, which is an indication of a lower shell contribution for the MCs' volume, increasing the possibility of a higher encapsulation yield. However, it is important for the shell to have the necessary thickness to offer enough mechanical strength and robustness, as the MCs need to endure handling and blending within the adhesive formulation, as well as to be capable to protect the IPDI from the exterior medium, in particular from the air humidity. Because both experiments were performed under the same conditions, it is possible to assume that the observed morphological differences are due to the distinct PCL MW.

Figure V.12 shows the FTIR spectra of the as-prepared MCs, of the shell-forming polymer, PCL, and of the encapsulated isocyanate, IPDI. The presence of unreacted isocyanate is confirmed by the intense peak at ca. 2260 cm^{-1} , ascribed to the $\text{N}=\text{C}=\text{O}$ bond stretching vibration, in both MCs' FTIR spectra. The PCL's most intense and distinct peak is related to the carbonyl group ($\text{C}=\text{O}$) stretching vibration, at $1715\text{--}1730\text{ cm}^{-1}$ [30, 32, 33]. The bands detected in the range of $2840\text{--}3000\text{ cm}^{-1}$ are associated with the stretching vibrations of the PCL' C-H groups from its aliphatic chain and the peaks at 1168 and 1300 cm^{-1} related to its C-O-C stretching, of the saturated ester groups, and C-O and C-C groups, respectively [33]. The MCs' shell material is herein shown to be PCL due to the presence of an intense peak at 1720 cm^{-1} , from the carbonyl stretch vibration, as well as the peak ascribed to the C-O stretching in both the MCs' FTIR spectra [33].

It should be stressed that any reaction between the isocyanate NCO groups and OH groups, resulting in urea moieties, can be discarded due to the absence of corresponding peaks in the FTIR spectra of the as-prepared MCs. The presence of urea moieties could be detected by its characteristic peaks at 1510 cm^{-1} and $3200\text{--}3400\text{ cm}^{-1}$, ascribed to the bending and stretching of the N-H group, respectively, as well as at $1680\text{--}1700\text{ cm}^{-1}$, from the urea carbonyl stretching vibration. This assures that if some reaction happened between the IPDI and the W phase, it was

in such a minimal extent that no PUa can be detected by FTIR analysis. From this it is possible to assume that the MCs' shell is composed mostly by PCL, with most of the isocyanate remaining unreacted. The developed MCs' fabrication procedure is basically a physical process.

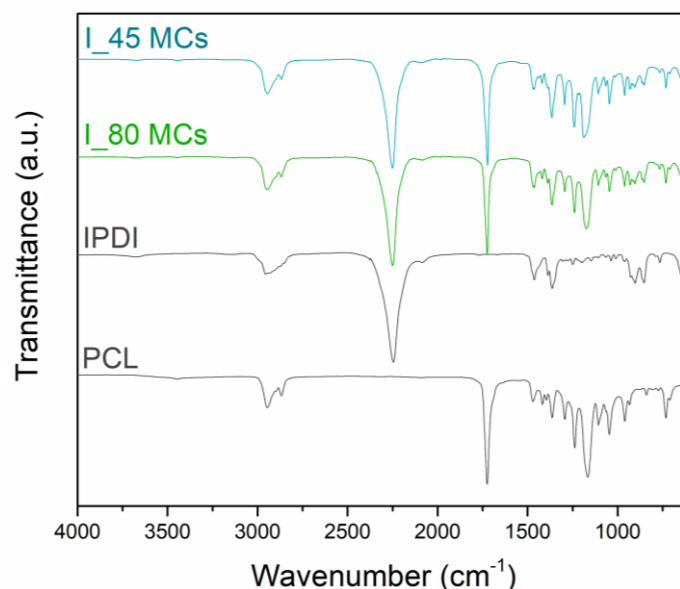


Figure V.12. FTIR spectra of the as-prepared MCs (I_45 and I_80), the shell-forming polymer PCL, and the encapsulated isocyanate, IPDI.

Table V.6 lists the Y values obtained from the FTIR spectra of the as-prepared MCs. By comparing the Y values of the I_45 and I_80 MCs, it can be concluded that, although by a small difference, the use of PCL80 enabled a higher isocyanate encapsulation. Despite the inhomogeneity of the sample in terms of size distribution, the I_80 MCs are the ones that exhibit an overall smaller value of the S/D ratio, enabling the encapsulation of a higher amount of IPDI.

The FTIR spectra of the I_45 and I_80 MCs, as-prepared and aged, are shown Figure V.13. The spectra of the three months old MCs, stored at room temperature and 60% of relative humidity, reveal a change in the chemical composition of its shell. New peaks can be identified in these MCs spectra, which were not present in the as-prepared samples, at 1690, 1626, and 1565 cm^{-1} as well as a band between 3420 and 3220 cm^{-1} . The peak at 1690 cm^{-1} can be associated with the presence of carbonyl groups from urea or tertiary urethanes, which indicates some possible reaction from the encapsulated isocyanate. The peak appearing at 1626 cm^{-1} is usually associated with the combined effect of the N-H in-plane bending, the C-N stretching, and the C-C stretching vibrations, typical of urea linkages, while the band at 1565 cm^{-1} is typical of secondary amides, in-plane N-H bending, which usually appears as an intense band between 1570 and 1510 cm^{-1} [32, 34]. The broad band between 3420 and 3220 cm^{-1} is correlated to the

presence of hydrogen bonding, N–H, or/and O–H stretching group vibrations [32, 34]. These new features in the FTIR spectra reveal the formation of urea and possibly urethane moieties, which are due to the contact between the encapsulated IPDI and active H groups. A possible diffusion of water from air moisture through the polymeric shell and/or some possible hydrolytic degradation of the PCL, might be responsible for the presence of active H groups in the MCs' interior. The PCL polymer might undergo hydrolytic degradation to some extent due to the presence of hydrolytically labile aliphatic ester linkages, as schematically represented in Figure V.14, reaction 1 [35, 36]. Cleavage of the PCL's ester bonds occurs upon its reaction with water, forming carboxyl end-groups, with the progressive reduction of its MW leading to a final biocompatible, water-soluble degradation product, as represented in Figure V.14 [36, 37]. The PCL carboxyl end-groups, resulting from its hydrolysis, have OH terminal groups that can react with the isocyanate, leading to urethane linkages and a biodegradable PU polymer (Figure V.14, reaction 1.1) [36, 38, 39]. According to the literature, the degradation of PCL in a living environment can result from simple chemical hydrolysis of the ester bonds and/or due to enzymatic attack, with a resulting decrease of the PCL's MW [36]. *Krasowska et al.* concluded that in a sterile aqueous medium only small changes are observed in the PCL's MW, due to a slow nonenzymatic hydrolytic degradation by ester cleavage [36]. On the other hand, it has been reported that the dissolution of PCL in sterile water requires the use of an external acid catalyst, due to its low acid dissociation constant, K_a , so that its hydrolysis is expected to be slow and dependent on the external acid concentration [40]. *França et al.* studied the degradability of PCL molded specimens when subjected to vacuum at 40 °C for up to 45 days, concluding that although PCL was not prone to hydrolytic degradation under the referred conditions, water diffusion and swelling of its polymeric matrix were observed [41].

The most likely hypothesis is that water, from the air moisture, might have diffused through the PCL MCs, with its subsequent reaction with the encapsulated isocyanate leading to the formation of PUa domains, as represented in Figure V.14, reaction 2. The presence of peaks related to the vibration of secondary amide groups, in the spectra of the 3 months old MCs, as well as the small peak at 1690 cm^{-1} , typically associated with the presence of urea carbonyl group, confirm this occurrence. The presence of a secondary PU could not be confirmed as its typical carbonyl peak, at $1715\text{--}1725\text{ cm}^{-1}$, if it exists, would be masked by the one of the PCL carbonyl group. Even though a few molecules of encapsulated IPDI have reacted, the high intensity of the NCO peak indicates the reactions occurred only in a small extent.

IPDI and of the I_45 MCs and I_80 MCs as-prepared and aged, after storage for 3 months at room temperature and 60% of relative humidity. The respective derivative curves are also displayed. PCLs with 45000 and 80000 Da present a similar degradation fingerprint, with the corresponding peak ranging from ca. 350 to 450 °C, indicating that the MW has only a slight effect on the polymer degradation temperature: higher MW results in an increase by ca. 6 °C of the degradation curve peak. The IPDI shows its first thermal event at lower temperatures, between 100 and 240 °C. The thermograms of both MCs samples exhibit its first significant thermal event at ca. 120 °C, which correspond to the IPDI. The second degradation step is referred to the PCL polymeric shell degradation. The amount of encapsulated isocyanate for both the I_45 and I_80 MCs was determined and is reported in Table V.6, along with the relative encapsulation yield (Y value) determined by FTIR.

Both the aged MCs first-derivative curves show two extra peaks, between 230 and 350 °C, not present in the as-prepared MCs first derivative curves, indicating that the samples chemical composition has changed during that period, corroborating the conclusions drawn by the FTIR analysis. It is reported for the PU/PUa material to show two degradation phenomena, the first occurring between 300 and 370 °C, correlated to the degradation of soft segments, and the second one above 370 °C. This might correspond to the extra peaks in the first derivatives of the aged MCs [42, 43]. Further evidence of the presence of PU/PUa moieties is the noncomplete shell degradation within the studied range of temperature, namely 96 and 98.78 wt%, for the aged I_45 MCs and I_80 MCs, respectively. It is possible that more PU/PUa has been formed in the aged I_45 MCs than in the aged I_80 MCs due to more water diffusion through the PCL45 shell.

MCs with a high degree of IPDI encapsulation, above 50% of the MCs' weight, were obtained with either PCL45 or PCL80, revealing the potential of this technique to encapsulate reactive isocyanate species. PCL80 was the one leading to a higher degree of encapsulation, confirmed both by TGA and by the Y value calculated through FTIR measurements.

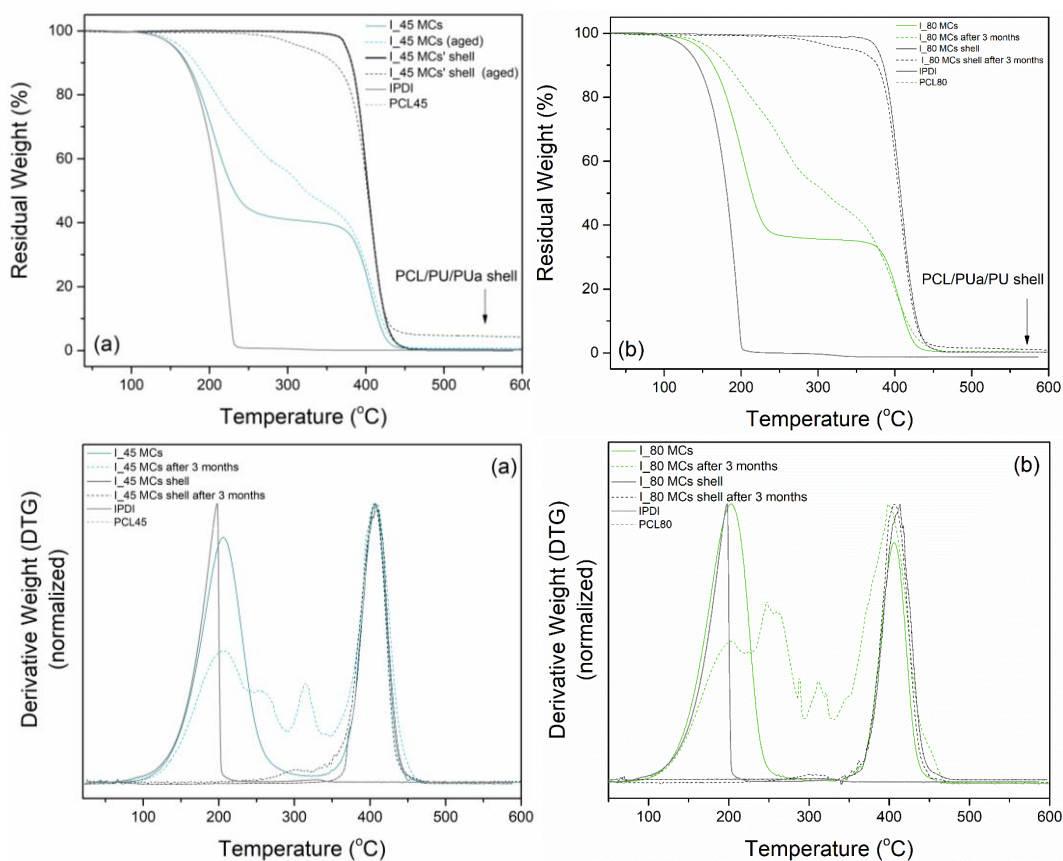


Figure V.15. (a) Thermogram of the as-prepared and aged (3 months) I₄₅ MCs (top), and the respective derivative curves (bottom); (b) thermograms of the as-prepared and aged (3 months) I₈₀ MCs (top), and the respective derivative curves (bottom).

Table V.6. Relative encapsulation yield (Y) and mass loss (%) of encapsulated IPDI for each experiment

MCs' acronym	Relative encapsulation yield (Y) from FTIR	Mass loss (%) from TGA (amount of pure encapsulated isocyanate) (from 115-320 °C *)
I ₄₅ MCs	2.4	54
I ₈₀ MCs	3.0	60.3

*Range of temperatures used for the encapsulated isocyanate quantification. The temperature range varied slightly depending on the MCs thermograms.

GPC analysis was performed to the I₄₅ and I₈₀ MCs' shell, as well as to the PCL45 and PCL80, to assess the MW distribution and the effect of the MCs' fabrication process conditions on the resulting polymeric shell, presented in Figure V.16. Neither the PCL80 nor the PCL45 have a unimodal distribution in what regards MW distribution. Both PCL45 and PCL80 both display high-MW chains, reaching ca. 90000 Da, however PCL45 has a wider MW distribution, with a stronger

contribution to lower MW peak, at ca. $\log(\text{MW}) = 3.2$. On the other hand, the PCL80 has a bimodal distribution, with the significantly most intense peak appearing at higher MW, at about $\log(\text{MW}) = 4.9$. During the MCs' preparation chains might have suffered some chain scission, as their corresponding peak decreased in intensity, with the microencapsulation process, and a new peak has appeared at lower $\log(\text{MW})$ values, in both the MCs' chromatograms. This might have occurred due to the strong mechanical stirring involved in the MCs' fabrication to which PCL is exposed while dissolved in DCM.

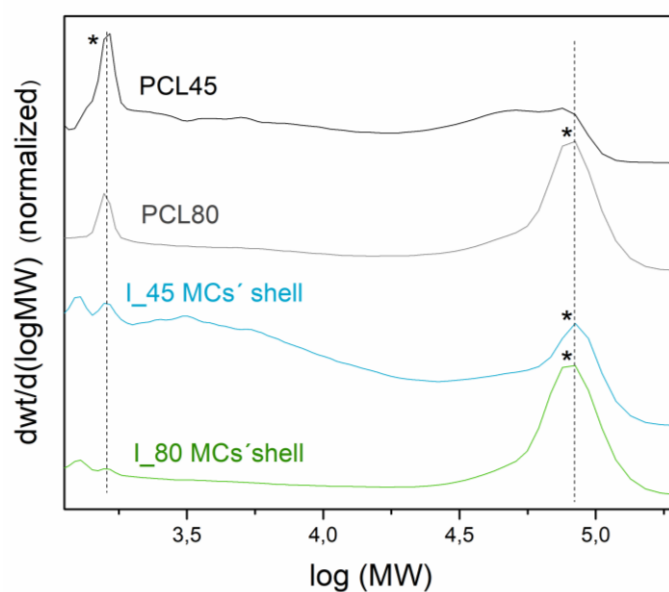


Figure V.16. Gel permeation chromatograms of the PCL45 and PCL80 raw materials, as well as that of the I_45 and I_80 MCs' shells.

The characteristic MW information, obtained by the GPC analysis, for both PCL as well as for the MCs is listed in Table V. S1, from the Supplementary Information. The M_p values were obtained from the most intense peak, marked in Figure V.16 with an asterisk. The MCs fabrication process affected the PCL45 and the PCL80 differently, as the M_p of the I_80 MCs' shell is identical to that of the PCL80, while the M_p for the I_45 MCs' shell varies from that of the PCL45. This further suggests that the PCL45' low-MW chains might have suffered some cleavage during the MCs fabrication. Accordingly, the polymer polydispersity shows some increase with the MCs fabrication process, revealing an increased heterogeneity of the molecular chains' distribution, for both cases.

Although the MCs' shells are composed of PCL, which has a melting temperature of ca. 60 °C, it is important to assess whether the presence of PUa domains, detected by FTIR and TGA in the aged MCs, affects its thermal response at the temperatures applied during the adhesion process,

in the footwear industry. For that purpose, the melting temperature of the aged MCs was evaluated by DSC analysis. The thermograms of the aged I_45 and I_80 MCs' shell are exposed in Figure V.17. Both samples show a low temperature endothermic peak at ca. 60 °C, correlated to the PCL melting point, revealing that the aged MCs can effectively respond to the range of temperatures involved in the adhesive's application process. It is also possible to observe that the I_45 MCs' shell melts at lower temperatures than the I_80 MCs' shell, possibly due to the lower MW of the polymeric shell.

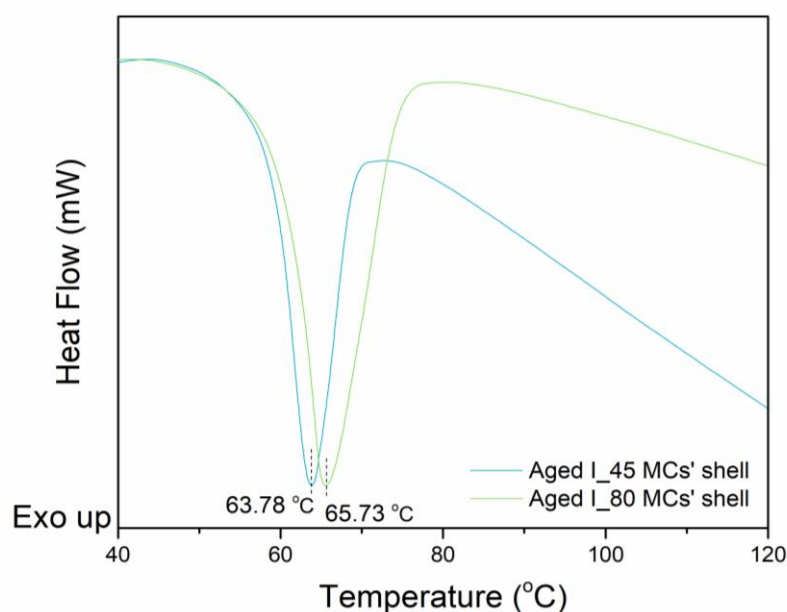


Figure V.17. DSC thermograms of the aged I_45 and I_80 MCs' shell.

To corroborate the results achieved by DSC, the aged MCs were mixed within the adhesive pre-polymer and subjected to 50 °C in an oven. During a 1 h long experiment, a sample was taken every 10 min and cooled to 27 °C, and its viscosity measured. It is hypothesized in this experiment that, once the MCs' shell melts, there is release of isocyanate, which will react with the OH groups of the pre-polymer, resulting in PU cross-links formation with a consequent increase of the pre-polymer viscosity. Two samples of the pre-polymer, without MCs, were also evaluated as a reference: one exposed to 50 °C and another one kept at room temperature. Figure V.18 shows that the pre-polymer, by itself, exhibits some viscosity increase along the experiment, probably due to some solvent evaporation. However, a notoriously higher increase in viscosity, by almost the triple of its initial value, is observed for the samples containing MCs. This is further evidence that the MCs, even the ones containing PU/PUa moieties, effectively can release the encapsulated isocyanate only by the effect of temperature, which makes them suitable for the present application. The low melting viscosity typical of PCL plays an important

role in the homogeneous distribution of the released isocyanate within the OH pre-polymer and therefore in the uniform responsiveness and reactivity of the system [44]. Also, the initial increase in the OH pre-polymer viscosity is not as pronounced with I_80 MCs as it is with the I_45 MCs, which is in accordance with the DSC results regarding the correlation between each PCL MW with the respective MCs' shell melting temperature.

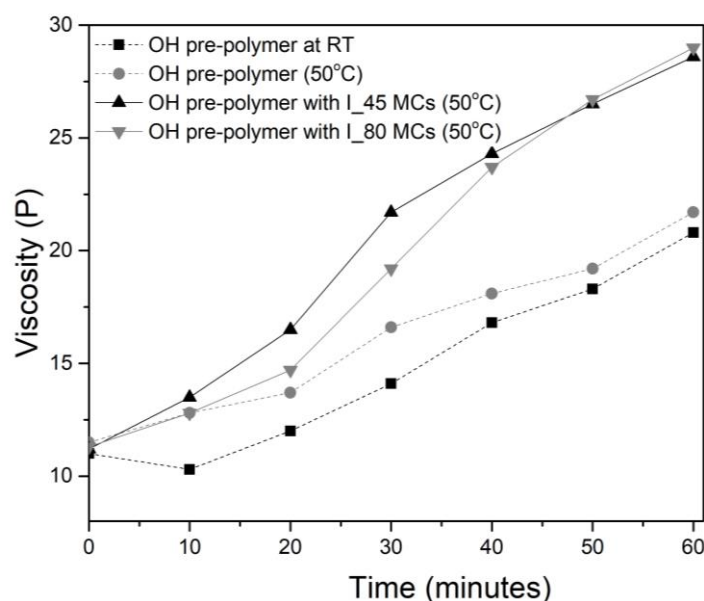


Figure V.18. Viscosities of the pre-polymer and its mixtures with aged MCs, measured every 10 minutes, during a 1-hour experiment.

Preliminary peeling strength tests were performed, at the labs of IST, as an indirect way to evaluate the MCs effectiveness as cross-linkers for the new adhesive formulation. In this case, the peeling strength of the pre-polymer containing encapsulated IPDI, was evaluated and compared to a reference sample composed by the pre-polymer with an equivalent amount of nonencapsulated IPDI.

Peeling strength and temperature resistance tests (creep tests) were posteriorly performed with PCL MCs at the CIPADE S.A. facilities, following the industry standards. Obtained results are shown in Chapter VI.

Figure V.19 shows the average maximum load obtained in the peeling strength tests, which are quite similar for both the adhesive joints prepared with encapsulated and nonencapsulated isocyanate. This reveals an effective release of the encapsulated IPDI, during the adhesive application, in part promoted by the low melting temperature and low melting viscosity of the PCL. By comparing the error bars, associated with the homogeneity of the adhesive joints, it is possible to conclude that the most homogeneous results were achieved with the

nonencapsulated isocyanate. The broad MC size distribution might be at the origin of such heterogeneity, confirming the importance of this feature in the final adhesive properties. Table V. S2 from of the Supplementary Information, lists the obtained average load measured per unit width of the bond, which, for all cases, was lower than 3N/mm. These low values are a result of the procedure for the specimen preparation in the university facilities, which is not an exact replication of the industrial process, due to the lack of proper equipment. Nevertheless, the specimens were all equally prepared so that the results can be compared, and conclusions can be drawn, regarding the release of the encapsulated content.

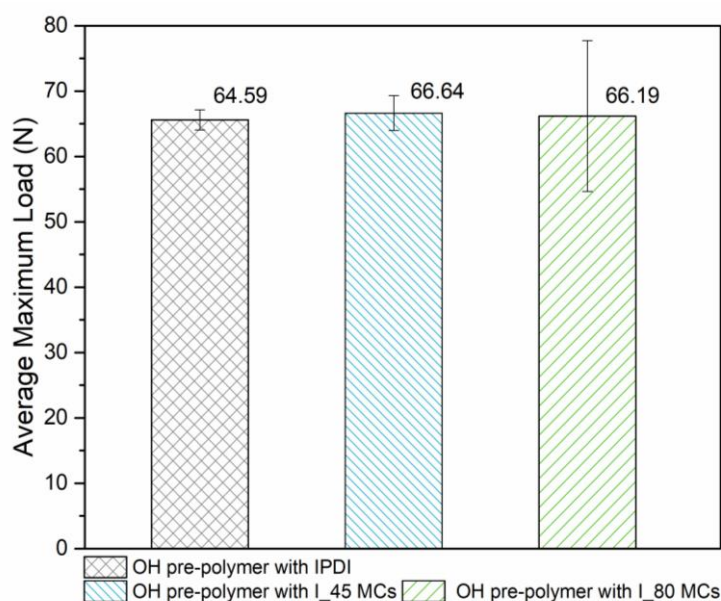


Figure V.19. Average maximum load obtained in the peeling strength tests for the adhesive joints prepared with the following formulations: OH pre-polymer with IPDI; OH pre-polymer with encapsulated IPDI in the form of I_45 MCs and I_80 MCs.

In conclusion, the solvent evaporation method demonstrated to be a simple and efficient approach for the encapsulation of reactive isocyanates. Spherical, disaggregated, and core-shell MCs were obtained, either with PCL45 as with PCL80 containing high loadings of pure liquid isocyanate, at 54 and 60.3 wt%, respectively. The MCs have a relatively steady encapsulated isocyanate content over a period of 3 months from its fabrication. Some enhanced characteristics were achieved when using the PCL80 for the MCs' shell fabrication, specifically in what regards a higher IPDI encapsulation, a smaller average shell thickness, a slightly longer shelf-life, and a higher melting temperature. The IPDI was found to be released from the MCs in response to the stimuli applied in the footwear industry during the adhesive application, enabling the cross-linking of the adhesive joint, which shows the large potential of these MCs for the current application.

Despite its advantages, the high viscosity of the O emulsion phase when using PCL with 80000 Da makes it very difficult to work with, leading to a low reproducibility, low production yield and bigger MCs sizes and sizes distribution comparing to the 45000 Da PCL. This could further lead to industrial difficulties when implementing the process in a larger scale. As the encapsulation content and shelf-life of the MCs obtained using PCL45 were not far from those obtained with the higher MW PCL, PCL45 was used in the following studies.

It should be noted that these findings were at the origin of a patent, which was granted in 2021 (PT 115312 B) and a subsequent R&D Project with the goal of further exploring MCs with biodegradable polymeric shell and establishing their production at the industrial level, in collaboration with an adhesive producer (CIPADE S.A.), an industrial automated machinery producer (JPM – Automação e Equipamentos Industriais, S.A.), and IPCA, for the life cycle assessment of the new adhesives.

V.3.2 Design of experiment to control the microcapsules size

The results exposed in this sub-chapter “V.3.2 Design of experiment to control the microcapsules size” are published in the paper “Design of Experiment for Optimizing Microencapsulation by the Solvent Evaporation Technique” [45].

PCL MCs obtained by the solvent evaporation technique, using PCL45, have a medium size of $326,39 \mu\text{m} \pm 157,26$. The main goal of this study is to decrease the size the MCs to a medium size between $70 \mu\text{m}$ to $80 \mu\text{m}$.

DOE has several advantages over the typical “one factor at a time” (OFAT). The OFAT encompasses the iterative experimentation of one factor, by fixing all process factors except the one that is under optimization [46, 47]. Adding to the inefficiency and time-consuming process, it is often inaccurate as an optimization technique for chemical processes as there are no considerations for synergistic effects between the factors under study [46, 48, 49]. Therefore, it is possible to deduce the individual impact of each factor on the reaction, but it is not possible to draw conclusions regarding their mutual influence on one another. As an alternative, the use of statistical or physical modeling might be considered [47].

DOE was used as a statistical method to optimize the size of the MCs. This method has been widely applied in different fields of science and industry to support the design, development, and optimization of products and processes [50]. It is used to systematically address cause and

effect relations between the variables in study and the outputs, enabling to optimize and identify its optimal values [50, 51]

For this purpose, the MODDE® Pro 13 (Umetrics, Sweden) software was used, by applying the response surface methodology (RSM) with a central composite design (CCD), in particular the central composite face design (CCF). RSM was used to reduce the number of synthesis necessary to recognize the influence of the process parameters in study, enabling to understand the effect of each one on the MCs size, and to develop a predictive model [51, 52]. This enables to determine which values to use, for the variables in study, to achieve any desired target. To the best of our knowledge, the use of DOE for the optimization of MCs, containing isocyanates, produced by the solvent evaporation technique is not yet reported.

Three critical and independent variables were considered, namely the PVA concentration, the GA concentrations and O to W phase volume, all known to impact in the emulsion system. In the production of MCs by the solvent evaporation technique, the size and stability of the emulsion droplets is closely correlated with the size of the final MCs, as they are formed by the polymer precipitation at the emulsion droplets' interface. The PVA and GA are used in the MCs' fabrication process as emulsions stabilizers, the first by rheological modification of the dispersed phase viscosity and the second by creating a steric barrier around the emulsion droplets, avoiding its coalescence [53-57]. Regarding the volume of the O phase in the emulsion, there is a correlation between this parameter and the droplets size of the dispersed phase [58-60]. The optimum range for the average MCs size was defined to be between 70µm to 80 µm, although MCs with a medium diameter of 100 µm are still fit for the application. This range was selected taking into consideration the performances of the MCs in the adhesive formulations. Large sized MCs have a poor distribution in the substrate, adding to a big disruption in the adhesive bondline. On the other hand, when the MCs are too small, a substantial quantity of them is required to ensure effective adhesive cross-linking. Furthermore, smaller MCs exhibit increased resistance to pressure-induced breakage.

Table V.7 lists the defined independent variables and respective ranges.

Table V.7. Selected independent variables and respective ranges

Independent variables	Factors	Coded levels		
		-1	0	1
PVA concentration (PVAc) % (w/w)	x_1	2	3	4
GA concentration (Gac) % (w/w)	x_2	0	1.75	3.5
O phase volume (V.r) % (v/v)	x_3	28	33.5	39

By using the CCF design, schematically represented in Figure V.20 (a), the response of the average MCs size (Y , μm) was given as a function of the three parameters according to the Equation 5:

$$Y = f(x_1, x_2, x_3) \quad \text{Equation 5}$$

where Y is the response of the model and x_n the independent variables, also known as factors [61]. For further development, the software compares the results obtained in a set of given experiments (output) with the theoretical results given by the model. The CCF used for the optimization is represented in Figure V.20 (b).

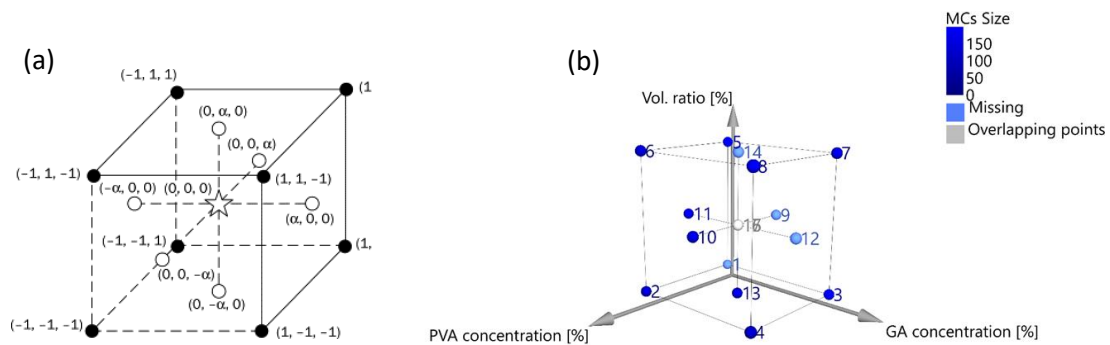


Figure V.20. Representation of a general central composite face design (CCF), reprinted with permission from [62] (a) and the CCF used for the optimization of the MCs average size.

The design consists of one experiment for each cube's vertices, face-centered, and three replicates of the cube's central point (0,0,0), on a total of 14 experiments and 3 replicates corresponding to the N15, 16 and 17. In Table V. 8 are indicated the proposed experiments, and the respective experimental responses. The N17 was deemed an outlier, and thus, only 16 runs were considered for the model development.

Table V. 8. Proposed experiments, by the DOE software, and respective experimental and predicted responses.

Exp Name	Experimental parameters			Response
	[PVAc] (% w/w)	[GAc] (% w/w)	V.r (% w/w)	MCs average size (μm)
N1	2	0	28	155.14 \pm 75
N2	4	0	28	41.36 \pm 16
N3	2	3.5	28	109.08 \pm 33
N4	4	3.5	28	46.48 \pm 14
N5	2	0	39	172.56 \pm 84
N6	4	0	39	82.81 \pm 23
N7	2	3.5	39	93.70 \pm 32
N8	4	3.5	39	91.83 \pm 46
N9	2	1.75	33.5	140.53 \pm 80
N10	4	1.75	33.5	65.54 \pm 22
N11	3	0	33.5	104.21 \pm 49
N12	3	3.5	33.5	70.81 \pm 25
N13	3	1.75	28	70.21 \pm 33
N14	3	1.75	39	109.36 \pm 30
N15	3	1.75	33.5	76.55 \pm 31
N16	3	1.75	33.5	81.23 \pm 25
N17	3	1.75	33.5	130.12 \pm 92

Figure V. 21 shows the coefficient plot, in which the size of the bars indicates the magnitude of the effect and the error bar the 95% confidence interval. All the terms are scaled and centered, allowing for the comparison of factors with different units, to assess their individual influence on the model. MODDE uses a saturated model, by which all terms, including all interactions and squared terms, are included. This ensures a high R^2 but a low Q^2 , as it usually includes non-significant terms [47]. The R^2 and the Q^2 , both between 0 and 1, represent how well a given predictive model fits the experimental data and the accuracy of the model in predicting new data, respectively. Ideally, the new model should have a high R^2 , which enables it to explain the dataset, and a high Q^2 to interpolate new data points accurately [47, 63]. In Figure V. 21, significant terms are those which have a magnitude far from zero and an uncertainty level that does not cross $y=0$ [47]. If both are combined, the term can be considered as non-significant. For the development of a model with a good output prediction, with a high Q^2 , it must be removed every non-significant term. Three terms were removed, and the new coefficient plot is

presented in Figure V. 22. By removing the non-significant terms, the Q^2 increased from 0.734 to 0.867.

The most significant factor showing a linear effect on the MCs' average size is the PVA concentration with its increase leading to a decrease in the MCs size. Additionally, PVA concentration is the only factor with a significant quadratic relationship with the MCs' average size as well as relevant interactions with the other parameters. The PVA concentration and its correlations with the other parameters have a higher impact on the average MCs size, while the amount of GA and the O phase volume in the emulsion were found to have a lower statistical significance.

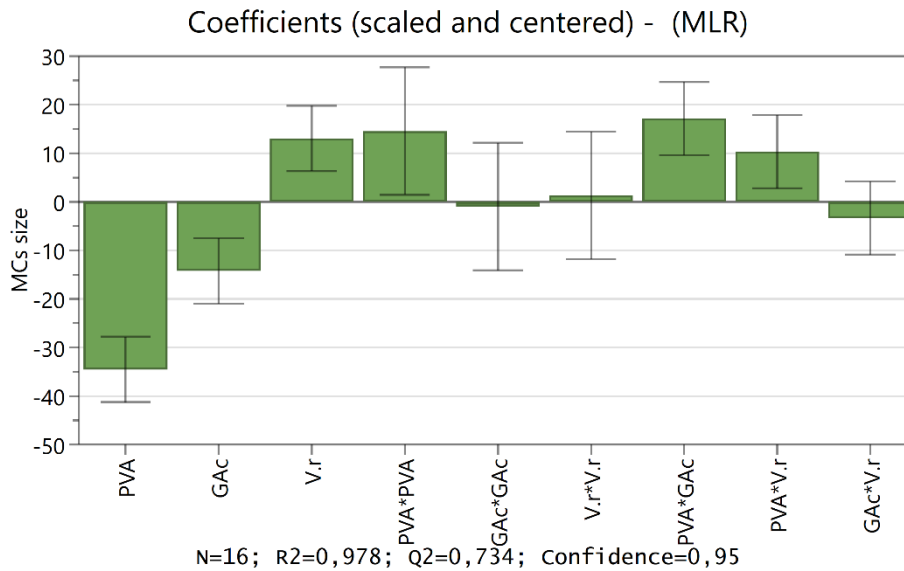


Figure V. 21. Coefficient plot for the DOE saturated model, showing the influence of individual and squared terms (where * represents multiplication) on the MCs' average size.

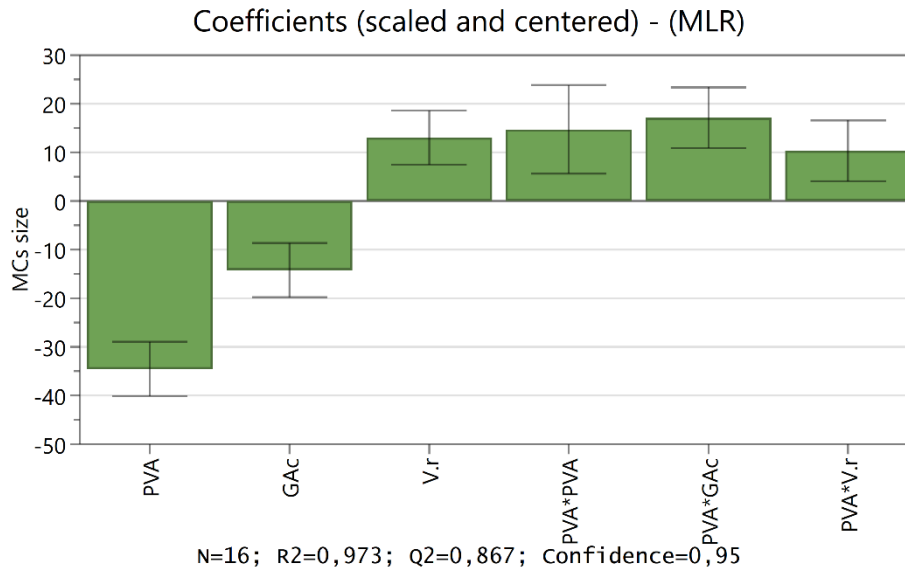


Figure V. 22. Coefficient plot for the DOE model, considering the significant terms, showing the influence of individual and squared terms (where * represents multiplication) on the MCs average size.

On Figure V.23 is the correlation plot between the experimental and predicted outcomes for the proposed experimental runs.

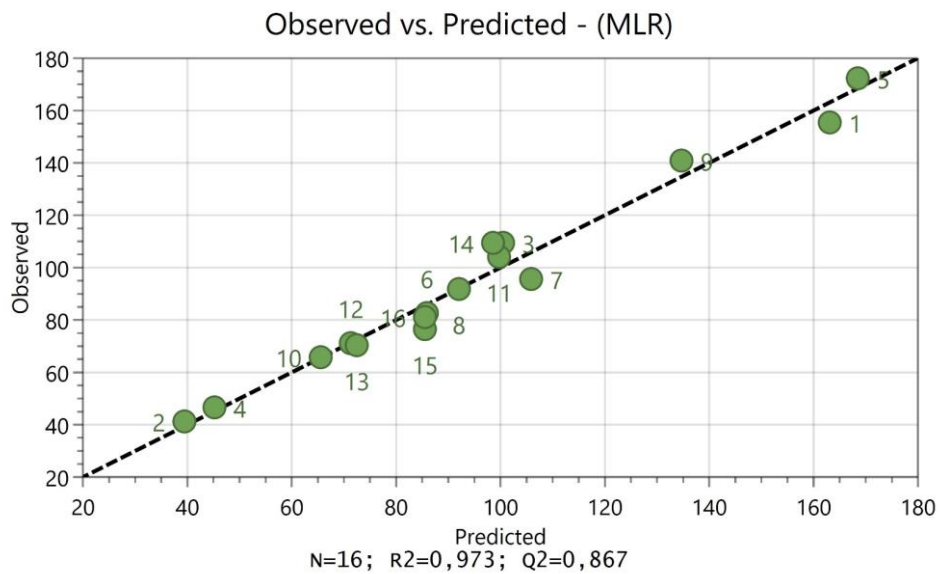


Figure V.23. Plot of the correlation between the observed vs predicted results.

A second-order analysis of the resulting experimental design showed a good correlation with the experimental data, with a R^2 of 0,973 and a Q^2 value of 0.867, exposed in Table V. 9. The

aptness of the model was determined based on the correlation between the predicted and the experimental responses.

Table V. 9. Results of the multiple regression analysis.

Regression Coefficients	R ²	R ² Adj.	Q ²	RDS
Coefficient Values	0.973	0.955	0.867	7.809

A multiple linear regression was used to fit the experimental data and the following second-order polynomial equation, Equation 6, was used to build a model to describe and predict the outcome responses to the factor's variations. The equation for the model, which enables to predict the values for the variables, was computed based upon the correlation coefficients and their effect on the MCs average size.

$$Y = \beta_0 + \sum_{i=1}^3 \beta_i x_i + \sum_{i=1}^3 \beta_{ii} x_i^2 + \sum_{i=1}^2 \sum_{j=i+1}^3 \beta_{ij} x_i x_j \quad \text{Equation 6}$$

For Equation 6, the Y represents the response (medium MCs' size, μm), x_i and x_j the independent variables and β_0 , β_i , β_{ii} , and β_{ij} the intercept, linear, quadratic, and interaction coefficients, respectively [61, 64]. The polynomial equation, Equation 7, obtained using multiple regression analysis, is the following:

$$Y (\mu\text{m}) = 85.395 - 34.5122x_1 - 14.2052x_2 + 13.0118x_3 + 14.7212x_1^2 + 17.1165x_1x_2 + 10.329x_1x_3 \quad \text{Equation 7}$$

For Equation 7, the Y is the medium MCs size (μm), x_1 is the PVA concentration in the W phase; x_2 the GA concentration in the W phase and x_3 is the O phase volume in the emulsion system.

The probability value (p-value) reveals the validity, significance, and acceptance of the developed model, for which it was considered a p-value lower than 0.05 as significant

(confidence level of 95%) [65]. The statistical significance of the equation coefficients is depicted on Table V.10.

Table V.10. Coefficients of model #2 and its statistical significance.

Variable	Coefficient (Scaled and Centered)	Standard Error	p-value
β_0	85,395	3.18793	6.81413e-10
x_1	-34.5122	2.46936	2.08123e-07
x_2	-14.2052	2.46936	0.00028
x_3	13.0118	2.46936	0.00051
x_1^2	14.7212	4.03245	0.00531
x_1x_2	17.1165	2.76083	0.00016
x_1x_3	10.329	2.76083	0.00461
	N=16	Q ² =0.867	
	DF=9	R ² =0.973	
	RSD = 7.809	R ² adj.=0.955	

The model presents a good correlation with the experimental data, with an R²= 0,973. This R² value implies that 97,3% of observations can be explained by the independent variables within the considered factor's range. The Q² value of 0.867, which should ideally be >0.5, demonstrated a good predictive capability, allowing for a confident prediction for the variables [63].

Figure V.24 shows the response contour and surface plots of the interactive effect between the variables in study on the average MCs size. For that, the PVA concentration was maintained constant, and the amount of GA and the O phase volume in the emulsion was varied. The contour plots show the behavior of the MCs size where the minimum diameters are represented as blue and the larger are represented as red. By increasing the PVA concentration from 2 wt% to 3 wt% it is clearly visible the shift of the MCs' size range, covered in the contour plot, to smaller values, confirming the effect of this variable. PVA was used as a rheology modifier, intend to increase the viscosity of the aqueous solutions, which is known to reduce the tendency for collisions between the O droplets as well as their sedimentation [56, 57]. For 2 and 3wt% of PVA in the W phase, the tendency is for smaller MCs to be obtained for higher concentrations of GA and lower concentrations of the O phase in the emulsion. GA is a branched polysaccharide, used in O/W emulsion stabilization by forming a protective film around emulsion droplets, which creates a steric barrier avoiding coalescence [53-55]. For a PVA concentration of 4 wt%, it is observed an increase in the MCs diameter with the increase of the GA concentration. High

concentrations of both PVA and GA might lead to an excessive increase in the emulsion viscosity, requiring a higher mechanical energy input to form smaller droplets during the emulsification process [58]. The necessary mechanical energy input might be given by an extended emulsification time or an increase in the emulsification rate. Regarding the emulsion phase ratios, a correlation between an increase in droplet size with an increase in the dispersed phase volume was already reported. This phenomenon can be correlated with a lack of emulsion stability leading to coalescence, due to an insufficient concentration of emulsifier, causing an inadequate cover of the O droplets [59, 60, 66]. It is also to consider that an increase of the O phase volume is also associated with a higher emulsion viscosity.

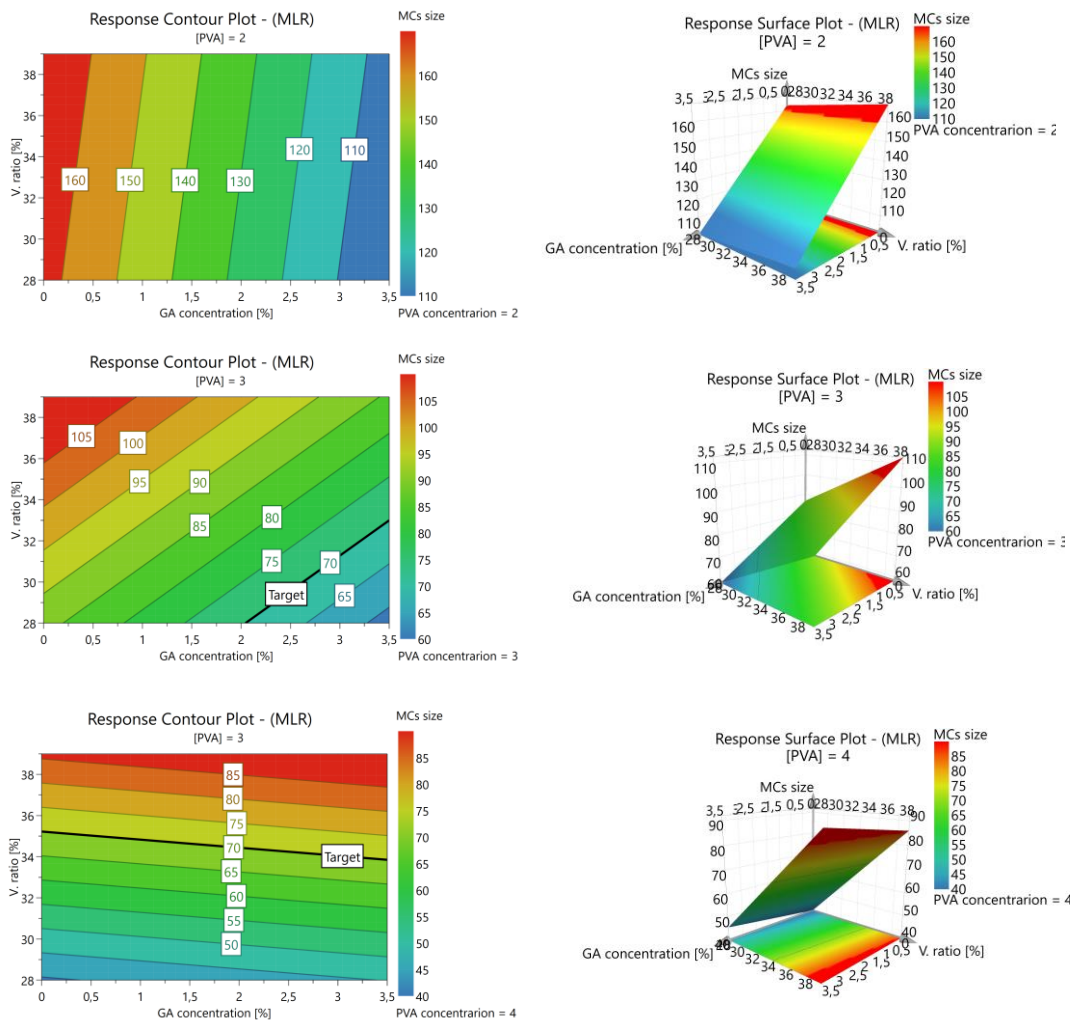


Figure V.24. Contour plots of the response (Mcs size, μm) to the variation of GA concentration (w/w%) vs volumetric ratio between the O and W phases (v/v %) for different PVA concentrations (left) and the respective 3-D surface plot (right).

Two additional validation experiments were conducted, aiming at an average diameter of 70 μm , with the variable's values given in Table V. 11, along with the predicted and experimental outcomes. The runs, N18 and N19, fall in the predicted values by the developed model, using a confidence level of 95%, validating the model. The obtained equation can be considered valid to predict the medium MCs sizes as a function of GA and PVA concentration and O phase volume in the emulsion.

Table V. 11. Experimental runs for validation of the model and respective predicted and experimental results.

Run	[PVA] (%)	[GA] (%)	O phase (%)	MCs average size (μm)	
				Predicted	Experimental
N18	3	1.5	28	58.64 – 93	90.27 \pm 25
N19	2.8	2	33.5	66.37 – 88	80.27 \pm 21

The SEM of the MCs obtained in the validation runs, as well as its size distribution, are exposed in Figure V.25. The MCs are loose and spherical with a core-shell morphology. Both syntheses have an identical size distribution range, with the N18 MCs having their distribution peak at smaller sizes than the N19 MCs. Both syntheses have a significantly narrower size distributions compared to the previously reported PCL MCs, which ranged from 75 to nearly 900 μm .

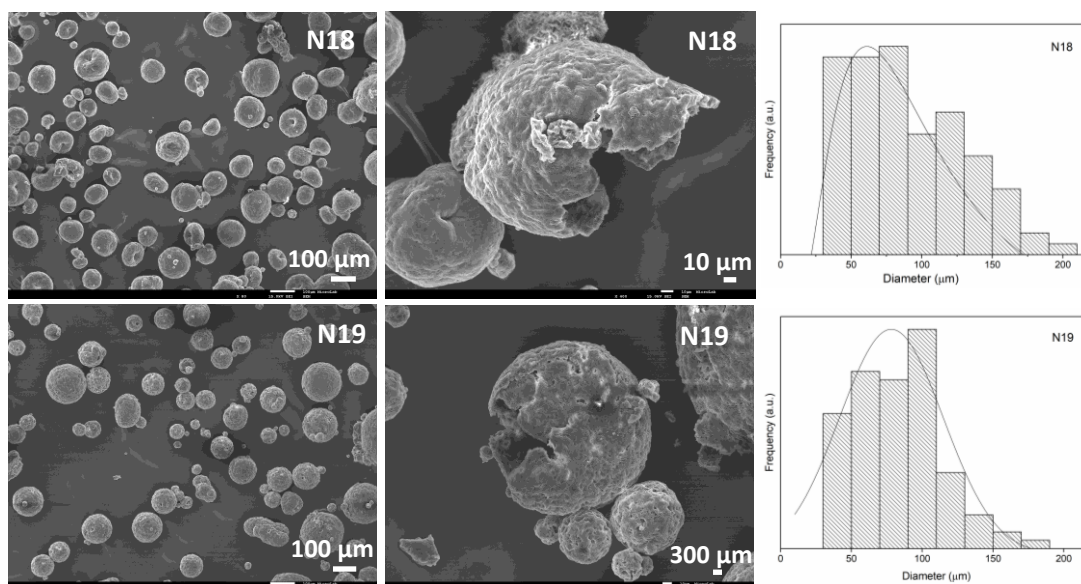


Figure V.25. SEM images (left) of the MCs obtained in the validation runs, N18 and N19, and respective size distribution histograms (right).

It is to notice that, although used for the model development, all the MCs obtained with a PVA concentration of 4wt% were considered not viable for the current application, as it has led to MCs without a spherical shape and, in some cases, with significant aggregation. In addition, it is

possible to identify some surface holes in the MCs' shell, which might compromise its shelf-life. In Figure V.26 are exposed SEM images of MCs produced using 4% of PVA, which are representative of all the MCs obtained with this concentration.

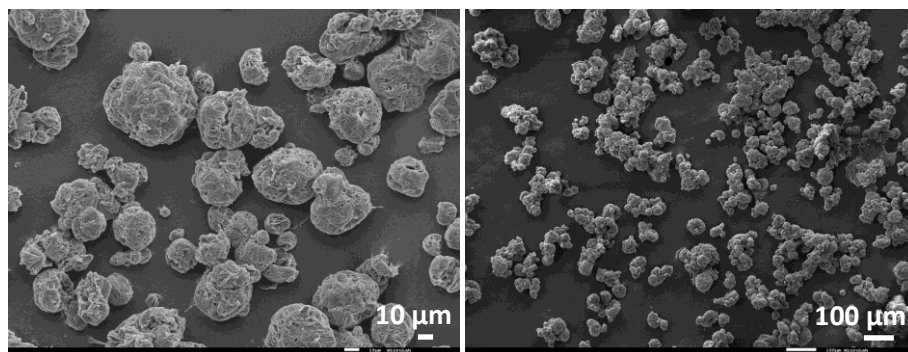


Figure V.26. SEM photomicrograph of MCs obtained using a PVA concentration of 4wt%.

By comparing all the remaining runs proposed by the DOE method, and having into consideration not only the MCs average size diameter but also its encapsulation content and shelf-life, the run N7 ([PVA]:2; [GA]:3.5; [O phase]:39) and the run N15 ([PVA]:3; [GA]:1.75; [O phase]:33.5) were considered the ones leading to the most suitable MCs. The SEM images of the MCs obtained in the referred runs, as well as the respective size distribution histograms, are depicted in Figure V.27. Although the N7 synthesis has led to MCs with an average size of about 90 μm and a bi-modal size distribution, these MCs have very satisfactory characteristics regarding their encapsulation content and shelf-life and were considered as a viable option. The average size distribution, respective mode and ratio between the average shell thickness and MCs' diameter (S/D ratio), for the N7, N15 and for the previously reported MCs (I_45 MCs), are exposed on Table V.12. Both the N7 and N15 samples have significantly smaller average size diameters than the I_45MCs. The size distribution was also decrease and transitioned from a trimodal distribution to a bimodal, for N7, and unimodal distribution, for N15, as a result of an improved emulsion stability.

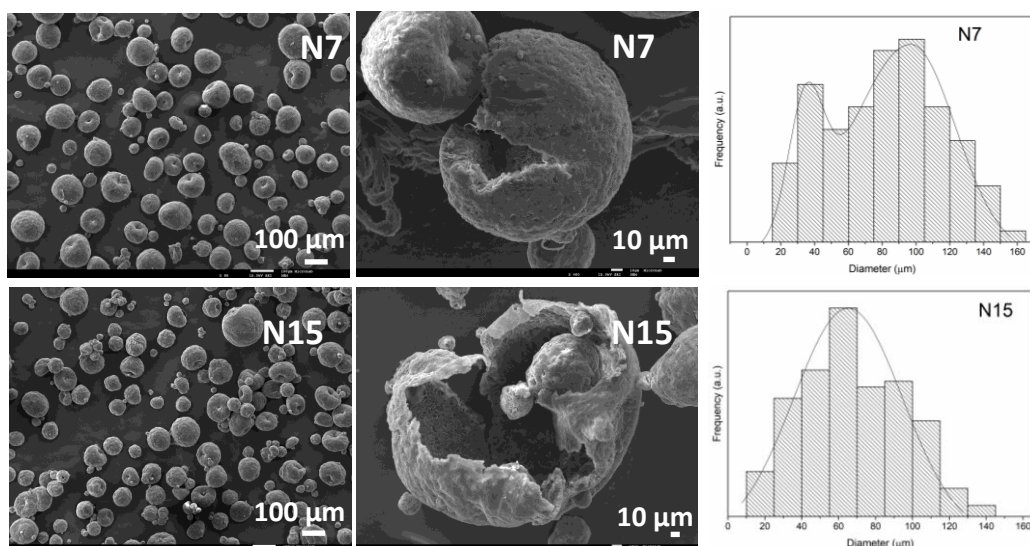


Figure V.27. SEM photomicrographs of the N7 and N15 MCs (left) and respective size distribution histograms (right).

Table V.12. N7, N15 and I_45MCs average diameter (D), size distribution mode and S/D ratio.

MCs' acronym	Average diameter	Mode	S/D ratio
N7	93.70 ± 32	36.73, 97,49	0.63, 0.24
N15	76.55 ± 31	62.83	0.087
I_45MCs	$326,39 \pm 157$	264, 416 and 637	0.11, 0.071 and 0.046

The MCs were also evaluated by thermogravimetric analysis to conclude about their encapsulation yield. Figure V.28 shows the thermograms of the shell-forming polymer, encapsulated IPDI and of the N7_MCs and N15_MCs, as-prepared and 3 months aged at room temperature and 60% of relative humidity. PCL has its degradation peak ranging from ca. 350 to 450 °C while the IPDI shows its first thermal event between 100 and 240 °C. Both MCs have their first thermal event at around 120 °C, corresponding to IPDI, which was used to quantify the encapsulation yield. The isocyanate content of both the N7 and N15_MCs, as prepared and 3 months aged, is exposed in Table V.13. Both the as prepared MCs have an IPDI content of around 60 wt% of the total MCs weight, with the N15_MCs having a slightly higher encapsulation. Both the DTG of the 3 months old MCs indicate the loss of some unreacted isocyanate, as a variety of low-MW species, oligomers, or low-MW polymeric species, by the presence of two extra peaks, between 280 and 350 °C, not present in the thermogram derivatives of the as-prepared MCs. Indeed, PU/PUa materials have two degradation peaks, the first one between 300 and 370 °C,

from the degradation of soft segments, and a second above 370 °C. Comparing with the aged I_45MCs thermogram and first-derivative curves, both the aged N7 and N15 MCs have less high-MW isocyanate species, especially the N7 MCs. Although in less extent, the N15 MCs seem to have species with a higher degree of polymerization. These differences might be due to the variation in the MCs' S/D ratio. A lower S/D ratio might contribute to a higher encapsulation content, however, it might also be responsible for a lower protection against the air moisture diffusion inside the MCs. Although there were variations in the MCs composition for 3 months they were not very significant, with the N7_MCs showing a decrease of only 7.43wt% of encapsulated isocyanate over that period of time, showing a great resistance to air moisture diffusion.

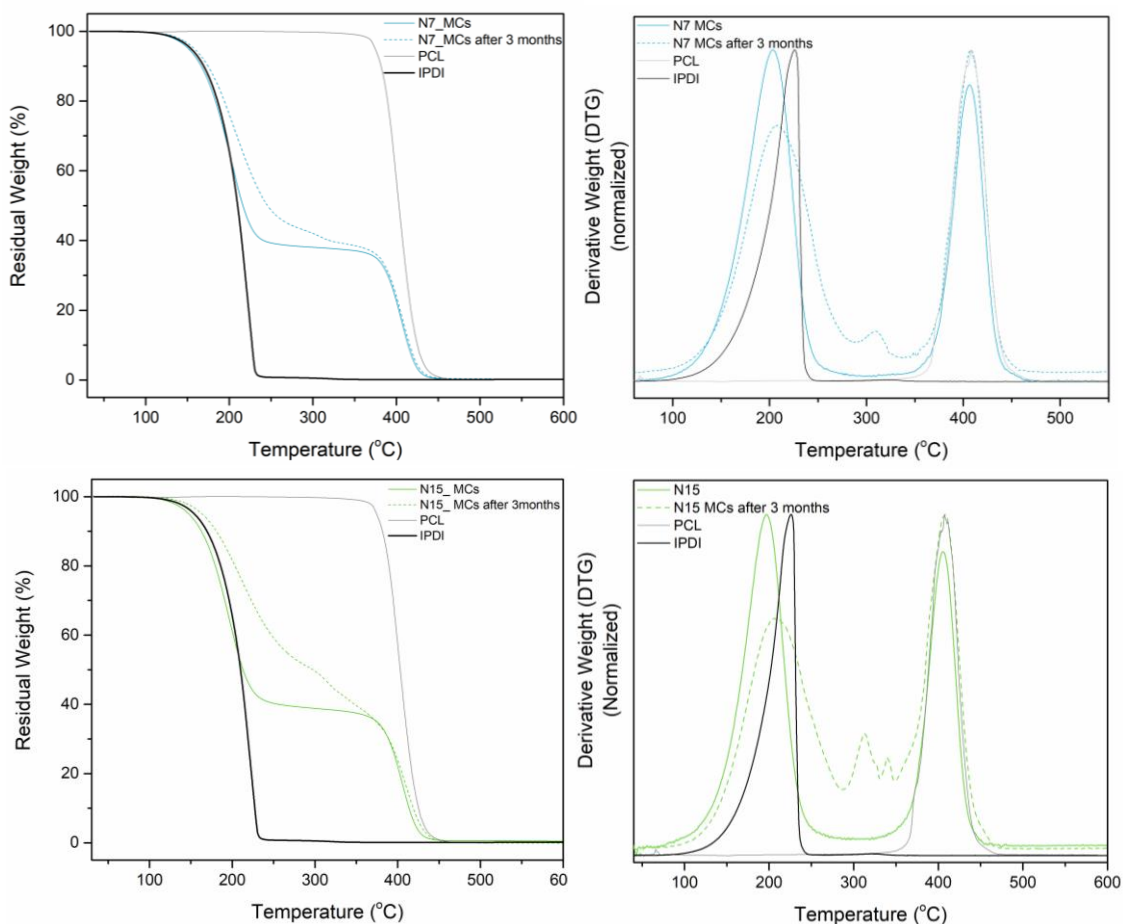


Figure V.28. Thermogram of the as-prepared and aged (by 3 months at room temperature and 60wt% of relative humidity) N7 MCs and N15 (left), and the respective derivative curves (right).

Table V.13. Relative encapsulation yield (Y value) and mass loss (%) of encapsulated IPDI for the N7_MCs and N15_MCs, as prepared and aged by 3 months (at room temperature and 60wt% of relative humidity).

MCs' acronym	Relative encapsulation yield (Y) from FTIR	Encapsulated isocyanate (wt%) from TGA (from 115-320 °C *)	Encapsulated isocyanate in the 3 months MCs (wt%) from TGA	% of isocyanate over a period of 3 months
N7_MCs	3.19	60.56	53.14	7.42
N15_MCs	2.67	58.24	44.75	13.49
I_45MCs	2.42	54.0	Not evaluated	Not evaluated

* Range of temperatures used for the encapsulated isocyanate quantification. The temperature range varied slightly depending on the MCs thermograms.

In conclusion, by using the DOE method, it was possible to develop a model to predict the optimum values for three pre-defined variables, that allowed to obtain MCs with a desired average size. The model was statistically evaluated employing the ANOVA test and was considered statistically significant, with a high R^2 of 0.973 and a Q^2 of 0.867, which makes it fit to be used to modulate and predict the MCs outcome.

PVA concentrations is, from the studied variables, the most influential to the MCs size and the O phase volume the one which influences the least. The developed model, enabled to obtain very satisfactory MCs with an average diameter between 76 to 94 μm , and to narrow its initial size distribution. An improvement in the encapsulation yield, when comparing with the previous results (I_45MCs), was also observed.

V.3.3 Polymers used for the shell formation

PCL has several advantages to be used as shell-forming polymer for the current application' MCs, as it has a low melting temperature and low melt viscosity. However, although it is a biodegradable polymer it is synthesized via ring opening polymerization of ϵ -caprolactone, which is petroleum derived monomer [67]. PHB has the advantage, compared to PCL, of being a biopolymer, obtained by biotechnological production. It is a polyhydroxyalkanoate (PHA), a type of polymer naturally produced by microorganisms, by the fermentation of sugars or lipids, when under stress conditions. PHB is the only considered biodegradable polyester that has a proven biodegradability in all natural environments, including in marine and freshwater environment,

according to the standards and certification in vigor. In contrast, PCL is only proven to biodegrade in industrial and home composting specific conditions [68]. PHAs are promising alternatives to petroleum-based plastics due to its mechanical and thermoplastic properties, comparable with polypropylene and polyethylene [69, 70]. PHB is stiffer and more brittle than PCL, with a high degree of crystallinity. For MCs with a PHB shell the isocyanate release would occur by pressure induced breakage of the MCs during the adhesive application. Although there are several advantages of using PHAs to substitute some of the petroleum-based plastics, there are still some limitations associated with its production at industrial scale. It has a relatively high-cost production, associated with a low yield, susceptibility to degradation and technology complexities including extraction difficulties [71, 72]. Several strategies have been developed to reduce the PHAs production costs and compete with the current petroleum based plastics, such as develop efficient bacterial strains, optimize the fermentation and polymer recovery processes and evaluate a series of new emerging bacterial fermentation processes which have the potential to accentuate the kinetics of microbial growth [72-74]. This polymer was used for the current work as it is not only biodegradable but also a biopolymer along with its high hydrophobicity and crystallinity, that ensures its breakage induced by the pressure applied during the adhesive joint preparation. The biodegradability of both PCL and PHB is already well characterized both *in vivo* as *in vitro*, occurring by bulk ester hydrolysis into carboxylic acids and alcohols [35-37, 75-77].

The production parameters of the N15 run were the ones selected to initiate the experiments to obtain PHB MCs. However, the PHB does not dissolve in DCM, as the PCL. Four different solvents, at several temperatures, were tested for the PHB dissolution, including acetic acid, acetone, chloroform, and ethyl acetate. The polymer was only possible to dissolve in chloroform by applying 50 °C. After several dissolution tests, it was concluded that PHB can only be used at a maximum concentration of 10 wt% in chloroform, leading to a saturated solution for higher concentrations. Possibly, the PCL has a better dissolution in DCM than the PHB has in chloroform, leading to this difference. Indeed, it is reported for the Hansen solubility parameters for PCL in DCM to be 17.8 MPa, 3.1 MPa and 5.7 MPa for the δ_d , δ_p and δ_h , respectively, with a R_0 of 3.7 MPa [78]. While, for the PHB in chloroform the values for the δ_d , δ_p and δ_h are 17.7-18.1 MPa, 3.1 MPa and 5.7 MPa, respectively, with a R_0 of 7.9-8.4 MPa [79] It is to notice that these values were obtained for different polymers and solvents combinations and were differently determined, with the ones for PCL obtained from experimental results and the ones for PHB theoretically calculated.

For the production of the PHB MCs, the polymer precipitation and consequent MCs formation, occurs much quicker than for the PCL MCs. This probably occurs as the PHB solution is almost saturated promoting the polymer precipitation with only a small percentage of solvent evaporation. A slow particle formation, as occurs for the PCL MCs production, leads to more homogeneous particles [80]. Due to the quick precipitation of the PHB, which occurs within an hour, most of the obtained particles have a non-uniform and non-spherical shape.

On Table V.14 are the parameters of the MCs fabrication procedure that were tested and optimized.

Table V.14. Optimized parameters for the PHB MCs production, and studied range of values.

Studied Parameters	Ranges			
GA wt% in the W phase	-	3.5wt%	5 wt%	-
volume ratio of the O₁:O₂ phases	1:3	1:3.7	1:4.7	-
Temperature	30 °C	40 °C	50 °C	-
Mechanical Stirring	500 rpm	750 rpm	850 rpm	-
PVA wt% in the W phase	2 wt%	3 wt%	4 wt%	-
Polymer wt% in the O₂ phase	5 wt%	8 wt%	10 wt%	12 wt%

The concentration of GA in the W phase and the O₁:O₂ proportion did not led to significant morphological modifications to the obtained MCs. The use of a GA concentration of 3.5 wt% and an O₁:O₂ proportion of 1:3.7 were chosen, as for higher IPDI concentrations the MCs were slightly more irregular. The temperature, on the other hand, had a major impact in the MCs production. It was not possible to obtain particles with temperatures lower than 40 °C, which leads to an agglomeration of the polymer around the agitation rod. As this, 50 °C was considered the optimal temperature value for the MCs production. The mechanical stirring also had an impact in the final particles, with an agitation of 500 rpm leading to the aggregation of the polymer at the bottom of the reactor. Figure V. 29 depicts the particles obtained using 750 rpm and 850 rpm, by which it is possible to verify a significant decrease in the particle's sizes with

the increase of the agitation speed, as expected. From this point, the particles were obtained using 850 rpm.

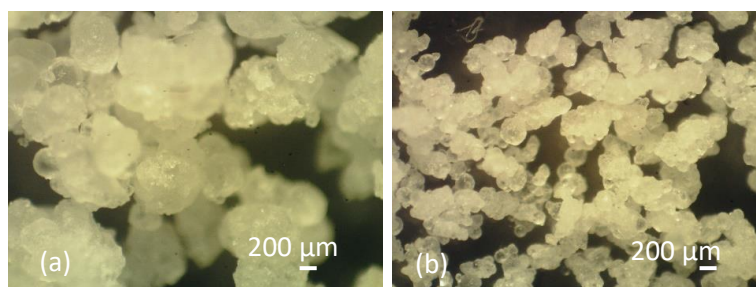


Figure V. 29. Optical microscopy photographs of the PHB MCs obtained using a mechanical stirring of 750 rpm (a) and of 850 rpm (b).

The PVA concentration in the W phase was varied from 2 to 4 wt%. PVA is used to stabilize the emulsion system by rheology modification of the continuous phase, increasing its viscosity. This will not only affect the stability of the emulsion, but also the evaporation of the chloroform, decreasing its rate. The increase of the system viscosity is expected to decrease the molecular transport rate and reduce the particle and droplet collision frequency. In this way, particles growth and their agglomeration will be reduced [81]. Indeed, as exposed in Figure V.30, a decrease of the particle size and the tendency for agglomeration when increasing the PVA concentration was observed. Having this into account 4 wt% was chosen as the PVA concentration.

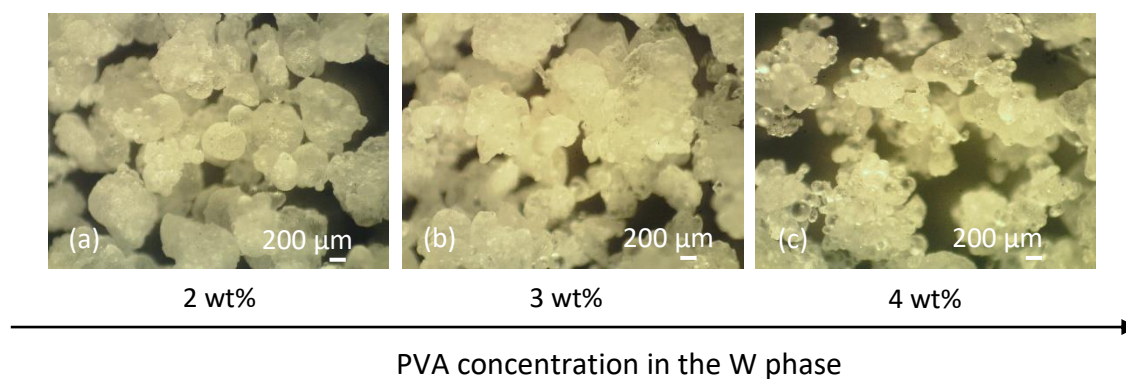


Figure V.30. Optical microscopy photographs of PHB MCs obtained with 2, 3 and 4wt% of PVA in the emulsion W phase.

Optical microscopy photographs of the MCs obtained with 5, 8, 10 and 12 wt% of PHB, in the emulsion O phase, are shown in Figure V.31. The PHB concentration affected the size of the particles, with higher polymer concentrations leading to bigger sized MCs. The polymer

concentration was varied from 5 to 12 wt%, with higher concentrations resulting in polymer agglomeration around the agitation rod. When the polymer concentration is higher than a critical value, it leads to a saturation of the solution, which is already the case for 12 wt% of PHB, resulting in an increased frequency of collisions of the particles, promoting a rapid nuclei growth [81]. It is also possible to observe a larger size distribution for higher concentrations. This occurs due to the non-homogeneity of supersaturated solutions during the process of precipitation in the poor solvent, making it difficult to control the uniformity of the particles [82, 83]. Both 5 and 8 wt% of PHB led to small MCs, however the ones obtained with 5 wt% were very fragile, which resulted in significant losses during the filtration process, due to the applied vacuum. As this, 8 wt% of polymer was the chosen ideal PHB concentration to use for the MCs production.

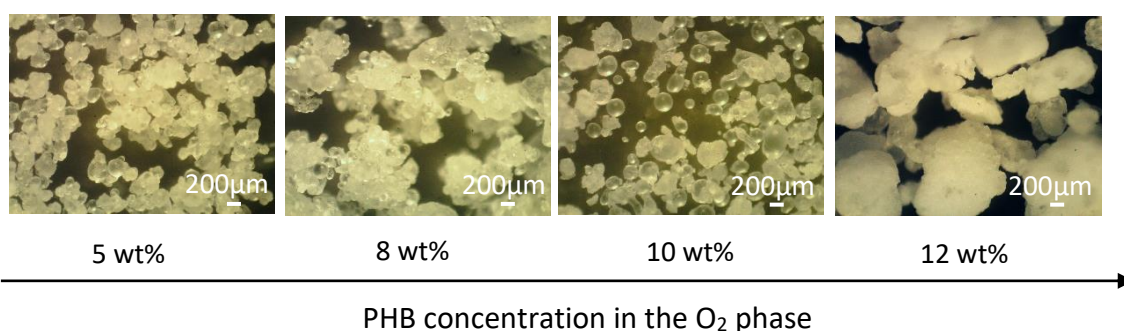


Figure V.31. Optical microscopy photographs of PHB MCs obtained using 5, 8, 10 and 12 wt% of PHB in the O phase of the emulsion.

Figure V.32 depicts the photomicrographs of the MCs obtained using 5, 8 and 10 wt% of PHB. It is possible to observe some loose and spherical MCs obtained with 5 wt% of polymer, as well as some irregular shaped, collapsed, MCs. Due to the small concentration of polymer, this MCs are very fragile, which makes them susceptible to collapse when submitted to the vacuum applied during the SEM analysis. The photomicrograph of the MCs produced using 8 wt% of PHB show some loose and spherical MCs, along with some that are irregularly shaped. However, for this case, the MCs do not seem to have been affect by the vacuum, confirming that higher concentrations of polymer confer some improved robustness to the shell.

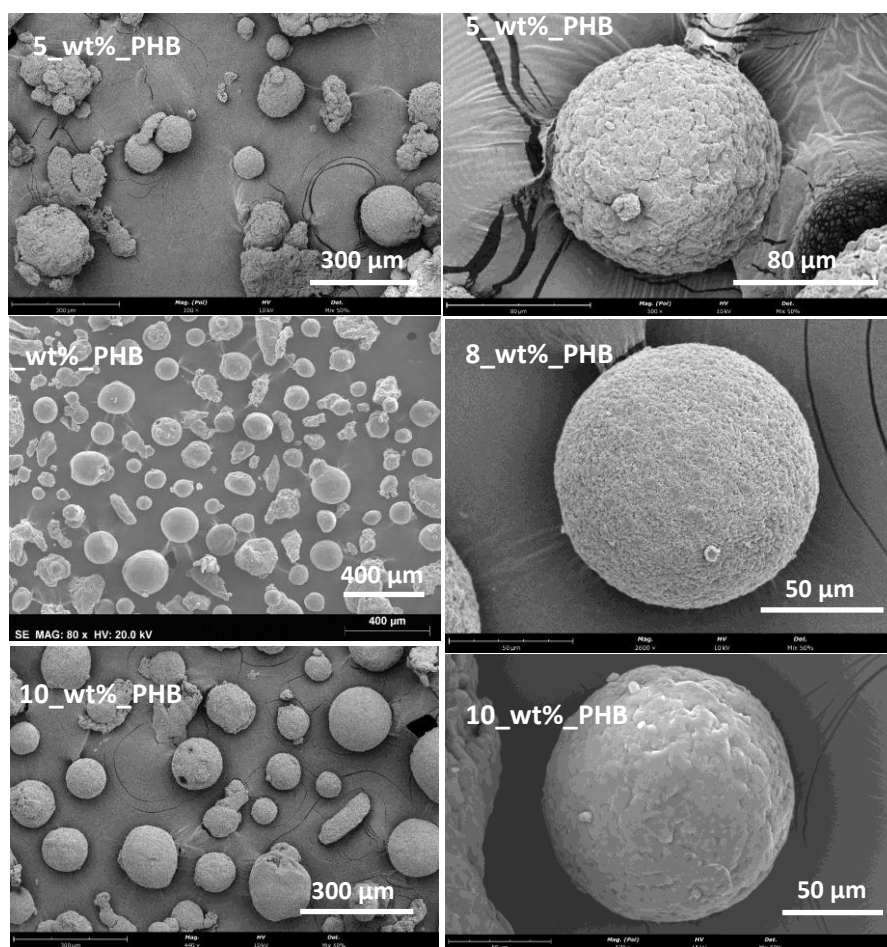


Figure V.32. SEM photomicrographs of the MCs obtained using 5, 8 and 10wt% of PHB in the O phase of the emulsion.

Figure V.33 displays the TGA and respective derivative curves of the MCs obtained using 5, 8 and 10 wt% of PHB, as well as of the polymer used for the shell formation and the encapsulated isocyanate. The PHB has a single thermal event, occurring between 220 °C and 275 °C. According to the literature, the maximum degradation temperature characteristic for PHBs is 290 °C [84, 85]. The thermal degradation of polyesters has been reported to occur by intramolecular ester exchange, transesterification, or by cis-elimination which is the case for PHB [84, 85]. The IPDI shows its first thermal event at lower temperatures, between 100 and 240 °C. The quantification of encapsulated IPDI on the as prepared MCs and on the 3 months aged MCs was determined having this into account, with the obtained values listed in Table V. 15. These MCs showed an incredibly high encapsulation content, up to 80% of the total MCs weight. It is possible to identify a correlation between the amount of PHB used for the shell formation and the encapsulated content, with higher PHB concentrations leading to lower IPDI values. PU/PUa soft segments are reported to degrade at a temperature between 300 and 370 °C [42, 43]. As there is no degradation curve at the referred temperatures in the as pre-prepared MCs thermograms it can be

stated that no reaction has occurred between the IPDI and the W phase during the MCs' fabrication process. However, this degradation curve is present in the 3 months old MCs thermograms and derivatives, indicating that some isocyanate has reacted during that period. The 3 months old 5 wt% PHB MCs were the ones with a higher degree of PUa formation, possibly due to a poorly protective shell, followed by the MCs produced with 10 wt%. Indeed, the 5 wt% PHB MCs have a rougher shell, with more pores and interfaces. It is to expect that a higher PHB content will create a more protective shell promoting a lower isocyanate loss over time. However, that was not the case as the 8 wt% MCs were the ones showing a better shelf-life with almost no significant changes in its composition, and a decrease of less than 20wt% in its isocyanate content over a period of 3 months. This might be due to the less controllable process with 10 wt% of PHB, which led to an incredibly quick precipitation and a non-uniform distribution of the polymer on the MCs' shell. The presence of isocyanate species with higher MW oligomers or low MW polymeric species can be identified, in the first derivative thermograms, by a larger band corresponding to the IPDI or by the presence of an extra band adjacent to this. Indeed, in the first derivative thermogram of the 5 wt% PHB MCs it is possible to identify this extra band at slightly higher temperatures than the one of pure IPDI, and, for the 10 wt% PHB MCs, the widening of the IPDI band.

A concentration of 8 wt% of PHB was considered the most suitable for the envisaged MCs.

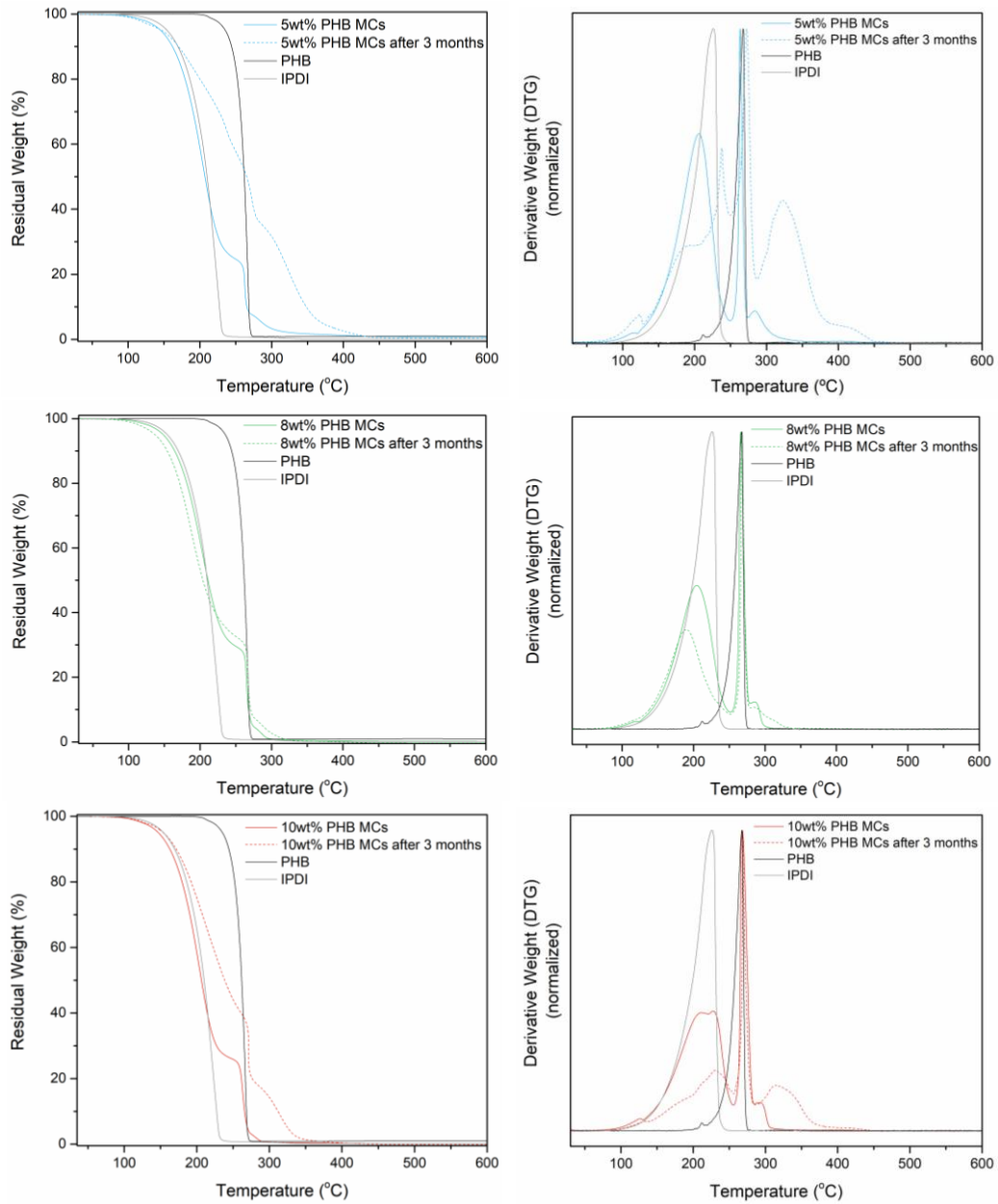


Figure V.33. Thermograms of the as-prepared and aged MCs obtained using 5, 8 and 10 wt% of PHB in the O phase of the emulsion, of the PHB and of the encapsulated isocyanate (left), as well as the respective derivatives (right), normalized by the division of each point by the maximum value.

Table V. 15. Mass loss (%) of encapsulated IPDI for the as-prepared PHB MCs obtained with 5, 8 and 10 wt% of dissolved polymer in the O phase of the emulsion, as well as for the aged MCs (by 3 months at room temperature and 60wt% of relative humidity).

MCs' sample	Encapsulated isocyanate in the as prepared MCs (wt%) (from 100-250 °C *)	Encapsulated isocyanate in the 3 months MCs (wt%)	% of isocyanate loss over a 3 month period
5_wt%_PHB	80.20	46.36	42.18
8_wt%_PHB	76.10	61.35	19.39
10_wt%_PHB	71.44	44.90	37.15

*Range of temperatures used for the encapsulated isocyanate quantification. The temperature range varied slightly depending on the MCs thermograms.

The optimized reactional parameters to produce PHB MCs are displayed in Table V.16. It is to notice that these parameters were the ones used for the 8 wt%_PHB_MCs formulation, which can be considered as the most promising for the envisaged application.

Table V.16. Optimized values for the reactional parameters to produce PHB MCs.

Reactional parameter	[GA] in the W phase	Volume ratio of O ₁ :O ₂ phases	Temperature	Mechanical Stirring	[PVA] in the W phase	[PHB] in the O ₂ phase
Optimal value	3.5 wt%	1:3.7	50 °C	850 rpm	4 wt%	8 wt%

MCs composed by a PHB shell, containing encapsulated IPDI, were obtained by using the solvent evaporation method. To the best of my knowledge, the encapsulation of isocyanates in MCs with a PHB shell was not yet reported in the state of the art. This MCs are composed by a biodegradable and a bio-derived polymeric shell. Its encapsulation content surpassed the values obtained using PCL as shell polymer, as well as the ones obtained for the MCs produced by interfacial polymerization technique, enabling to reach values between 70 and 80 wt% of encapsulated content, with the most suitable MCs having 76 wt%. The number of publications regarding MCs containing more than 75 wt% of core content in isocyanate microencapsulation is very scarce [86-89]. It is also important to notice that the core content of the developed MCs is composed only by IPDI, without any solvent or other additives. Also, the isocyanate loss in the 8 wt% PHB MCs over a period of 3 months was minimum, showing a good shelf-life. However, the synthesis process to obtain this MCs is very difficult to control, due to the quick precipitation of the PHB, making the industrial implementation of the process a challenge. Nevertheless, the

effectiveness of this MCs, as adhesive cross-linkers, was tested, with its results exposed in Chapter VI.

V.3.4 Encapsulation of highly reactive isocyanate species

In addition to the encapsulation of the monomeric IPDI, the solvent evaporation technique was employed to encapsulate pre-polymeric MDI species, in particular Ongronat® 2500 and Suprasec® 2234, the last one commercially used by CIPADE, S.A. With that purpose, the MCs production' parameters, previously optimized using the MODDE® Pro 13 software, in particular for the N15 run, were used. These isocyanates are far more reactive than the previously encapsulated IPDI, which makes their encapsulation particularly challenging. All the adopted procedures for the MCs production are in combination with a microemulsion system involving water as the continuous phase. Due to the high reactivity of these isocyanate species the minimal contact with water promotes a quicker PUa formation with consequent loss of available isocyanate to be encapsulated. The characteristics of the isocyanates in study are exposed in Table IV.2, and the adopted synthesis parameters on Table V.17.

Table V.17. Microcapsules' acronyms and emulsion composition.

MCs' acronyms	W phase (wt%)	O ₁ phase (wt%)	O ₂ phase (wt%)
Ongronat_MCs	PVA aqueous solution at 3 wt%	Ongronat® 2500 (26.2% of the emulsion)	PCL with 45000 Da at 16 wt% in DCM
Suprasec_MCs	GA at 1.75 wt% (66.5 % of the emulsion)	Suprasec® 2234 (26.2% of the emulsion)	(7.3% of the emulsion)

Figure V.34 shows the photomicrographs of the MCs containing Ongronat® 2500 and Suprasec® 2234, as well as their size distribution histograms. For both cases, loose, disaggregated MCs with a spherical shape were obtained, with the Ongronat_MCs having a core-shell morphology. On the other hand, the Suprasec_MCs have a very rigid shell which makes them difficult to break and to access their interior. This is an indication that the shell might be composed not only by PCL but also a significant amount of polymerized species, namely PUa.

Although the optimized N15 run parameters were used, the obtained MCs have a medium size higher than 70 μm , of ca. 150 μm for the Ongronat_MCs and of 268 μm for the Suprasec_MCs. This is due to the increased viscosity of the O phase when using higher MW isocyanate species, which was also observed for the MCs obtained with PCL80, comparing with the ones composed by PCL45. Indeed, the IPDI has a viscosity of 10 mPa.s, while the Ongronat[®] 2500 and the Suprasec[®] 2234 have a viscosity of 520-680 mPa.s and of 2500 mPa.s, respectively, which strongly influence the viscosity of the oil phase.

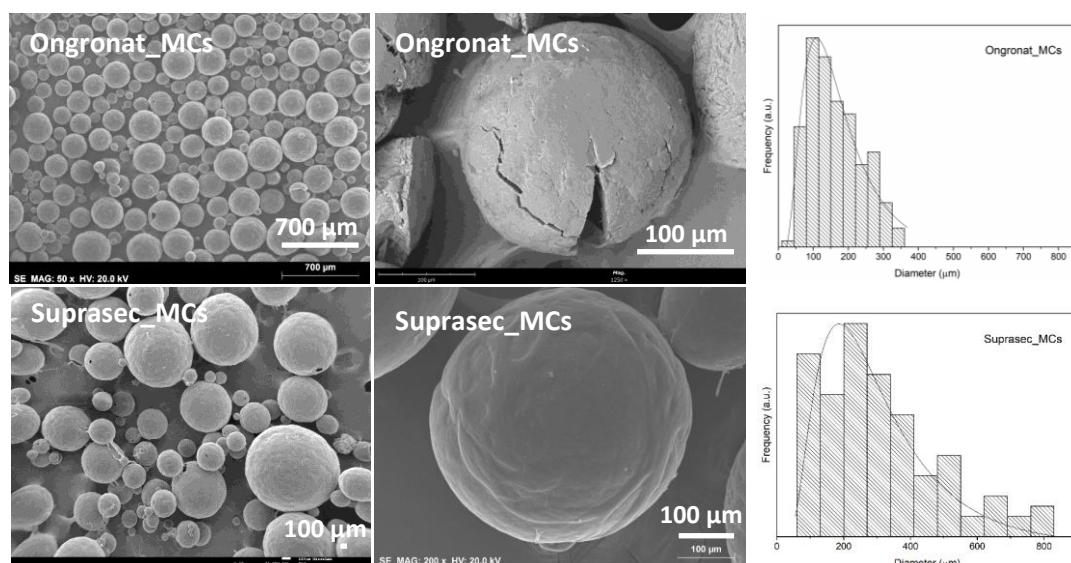


Figure V.34. SEM photomicrographs of the Ongronat_MCs and of the Suprasec_MCs (right) as well as of the respective size distribution histograms (left).

The FTIR spectra of both the Ongronat_MCs and the Suprasec_MCs, as well as of the PCL and respective isocyanates are depicted in Figure V.35. The peak at ca. 2260 cm^{-1} , which is ascribed to the N=C=O bond stretching vibration from unreacted isocyanates, is visible in both the Ongronat[®] 2500 and Suprasec[®] 2234 MCs' spectra, however with a significantly lower intensity in the last. This is an indication of a lower encapsulation efficiency. The PCL's most intense peak, related to the carbonyl group (C=O) stretching vibration, is identifiable in both the MCs' spectra, at 1715–1730 cm^{-1} , confirming the shell composition [30, 33]. However, distinctly from what was observed for the IPDI containing MCs, the carbonyl peak from PUa, at 1660 cm^{-1} , is also visible, adjacent to the one from the PCL, in both the as prepared MCs' spectra. This confirms that indeed some isocyanate reacted during the MCs' production process forming a hybrid shell composed by both PCL and PUa moieties. Having this into consideration, for the Y value calculation, the area related to the shell was that of both the PCL and PUa carbonyl peaks, as exposed in Equation 8. The Y value for the aged MCs is presented as a % of the first. When comparing the PUa carbonyl peak of the as prepared and aged MCs' spectra, it is clear the

increase of its intensity, indicating that the encapsulated isocyanate reacted over time. This leads to an increase of the PUa moieties on the shell and a decrease of the unreacted encapsulated isocyanate. By looking at the Y values, exposed on Table V.18, the difference between the Ongronat_MCs and the Suprasec_MCs is clear, with the last having a significantly lower value.

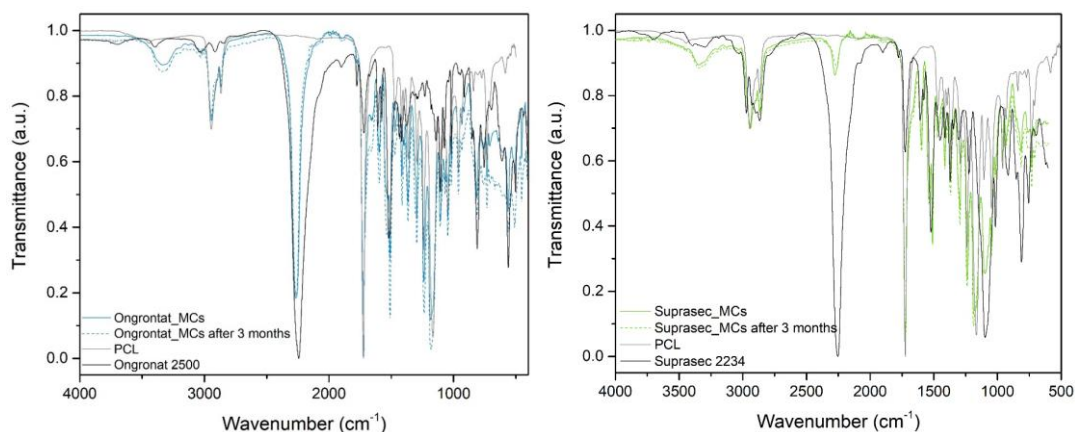


Figure V.35. FTIR-ATR spectra of the Ongronat_MCs and Suprasec_MCs as prepared and aged (by 3 months at room temperature and 60wt% of relative humidity), and of the PCL and respective isocyanate.

$$Y = \frac{Area_{NCO} (2260cm^{-1})}{Area_{shell} (1760-1621cm^{-1})} \quad \text{Equation 8}$$

The thermogram of the Ongronat_MCs, as well as that of the PCL and encapsulated isocyanate, are exposed on Figure V.36. PCL has his degradation peak ranging from ca. 350 to 450 °C while the Ongronat®2500 shows its first thermal event between 175 and 340 °C. The amount of encapsulated isocyanate, determined having these findings into consideration, is about 21% of the total MCs' weight. This is a significantly lower value compared to that obtained for the PCL MCs containing IPDI, which varied between 54 and 60 wt%. The presence of PUa can also be confirmed by the DTG thermogram, from the identification of a band above 430 °C [42, 43]. In the aged MCs' DTG there is a band at 345 °C, not present in the as prepared MCs, which regards to Ongronat®2500 higher MW species, indicating the occurrence of polymerization reactions over time.

The TGA of the Suprasec_MCs cannot be used to draw conclusions regarding this MCs encapsulation content. Suprasec is a pre-polymer, with low NCO value, which results in the overlap of the thermal events of its unreacted form with those of PUa. The thermogram of the Suprasec_MCs is exposed on Figure V. S2, from Supplementary Information.

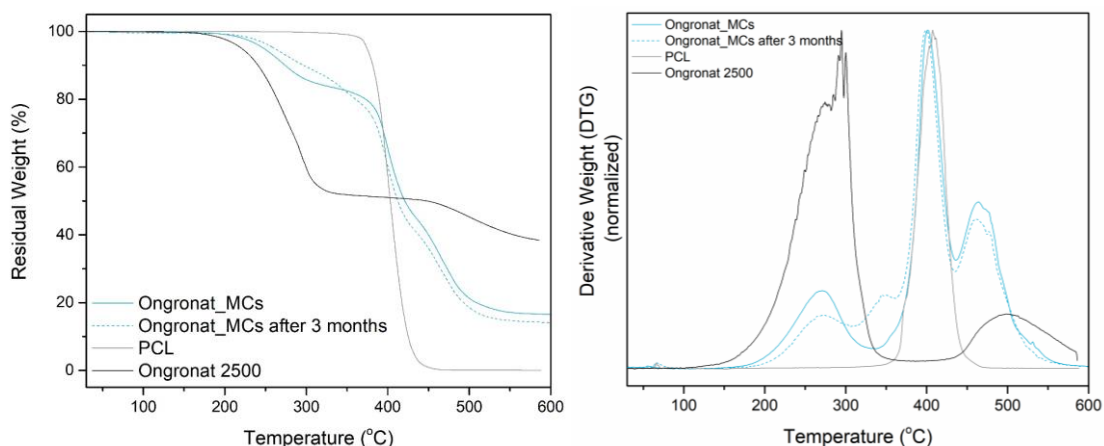


Figure V.36. Thermogram of the Ongronat_MCs as prepared and aged (by 3 months at room temperature and 60wt% of relative humidity), of the shell polymer and encapsulated isocyanate (left) and respective derivatives (right), normalized by the division of each point by the maximum value.

Table V.18 Mass loss (%) of encapsulated IPDI, by TGA and relative encapsulation yield (Y value) of the as-prepared MCs and aged by 3 months (at room temperature and 60wt% of relative humidity).

MCs' acronyms	Encapsulated isocyanate	Relative encapsulation yield (Y)	Y1 (%) 3 month after the synthesis
	from TGA (%) (from 190-330 °C)		
Ongronat_MCs	21.17	2.21	82.35
Suprasec_MCs	-	0.27	74.07

MCs with a PCL shell containing higher MW isocyanates, in particular Ongronat[®]2500 and Suprasec[®]2234, were obtained using the solvent evaporation technique. The MCs are spherical, loose and, in the case of Ongronat_MCs, have a core-shell morphology. Due to the high reactivity of these isocyanates, a pure PCL shell was not possible to obtain, but instead a combination of PCL with PUa, resulting from some isocyanate reaction with the OH groups during the MCs' production process. Due to this, the encapsulation yield was lower than that of the IPDI containing MCs, obtained from a purely physical process, especially for the Suprasec[®]2234. Although the encapsulation content of the Suprasec_MCs was not possible to quantify, FTIR analysis show it is far lower than that of the Ongronat_MCs, which is ca. of 21 wt%. This is considered a low encapsulation yield for the envisaged application as the lower the encapsulation content, the higher the amount of MCs that are necessary to add to the adhesive formulation, which can impact the adhesive performance. Due to this reason, the Suprasec_MCs cannot be considered viable for the envisaged application. On the other hand, the Ongronat_MCs, although their low isocyanate content, were tested as cross-linkers, whose results can be found in Chapter VI.

V.4 Scale-up of the syntheses processes

After the above reported optimization studies, a laboratorial scale-up of the process to encapsulate IPDI was carried out. The initial reactional volume of 85ml was scaled-up to 425 ml, which corresponds to an increase of 5 times the initial volume. The O and W phase compositions of the pre-scaled-up process as well as those of the scale-up are described in Table V.19.

Table V.19. Microcapsules' acronyms and emulsion composition.

MCs acronym	Synthesis volume	Water phase (wt%)	Oil ₁ phase (wt%)	Oil ₂ phase (wt%)	Time of synthesis
Pre_scaled-up_MCs	85ml	PVA aqueous solution	IPDI	PCL with 45000 Da at 16 wt% in DCM (26% of the emulsion)	3h30
Scaled-up_MCs	425 ml	GA (66.9 % of the emulsion)	(7.1% of the emulsion)		2h

The scale-up microencapsulation process was maintained identical to the pre-scale-up one, represented by the flow diagram in Figure V.37

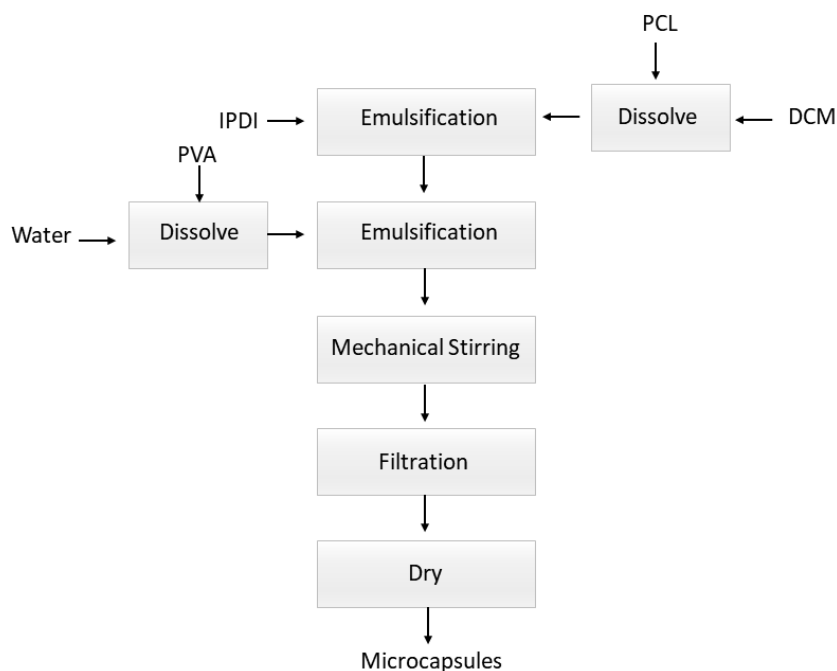


Figure V.37. Flow diagram of the scale-up process for the PCL MCs fabrication.

The MCs' production apparatus used for the pre-scale-up process is depicted in Figure V.38 (a) and the one of the scale-up on Figure V.38 (b). An extremely simple apparatus is enough to obtain this type of MCs. Figure V.39 shows the stirring rods used in the pre-scale-up process and the one used in the scale-up process, with an indication of the respective blade diameter. By applying Equation 4, Chapter IV, the 750rpm, used in the pre-scale-up, were decreased to 430 rpm in the scale-up. The duration of the encapsulation process was also adjusted, suffering a decrease by 1h30. By the solvent evaporation technique, the duration of the process can be decreased by increasing the contact between the reactional medium and the air (exterior medium), which promotes a quicker evaporation of the organic solvent. For the scale-up the contact between the reactional medium and the air should have decreased, due to a significantly higher amount of fluid, slowing the MC's production. However, the difference between the mechanical stirring rods used in both processes might have contributed to a different fluid dynamic, promoting an increased contact between the fluid and the air, leading to a quicker DCM evaporation and MCs' formation.

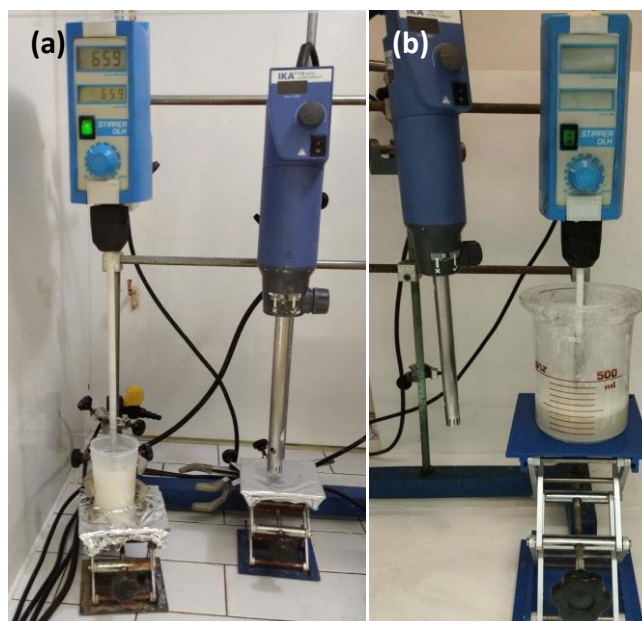


Figure V.38. PCL MCs' production apparatus used for the pre-scale-up reactional volume (a) and for the scale-up volume (b).

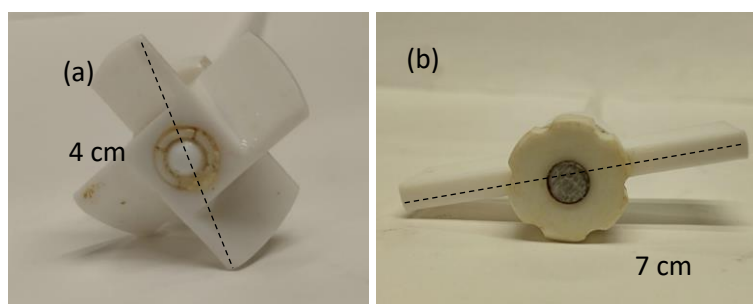


Figure V.39. Stirring rods used in the pre-scale-up (a), and in the scale-up (b) process.

The SEM photomicrographs of the pre-scale-up_MCs and scale-up_MCs are exposed in Figure V.40, along with the respective size distribution histogram. Both have a unimodal size distribution, although the scaled-up MCs have significantly larger sizes, with an average of 170 μm contrasting with the 76.55 μm obtained in the pre-scale-up process. It is to notice that, for the size distribution histograms there were only used intact, spherical MCs, which is particularly relevant for the Scale-up_MCs. In the SEM photomicrograph of the scale-up process it is possible to observe some broken MCs, particularly the ones with larger dimensions. A lower S/D ratio could contribute to an increased fragility of the MCs, however its value was identical for the MCs obtained by both processes, as exposed in Table V.20. The observed difference might be correlated with the stirring rod used in the scale-up which might be damaging the MCs during their fabrication process, despite the adjustment in the used rpm. Indeed, after the PCL

precipitation, the solid MCs' shell can be damaged by the mechanical impact of the blades, which can lead to their rupture. Also, both the MCs sizes and size distribution have increased with the scale-up. Since the GA and PVA concentrations, as well as the O volume and the shape of the reactor were maintained, this is possibly correlated with an improper system agitation. This might indicate a necessity to substitute the stirring rod for a more appropriate one.

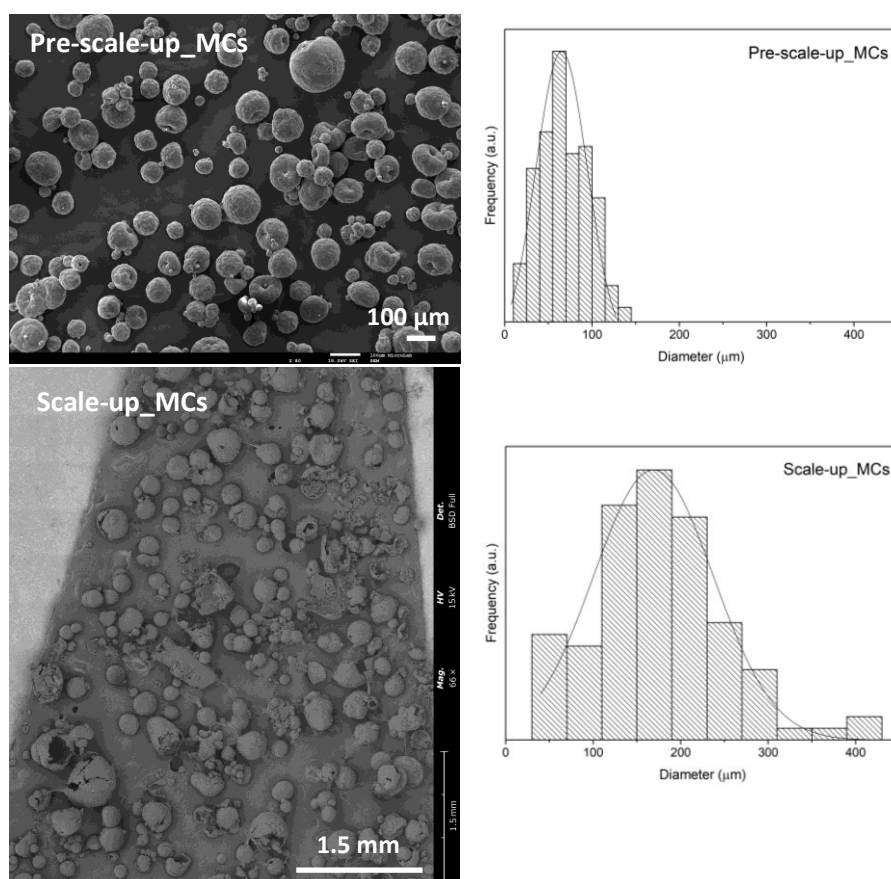


Figure V.40. SEM photomicrographs of the pre-scale-up_MCs and of the Scale-up_MCs (left) and respective size distribution histograms (right).

Figure V.41 depicts the thermograms and the respective derivatives of the MCs obtained for both reaction volumes, the PCL and the IPDI. Due to the similarity of the MCs' thermograms it is possible to state that both have an identical composition. Indeed, the difference in the encapsulation yield is of only 2.9 wt% between samples, with the ones obtained in the scale_up process having the slightly lower IPDI amount. It is also possible to state that the scale-up process did not influence the MCs' shell composition, as no fingerprint of PUa can be observed in this MCs' thermogram.

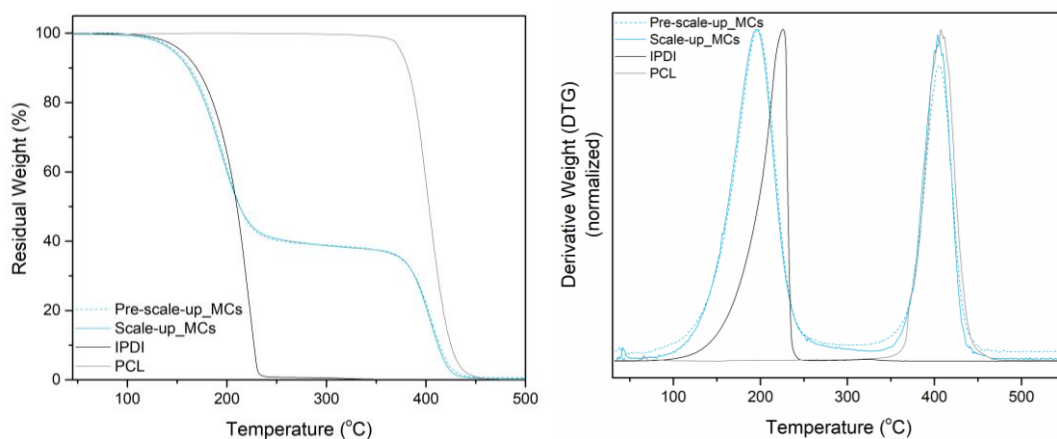


Figure V.41. Thermogram of the Pre-scale-up_MCs, of the Scale-up_MCs, shell polymer and encapsulated isocyanate (left) and respective derivative curves (right).

The encapsulation yield determined by the TGA analysis, as well as the relative encapsulation yield calculated by FTIR and the respective MCs S/D ratio are exposed in Table V.20. The FTIR spectra of both the MCs synthesis, as well as of the PCL and IPDI, are exposed in Figure V. S3, from Supplementary Information.

Table V.20. Mass loss (%) of encapsulated IPDI, by TGA, relative encapsulation yield (Y value) and S/D ratio for the as-prepared Pre-scale-up_MCs and Scale-up_MCs.

MCs' acronyms	Encapsulated isocyanate from TGA (%) (from 115-320 °C*)	Relative encapsulation yield (Y)	S/D ratio
Pre scale-up_MCs	61.2	2.97	0.087
Scale-up_MCs	58.3	2.45	0.088

*Range of temperatures used for the encapsulated isocyanate quantification. The temperature range varied slightly depending on the MCs thermograms.

The scale-up of the MCs production, by the solvent evaporation method, was made from an initial reactional volume of 85ml to a final volume of 425 ml, which enabled to increase the amount of obtained MCs from 6.5g to ca. 47g per batch. The ULTRA-TURRAX rpm, for the O phase preparation, was adjusted due to the higher reactional volume. As for the mechanical stirring, the agitation rod was substituted for a more appropriate one, according to the new reactor diameter. However, and although the rpm was adjusted, the obtained MCs had bigger sizes and size distributions than the pre-scale-up MCs, and some appeared to be broken. This might indicate an improper agitation of the reactional medium, probably due to the shape of the new mechanical rod. Nonetheless, the obtained S/D ratio is identical for both MCs, which reflects a similar contribution of the shell to the MCs overall morphology. In accordance, the

encapsulation yield between samples was also identical, with a difference lower than 3 wt% between samples, as well as the MCs' shell composition with both being composed solely by PCL. Despite some required adjustments in what regards the mechanical stirring rod and rpm, this preliminary lab scale-up reveals the viability of industrial implementation of these MCs' production.

V.5 Final remarks

The solvent evaporation technique, which has been used to produce polymeric MCs containing hydrophilic content by means of a single water-in-oil (W/O) or W/O/W emulsion system, was herein employed to produce core-shell MCs containing reactive isocyanate species in the core and a biodegradable polymeric shell. To the best of my knowledge this technique was not used before for the encapsulation of any type of isocyanate and the publications regarding hydrophobic species are scarce. Therefore, the fabrication process was adapted and optimized, by studying several processing parameters.

To prevent any contact between the isocyanates and the emulsion W phase, aiming to avoid the formation of PUa moieties, the strategy employed was to use a double O/O/W emulsion system. However, the existence of a O/O emulsion was only possible to confirm, by optical microscopy, for the encapsulation of Ongronat®2500, as IPDI is not visually distinguishable from the O phase containing the dissolved polymer. Nevertheless, the shell of both the PCL and PHB MCs containing IPDI, was composed only by the desired polymer and no PUa was detected neither by FTIR spectroscopy or TGA/DTG.

It is herein reported the use of two distinct PCL grades with different MW, for the shell formation, and its effect on the morphology, encapsulation content and shelf-life of the resulting MCs. Design of Experiments (software MODDE® Pro 13) was carried out to control and tune the size of the MCs, i.e. to develop a model that predicts the optimum value for predefined reactional parameters to produce MCs with a specific average size. After the process optimization, isocyanates of higher reactivity than IPDI, were possible to be encapsulated, by using PCL as the shell forming polymer. Moreover, MCs with a polymeric shell of PHB, that is not only biodegradable but also bioderived, were possible to be fabricated through a combination of solvent evaporation technique with the self-organized precipitation method. Finally, a lab scale-up of the process was carried out, corresponding to an increase in 5 times the initial reactional volume, which allowed to show that this is a simple process possible to be

implemented at the industrial level. It should be added that the infrastructure for the industrial fabrication of this type of MCs has been recently set at CIPADE S.A., main partner in the projects “ECOBOND” (POCI-01-0247-FEDER-017930) and “BEYOND ECOBOND” (POCI-01-0247-FEDER-046991), the main funders of this Ph.D. work.

Polycaprolactone’ molecular weight

PCL was the chosen polymer for the MCs’ shell formation due to its biodegradability, low melting point of 60°C, low melt viscosity and low glass transition temperature, of about -60 °C. These features enable the MCs to release the isocyanate not only by breakage but also by the melting of the shell, during the adhesive application.

Two PCL grades with different MW, of 45000 and 80000 Da, were used for the MCs’ shell formation. It was hypothesized that the MW might affect the final MCs characteristics, as it can have an impact on the polymer permeability and thermal/mechanical resistance. It was possible to obtain spherical, disaggregated, and core-shell MCs, using both PCL grades, by means of the solvent evaporation technique. The polymer MW has shown to have an impact on the MCs characteristics, with the 80000 Da PCL resulting in MCs with more 6 wt% of isocyanate and less 3 wt% of PUa formation after an ageing of 3 months. **The increased MW was responsible for improving the resistance to the water moisture diffusion as well as for providing a better encapsulation yield. However, it greatly increases the viscosity of the respective O phase. This brings difficulties to the MCs production process, leading to a low reproducibility, low production yield and bigger MCs and sizes distribution.** As the encapsulation content and shelf-life of the MCs obtained using PCL45 were quite similar to those obtained with the higher MW PCL, and their production is much more straightforward, this MW was selected as the most suitable for the current MCs production.

The solvent evaporation technique has shown to be a simple and efficient method for the encapsulation of isocyanate, enabling to obtain MCs only by physical means, due to the precipitation of the PCL, avoiding the reaction of the isocyanate to be encapsulated. As referred before, this process was patented, (PT 115312 B), and is now being industrially implemented at CIPADE, S.A. in the scope of the project “BEYOND ECOBOND”, POCI-01-0247-FEDER-046991.

The developed technology can be used as a technology platform for the encapsulation of other reactive hydrophobic species by means of a purely physical process, using biodegradable polymers.

Design of Experiment to control the microcapsules size

The solvent evaporation technique has shown to be a simple and reliable method to produce MCs containing encapsulated isocyanate. Despite the favorable characteristics of the resulting MCs, their average size of $326.39 \mu\text{m} \pm 157.26$ and a size distribution ranging from 96 to 685 μm is not adequate for the current application. Such large dimensions and size distribution are associated with a worse performance of the final adhesive formulation as it leads to a poor distribution of the MCs in the substrate to be adhered. With the aim of decreasing the MCs size, the MODDE® Pro 13 software was used, as a design of experiment tool, by applying the response surface methodology (RSM) with a central composite design (CCD), in particular the central composite face design (CCF). The variables in study were the GA and PVA concentrations and the O phase volume, which are known to influence the stability of emulsions. By controlling the size and stability of the emulsion it is possible to control the size of the final MCs, as they are formed by the dissolved polymer precipitation at the emulsion droplets' interface. **The optimum range for the average MCs size was defined to be between 70 μm to 80 μm , although MCs with a medium diameter of 100 μm can still be used for the application.**

By using the MODDE® Pro 13 software, it was possible to develop a model, considered to be statistically significant, with a R^2 of 0.973 and a Q^2 of 0.867, fit to be used to modulate and predict the synthesis outcome.

PVA concentration was in fact the most significant to control the average MCs sizes, as it is the one that has the most impact in the emulsion stability. The values for the tested variable were adjusted, and it was possible to obtain MCs with an average diameter between 76 and 94 μm .

Polymers used for the shell formation

The solvent evaporation technique was used to produce polymeric MCs with a PCL shell. It is a versatile technique that can be used with other polymers possible to be dissolved in a solvent with a boiling point lower than that of the emulsion' continuous phase. MCs with a PHB shell, which is not only a biodegradable but also a bioderived polymer, were also developed. This polymer is a PHA which has been used as substitutes to petroleum-based plastics due to its promising characteristics.

Although the synthesis of PCL MCs was already optimized, the process needed to be adapted for the PHB due to this polymer lower solubility. Chloroform was the only tested solvent able to dissolve the PHB, up to a maximum concentration of 10wt%. Due to the saturation of the O

phase, the PHB rapidly precipitates during the MCs fabrication process. **From the studied parameters, the PHB concentration, the mechanical stirring and, lastly, the PVA concentration were the ones having the most significant impact on the final MCs properties.** The first parameter is related to the precipitation phenomenon, while the last two are known to affect the emulsion stability. **MCs containing high loads of encapsulated content, up to 80 wt% were obtained.** However, the process to obtain this MCs is difficult to control, due to the quick precipitation of the PHB, which makes its industrial implementation a challenge by now.

Contributions:

- The use of a double emulsion system containing an O/O template for the encapsulation of water-sensitive species.
- The encapsulation of isocyanate through the solvent evaporation technique.
- The encapsulation of isocyanates by a biodegradable PCL shell.
- Development of a new model to tune the average sizes of the PCL MCs containing IPDI, by the solvent evaporation technique.
- Evaluation of the most statistically significant parameters on the emulsion stability and MCs average sizes.
- Adaptation of the solvent evaporation technique for the encapsulation of isocyanate by a biodegradable and bio-derived PHB shell.

Bibliography:

- 1 Li, M.;Rouaud, O.;Poncelet, D., *Microencapsulation by solvent evaporation: State of the art for process engineering approaches*. International Journal of Pharmaceutics, **2008**, 363, 26-39.
- 2 Aliabadi, H. M.;Elhasi, S.;Mahmud, A.;Gulamhusein, R.;Mahdipoor, P.;Lavasanifar, A., *Encapsulation of hydrophobic drugs in polymeric micelles through co-solvent evaporation: The effect of solvent composition on micellar properties and drug loading*. International Journal of Pharmaceutics, **2007**, 329, 158-165.
- 3 Teeka, P.;Chaiyasat, A.;Chaiyasat, P., *Preparation of Poly (methyl methacrylate) Microcapsule with Encapsulated Jasmine Oil*. Energy Procedia, **2014**, 56, 181-186.
- 4 Winkler, J. S.;Barai, M.;Tomassone, M. S., *Dual drug-loaded biodegradable Janus particles for simultaneous co-delivery of hydrophobic and hydrophilic compounds*. Experimental Biology and Medicine, **2019**, 244, 1162-1177.
- 5 Tang, S.;Yourdkhani, M.;Casey, C. M. P.;Sottos, N. R.;White, S. R.;Moore, J. S., *Low-Ceiling-Temperature Polymer Microcapsules with Hydrophobic Payloads via Rapid Emulsion-Solvent Evaporation*. ACS Applied Materials & Interfaces, **2017**, 9, 20115-20123.
- 6 Iqbal, M.;Valour, J.-P.;Fessi, H.;Elaissari, A., *Preparation of biodegradable PCL particles via double emulsion evaporation method using ultrasound technique*. Colloid and Polymer Science, **2015**, 293, 861-873.
- 7 Lamprecht, A.;Ubrich, N.;Pérez, M. H.;Lehr, C.;Hoffman, M.;Maincent, P., *Influences of process parameters on nanoparticle preparation performed by a double emulsion pressure homogenization technique*. International Journal of Pharmaceutics, **2000**, 196, 177-82.
- 8 Hwang, Y. M.;Pan, C. T.;Lin, Y.-M.;Zeng, S.-W.;Yen, C. K.;Wang, S.-Y.;Kuo, S. W.;Ju, S.-P.;Liang, S.-S.;Zong-Hsin, L., *Preparation of Biodegradable Polycaprolactone Microcarriers with Doxorubicin Hydrochloride by Ultrasonic-assisted Emulsification Technology*. Sensors and Materials, **2019**, 31, 301-310.
- 9 Iqbal, M.;Zafar, N.;Fessi, H.;Elaissari, A., *Double emulsion solvent evaporation techniques used for drug encapsulation*. International Journal of Pharmaceutics, **2015**, 496, 173-190.
- 10 Imbrogno, A.;Dragosavac, M. M.;Piacentini, E.;Vladisavljević, G. T.;Holdich, R. G.;Giorno, L., *Polycaprolactone multicore-matrix particle for the simultaneous encapsulation of hydrophilic and hydrophobic compounds produced by membrane emulsification and solvent diffusion processes*. Colloids and Surfaces B: Biointerfaces, **2015**, 135, 116-125.
- 11 Gürsel, I.;Hasirci, V., *Properties and drug release behaviour of poly(3-hydroxybutyric acid) and various poly(3-hydroxybutyrate-hydroxyvalerate) copolymer microcapsules*. Journal of Microencapsulation, **1995**, 12, 185-93.
- 12 Arjona, J.;Valenzuela-Díaz, F.;Wiebeck, H.;Hui, W.;Silva-Valenzuela, M., *Physical Properties of PHB/VMF2 Nanocomposite Microcapsules in Water*. Materials Science Forum, **2018**, 930, 190-194.
- 13 Cao, L.;Liu, Y.;Xu, C.;Zhou, Z.;Zhao, P.;Niu, S.;Huang, Q., *Biodegradable poly(3-hydroxybutyrate-co-4-hydroxybutyrate) microcapsules for controlled release of trifluralin with improved photostability and herbicidal activity*. Materials Science and Engineering: C, **2019**, 102, 134-141.
- 14 Arjona, J. C.;Silva-Valenzuela, M. G.;Wang, S. H.;Valenzuela-Díaz, F. R., *Biodegradable Nanocomposite Microcapsules for Controlled Release of Urea*. Polymers, **2021**, 13, 722.
- 15 Zernov, A. L.;Ivanov, E. A.;Makhina, T. K.;Myshkina, V. L.;Samsonova, O. V.;Feofanov, A. V.;Volkov, A. V.;Gazhva, J. V.;Muraev, A. A.;Ryabova, V. M.;Shaitan, K. V.;Ivanov, S.

- Y.;Bonartseva, G. A.;Bonartsev, A. P., *Microcapsules of poly(3-hydroxybutyrate) for sustained protein release*. *Sovremennye Tehnologii v Medicine*, **2015**, 7, 50-56.
- 16 Perignon, C.;Ongmayeb, G.;Neufeld, R.;Frere, Y.;Poncelet, D., *Microencapsulation by interfacial polymerisation: membrane formation and structure*. *Journal of Microencapsulation*, **2015**, 32, 1-15.
- 17 Lu, X.;Katz, J. S.;Schmitt, A. K.;Moore, J. S., *A Robust Oil-in-Oil Emulsion for the Nonaqueous Encapsulation of Hydrophilic Payloads*. *Journal of the American Chemical Society*, **2018**, 140, 3619-3625.
- 18 Zia, A.;Pentzer, E.;Thickett, S.;Kempe, K., *Advances and Opportunities of Oil-in-Oil Emulsions*. *ACS Applied Materials & Interfaces*, **2020**, 12, 38845-38861.
- 19 Meng, F.;Wang, S.;Wang, Y.;Liu, H.;Huo, X.;Ma, H.;Ma, Z.;Xiong, H., *Microencapsulation of oxalic acid via oil-in-oil (O/O) emulsion solvent evaporation*. *Powder Technology*, **2017**, 320, 405-411.
- 20 Loxley, A.;Vincent, B., *Preparation of Poly(methylmethacrylate) Microcapsules with Liquid Cores*. *Journal of Colloid and Interface Science*, **1998**, 208, 49-62.
- 21 Wang, Y.;Guo, B.-H.;Wan, X.;Xu, J.;Wang, X.;Zhang, Y.-P., *Janus-like polymer particles prepared via internal phase separation from emulsified polymer/oil droplets*. *Polymer*, **2009**, 50, 3361-3369.
- 22 Loureiro, M. V.;Vale, M.;Galhano, R.;Matos, S.;Bordado, J. C.;Pinho, I.;Marques, A. C., *Microencapsulation of Isocyanate in Biodegradable Poly(ϵ -caprolactone) Capsules and Application in Monocomponent Green Adhesives*. *ACS Applied Polymer Materials*, **2020**, 2, 4425-4438.
- 23 Ansari, T. H.;Hasnain, M.;Hoda, M. N.;Nayak, A. K., *Microencapsulation of pharmaceuticals by solvent evaporation technique: A review*. *Elixir Pharmacy*, **2012**, 47, 8821-8827.
- 24 Aberturas, M. R.;Molpeceres, J.;Guzmán, M.;García, F., *Development of a new cyclosporine formulation based on poly(caprolactone) microspheres*. *Journal of Microencapsulation*, **2002**, 19, 61-72.
- 25 Fournier, C. O.;Fradette, L.;Tanguy, P. A., *Effect of dispersed phase viscosity on solid-stabilized emulsions*. *Chemical Engineering Research and Design*, **2009**, 87, 499-506.
- 26 Liu, C. W.;Li, M. Z., *Effect of Dispersed Phase Viscosity on Emulsification in Turbulence Flow*. *Applied Mechanics and Materials*, **2014**, 446-447, 571-575.
- 27 Abbott, S., *Surfactant Science: Principles and Practice*. **2015**: DEStech Publications, Inc.
- 28 Briceño, M.;Salager, J. L.;Bertrand, J., *Influence of Dispersed Phase Content and Viscosity on the Mixing of Concentrated Oil-in-Water Emulsions in the Transition Flow Regime*. *Chemical Engineering Research and Design*, **2001**, 79, 943-948.
- 29 Wang, W.;Liu, D.;Lu, L.;Chen, H.;Gong, T.;Lv, J.;Zhou, S., *The improvement of the shape memory function of poly(ϵ -caprolactone)/nano-crystalline cellulose nanocomposites via recrystallization under a high-pressure environment*. *Journal of Materials Chemistry A*, **2016**, 4, 5984-5992.
- 30 Yu, X.;Wang, N.;Lv, S., *Crystal and multiple melting behaviors of PCL lamellae in ultrathin films*. *Journal of Crystal Growth*, **2016**, 438, 11-18.
- 31 Schindelin, J.;Arganda-Carreras, I.;Frise, E.;Kaynig, V.;Longair, M.;Pietzsch, T.;Preibisch, S.;Rueden, C.;Saalfeld, S.;Schmid, B.;Tinevez, J. Y.;White, D. J.;Hartenstein, V.;Eliceiri, K.;Tomancak, P.;Cardona, A., *Fiji: an open-source platform for biological-image analysis*. *Nat Methods*, **2012**, 9, 676-82.
- 32 Smith, B. C., *Infrared Spectral Interpretation: A Systematic Approach*. 1st ed. **1998**: CRC Press.
- 33 Smith, B. C., *The carbonyl group, part I: Introduction*. *Spectroscopy*, **2017**, 32, 31-36.
- 34 Delpech, M. C.;Miranda, G. S., *Waterborne polyurethanes: influence of chain extender in ftir spectra profiles*. *Central European Journal of Engineering*, **2012**, 2, 231-238.

- 35 Sánchez-González, S.;Diban, N.;Urriaga, A., *Hydrolytic Degradation and Mechanical Stability of Poly(ϵ -Caprolactone)/Reduced Graphene Oxide Membranes as Scaffolds for In Vitro Neural Tissue Regeneration*. *Membranes*, **2018**, *8*.
- 36 Krasowska, K.;Heimowska, A.;Morawska, M., *Environmental degradability of polycaprolactone under natural conditions*. *E3S Web of Conferences*, **2016**, *10*, 00048.
- 37 Wang, S. H.;Silva, L. F.;Kloss, J.;Munaro, M.;Souza, G. P.;Wada, M. A.;Gomez, J. G. C.;Zawadzki, S.;Akcelrud, L., *Polycaprolactone based biodegradable polyurethanes*. *Macromolecular Symposia*, **2003**, *197*, 255-264.
- 38 Blackwell, C. J., *Synthesis and Degradation of Biodegradable Polyurethanes*, in *Department of Chemistry*, **2016**, Doctor of Philosophy dissertation, Durham University.
- 39 Xiao, Y.;Wu, B.;Fu, X.;Wang, R.;Lei, J., *Preparation of biodegradable microcapsules through an organic solvent-free interfacial polymerization method*. *Polymers for Advanced Technologies*, **2019**, *30*, 483-488.
- 40 Siparsky, G. L., *Polymers from Renewable Resources*. 1st ed. **2001**: American Chemical Society.
- 41 França, D.;Bezerra, E.;Morais, D.;Araujo, E.;Wellen, R., *Hydrolytic and Thermal Degradation of PCL and PCL/Bentonite Compounds*. *Materials Research*, **2016**, *19*, 618-627.
- 42 Attaei, M.;Loureiro, M. V.;Vale, M.;Condeço, J.;Pinho, I.;Bordado, J. C.;Marques, A. C., *Isophorone Diisocyanate (IPDI) Microencapsulation for Mono-Component Adhesives: Effect of the Active H and NCO Sources*. *Polymers*, **2018**, *10*, 825.
- 43 Koh, E.;Kim, N.-K.;Shin, J.;Kim, Y.-W., *Polyurethane microcapsules for self-healing paint coatings*. *RSC Advances*, **2014**, *4*, 16214-16223.
- 44 Avella, A.;Mincheva, R.;Raquez, J. M.;Lo Re, G., *Substantial Effect of Water on Radical Melt Crosslinking and Rheological Properties of Poly(ϵ -Caprolactone)*. *Polymers*, **2021**, *13*, 491.
- 45 Loureiro, M. V.;Aguiar, A.;Santos, R. G. d.;Bordado, J. C.;Pinho, I.;Marques, A. C., *Design of Experiment for Optimizing Microencapsulation by the Solvent Evaporation Technique*. *Polymers*, **2024**, *16*, 111.
- 46 Taylor, C. J.;Pomberger, A.;Felton, K. C.;Grainger, R.;Barecka, M.;Chamberlain, T. W.;Bourne, R. A.;Johnson, C. N.;Lapkin, A. A., *A Brief Introduction to Chemical Reaction Optimization*. *Chemical Reviews*, **2023**, *123*, 3089-3126.
- 47 Taylor, C. J.;Baker, A.;Chapman, M. R.;Reynolds, W. R.;Jolley, K. E.;Clemens, G.;Smith, G. E.;Blacker, A. J.;Chamberlain, T. W.;Christie, S. D. R.;Taylor, B. A.;Bourne, R. A., *Flow chemistry for process optimisation using design of experiments*. *Journal of Flow Chemistry*, **2021**, *11*, 75-86.
- 48 Peris-Díaz, M. D.;Sentandreu, M. A.;Sentandreu, E., *Multiobjective optimization of liquid chromatography–triple-quadrupole mass spectrometry analysis of underivatized human urinary amino acids through chemometrics*. *Analytical and Bioanalytical Chemistry*, **2018**, *410*, 4275-4284.
- 49 Fu, F.;Hu, L., *Advanced High Strength Natural Fibre Composites in Construction*. **2017**: Woodhead Publishing.
- 50 Jankovic, A.;Chaudhary, G.;Goia, F., *Designing the design of experiments (DOE) – An investigation on the influence of different factorial designs on the characterization of complex systems*. *Energy and Buildings*, **2021**, *250*, 111298.
- 51 Kumari, M.;Gupta, S. K., *Response surface methodological (RSM) approach for optimizing the removal of trihalomethanes (THMs) and its precursor's by surfactant modified magnetic nanoadsorbents (sMNP) - An endeavor to diminish probable cancer risk*. *Scientific Reports*, **2019**, *9*, 18339.
- 52 Rajkumar, K.;Muthukumar, M., *Response surface optimization of electro-oxidation process for the treatment of C.I. Reactive Yellow 186 dye: reaction pathways*. *Applied Water Science*, **2017**, *7*, 637-652.

- 53 Wang, B.;Tian, H.;Xiang, D., *Stabilizing the Oil-in-Water Emulsions Using the Mixtures of Dendrobium Officinale Polysaccharides and Gum Arabic or Propylene Glycol Alginate*. *Molecules*, **2020**, 25, 759.
- 54 Niu, F.;Niu, D.;Zhang, H.;Chang, C.;Gu, L.;Su, Y.;Yang, Y., *Ovalbumin/gum arabic-stabilized emulsion: Rheology, emulsion characteristics, and Raman spectroscopic study*. *Food Hydrocolloids*, **2016**, 52, 607-614.
- 55 Huang, M.;Yang, J., *Facile microencapsulation of HDI for self-healing anticorrosion coatings*. *Journal of Materials Chemistry*, **2011**, 21, 11123-11130.
- 56 Costa, C.;Medronho, B.;Filipe, A.;Mira, I.;Lindman, B.;Edlund, H.;Norgren, M., *Emulsion Formation and Stabilization by Biomolecules: The Leading Role of Cellulose*. *Polymers*, **2019**, 11, 1570.
- 57 Walstra, P., *Physical Chemistry of Foods*. 1st ed. **2001**: CRC Press, Boca Raton.
- 58 Tamara, D. H.;Dokić, P.;Krstonošić, V.;Hadnađev, M., *Influence of oil phase concentration on droplet size distribution and stability of oil-in-water emulsions*. *European Journal of Lipid Science and Technology*, **2013**, 115, 313-321.
- 59 Taherian, A. R.;Fustier, P.;Ramaswamy, H. S., *Effect of added oil and modified starch on rheological properties, droplet size distribution, opacity and stability of beverage cloud emulsions*. *Journal of Food Engineering*, **2006**, 77, 687-696.
- 60 Mirhosseini, H.;Tan, C. P.;Hamid, N. S. A.;Yusof, S., *Optimization of the contents of Arabic gum, xanthan gum and orange oil affecting turbidity, average particle size, polydispersity index and density in orange beverage emulsion*. *Food Hydrocolloids*, **2008**, 22, 1212-1223.
- 61 Ye, G.;Ma, L.;Li, L.;Liu, J.;Yuan, S.;Huang, G., *Application of Box–Behnken design and response surface methodology for modeling and optimization of batch flotation of coal*. *International Journal of Coal Preparation and Utilization*, **2020**, 40, 131-145.
- 62 Davim, J. P., *Mechatronics and Manufacturing Engineering: Research and Development. From Woodhead Publishing Reviews: Mechanical Engineering Series*. 1st ed. **2016**: Woodhead Publishing.
- 63 Dennison, T. J.;Smith, J.;Hofmann, M. P.;Bland, C. E.;Badhan, R. K.;Al-Khattawi, A.;Mohammed, A. R., *Design of Experiments to Study the Impact of Process Parameters on Droplet Size and Development of Non-Invasive Imaging Techniques in Tablet Coating*. *PLoS One*, **2016**, 11, e0157267.
- 64 Akkaya, G. K.;Öden, M. K., *Optimization of the effect of copper electrodes on the removal efficiency of 4-chlorophenol from aqueous solution by electrocoagulation*. *Environmental Research and Technology*, **2022**, 5, 33-43.
- 65 Mateus, M. M.;Matos, S.;Guerreiro, D.;Debiagi, P.;Gaspar, D.;Ferreira, O.;Bordado, J. C.;Santos, R. G. d., *Liquefaction of almond husk for assessment as feedstock to obtain valuable bio-oils*. *Pure and Applied Chemistry*, **2019**, 91, 1177-1190.
- 66 Ferguson, P. D.;Shaw, R.;McCudden, A.;Elliot, C.;Welham, M.;McAlpine, V.;Castel, C.;Armstrong, T.;Yang, Q.;Qiu, W., *Improving Robustness of Pharmaceutical Dosage form Sample Preparation Using Experimental Design and Process Understanding Tools*. *Chromatographia*, **2020**, 83, 1525-1538.
- 67 Niaounakis, M., *Biopolymers: Applications and Trends*. 1st Edition ed. **2015**: Elsevier.
- 68 nova-Institute, OWS , Hydra Marine Science, IKT Stuttgart and Wageningen University & Research in cooperation with DIN CERTCO and TÜV Austria. *Biodegradable Polymers in Various Environments According to Established Standards and Certification Schemes*. **2021**; Available from: <https://renewable-carbon.eu/publications/product/biodegradable-polymers-in-various-environments-according-to-established-standards-and-certification-schemes-graphic-pdf/>.
- 69 Pettinari, M. J.;Egoburo, D. E., *Microbial Cell Factories Engineering for Production of Biomolecules*. 1st ed. **2021**: Elsevier.

- 70 Ushani, U.;Sumayya, A. R.;Archana, G.;Rajesh, B. J.;Dai, J., *Food Waste to Valuable Resources*. **2020**: Academic Press.
- 71 Pernicova, I.;Novackova, I.;Sedlacek, P.;Kourilova, X.;Kalina, M.;Kovalcik, A.;Koller, M.;Nebesarova, J.;Krzyzanek, V.;Hrubanova, K.;Masilko, J.;Slaninova, E.;Obruca, S., *Introducing the Newly Isolated Bacterium Aneurinibacillus sp. H1 as an Auspicious Thermophilic Producer of Various Polyhydroxyalkanoates (PHA) Copolymers-1. Isolation and Characterization of the Bacterium*. *Polymers*, **2020**, *12*, 1298.
- 72 McAdam, B.;Brennan, M. F.;McDonald, P.;Mojicevic, M., *Production of Polyhydroxybutyrate (PHB) and Factors Impacting Its Chemical and Mechanical Characteristics*. *Polymers*, **2020**, *12*, 2908.
- 73 Koller, M., *A Review on Established and Emerging Fermentation Schemes for Microbial Production of Polyhydroxyalkanoate (PHA) Biopolyesters*. *Fermentation*, **2018**, *4*, 30.
- 74 Adnan, M.;Siddiqui, A. J.;Ashraf, S. A.;Snoussi, M.;Badraoui, R.;Alreshidi, M.;Elasbali, A. M.;Al-Soud, W. A.;Alharethi, S. H.;Sachidanandan, M.;Patel, M., *Polyhydroxybutyrate (PHB)-Based Biodegradable Polymer from *Agromyces indicus*: Enhanced Production, Characterization, and Optimization*. *Polymers*, **2022**, *14*, 3982.
- 75 Altaee, N.;El-Hiti, G. A.;Fahdil, A.;Sudesh, K.;Yousif, E., *Biodegradation of different formulations of polyhydroxybutyrate films in soil*. *SpringerPlus*, **2016**, *5*, 762.
- 76 Mabrouk, M. M.;Sabry, S. A., *Degradation of poly (3-hydroxybutyrate) and its copolymer poly (3-hydroxybutyrate-co-3-hydroxyvalerate) by a marine *Streptomyces sp. SNG9**. *Microbiological Research*, **2001**, *156*, 323-335.
- 77 Tarazona, N. A.;Machatschek, R.;Lendlein, A., *Influence of Depolymerases and Lipases on the Degradation of Polyhydroxyalkanoates Determined in Langmuir Degradation Studies*. *Advanced Materials Interfaces*, **2020**, *7*, 2000872.
- 78 Zhang, S.;Campagne, C.;Salaün, F. *Influence of Solvent Selection in the Electrospraying Process of Polycaprolactone*. *Applied Sciences*, 2019. **9**, DOI: 10.3390/app9030402.
- 79 Terada, M.;Marchessault, R. H., *Determination of solubility parameters for poly(3-hydroxyalkanoates)*. *International Journal of Biological Macromolecules*, **1999**, *25*, 207-215.
- 80 Yabu, H.;Higuchi, T.;Ijiri, K.;Shimomura, M., *Spontaneous formation of polymer nanoparticles by good-solvent evaporation as a nonequilibrium process*. *Chaos: An Interdisciplinary Journal of Nonlinear Science*, **2005**, *15*, 047505.
- 81 Joye, I. J.;McClements, D. J., *Production of nanoparticles by anti-solvent precipitation for use in food systems*. *Trends in Food Science & Technology*, **2013**, *34*, 109-123.
- 82 Arita, T.;Kanahara, M.;Motoyoshi, K.;Koike, K.;Higuchi, T.;Yabu, H., *Localization of polymer-grafted maghemite nanoparticles in a hemisphere of Janus polymer particles prepared by a self-organized precipitation (SORP) method*. *Journal of Materials Chemistry C*, **2013**, *1*, 207-212.
- 83 Sun, Y.;Chai, X.;Han, W.;Farah, Z.;Tian, T.;Xu, Y.-J.;Liu, Y., *Pickering emulsions stabilized by hemp protein nanoparticles: Tuning the emulsion characteristics by adjusting anti-solvent precipitation*. *Food Hydrocolloids*, **2023**, *138*, 108434.
- 84 Kopinke, F. D.;Remmler, M.;Mackenzie, K., *Thermal decomposition of biodegradable polyesters—I: Poly(β -hydroxybutyric acid)*. *Polymer Degradation and Stability*, **1996**, *52*, 25-38.
- 85 Schröpfer, S.;Bottene, M. K.;Bianchin, L.;Robinson, L.;Lima, V.;Jahno, V.;Barud, H.;Ribeiro, S., *Biodegradation evaluation of bacterial cellulose, vegetable cellulose and poly (3-hydroxybutyrate) in soil*. *Polímeros*, **2015**, *25*, 154-160.
- 86 Ma, Y.;Zhang, Y.;Liu, X.;Gu, J., *Synthesis of isocyanate microcapsules as functional crosslinking agent for wood adhesive*. *The Journal of Adhesion*, **2021**, *97*, 38 - 52.
- 87 He, Z.;Jiang, S.;An, N.;Li, X.;Li, Q.;Wang, J.;Zhao, Y.;Kang, M., *Self-healing isocyanate microcapsules for efficient restoration of fracture damage of polyurethane and epoxy resins*. *Journal of Materials Science*, **2019**, *54*, 8262-8275.

- 88 Sun, D.;Chong, Y. B.;Chen, K.;Yang, J., *Chemically and thermally stable isocyanate microcapsules having good self-healing and self-lubricating performances*. Chemical Engineering Journal, **2018**, 346, 289-297.
- 89 Yi, H.;Yang, Y.;Gu, X.;Huang, J.;Wang, C., *Multilayer composite microcapsules synthesized by Pickering emulsion templates and their application in self-healing coating*. Journal of Materials Chemistry A, **2015**, 3, 13749-13757.

Supplementary Information

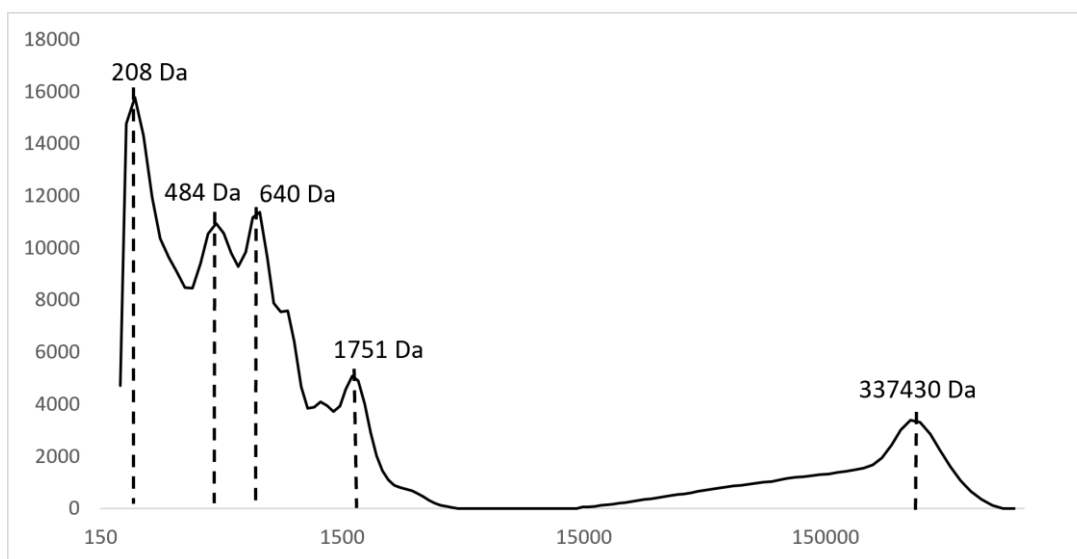


Figure V. S 1. Gel permeation chromatogram of the PHB.

Table V. S1. GPC results for the PCL polymers with 45000 Da and 80000 Da and for the I_45 and I_80 MCs' shell.

Sample	Mn [kDa]	Mw [kDa]	Mp [kDa]	PDI
PCL45	2.7	19.9	16.20	7.17
PCL80	2.6	35.7	82.00	13.85
I_45	2.1	17.8	86.60	8.57
I_80	2.8	44.6	82.77	15.50

Table V. S2. Preliminary peeling strength test results of adhesive bonds adhered using the I_45 and I_80 MCs as cross-linkers.

Cross-linker added to the OH Pre-polymer	Av load per unit width of the bond (N/mm)	Adhesive system
IPDI	2.15	2K
Microencapsulated IPDI (I_45 MCs)	2.21	1K
Microencapsulated IPDI (I_80 MCs)	2.20	1K

Table V. S3. Coefficients of model #1 and its statistical significance.

Variable	Coeff. SC	Std. Err.	p-value
β_0	329,128	172,679	0,0983
x_1	-49,0026	127,613	0,7123
x_2	-13,588	127,613	0,9181
x_3	19,547	127,613	0,8825
x_1^2	-68,4966	246,542	0,7891
x_2^2	-131,784	246,541	0,6095
x_3^2	-56,0187	246,541	0,8267
x_1x_2	19,9966	142,676	0,8926
x_1x_3	13,2912	142,676	0,92839
x_2x_3	-0,2333	142,676	0,99868
	N=17	Q ² =-0,605	
	DF=7	R ² =0,164	
	RSD = 403,5	R ² adj.=-0,911	

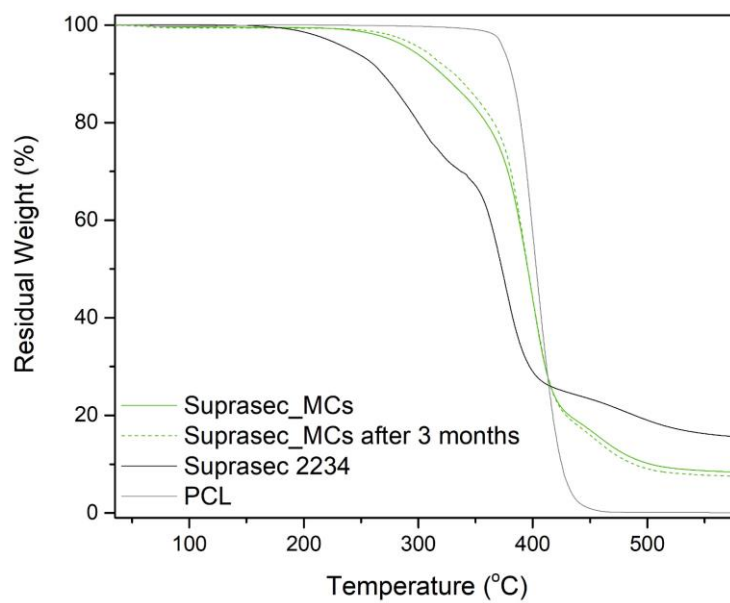


Figure V. S2. Thermogram of the PCL MCs containing encapsulated Suprasec[®]2234, Suprasec_MCs, after the synthesis and aged (by 3 months at room temperature and 60wt% of relative humidity), as well as of the Suprasec[®]2234 and PCL.

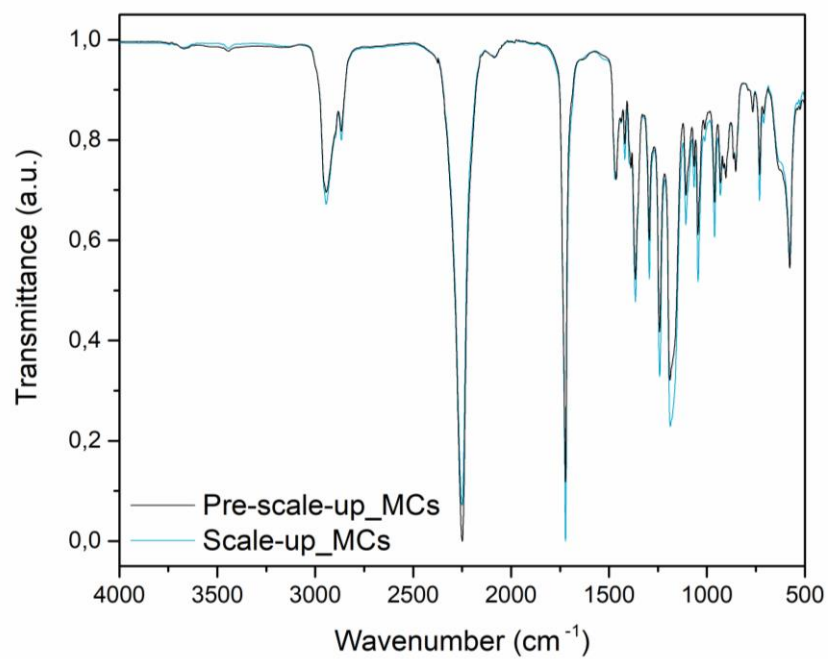


Figure V. S3. FTIR-ATR spectra of the PCL MCs, containing encapsulated IPDI, obtained in the pre-scale-up process and in the scale-up.

Chapter VI

Adhesive Development

Chapter VI - Adhesive development

This chapter exposes the development of PU and PCP adhesive formulations containing the MCs as cross-linkers. Due to the presence of organic solvents in the pre-polymer compositions, the study of the MCs chemical resistance to dissolution is essential, to conclude regarding the viability to develop 1K or 2K adhesive formulations. The capability of the MCs to act as cross-linkers, i.e. its response to the stimulus applied during the adhesive joint preparation and its effect on the final bondline, is also described. Optimization studies regarding the optimal concentration of MCs in the new PU and PCP adhesive formulations are here exposed, which enables to conclude regarding the most promising adhesive formulation.

VI.1 Adhesives testing and characterization

The developed MCs are to be used as cross-linkers for new PU and PCP adhesive formulations. In addition to the MCs characterization, the testing of the new adhesive enables to confirm the MCs adequacy for the application. For that purpose, the adhesive joints were subjected to both a peeling strength test and a temperature resistance test when submitted to constant force herein referred as creep test. These experiments were carried out at the facilities of CIPADE S.A. (S. João da Madeira - Portugal) according to their current procedures to test adhesive joints. Two different pre-polymers were tested for the development of the new adhesive formulation, namely Ciprene®2000, a PCP pre-polymer, and Plastik® 6275, a PU pre-polymer, both kindly supplied by CIPADE S.A. The adhesive containing the MCs as cross-linkers was always compared to the adhesive prepared with the same non-encapsulated isocyanate, respective benchmark (non-encapsulated commercial isocyanate), as well as with the adhesive pre-polymer without any isocyanate (without cross-linker). The main characteristics of the pre-polymers and isocyanates used for the testing are described in Table VI.1.

Table VI.1. PU and PCP pre-polymers, as well as isocyanate cross-linkers (to be encapsulated and benchmark) used in the development of the new adhesive formulation.

Classification	Chemical	Commercial name	NCO content (%)	Isocyanate Properties	Supplier
Adhesive pre-polymers	PCP base	CIPRENE® 2000	-	-	CIPADE S.A.
	PU base	PLASTIK® 6275	-	-	CIPADE S.A.
Cross-linkers	MDI	Suprasec® 2234	15.9	Pre-polymeric MDI	CIPADE S.A.
	TDI	Desmodur® RC	7.0 ± 0.2	Poly-isocyanurate of TDI (35%) in ethyl acetate	CIPADE S.A.
	IPDI	Desmodur® I	≥ 37.5	Aliphatic diisocyanate	Covestro AG
	MDI	Ongronat® 2500	30-32	Oligomeric MDI	BorsodChem

It should be referred that Suprasec® 2234 is the commercial cross-linker typically used with Ciprene® 2000 and Desmodur® RC the one used with Plastik® 6275, both at a concentration of 2.5 wt%.

To calculate the quantity of MCs to be added to the formulation, the amount of encapsulated isocyanate, previously determined by TGA, was considered and not the total weight of the MCs.

The specimens used for the testing were composed of two Neolite substrates, an artificial substitute to leather which is widely used in the footwear industry, with 13 cm × 3 cm, glued together in an area of 10 cm × 3 cm. The substrates were subjected to a mechanical carding previously to the joint preparation and, for the ones prepared with Plastik® 6275 an additional chemical treatment of halogenation, with the solution 2190 Halinov (CIPADE S.A.), was also necessary. The adhesive formulation, composed by the pre-polymer and cross-linker, which were previously mixed together, was applied in both substrates with a brush and allowed to dry for 15 minutes at room temperature. Posteriorly, the substrates prepared with CIPRENE® 2000 were pressed together at 4 bar for 10 seconds, while the ones prepared with Plastik® 6275 (PCP base) required an additional activation processed by IR radiation at 70 °C for 6 seconds, using a heat activator. The adhesive joints were stored for 7 days in standard conditions (23 °C, 50% RH) to ensure the complete cure of the adhesive.

The process for the adhesive joint preparation, using Plastik® 6275, is depicted in Figure VI.1.



Figure VI.1. Photographs of the several steps involved in the adhesive joint preparation: (a) adhesive dispersion in the substrate, (b) drying, (c) reactivation and (d) pressing.

VI.1.1 Peeling strength test

The peeling strength test was performed to measure the adhesive strength of the bond, as the peel strength is the mechanical force per unit width required to separate two bonded materials. The strength was calculated during the test by dividing the average force by the unit width of the bonded samples. This test was performed at the CIPADE S.A. facilities using an Instron 5566 universal testing machine and following the ISO 20344:5.2 norm, at a constant speed of 1 cm/min and an angle of 180°. In addition to the peel strength, the type of bond failure was also evaluated. As previously referred, there are three primary types of bond failure, i.e adhesive, cohesive, and at the substrate. Adhesive failure occurs when the adhesive loses the adhesion from one of the bonded surfaces, cohesive failure occurs due to the breakdown of the intermolecular bondings within the adhesive and, finally, the substrate failure occurs when the strength of the adhesive bond exceeds the strength of the substrate itself, leading to the substrate damage.

VI.1.2 Creep test

This test measures the adhesive resistance to temperature, which is a manifestation of the adhesive cross-linking. The test was performed at CIPADE S.A. facilities, using a climatic chamber heat activator from Aralab (Portugal, Rio de Mouro). For that, one of the unbonded ends of the specimen was fixed on the cabinet of the oven, and the other unbonded end was loaded with a

force of 2.94N, as depicted in Figure VI.2. The creep test was performed in a controlled environment at a starting temperature of 60 °C at which the samples were subjected for 2 hours. After this period, the displacement, in centimeters (cm), of the sample was measured. For the samples that did not open completely, the same procedure was repeated at 70 °C and, posteriorly, at 80 and 90 °C. A lower displacement represents a better adhesive joint resistance to temperature, which is a sign of a more effective cross-linking.



Figure VI.2. Specimen under the creep test, in the climatic chamber.

VI.2 MCs solvent resistance and behavior in the adhesive pre-polymer

The MCs resistance to solvents was studied to assess the viability to develop a mono-component adhesive. Due to the solvents present in the pre-polymer composition, it is of great importance to guarantee that the MCs' shell is not prone to dissolve in their presence, which would lead to the undesired contact between the isocyanate and the pre-polymer before the adhesive joint preparation, while still inside the container.

The MCs were submersed in each one of the solvents, that make part of the pre-polymer's composition, for one week at room temperature. After 24h, 96h and 168h of immersion, a sample of MCs was obtained by filtration and evaluated by ATR-FTIR. The dissolution of the MCs' polymeric shell leads to the loss of isocyanate core content, with a consequent decrease in the intensity of the NCO stretching peak in the FTIR spectrum. The MCs resistance to each solvent over the period of one week, was followed by the Y value, with the decreasing of its value meaning the dissolution of the polymeric shell.

In addition, the same procedure was followed with water. This would enable to conclude regarding the MCs' shell hydrophobicity, which is of great importance for the MCs' storage due to the possibility of water diffusion from air humidity towards their inside. For this case, the encapsulated isocyanate does not decrease due to its leaching, but by its reaction with water, forming urea moieties.

Table VI.2 describes the properties of the solvents used to test the MCs' shell chemical resistance.

Table VI.2. Solvents used to test the chemical resistance of the developed MCs, their purity and manufacturer.

Classification	Chemical	Commercial name	Purity	Manufacturer
Solvent	Acetone	-	99.7%	JMGS
	Toluene	-	100%	VWR Chemicals
	Hexane	-	95%	Fisher Chemical
	Ethyl acetate	-	99.99%	Fisher Chemical

The MCs resistance to solvents was studied both on the MCs obtained by interfacial polymerization technique (Ongronat[®]2500_MCs, Suprasec[®]2234_MCs and Desmodur[®]RC_MCs) as on the MCs obtained by solvent evaporation (PCL_MCs, PHB_MCs and PCL/PHB_MCs), all containing IPDI as core content. Three different PUa MCs were tested, obtained using different isocyanates for the shell formation, namely Ongronat[®]2500, Suprasec[®]2234 and Desmodur[®]RC, with the results displayed in Figure VI.3. All the MCs were affected by the solvents, with acetone and ethyl acetate showing a more aggressive effect, for all cases, evidenced by the more significant decrease of the MCs' Y value when submerged in these solvents. For the MCs with a shell made from Desmodur[®]RC, toluene had an effect identical to that of ethyl acetate.

MCs obtained with Ongronat[®]2500 seem to have a better chemical resistance to the tested solvents and also to the water diffusion. Although the solvent resistance exhibited by them is not enough to develop a mono-component adhesive, the increased resistance to water diffusion is associated with a longer shelf-life. Indeed, this it is in accordance with the results exposed in Chapter IV.

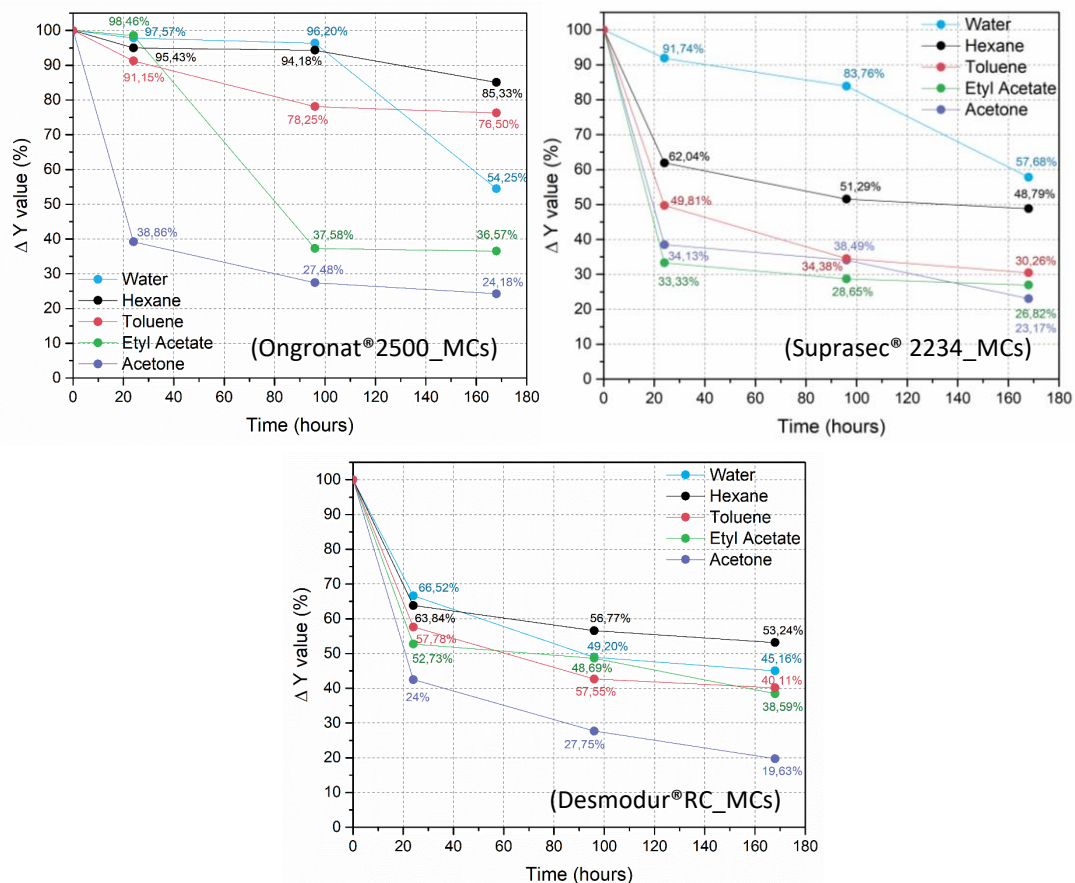


Figure VI.3. Ongronat_MCs, Suprasec®2234_MCs and Desmodur®RC_MCs Y value variation over 180h, while submerged in organic solvents and water.

Figure VI.4 displays the results of the PCL, PHB and PCL/PHB MCs resistance both to solvent dissolution and to water diffusion through the shell. All the MCs were severely affected by the solvents with the PCL MCs showing a complete dissolution in acetone and toluene in 24h. Indeed, it has been reported a great PCL solubility in chlorinated hydrocarbons, polar solvents, and in most aromatic solvents [1, 2]. Although PHB shows a better solvent resistance it is far less than that showed by the PUa MCs, and therefore not enough to develop a mono-component adhesive. On the other hand, PCL MCs showed an excellent resistance to water diffusion, outstanding all the studied MCs, which explains their superior shelf-life. Although polyesters are prone to suffer from hydrolysis in the ester bond, it is only when in a living environment, due to enzymatic degradation [3]. It is possible to occur chemical hydrolysis in an aqueous sterile medium, however only in a small extent and it usually requires the presence of an external catalyst [4, 5]. The obtained results are in accordance with the literature. *Bagheri A. R. et al.* reported on a higher biodegradability of PHB comparing to PCL, when immersed in both seawater and freshwater [6]. Also, PCL, when compared to other polyesters, including PHA, has the lowest oxygen to carbon ratio, which is an indicator of a higher hydrophobicity [7, 8].

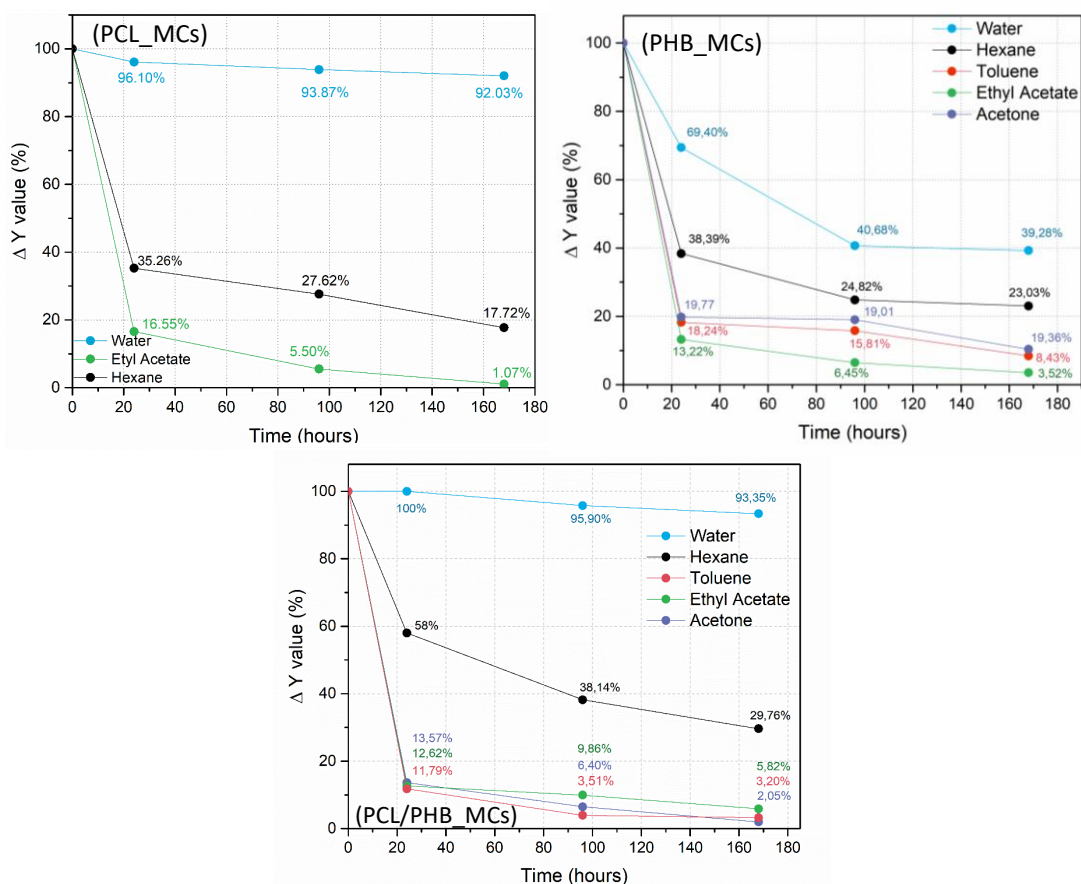


Figure VI.4. PCL_MCs, PHB_MCs and PLC/PHB_MCs Y value variation over 180h, while submerged in organic solvents and water.

The chemical resistance of the MCs in the adhesive pre-polymers was also tested, both in PU (Ciprene®2000) and in PCP (Plastik® 6275), exposed in Figure VI.5. For that purpose, the MCs were added to the pre-polymer at the commercial cross-linker concentration, and its viscosity was measured over a one-week period. In case of MCs' dissolution, the isocyanate is released and enters in contact with the pre-polymer, leading to cross-linking reactions and viscosity increase of the mixture. Although the chemical resistance of the MCs' shell was already assessed in each of the solvents, it is also important to study its resistance to the solvents combination and concentrations present in the pre-polymer composition.

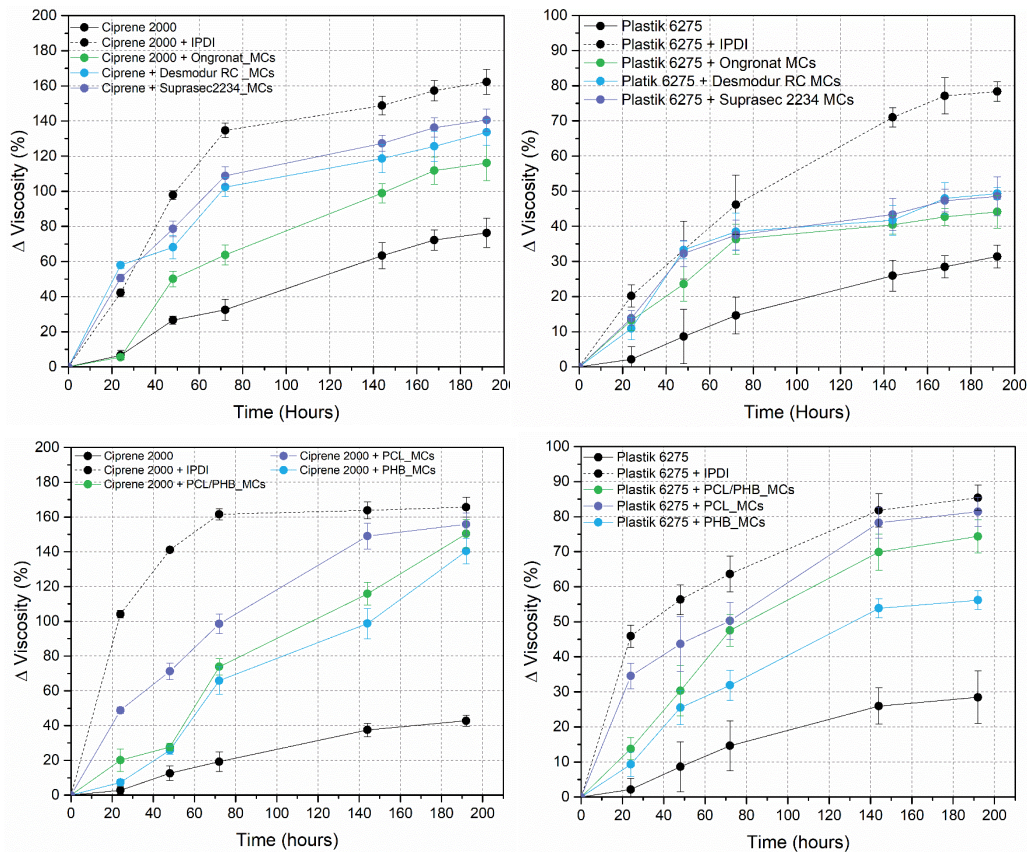


Figure VI.5 Viscosity variation, over 190 hours, of the Plastik®6275 and Ciprene®2000, containing PU/PUa, PCL or PHB MCs, to evaluate the MCs resistance in the adhesive pre-polymers.

Ciprene® 2000 is more aggressive to the PUa MCs' shell than Plastik® 6275, in general, with the Ongronat® MCs leading to the lower viscosity increase, indicating a better chemical resistance. The MCs produced using the solvent evaporation technique seem to be more prone to be affected by the pre-polymers, leading to identical results in both Plastik® 6275 and Ciprene® 2000. PCL MCs are the ones leading to the higher viscosity increase of the pre-polymer, which is in line with the low chemical resistance to solvents, such as acetone and toluene, exhibited above. PHB has a better chemical resistance than PCL, with both the PHB and PCL/PHB MCs showing a lower viscosity increase. These results are all in accordance with the ones obtained from the MCs immersion directly in the solvents. To conclude, the chemical resistance observed, even in the best performing MCs, namely the Ongronat®2500_MCs, is not high enough for the development of a mono-component adhesive with an acceptable shelf-life. On the other hand, these MCs display an acceptable shelf-life when not in direct contact with the solvents existent in the adhesive pre-polymer. Therefore, it is suggested to mix the MCs with the pre-polymer before the application, which successfully addresses the main goal of this work: protection of the workers from isocyanates, together with the achievement of high-performing adhesive joints.

VI.3 MCs effectiveness as cross-linkers

In the footwear industry, to guarantee the durability of the product, the adhesive joints must meet certain specifications regarding the minimum values obtained in the peel strength test, regardless of the type of substrate. These depend on the type of footwear, age and gender of the end user, accordingly with the Table II.2, on Chapter II. For casual footwear, the peel strength must be higher than 3 N/mm.

For the MCs to be considered effective cross-linkers it is mandatory that the encapsulated isocyanate is released during the adhesive joint preparation, by the effect of pressure (4 kg/cm²) and/or by the effect of temperature (70 °C) applied in the adhesion process, otherwise the cross-linking of the pre-polymer, required for high-performing adhesive joints, does not occur.

The size of the MCs has an important impact on the adhesive joint quality, in particular due to the homogeneity of the adhesive distribution on the substrate. Bigger sized MCs or MCs that tend to aggregate in the pre-polymer display a poorer distribution on the substrate, as shown in Figure VI.6, where the white regions represent a higher concentration of MCs. Bigger sized MCs can also have a negative effect on the appearance of the adhered substrates, especially for thin and flexible materials.



Figure VI.6. Photographs exposing an improper adhesive distribution on the substrate.

The amount of encapsulated isocyanate can also affect the adhesive joint quality, as a lower content imposes the need of a higher concentration of MCs in the pre-polymer to guarantee that the isocyanate concentration is the required one (2.5wt%).

Three different isocyanates were encapsulated throughout this work, namely Suprasec® 2234, IPDI and Ongronat® 2500. The cross-linking efficiency of each one was considered for both the PU and PCP pre-polymers and was compared with the respective benchmark, when applicable. Table VI.3 compiles the peel strength test results obtained for all the cross-linkers, at the commercial concentration in the pre-polymer (2.5 wt% of absolute isocyanate value). However, instead of the usual protocol which stipulates that the opening should occur after 48h from the bonding, the substrates were only opened after a curing time for one week, due to the lower IPDI reactivity. The obtained results show that, by increasing the cross-linking time to one week, the IPDI can lead to results similar to the benchmark isocyanates in the peeling strength tests. Particularly for Ciprene® 2000, the results obtained with both IPDI and Ongronat® 2500 were very satisfactory. For the Plastik® 6275 these isocyanates led to results slightly lower than the benchmark (non-encapsulated Desmodur®RC), nevertheless superior to the 3 N/mm required for casual footwear. Having these results into consideration, both IPDI and Ongronat® 2500 the isocyanates were the isocyanates considered for this application.

Table VI.3. Peel strength test results obtained for the IPDI, Ongronat®2500 and respective benchmarks, at 2.5 wt%, in both the PU and PCP pre-polymers.

Cross-linker	Pre-polymer	Peel strength per unit width (N/mm)
-		4.95
Suprasec® 2234	Ciprene® 2000	4.70
IPDI		5.68
Ongronat® 2500		5.24
-		4.83
Desmodur® RC	Plastik® 6275	4.89
IPDI		4.22
Ongronat® 2500		4.36

Figure VI. 7 relates to the peel strength test results obtained with PUa MCs containing Suprasec® 2234 (shell made with Desmodur® RC) and IPDI (shell made with Ongronat® 2250), using the Ciprene® 2000 as pre-polymer. It is to notice that the specimens prepared with IPDI_MCs were opened 48 hours after their preparation, instead of the required 1 week, which explains the low N/mm values. Nevertheless, the similar results obtained with encapsulated and non-encapsulated IPDI indicate that the MCs were able to release the content during the adhesive application, leading to cross-linking reactions in the pre-polymer. On the opposite, the significantly lower value obtained with the encapsulated Suprasec® 2234, comparing with its

non-encapsulated form, indicates that the MCs were not able to release its content. Several attempts were made to obtain more responsive Suprasec® 2234 containing MCs, however with no better results. This is due to the very stiff MCs that are obtained when encapsulating this isocyanate. They are not able to break, melt, at the conditions used for the adhesive joint preparation, employed in the footwear industry. Confirming this fact, Figure VI.8 reveals the presence of intact Suprasec 2234_MCs in the adhesive joint after its opening in the peel strength test.

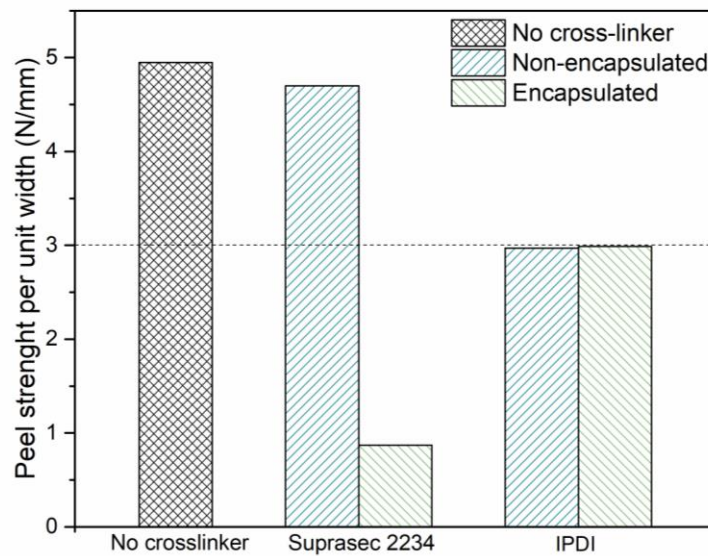


Figure VI. 7. Peel strength test results obtained with PU/PUa MCs containing Suprasec® 2234 and IPDI, at 2.5wt% in the CIPRENE® 2000 pre-polymer.

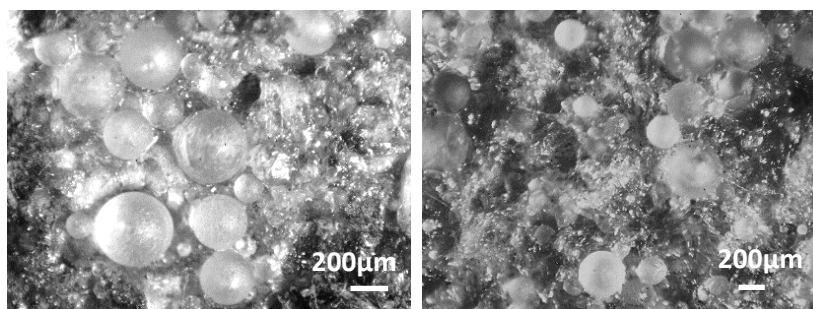


Figure VI.8. Optical microscopy photographs depicting intact Suprasec 2234_MCs in the adhesive joint, after its opening in the peel strength test.

Table VI. 4 exposes the results obtained in the creep test. In accordance with the peeling strength tests, the Suprasec®2234_MCs led to significantly distinct results to its non-encapsulated form, indicating that no significant cross-linking of the pre-polymer has occurred. When comparing with the sample prepared with no cross-linker it can be conclude that these

MCs had a negative contribution to the adhesive joint, worsening the adhesive joint performance. On the contrary, the IPDI_MCs only showed a significant displacement at 90 °C, and a full opening of the specimen at 100 °C. It is to refer that these samples were tested one week after their preparation, stressing the importance of the curing time for this isocyanate. When given enough time, IPDI can lead to a well cross-linked adhesive with good resistance to temperature.

Table VI. 4. Results obtained in the creep tests for substrates adhered with the pre-polymer and adhesive formulations containing Suprasec®2234 and IPDI as crosslinkers, as well as MCs with the encapsulated isocyanates, using Ciprene® 2000 as pre-polymer.

Crosslinker	d (cm) 50°C	d (cm) 60°C	d (cm) 70°C	d (cm) 80°C	d (cm) 90°C	d (cm) 100°C
-	0.2	6.7	FO	--	--	--
Suprasec® 2234	0	0	0	0	0	0
IPDI						--
IPDI_MCs	0	0	0.3	0.9	2.6	FO
Suprasec®2234_MCs	0.1	FO	--	--	--	--

Regarding the PCL MCs, their initial big dimensions, with a large size distribution, of $326,39 \mu\text{m} \pm 157,26$, led to a poor distribution of the MCs in the substrate, as can be seen in Figure VI.6. However, after several optimization trials carried out in this work, the size and size distribution of this MCs were decreased, improving its performance in the adhesive formulation. Figure VI.9 displays images of the substrates in which it was applied a formulation with 5wt% of PCL MCs (a) and PHB MCs (b), both containing IPDI, showing a homogeneously dispersed adhesive.

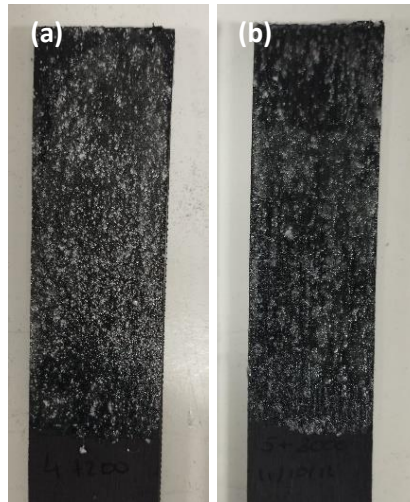


Figure VI.9. Photographs of substrates with a homogeneously dispersed adhesive. Formulation with 5wt% of PCL MCs (a) and 5wt% of PHB MCs (b), both containing IPDI.

Figure VI.10 exposes the peel strength test results obtained with PCL and PHB MCs, in the Ciprene® 2000 and the Plastik® 6275 pre-polymers. It is to notice that, for the adhesive joints prepared with Ciprene® 2000 only the stimulus of pressure contributed for the isocyanate release from the MCs, while for the joints prepared with Plastik® 6275 both the stimuli of pressure and temperature (reactivation at 70 °C) were applied. For all the tests there were achieved peel strength values above the 3 N/mm required in the industry for casual footwear.

For Ciprene®2000 the impact of the MCs on the adhesive joints is evident, as the specimens with MCs exhibit lower peel strength values than those with no-encapsulated isocyanates. In Figure VI.11 are exposed the opened bondlines, after the peeling strength tests, adhered with Ciprene® 2000 and PCL MCs as cross-linkers. Most of the Ongronat_MCs are still intact, indicating that they were not able to release the isocyanate during the specimen preparation. The shell of the Ongronat_MCs is composed not only by PCL but also some PUa, due to the reaction between this isocyanate and the water during the MCs' fabrication process. This leads to a PCL/PUa shell, which might have difficult the MCs breakage at the 4 bar applied during the specimens preparation. Regarding the IPDI_MCs, the majority seem to be broken, indicating that the applied pressure is enough to trigger its isocyanate release.

Plastik® 6275 pre-polymer led to far better results. For this case, both the specimens prepared with IPDI and Ongronat®2500 MCs resulted in very satisfactory results, of a peel strength above 5 N/mm. PCL is a low temperature responsive polymer, with a melting temperature lower than that used in the adhesion process, during the reactivation process, which contributes to the

isocyanate release. To study the PCL ability to respond to the conditions used during the reactivation, a sample of MCs was submitted to the process and its melting was confirmed, Figure VI. S1 from Supplementary Information. By comparing the bondlines of the specimens prepared with both the pre-polymers and the Ongronat_MCs as crosslinkers, it is clear the effect of the temperature on this MCs' responsiveness. For the bondline prepared with Plastik® 6275 the MCs can barely be detected, indicating its melting during the adhesive joint preparation, exposed in Figure VI.12.

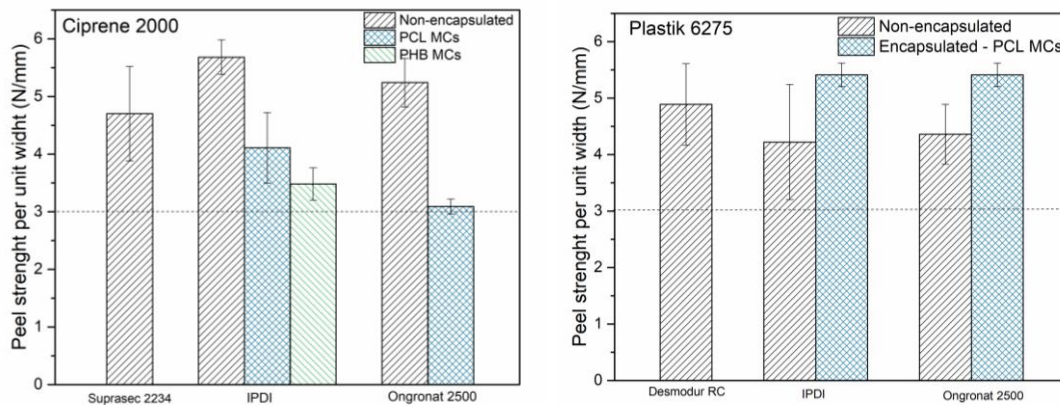


Figure VI.10. Peel strength test results obtained with PCL and PHB MCs in both the CIPRENE® 2000 (left) and the Plastik® 6275 (right) pre-polymers, at 2.5wt%.

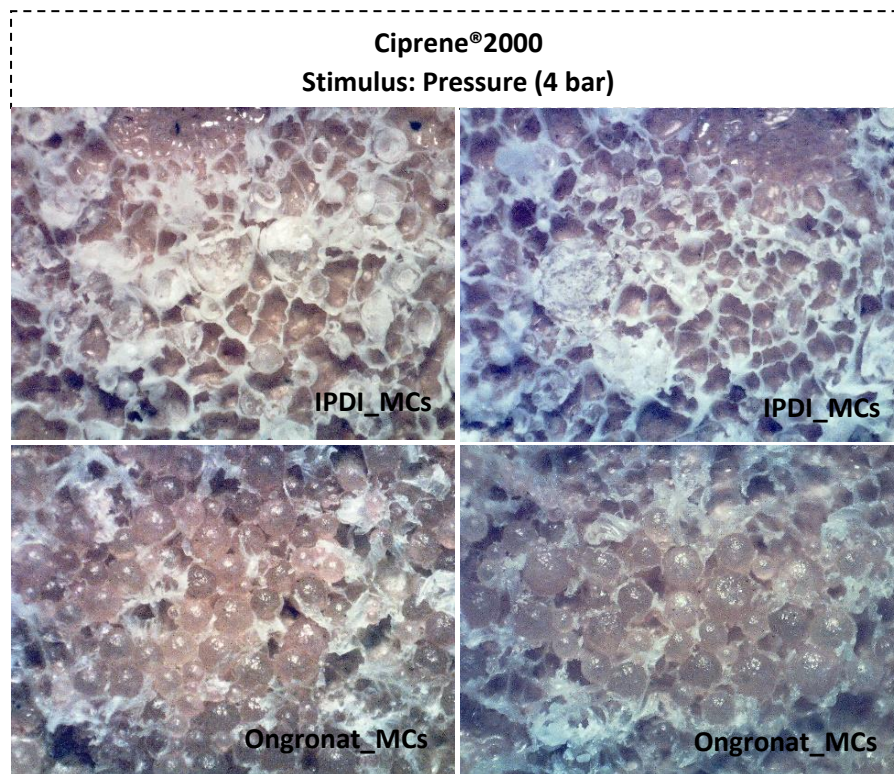


Figure VI.11. Photographs of the opened bondlines, after the peeling strength tests, using Ciprene® 2000 and PCL MCs, containing IPDI or Ongronat®2500, as cross-linkers.

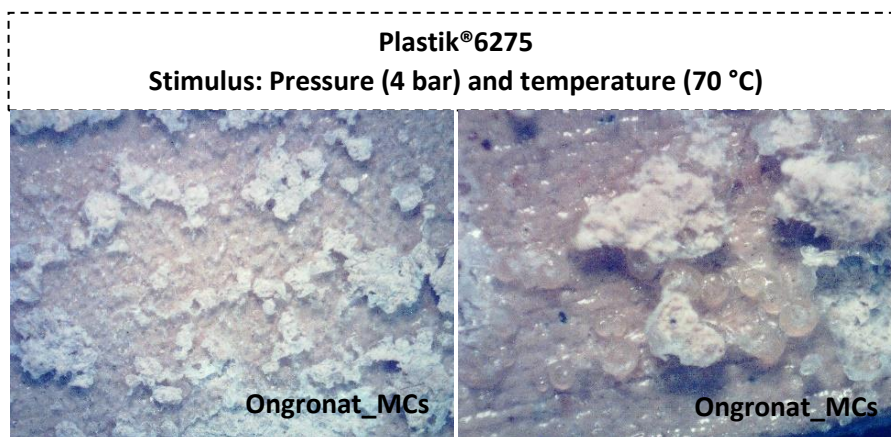


Figure VI.12. Photographs of the opened bondlines, after the peeling strength tests, using Plastik® 6275 and PCL MCs, containing Ongronat® 2500, as cross-linker.

VI.4 Optimization of the final adhesive

The developed MCs are to substitute the isocyanate cross-linkers typically used in PU and PCP adhesives and not only are they a different type of cross-linker agent, but the encapsulated isocyanate is also distinct from the ones commercially used. Different concentrations of both PCL and PHB MCs were tested as cross-linkers, aiming at optimizing the ideal concentration in the adhesive formulation. Figure VI.13, shows the peel strength test results obtained using both Ciprene® 2000 and Plastik® 6275 as pre-polymers.

Both IPDI and Ongronat® 2500 led to a high peel strength of the adhesive joints when added at the same concentration as the commercially used cross-linker. For Plastik® 6275 the adhesive peel strength improves with the increase of IPDI in the formulation. Contrarily, for Ciprene® 2000 the strength of the adhesive joint seems to decrease for higher isocyanate concentrations. This can be attributed to an excess of free NCO groups in the formulation, which can increase too much the cross-linking density, affecting the adhesion performance [9, 10].

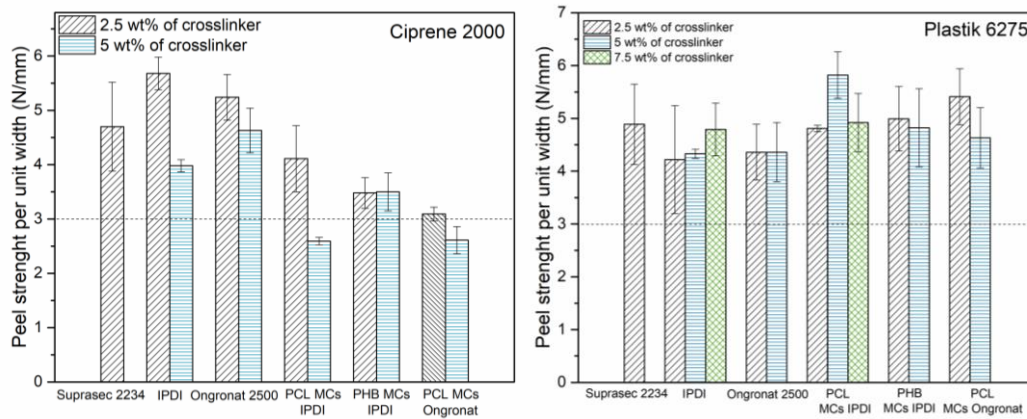


Figure VI.13. Peel strength test results using adhesive formulations with different concentrations of MCs, both with Ciprene® 2000 (left) and Plastik® 6275 (right) as pre-polymers.

For adhesive formulations using Ciprene® 2000, the MCs had a negative effect in the adhesive joint properties. The specimens adhered using MCs as cross-linkers have lower peeling strengths values and the higher the concentration of MCs, the poorer the adhesion. Nonetheless, almost all the samples prepared with IPDI containing MCs had peel strength values above the required 3 N/mm and a cohesive type of failure, or a mixture of cohesive with adhesive (Figure VI.14). The specimens prepared with Ongronat_MCs, barely led to the required 3N/mm when at 2.5%, leading to lower values for higher concentrations of MCs.

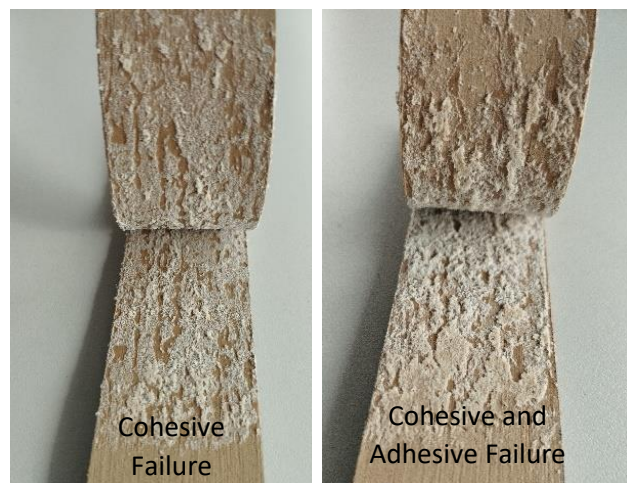


Figure VI.14. Photographs depicting a cohesive (left) and mixture of cohesive with adhesive type of failure (right). Substrates previously adhered with IPDI_MCs as cross-linkers in Ciprene® 2000.

All the substrates adhered using Plastik® 6275 resulted in peeling strength values well superior to 3 N/mm. Plastik®6275 is a high-strength bonding adhesive leading to a cohesive or substrate type of failure, even for the specimens adhered with no cross-linkers (Figure VI. 15). The

substrates prepared with MCs led to peel strength values higher than the specimens prepared with the same non-encapsulated isocyanates. Nevertheless, there seems to be a concentration threshold above which the negative effect of the MCs in the bondline seem to surpass the benefits of adding more cross-linker. For the IPDI_MCs its presence at 5 wt% led to the best results and, for both the PHB_MCs and Ongronat_MCs, the commercially used 2.5 wt% is the most favorable concentration.

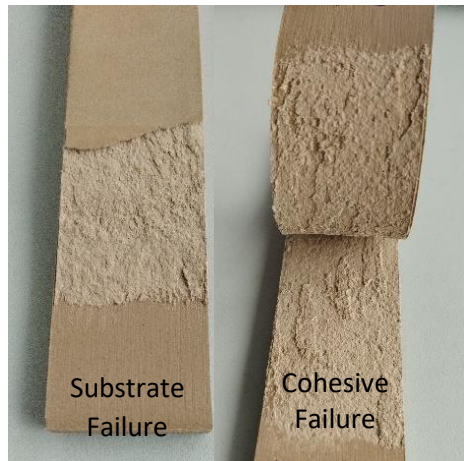


Figure VI. 15. Photographs depicting a substrate (left) and a cohesive type of failure (right). Substrates previously adhered with IPDI_MCs as cross-linkers in Plastik®6275.

The creep test results are listed on the Table VI.5 and Table VI.6 for Plastik® 6275 and Ciprene® 2000, respectively. The Ongronat_MCs have shown to be less effective cross-linkers and considering the time required for this test, IPDI containing MCs were tested, both with a PHB and PCL shell. The MC s performance is compared with the adhesive pre-polymer without cross-linker, with non-encapsulated IPDI and with the respective benchmark.

Table VI.5. Results obtained in the creep tests for substrates adhered with a pre-polymer and adhesive formulations containing Desmodur®RC and IPDI as crosslinkers, as well as PCL and PHB MCs containing the last, using Plastik®6275 as pre-polymer.

Crosslinker	Percentage in the pre-polymer (wt%)	d (cm)	d (cm)	d (cm)	d (cm)
		60°C	70°C	80°C	90°C
-	-	1	FO	FO	FO
Desmodur® RC	2.5	0	0	0	0
IPDI	2.5	0.3	0.96	FO	FO
	5	0	0	0	1.43
PCL_MCs	2.5	0	0.33	2.07	FO
	5	0	0.2	0.27	0.93
PHB_MCs	2.5	0	0.13	0.13	0.33
	5	0	0.07	0.13	0.22

Table VI.6. Results obtained in the creep tests for substrates adhered with a pre-polymer and adhesive formulations containing Suprasec®2234 and IPDI as crosslinkers, as well as PCL and PHB MCs containing the last, using Ciprene®2000 as pre-polymer.

Crosslinker	Percentage in the pre-polymer (wt%)	d (cm)	d (cm)	d (cm)	d (cm)
		60°C	70°C	80°C	90°C
-	-	FO	FO	FO	FO
Suprasec® 2234	2.5	0.35	1.05	3.35	FO
IPDI	2.5	-	-	--	-
	5	0.65	2.75	3.25	FO
PCL_MCs	2.5	1	1.93	3.95	FO
	5	0.83	2.30	3.40	FO
PHB_MCs	2.5	0.73	1.93	3.03	FO
	5	0.73	2.50	2.47	FO

The creep test is particularly important to understand the cross-linking effect on the PU adhesive formulation (Plastik® 6275). This adhesive pre-polymer already has a high-strength bonding per se, and the cross-linking main advantage is to improve its resistance to temperature. Even though the difference with and without cross-linker was not so notorious in the peeling strength test, its response to temperature is very distinct with a full opening of the non-crosslinked specimen at only 70 °C. The increase from 2.5 to 5 wt% of the IPDI and PCL' MCs in the formulation led to significant improvements. The use of PCL_MCs at 5 wt% enabled to obtain a displacement inferior to 1 cm at 90 °C indicating a good cross-linking of the pre-polymer. These results confirm the ability of using PCL MCs, containing encapsulated IPDI, as cross-linkers for PU adhesive formulation, at a concentration of 5 wt%. The PHB MCs led to the lower displacement, when compared with the PCL MCs and the non-encapsulated isocyanate, with its use at 5 wt% leading to the most promising results. The PHB MCs have smaller sizes and show a

lower aggregation tendency, resulting in a better dispersion in the pre-polymer, which might have contributed to a better cross-linking performance.

The bondline prepared with Ciprene® 2000 adhesive has a lower resistance to temperature, resulting in a full opening at 90°C for all cases. The displacement observed for the IPDI and PCL MCs at 5 wt%, is similar to that of the benchmark at 80°C, confirming their ability to act as cross-linker for the PCP adhesive. As observed for the PU adhesive, the PHB MCs led to lower displacements than the PCL MCs.

VI.5 Final remarks

The high reactivity and relatively high degree of polymerization characteristic of the cross-linker isocyanate commercially used by CIPADE (Suprasec® 2234), made their encapsulation a difficult task. Resulting MCs were too stiff, inhibiting their response to the stimuli of pressure and temperature applied during the adhesive joint preparation. In addition, these MCs had a low yield of encapsulation, which required the use of a large amount of MCs in the adhesive formulation to assure the 2.5 wt% of isocyanate in the final composition. Nevertheless, the Suprasec_MCs were tested in the commercial pre-polymer, Ciprene®2000, confirming its inability to act as cross-linkers for this application. Adding to the inability of this MCs to release the encapsulated isocyanate, they also show a negative effect on the adhesive joint, resulting in a peel strength much lower than that of the joint prepared without cross-linker.

Therefore, two other isocyanates were tested as cross-linkers for the adhesive's formulations, namely IPDI and Ongronat® 2500.

The IPDI containing MCs, obtained both by interfacial polymerization and solvent evaporation techniques, were able to respond either to one, or both, stimuli applied in the adhesive joint preparation. Adhesive joints prepared with Ciprene®2000 are more susceptible to be negatively affected by the MCs. A peel strength value higher than 3 N/mm was obtained, when using MCs with a PCL shell, at a concentration of 2.5 wt%, however resulting in lower values than the same non-encapsulated isocyanate. Nevertheless, the MCs were able to release its content during the adhesion process and act as cross-linkers, confirmed by the increased temperature resistance.

The bondlines prepared with the Plastik® 6275 pre-polymer were not affected by the presence of MCs, with both the PCL and PHB MCs showing to be effective cross-linkers by the peeling strength and temperature resistant tests.

For both the PU and PCP adhesives the PHB_MCs seem to lead to the lower displacements in the creep tests, which can be a result of its smaller sizes and better dispersion in the adhesive. The most promising adhesive formulation was obtained for Plastik® 6275 pre-polymer both with the PCL and PHB MCs at a concentration of 5 wt% in the adhesive formulation, leading to adhesive joints which responded to both the peeling strength and creep tests similarly to those prepared with the benchmark cross-linker.

Bibliography:

- 1 Arakawa, C. K.;DeForest, C. A., *Biology and Engineering of Stem Cell Niches*. **2017**: Academic Press.
- 2 McGrath, J. E.;Hickner, M. A.;Höfer, R., *Polymer Science: A Comprehensive Reference*. 2nd ed. **2012**: Elsevier.
- 3 Krasowska, K.;Heimowska, A.;Morawska, M., *Environmental degradability of polycaprolactone under natural conditions*. E3S Web of Conferences, **2016**, 10, 00048.
- 4 Siparsky, G. L., *Polymers from Renewable Resources*. 1st ed. **2001**: American Chemical Society.
- 5 Loureiro, M. V.;Vale, M.;Galhano, R.;Matos, S.;Bordado, J. C.;Pinho, I.;Marques, A. C., *Microencapsulation of Isocyanate in Biodegradable Poly(ϵ -caprolactone) Capsules and Application in Monocomponent Green Adhesives*. ACS Applied Polymer Materials, **2020**, 2, 4425–4438.
- 6 Bagheri, A. R.;Laforsch, C.;Greiner, A.;Agarwal, S., *Fate of So-Called Biodegradable Polymers in Seawater and Freshwater*. Global Challenges, **2017**, 1, 1700048.
- 7 Zhang, X.;Peng, X.;Zhang, S. W., *Science and Principles of Biodegradable and Bioresorbable Medical Polymers*. 1st ed. **2016**: Woodhead Publishing.
- 8 Spicer, C. D., *Hydrogel scaffolds for tissue engineering: the importance of polymer choice*. Polymer Chemistry, **2020**, 11, 184-219.
- 9 Jiang, W.;Hosseinpourpia, R.;Biziks, V.;Ahmed, S. A.;Militz, H.;Adamopoulos, S., *Preparation of Polyurethane Adhesives from Crude and Purified Liquefied Wood Sawdust*. Polymers, **2021**, 13, 3267.
- 10 Lee, J.-H.;Lee, T.-H.;Shim, K.-S.;Park, J.-W.;Kim, H.-J.;Kim, Y.;Jung, S., *Effect of crosslinking density on adhesion performance and flexibility properties of acrylic pressure sensitive adhesives for flexible display applications*. International Journal of Adhesion and Adhesives, **2017**, 74, 137-143.

Supplementary Information

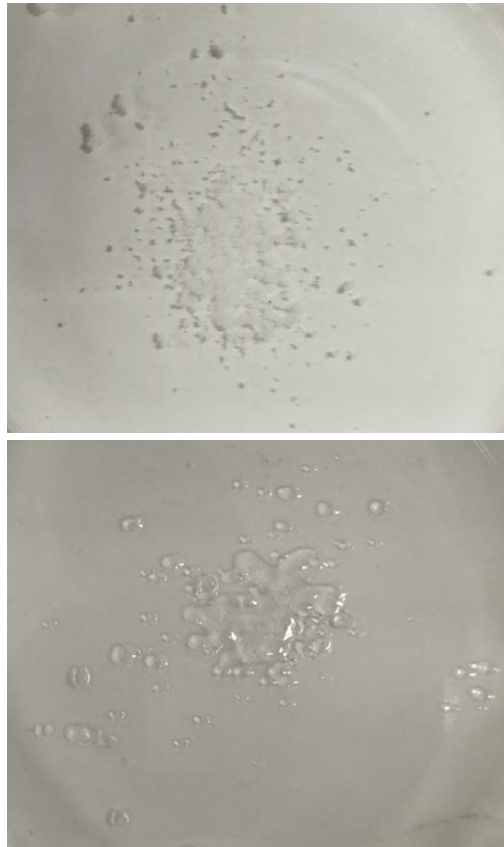


Figure VI. S1. Photographs of the PCL MCs before (above) and after (bottom) being submitted to the reactivation process used during the adhesion process, when using a PCP adhesive (Plastik® 6275).

CHAPTER VII

Summary

Chapter VII – Final remarks and conclusions

This dissertation reports on the development of polymeric microcapsules (MCs) containing a high amount of encapsulated isocyanate species (reaching c.a. 80wt%), to be used as cross-linkers for polyurethane (PU) and polychloroprene (PCP) pre-polymer adhesive formulations aimed at the footwear industry. The encapsulation of the isocyanate species, which are considered to be toxic substances, avoids their direct contact with the operator, as they are only to be released during the adhesive joint preparation. The adhesive is to be supplied as one-component (1K), with the MCs and the pre-polymer mixed together, or as two-component (2K), with the two being supplied separately.

In the previous chapters two distinct techniques are reported for the encapsulation of isocyanate species, namely the interfacial polymerization and the solvent evaporation, both in combination with a microemulsion system. By the first technique, the MCs are produced by chemical reactions of the involved reagents while, by the latter one, MCs are formed by means of a physical process, due to polymer precipitation on the surface of the emulsion droplets. Spherical, loose and core-shelled MCs were obtained by both techniques containing not only monomeric, but also oligomeric and pre-polymeric species. Figure VII. 1 schematizes the experimental work exposed in this dissertation.

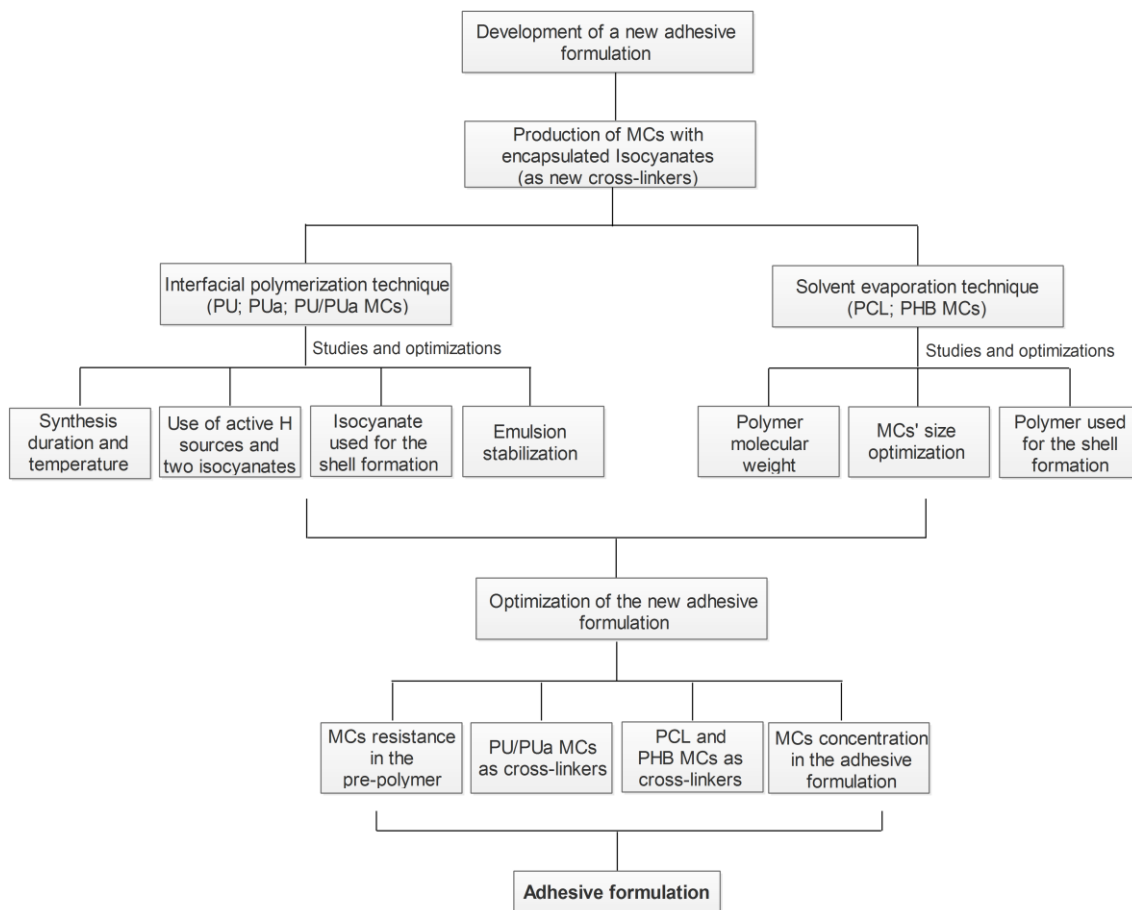


Figure VII. 1. Schematization of the experimental work exposed in this dissertation.

Interfacial Polymerization:

The interfacial polymerization technique is largely used in the state of the art for the encapsulation of isocyanate monomeric species, producing polyurea (PUa) and PU/PUa MCs. However, in this thesis, a comprehensive study for the optimization of this method was carried out. It targets MCs with high encapsulation efficiency, acceptable shelf-life and able to effectively release their content during the adhesive joint preparation by the effect of pressure (4 bar) and temperature (70 °C) applied in the process. To the best of my knowledge, there are no isocyanate MCs available in the market, and they have never been tested before for the application of focus in this thesis. The main parameters that were found to most influence the performance of the MCs as cross-linkers, in the adhesive formulations, are encapsulation efficiency, the MCs' shelf-life and the MC's size distribution. To optimize the encapsulation efficiency, it was used a combination of active H sources in the W phase of the emulsion and two isocyanates in the oil (O) phase, one of them much more reactive than the other. The active H sources promote a quicker shell formation, and the second (most reactive) isocyanate is here

used to produce the shell, so that the isocyanate intended to be encapsulated does not participate in the shell formation. The active H sources were used with a double intent, not only to promote a quicker shell formation, but also to improve the MCs' shell features, namely lower toughness and higher hydrophobicity, targeting an effective isocyanate release when desired and a longer shelf-life of the MCs. MCs with 46.3% of its weight in isocyanate were obtained, by this method.

All the tested active H sources were able to improve the MCs' shelf-life, particularly Jeffamine® D2000 and the combination of polyethylenimine (PEI) and n-octyl triethoxysilane (n-OTES). Both the repeating oxypropylene units of the Jeffamine® D2000 and the long aliphatic carbohydrate chain from n-OTES were found to increase the hydrophobicity and flexibility of the shell. PEI, on the other hand, contributed to increase the cross-linking of the shell.

To optimize the size distribution of the MCs, the size and stability of the emulsion droplets was improved. With that purpose, the effect of several emulsion stabilization systems were evaluated, namely the effect of emulsifiers, a polysaccharide, and a rheology modifier, as well as combinations between them. Rheology modification was shown to be the most effective strategy to stabilize the oil-in-water (O/W) emulsion system, since it prevents droplets sedimentation. The use of polyvinyl alcohol (PVA) at 2 wt% in the water (W) phase enables to increase its viscosity to 5-6 cP, which led to a minimum variation between the size of the initial emulsion droplets and that of the final MCs. This enabled a fine control over the MCs sizes.

By applying all these strategies, it was able to obtain fine-tuned PUa and PU/PUa MCs containing not only isophorone diisocyanate (IPDI) but also oligomeric methylene diphenyl diisocyanate (MDI) species and pre-polymeric isocyanate species.

The following scheme, Figure VII. 2, shows the reactional conditions for the best performing MCs of PU/PUa shell, as well as the impact of the referred MCs for the present work. **Erro! A origem da referência não foi encontrada.** lists the range of values for the studied reactional parameters that enable to obtain satisfactory MCs.

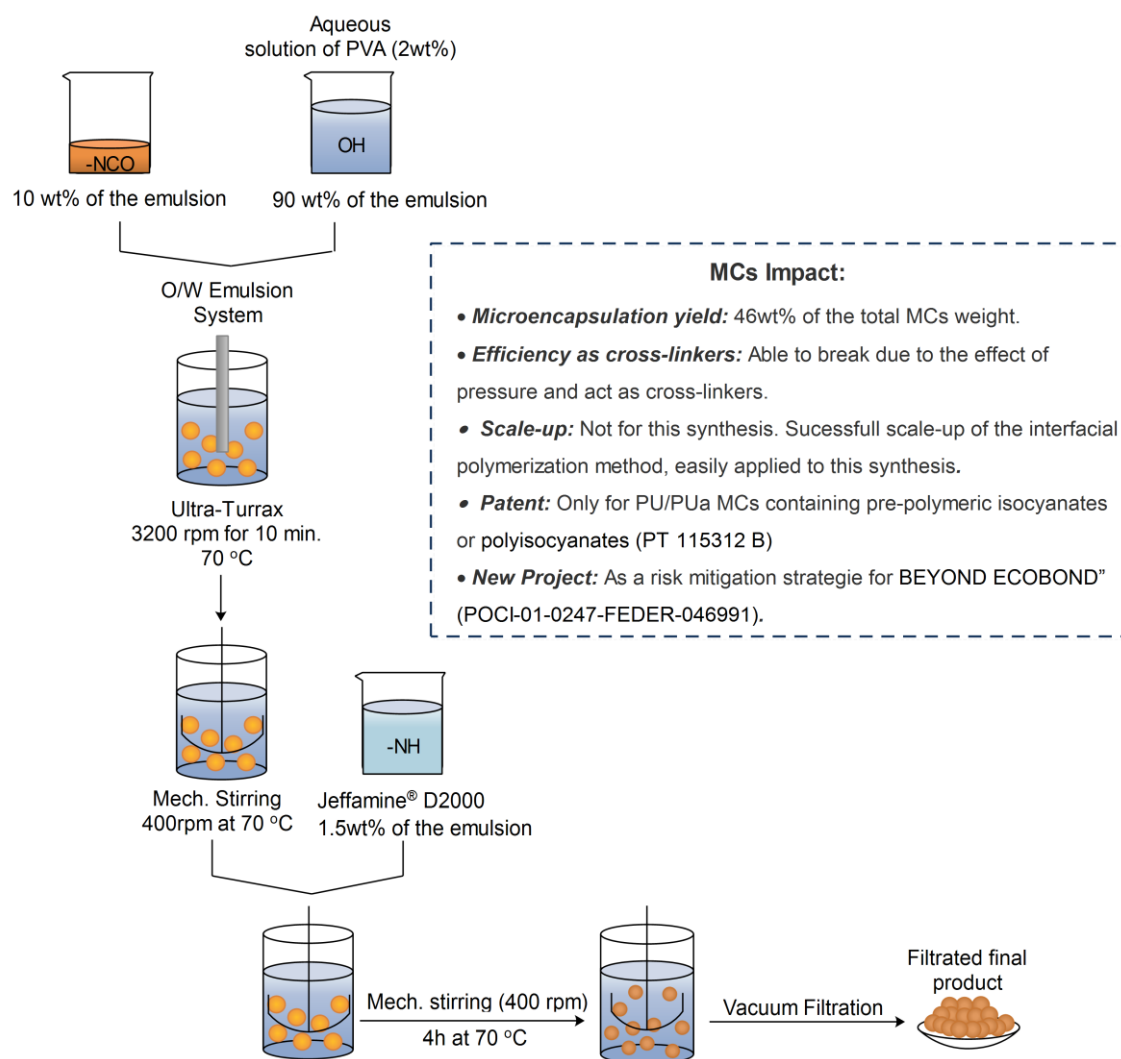


Figure VII. 2. Reactional scheme for the best performing MCs of PU/PUa shell.

Table VII. 1. Range of values for the studied reactional parameters that allow to obtain satisfactory MCs by interfacial polymerization technique.

Reactional Parameters	Range of values
Emulsification time	10 minutes
Synthesis Temperature	60 - 70°C
Emulsification stirring	3200 – 3400 rpm
Mechanical stirring	400 – 500 rpm

Solvent evaporation:

This technique has only been scarcely reported for the encapsulation of hydrophobic species and was never used before for the encapsulation of isocyanate species. Adding, effectively encapsulate a variety of isocyanates in MCs with a biodegradable shell is one of the biggest novelties presented in this thesis. Several reactional parameters had to be optimized and several specific studies were carried out, namely the effect of the polycaprolactone (PCL) MW on the MCs final characteristics, as well as the effect of the PVA and gum arabic (GA) concentration and the O phase volume on the MCs average sizes. A Design of Experiment (MODDE® Pro 13 software) was employed, which enabled to conclude regarding the relative importance of each parameter in study, as well as to develop a model to predict the optimum values for these reactional parameters to obtain MCs with a pre-defined average size.

Two PCL with distinct MW, of 45000 and 80000 Da, were tested as polymers for the MCs' shell formation. Both PCL led to spherical, disaggregated, and core-shell MCs, with the ones obtained with the higher MW PCL having bigger sizes and size distributions. The MW of the shell polymer has shown to also influence the encapsulation content and the MCs' shelf-life. The MCs obtained with the higher MW PCL had more 6% of its weight in isocyanate, compared to the ones obtained with the 45000 Da PCL and demonstrated to form less PUa over time, showing an improved shelf-life. Despite the advantages regarding the use of a higher MW PCL, it greatly increases the viscosity of the respective O phase, which brings issues on the MCs production process, namely a low reproducibility, low production yield and bigger MCs sizes and sizes distribution. Due to these reasons, PCL with 45000 Da was selected as the ideal for the MCs production. The size of the MCs was optimized, to ca. of 94 μm , by DOE, using as main variables GA and PVA concentrations as well as the O phase volume, being the PVA concentration in the W phase the most significant parameter on the emulsion stability and consequently on the control of the average MCs sizes.

MCs containing highly reactive pre-polymeric isocyanate species, namely Ongronat® 2500 and Suprasec® 2234, were also achieved by this methodology. They were spherical, loose and disaggregated, but with a larger average size than IPDI MCs: ca. 150 μm (Ongronat® 2500) and ca. 268 μm (Suprasec® 2234). Only Ongronat® 2500 MCs contained isocyanate, with an encapsulation content of about 21 wt%. This value is lower than desired for the current application, nevertheless it is an improvement in the state of the art as the publications regarding the encapsulation of non-monomeric isocyanates are scarce and none by the solvent evaporation technique, containing a biodegradable shell.

The following scheme, Figure VII. 3, shows the reactional conditions for the best performing MCs composed by a PCL shell, as well as the impact of the referred MCs for the present work. Table VII. 2 lists the range of values for the studied reactional parameters that enable to obtain satisfactory MCs.

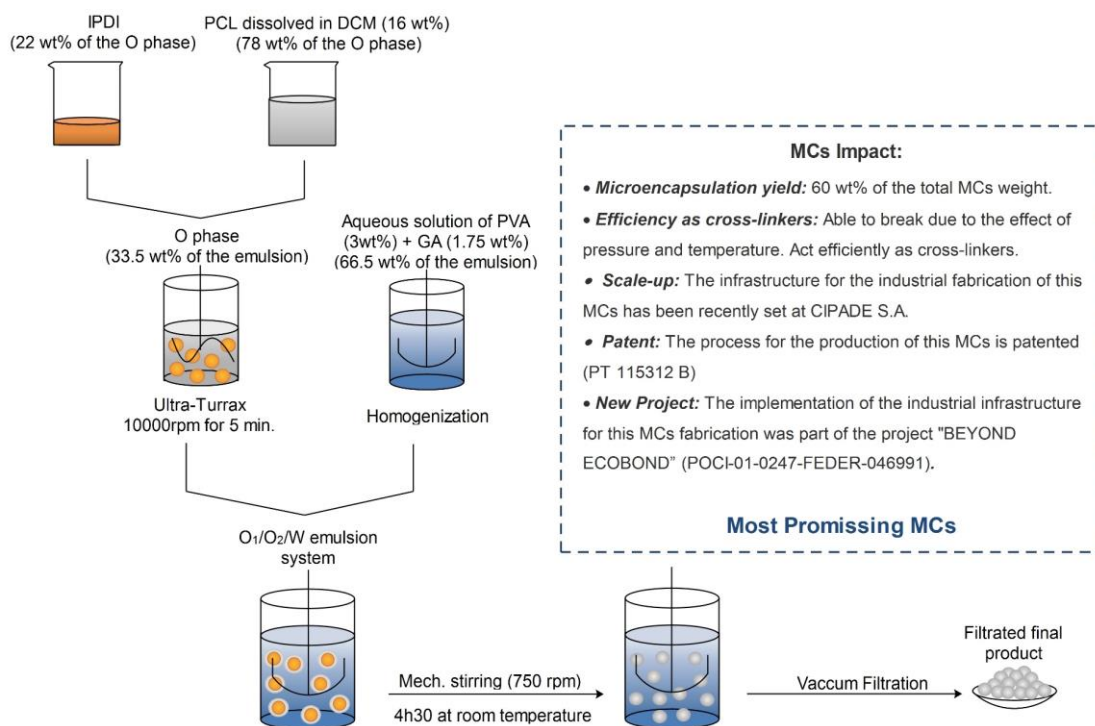


Figure VII. 3. Reactional scheme for the best performing MCs composed by a PCL shell.

Table VII. 2. Range of values for the studied reactional parameters that allow to obtain satisfactory MCs by the solvent evaporation technique, using PCL as shell forming polymer.

Reactional parameters	Range of values
PVA concentration	2 - 3 wt% in the W phase
GA concentration	0 - 3.5 wt% in the W phase
Emulsification time	10 minutes
Emulsification stirring	8500 -10000 rpm
Mechanical stirring	800 -850 rpm
Polymer concentration	10-16 wt% in the organic solvent
Isocyanate concentration	16-20 wt% of the O phase
O/W ratio	28 - 39 wt%

In addition to PCL, MCs with a polyhydroxybutyrate (PHB) shell were also obtained by using an adaptation of the solvent evaporation technique with the self-organized precipitation method, enabling to encapsulate high isocyanate loads, of 80 wt%.

The following scheme, Figure VII. 4, shows the reactional conditions for the best performing MCs, of PHB shell. Table VII. 3 lists the range of values for the studied reactional parameters that enable to obtain satisfactory MCs.

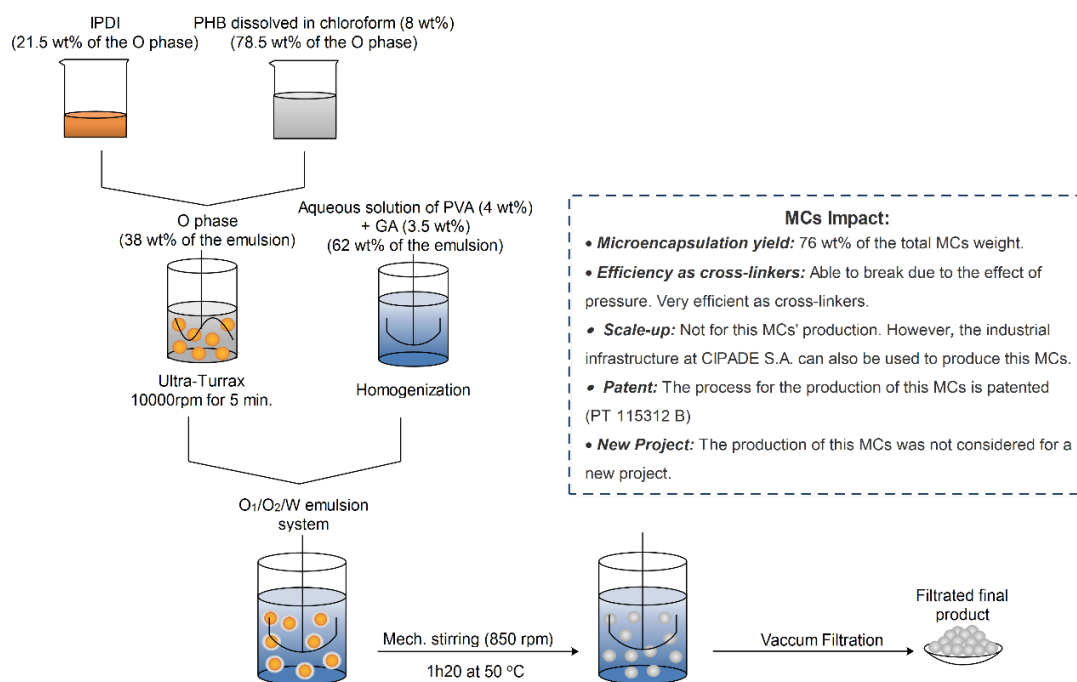


Figure VII. 4. Reactional scheme for the best performing MCs composed by a PHB shell.

Table VII. 3. Range of values for the studied reactional parameters that allow to obtain satisfactory MCs by the solvent evaporation technique, using PCL as shell forming polymer.

Reactional parameters	Range of values
GA wt% in the W phase	3.5wt%- 5 wt%
volume ratio of the O1:O2 phases	1:3 – 1:4.7
Temperature	40 °C – 50 °C
Mechanical Stirring	850 rpm
PVA wt% in the W phase	4 wt%
Polymer wt% in the O ₂ phase	8 wt% - 10 wt%

The MCs obtained by the interfacial polymerization and solvent evaporation methods were tested as cross-linkers in the PU and PCP adhesive formulation. The peel strength and creep test results obtained for the adhesive formulations composed by the MCs, in its optimized concentrations, and the Ciprene®2000 and Plastik®6275 pre-polymers, are summarized in Table VII. 4 and Table VII. 5, respectively.

Table VII. 4. Peel strength and creep test results obtained with adhesive formulations composed by the Ciprene®2000 pre-polymer and the optimized MCs' concentration, for each type of MCs.

MCs production technique	Interfacial Polymerization		Solvent Evaporation		
	PU/PUa		PCL		PHB
MCs' shell					
Encapsulated isocyanate	IPDI	Suprasec® 2234	IPDI	Ongronat® 2500	IPDI
Optimized concentration (wt%)	2.5	2.5	2.5	2.5	5
Peel Strength test (N/mm)	2.99	0.87	4.11	3.09	3.5
Creep test	FO* at 100 °C	FO* at 60 °C	FO* at 90 °C (3.95 cm at 80 °C)	-	FO* at 90 °C (2.47 cm at 80 °C)

*FO - Full opening

Table VII. 5. Peel strength and creep test results obtained with adhesive formulations composed by the Plastik®6275 pre-polymer and the optimized MCs' concentration, for each type of MCs.

MCs production technique	Solvent Evaporation		
	PCL		PHB
MCs' shell			
Encapsulated isocyanate	IPDI	Ongronat®2500	IPDI
Optimized concentration (wt%)	5	2.5	5
Peel Strength test	5.82	5.41	4.82
Creep test	Resisted to 90 °C (0.93cm)	-	Resisted to 90 °C (0.22cm)

MCs containing Suprasec®2234 needed to be in a large amount in the adhesive formulation, due to its low encapsulation yield. Also, this MCs rigid shell did not break during the adhesive application. For these reasons, the referred MCs were not considered fit for the application.

Bondlines prepared with Ciprene®2000 seem to be negatively affected from the presence of MCs, which is not observable for the specimens prepared with Plastik® 6275. Due to this, there were only obtained satisfactory peeling strength tests results, with the Ciprene®2000 pre-polymer, for a concentration of 2.5 wt% of MCs, either way leading to lower values than the same non-encapsulated isocyanate.

The adhesive joints adhered with Plastik® 6275 pre-polymer, seem to not be affected by the presence of MCs. The specimens prepared with this adhesive have the advantage to be submitted not only to pressure but also to temperature during the adhesion process, which contributes to the isocyanate release from the MCs.

For both pre-polymers the PHB MCs are the most promising cross-linkers, leading to the lower displacements in the creep tests, with similar results to the benchmark cross-linker.

Table VII.6 lists the advantages and disadvantages of the MCs obtained by both methods addressed in this dissertation.

Table VII.6. Advantages and disadvantages of each MCs' production method and of the respective MCs characteristics.

Production method	Advantages	Disadvantages
Interfacial polymerization	<ul style="list-style-type: none"> • Well established method for the encapsulation of isocyanates, with extensive information on the state of the art • Small sized MCs with a spherical morphology • PU and PUa shelled MCs have a better resistance to solvents 	<ul style="list-style-type: none"> • Lower encapsulation content • Lower shelf-life • High stiffness of the shell • Difficult to respond to the stimuli applied during the adhesion • Lower resistance to water and moisture diffusion
Solvent Evaporation	<ul style="list-style-type: none"> • Higher encapsulation content • Prolonged shelf-life • Versatility of the shell material • Biodegradable shell • Temperature responsive shell • Capability to respond to the stimuli applied during the adhesion • Higher resistance to water and moisture diffusion 	<ul style="list-style-type: none"> • Poorly studied technique for the isocyanate encapsulation with no information on the state of the art • Bigger sized MCs • Reproducibility and morphological issues along with low production yield when using PCL with high MW • PHB and PCL have a lower resistance to solvents

Considering the advantages and disadvantages of each production process the solvent evaporation method stands for the most potential one, for this application. Although the interfacial polymerization method is a reliable method, very well studied and documented for the encapsulation of isocyanates, the obtained MCs cannot be considered adequate for the application. The lower encapsulation content make it necessary to add more MCs to the bondline to ensure the necessary isocyanate for the cross-linking, which causes disruption on the bondline, specially on Ciprene®2000. This is associated with the inability of this MCs to burst during the adhesive application, due to the high stiffness of the shell, which makes them

inadequate. On the contrary the MCs obtained by the solvent evaporation technique have higher encapsulation content and are able to respond both to the stimuli of pressure and temperature, for the PCL MCs. However, due to their poor solvent resistance it is not possible for the adhesive to be supplied as 1K adhesive. One important feature for the MCs when supplied separately is their resistance to the air moisture diffusion, as the isocyanate reacts with water. PUa and PU/PUa show a poor shelf-life due to this phenomenon, which adds to the inadequacy of this MCs. On the other hand, the ones obtained by the solvent evaporation method show a good shelf-life for a period of 3 months, due to the higher hydrophobicity of its shell.

Although MCs containing pre-polymeric encapsulated isocyanates were possible to be obtained, by both techniques, its encapsulation content was lower and it increased the stiffness of the shell. The ones containing Ongronat®2500 were tested as cross-linkers leading to poorly results. The IPDI, when used at 5 wt% in the pre-polymer, has showed to be fit for the application, leading to results similar to those of the commercially used isocyanates. Having this into account, IPDI was considered the most fit isocyanate to be used as encapsulated cross-linker.

In which regards the shell material, although the PHB lead to the highest encapsulation content, smaller MCs and to the most promising results as cross-linkers, this MCs production process is difficult to control and has a high irreproducibility, which might bring challenges in its industrial implementation. For this reason, the PCL MCs, using the PCL with 45000 Da and containing encapsulated IPDI, were considered the most promising for this application.

Concluding, a new adhesive formulation was developed, containing solid MCs as cross-linkers, with identical properties to the ones currently commercially available. The new formulation is to be supplied as 2K, with the MCs to be mixed with the adhesive pre-polymer during the adhesive application, in a concentration of 5 wt% in the Plastik® 6275 pre-polymer and at 2.5 wt% in the Ciprene®2000. The MCs have a shelf-life of 3 months and ideally should be stored in a low humidity environment. Its PCL shell enable this MCs to release its content either by the effect of pressure and/or temperature usually applied in the footwear industry, avoiding the need to adapt the currently implemented adhesion process. These newly developed MCs gave rise to the patent PT 115312 B A pilot plant for the production of these MCs has been recently established at CIPADE S.A. facilities, which, after optimization trials will culminate in commercially available isocyanate MCs, with a wide range of applications, such as in the adhesive field, self-healing, smart coatings, etc..